A REPORT OF RESEARCH CONDUCTED UNDER MARAD TASK S-11

OF THE SHIP PRODUCIBILITY RESEARCH PROGRAM

TO DETERMINE THE VALUE OF STANDARD STRUCTURAL ARRANGEMENTS

STANDARD STRUCTURAL ARRANGEMENTS

Prepared by:

General Dynamics Corp.

Quincy Shipbuilding Division

Report Documentation Page

Public reporting burden for the collection of information is estimated to average 1 hour per response, including the time for reviewing instructions, searching existing data sources, gathering and maintaining the data needed, and completing and reviewing the collection of information. Send comments regarding this burden estimate or any other aspect of this collection of information, including suggestions for reducing this burden, to Washington Headquarters Services, Directorate for Information Operations and Reports, 1215 Jefferson Davis Highway, Suite 1204, Arlington VA 22202-4302. Respondents should be aware that notwithstanding any other provision of law, no person shall be subject to a penalty for failing to comply with a collection of information if it does not display a currently valid OMB control number.

1. REPORT DATE **1976**	2. REPORT TYPE **N/A**	3. DATES COVERED **-**

4. TITLE AND SUBTITLE	5a. CONTRACT NUMBER
A Report of Research Conducted Under MARAD Task S-11 of the Ship Producibility Research Program to Determine the Value of Standard Structural Arrangements	5b. GRANT NUMBER
	5c. PROGRAM ELEMENT NUMBER

6. AUTHOR(S)	5d. PROJECT NUMBER
	5e. TASK NUMBER
	5f. WORK UNIT NUMBER

7. PERFORMING ORGANIZATION NAME(S) AND ADDRESS(ES)	8. PERFORMING ORGANIZATION REPORT NUMBER
Naval Surface Warfare Center CD Code 2230 - Design Integration Tools Building 192 Room 128-9500 MacArthur Blvd Betheda, MD 20817-5700	

9. SPONSORING/MONITORING AGENCY NAME(S) AND ADDRESS(ES)	10. SPONSOR/MONITOR'S ACRONYM(S)
	11. SPONSOR/MONITOR'S REPORT NUMBER(S)

12. DISTRIBUTION/AVAILABILITY STATEMENT
Approved for public release, distribution unlimited

13. SUPPLEMENTARY NOTES

14. ABSTRACT

15. SUBJECT TERMS

16. SECURITY CLASSIFICATION OF:			17. LIMITATION OF ABSTRACT	18. NUMBER OF PAGES	19a. NAME OF RESPONSIBLE PERSON
a. REPORT **unclassified**	b. ABSTRACT **unclassified**	c. THIS PAGE **unclassified**	**UU**	**303**	

Preface

        The three individual technical reports which follow were written as the result of the Ship Producibility Task S-11, "Standard Structural Arrangements". The work was performed by the Quincy Shipbuilding Division of General Dynamics under contract to Bath Iron Works Corporation.

        Industry groups meeting in advance of the formulation of Task S-11 had recommended a number of structural arrangements to be investigated for standardization. These were augmented in the pre-award proposal.

        The complete candidate list was forwarded for evaluation to ten major U.S. shipyards, with follow-on visits to each yard. The results of interviews were summarized for each category under the following format:

        Iterm:

        Definition:

1. What are most likely areas of use

2. How prevalent is current use?

3. Is there a qualitative rationale?

4. Is there a quantitative rationale?

5. Is there a potential for developing the rationale and for the development of standards?

6. Can cost advantages of standards be establ shed ?

7. Existing technical criteria and guidelines

8. Potential Marine Graphics Handbook entry.

9. Potential design application for evaluation of benefit.

10. Estimated study manhours.

Results were summarized in the "Progress Summary, Task S-11", July 1976, which is on file at Bath Iron Works.

An advisory group appointed by the contractor evaluated all proposed catgeories for greatest usefulness to the industry and for compliance with the essential objective to reduce the cost of building ships in the United States.

Nineteen categories were ranked numerically and assigned three levels of priority:

<u>Priority 1</u>

1   Structural Details

2   Alignment Criteria

3   Repair Standards

4   Standard Frame Spacing

5   Construction Openings

6   Straight Line Frames

7   Standard Welding, Details

<u>Priority 2</u>

8   Level Longitudinal

9   Bow Framing

10   Stern Framing

11   Tripping Brackets

12   Parallel Decks and Standard Deck Framing

13   Foundations

14   Erection Breaks at In-plane Structure

Priority 3

15   Consideration of Deflection to Minimize Distortion and Vibration

16   Rudders

17   Water Scoops and Sea Chests

18   Reinforcing and Racking Preventatives for Heavy Lifts

19   Bilge Keels

Items 1, 2 and 11 (structural details, alignment criteria and tripping brackets) were ultimately selected for detailed study. The consensus lower priority item on tripping brackets was considered because of special interest to the investigators.

The authors gratefully acknowledge the guidance of Mr. John Mason, Bath Iron Works Project Manager, the funding contributed by MarAd and the time and courtesy extended by all shipyards visited. Thanks are due also to the members of the Advisory Committee.

Standard Structural Arrangements,

Task S-11 of the Ship Producibility Program

Executive Summary

The intent of Task S-11 was to reduce the cost of U.S. built ships by
producing a series of standard structural arrangements. Study objectives were
eventually modified to the formulation of design guidelines. Twenty candidate
subjects were investigated for inclusion in the study, and three were selected:

Structural Details

Misalignment Tolerance

Tripping Brackets

The report on "Potential Ship Structural Details Guidelines" defines common
structural details and provides brief descriptive narrative of application and
attributes. Detailed static analysis was performed for structural intersections,
generally the most common and troublesome structural detail.

Illustrations are provided for details in sixteen categories. These
details represent what is best in U.S. shipbuilding practice, or the development
of slightly modified configurations.

The report on "Potential Ship Structure Misalignment Tolerance Guidelines"
presents a review of available standards and guidelines and of published experi-
mental and theoretical data.

Analysis of butt and cruciform joints is combined with available fatigue
data to produce specific guidelines for permissible static and dynamic misalign-
ment Of common shipbuilding Joints.

The third report in this program, "Potential Ship Structure Tripping Bracket Guidelines" was motivated by current lack of suitable guidance to the need for tripping brackets in ship structure. The report is a designer-oriented compendium of the necessary theoretional formulatlons.

It is expected that thorough and deliberate review of these reports by industry groups such as SNAME panel SP-6 and ASTM Subcommittee F-25 can develop these tentative proposals into detailed consensus guidelines or standards.

The adoption of uniform structural details will generate specific performance feedback leading to reduced repair costs. Overall ship scantlings may eventually be reduced if margins for assumed stress concentrations or defects at structural details can be eliminated.

The misalignment criteria should be extended to the analysis of greater extent of misalignment and to the systematic investigation of suitable repair. Confirming full scale fatigue testing is desirable. Consensus guidelines will save considerable time now devoted to qualitative and quantitative arguments between builder, owner and regulatory agency inspectors, while improving ship reliability anti possibly decreasing fitup costs.

Guidelines for tripping bracket location are of significant economic value in ships with deep web frames, where frequent and arbitrary use of large brackets may greatly add to shipbuilding expense. General Dynamics has already employed this analysis to justify design alteration resulting in removal of several hundred large brackets per ship.

To complete these guidelines it remains to formulate a solution for asymmnetric stiffeners (angles) in bending.

All three reports on potential guidelines are expected to be of immediate use to ship structural designers.

FINAL TECHNICAL REPORT

ON

POTENTIAL SHIP STRUCTURE
MISALIGNMENT TOLERANCE
GUIDELINES

PART NO. 1 OF

STANDARD
STRUCTURAL ARRANGEMENTS
TASK S-11
OF THE
SHIP PRODUCIBILITY PROGRAM

GENERAL DYNAMICS
QUINCY SHIPBUILDING DIVISION

TABLE OF CONTENTS

TABLE OF CONTENTS (Cont'd)

LIST OF ILLUSTRATIONS

LIST OF ILLUSTRATIONS (Cont'd)

LIST OF ILLUSTRATIONS (Cont'd)

LIST OF TABLES

Section 1

INTRODUCTION AND SUMMARY

The aim of this report is to establish a basis for a set of guidelines to be used in the evaluation of errors in alignment. The importance of alignment criteria is clear:

1. Reference 1 states "The most commonly suggested tolerance problem was misalignment, especially misalignment of inter-costal at cruciform intersections". This was noted after discussions with ship owner/operator executives and yard executives.

2. Correction and rework of structural deviations may introduce locked-in stresses, flaws or weld defects which may be more detrimental to overall strength than the original defect.

3. The cost involved in repairing, inspecting, and re-repairing where necessary, while large, is probably small compared with the cost of delays, late delivery and consequent loss of goodwill.

Due to the lack of specific guidelines for dealing with mis-alignment, designers and engineers have had to evaluate each case using judgment and rules of thumb, and have had to convince inspectors and surveyors that the structural integrity has not been jeopardized.

Sections 2 and 3 of this study present a summary of published standards and guidelines and of the technical literature most applicable to the alignment subject.

Sections 4 and 5 present analytical work leading to the basis for design guidelines (Section 6) for static and fatigue strength of misaligned joints, respectively. Section 6 is esscntially a self contained summary of the potential design guidelines derived in this report, and could be used independently.

A limited survey of reported cases of misalignment indicates that there is no predominant pattern of occurrence or repair. Guidelines for alignment criteria and for related structural alterations should lead to significant savings of ship con-struction time and cost.

Section 2

COLLECTION OF EXISTING STANDARDS AND GUIDELINES

2.1 <u>GENERAL</u>

This section is an attempt to list standards and guidelines
applicable to alignment criteria contained in the rules of the
major classification societies and of other applicable rule-
making technical societies. Only those guidelines are
presented that define numerical limits for misalignment.

The American Bureau of Shipping (ABS) has no formal set of
quality control standards but generally agrees that structural
tolerance limits depend on the location of the joint, quality
of material and the allowable stress level. Bureau Veritas
and Lloyd's Register of Shipping likewise have no published
standards for tolerances.

Nippon Kaiji Kyokai has a set of standards "Japanese Shipbuilding
Quality Standards - 1975" developed by the societyiety of Naval
Arhitects of japan and the University of Tokyo. These
standards provide numerical limits for strength **and other members.**
The German Shipbuilding Industry developed the "Production
Standard of the German Shipbuilding Industry" which is non-
binding and not enforced by Germanischer Lloyd surveyors. The
final set of formal standards presented is VIS 530, "Accuracy
In Hull Construction", prepared by the Swedish Shipbuilding
Standards Center.

Reference 1 is a timely summary of all applicable guidelines.

The following references have been reviewed and excerpted.
Throughout the remainder of this report the following indicated
abbreviations will apply:

REF. NO.	TITLE/SOCIETY	ABBREVIATION
1)	Swedish Shipbuilding Standards Institute	VIS-530
3	Japanse Shipbuilding Quality Standards	JSQS
4	Association of.German Shipbuilding Industry	PSGS
5	Ikawajima-Harima Heavy Industries	IHI
6	American Bureau of Shipping	ABS
7	Bureau Veritas	BV
8	Det Norske Veritas	DNV
9	Germanischer Lloyd	GL
10	Lloyd's Register	LR
11	Nippon Kaiji Kyokai	NKK

2.2 ALIGNMENT STANDARDS

2.2.1 Fillet Welded Cruciform Joints

Cruciform joints with fillet welds are the classic tolerance
problem. This detail will be found in the fitting of brackets,
intercostal, webs, bulkheads, longitudinals, etc. Figure 2-1
details the joint with respect to the documented standards.

THROUGH PLATE

T_3

T_2

A

T_1
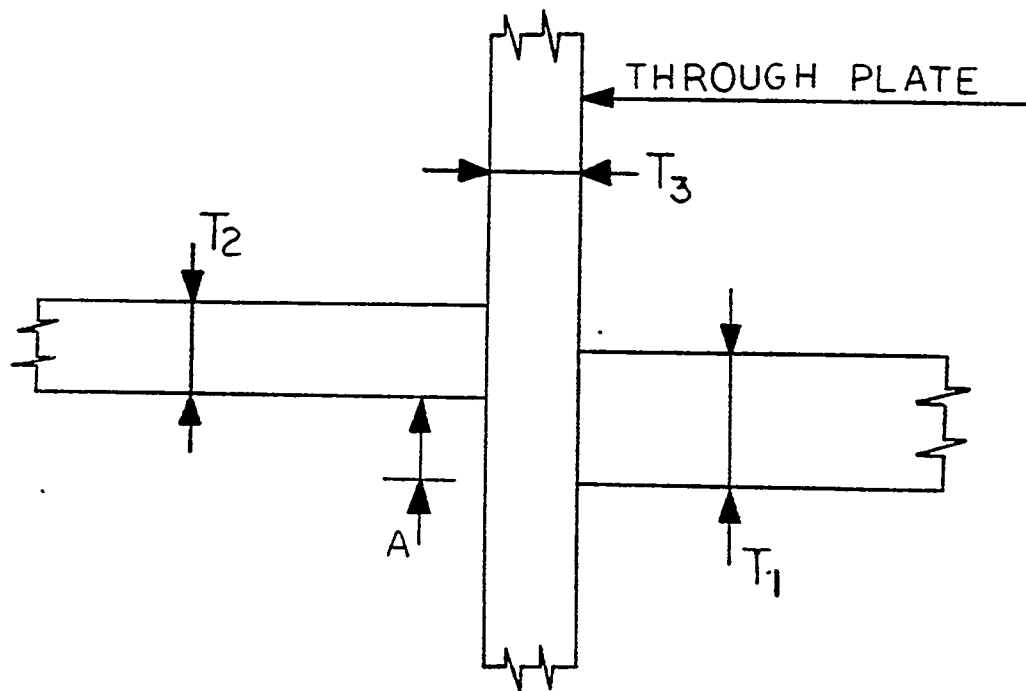
$T_1 \geqq T_2$

FIGURE 2-1

ALIGNMENT OF FILLET WELDED CRUCIFORM JOINTS

1. JSQS :   For strength   members:

   Tolerance Limit: $A \leqq 1/3 \ T_1$

   For other members:

   Standard Limit $A \leqq 1/3 \ T_2$

   Tolerance Limit $A \leqq 1/2 \ T_2$

2. PSGS :   Assembly misalignment: internal members (Stiffening)
   Out of alignment by more than 1/2 the plate or
   profile thickness will bc disconnected and realigned.

3. VIS-530:   For strength members; maximum divergence:

   $A \leqq 1/4 \ T_3 + 1/8 \ \text{in.} \leqq 1/2 \ T_2$

   For local members; maximum divergence:

   $A \leqq 1/4 \ T_3 + 1/8 \ \text{in.}$

4. IHI :   For longitudinal members within 0.6L of
   and for principal transverse supporting members:

   $A \leqq 1/3 \ T_2$

   For all others the allowable limit:

   $A \leqq 1/2 \ T_2$

5. BV: Plates are to bc properly adjusted; a slight offset
   is however tolerated over part of the lenqth of the
   joint, provided it does not exceed:

   -0.08 in.   where $T_2 < 0.25$ in.

   -0.12 in.   where $T_2 \geqq 0.25$ in

   -0.08 in.   for overhead fillet welds

2 .2.2 Butt Welds in Continous Plating

1. JSQS :   For strength members the tolerance limit:
$$A \leq 0.15 \ T \leq 0.12 \ in.$$
            For other members the tolerance limit:
$$A \leq 0.20 \ T \leq 0.12 \ in.$$

2. PSGS :   In butt welds, plate misalignment may be:
$$A \leq 0.15 \ T \leq 0.16 \ in.$$

3. VIS-530:   For plate members:
$$A \leq 0.15 \ T \leq 0.16 \ in.$$

4. 1II1:   Skin plates (bottom shell, side shell and deck
            plate) and longitudinal strength members, the
            allowable limit: $A \leq 0.15 \ T \leq 0.12 \ in.$
            Bulkhead plates and interior members, the
            allowable limit: $A \leq 0.20 \ T \leq 0.12 \ in.$

5. BV::   When assembling plates of the same thickness,
            it is to be checked that they are correctly
            adjusted in height, a slight offset is however
            tolerated where this cannot be reduced in the
            normal way, provided it is not greater than the
            greater of the values:
$$A = 0.1T + 0.04 \ in.$$
            0.08 in. for butts
            0.12 in. for longitudinal seams
            The last two values may be increased by 0.04 in.
            where the joints are double vee groove.

T-THICKNESS THINNER
MEMBER

A
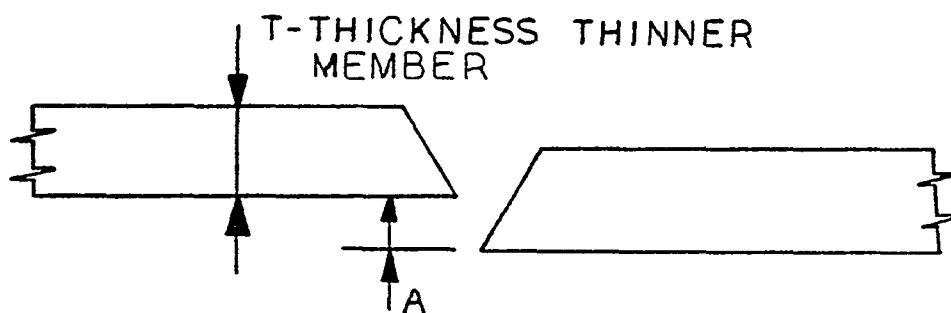
FIGURE 2-2

ALIGNMENT OF BUTT WELDED JOINTS

2.2.3 Butt Welds in Flanges And Webs

1. VIS-530:   Flange breadth (see Figure 2-3).

The maximum divergence:

$$A \leqq 0.04B \leqq 0.31 \text{ in.}$$

Flange height (see Figure 2-4).

The maximum divergence:

$$A \leqq 0.2T_1$$
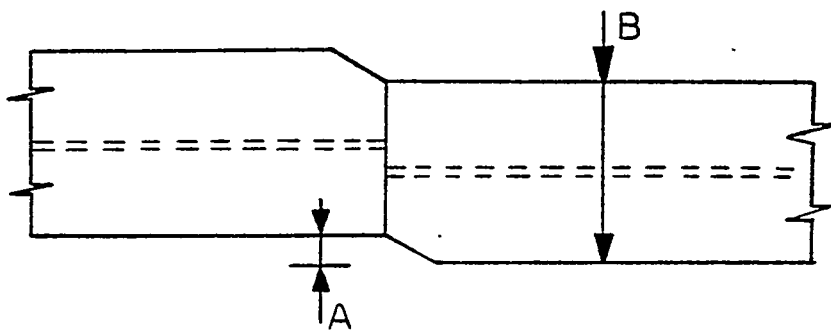
FIGURE 2-3

ALIGNMENT OF LONGITUDINAL FLANGES
W/ RESPECT TO BREADTH
(REFERENCE 2)

T_1 A 18° T_2

$T_1 \leqq T_2$
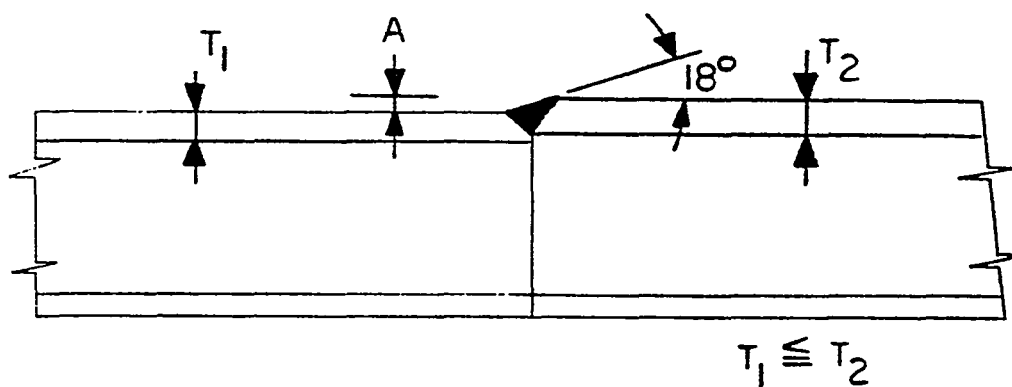
$\underline{\mathsf{FIGURE\ \ 2\text{-}4}}$

$\underline{\mathsf{ALIGNMENT\ OF\ LONGITUDINAL\ \ FLANGES}}$

$\underline{\mathsf{W/RESPECT\ TO\ HEIGHT}}$
(REFERENCE 2)

Section 3
LITERATURE SURVEY OF EXPERIMENTAL
AND THEORETICAL DATA

3.1   GENERAL

Published papers on the subject of misalignment are few, and by
their number do not reflect the industry's interest in the
problem.   A non-exhaustive review of the literature focuses
attention on two papers on fatigue which provide valuable
numerical data to this study, and on two papers on quality
assurance which could provide the framework for design guide-
lines and standards.

3.2   FATIGUE TESTING

A.   "Fatigue Strength Of Butt Joint With Misalignment",
 (Reference 12)

This paper presents the results of a study of the effect of
misalignment in butt welded joints on fatigue strength.   The
paper also seeks to find allowable amounts of misalignment
and a method for improving joint strength.

Test specimens were made of mild steel and two types of high
tensile steel with thicknesses equal to 0.25 in. and 0.63 in.and
mechanical properties as shown in Table 3-1.

The sizes and shapes of the test specimens are shown in
Figures 3-1 and 3-2, along with the ratio of the amount of
misalignment, δ , to the thickness of the specimens, T.

Two types of tests were carried out by the investigator: a
static tension test and a series of fatigue tests.

TABLE 3-1
MECHANICAL PROPERTIES
OF TEST SPECIMENS

TYPE OF STEEL	PLATE THICK (IN)	σ_Y KSI	σ_B KSI	ELONG. (%)
SS-41	0.250	39.4	63.2	24.0
	0.625	34.4	60.4	24.5
HT-50	0.250	55.5	78.5	26.0
	0.625	51.9	81.7	24.3
HT-60	0.625	79.8	96.8	12.0

GAGE LENGTH = 7.875 IN

σ_Y —YIELD STRESS

σ_B —ULTIMATE TENSILE STRESS

δ/T	0.0	0.2	0.4	0.6
δ IN	0.0	0.05	0.10	0.15

2.375 IN

3.95 IN

4.75 IN

11.0 IN

δ

T=0.25 IN
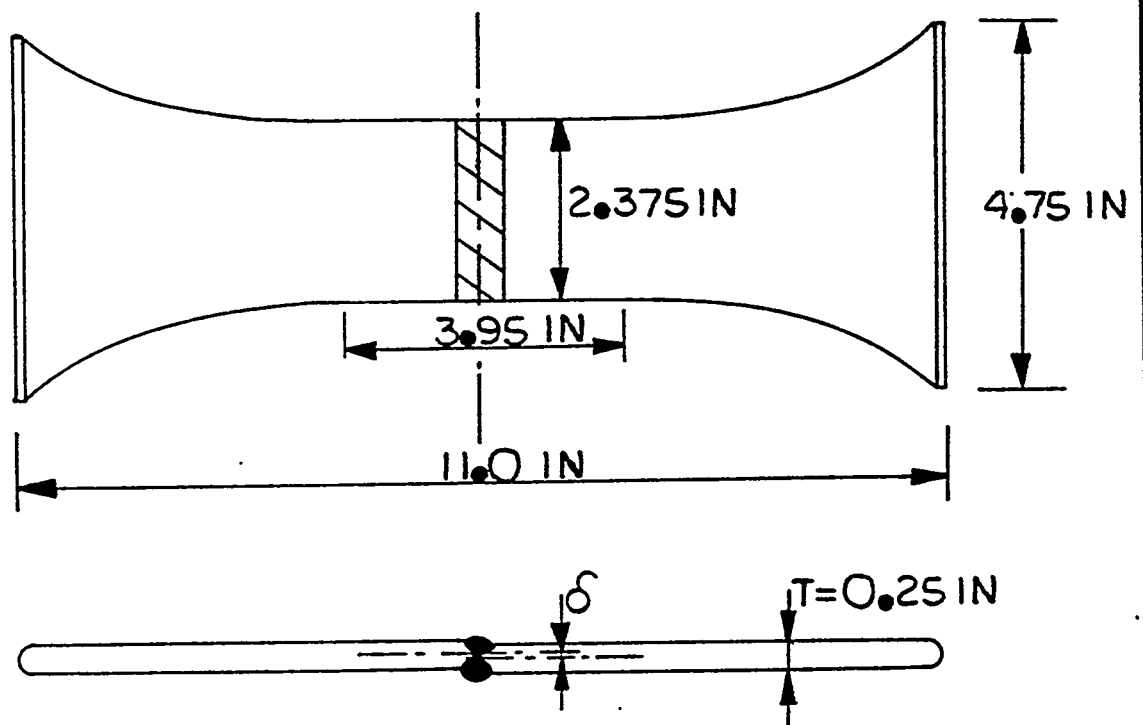
FIGURE 3-1

DETAILS OF EXPERIMENTAL

TEST SPECIMEN

δ/T	0.0	0.2	0.4	0.6
δ IN	0.0	0.125	0.25	0.375

2.375 IN

5.5 IN

3.95 IN

11.0 IN

δ

T=0.625 IN
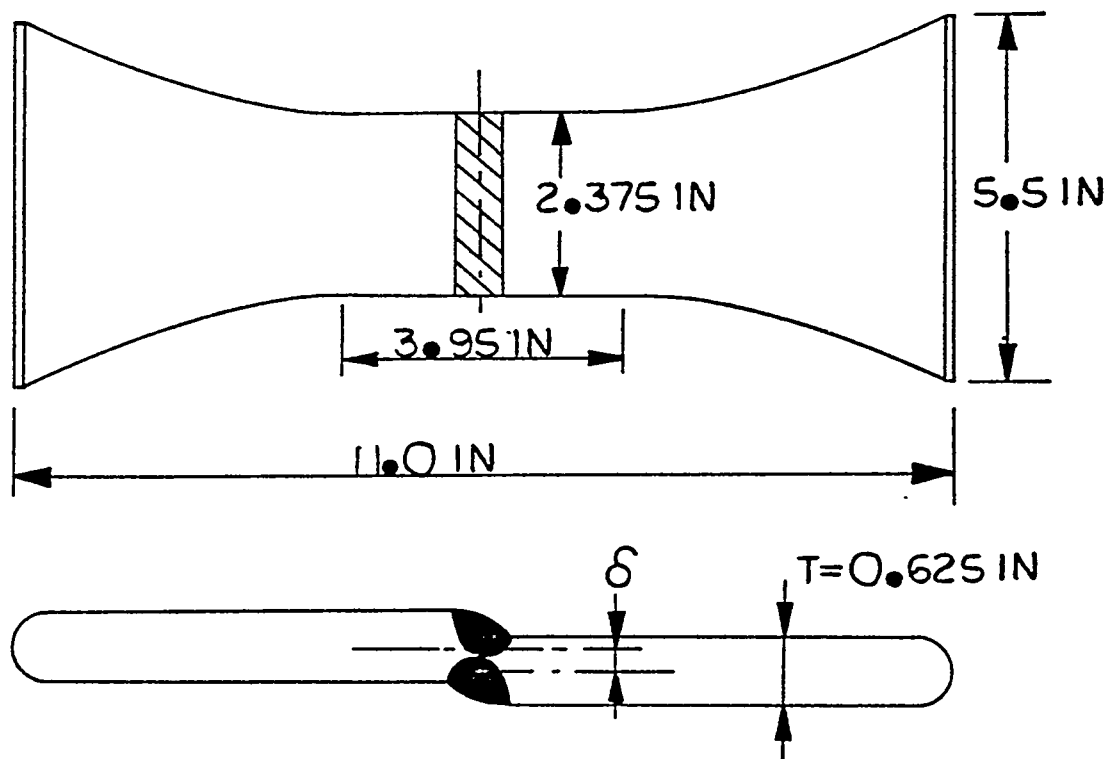
FIGURE 3-2
DETAILS OF EXPERIMENTAL
TEST SPECIMEN

The static tension tests were performed on the 0.63 in.
specimens. Results of the static tension tests are shown in
Figures 3-3, 3-4 and 3-5. The ordinate in the figures represents
the tensile stress (P/A) and the abscissa shows mean strain over
a gauge length of 3.9.5 in. including the butt welded joint. From
these results it is found that the static ultimate strength of
the test specimens decreases as misalignment ratio increases.
Figure 3-3 indicates that mild steel specimens with misalignment
ratios equal to 0.4 and less have a significant plastic deforma-
t,ion range, while the $\frac{\delta}{T}$ = 0.6 specimen sustains about half that
deformation.

Misalignment ratios of up to 0.4 appear, from a pure stress
stand point, to be acceptable. **Revised σ_B is as follows:**

$\frac{\delta}{T}$ = 0.2; σ_B =   59.0 ksi

$\frac{\delta}{T}$ = 0.4; σ_B =   57.8 ksi

$\frac{\delta}{T}$ = 0.6; σ_B =   52.0 ksi

All four specimens of HT-50 exhibit a large plastic strain zone,
and the HT-60 specimens do not.

Failure of the specimens generally occurred in the base metal.
and not in the welded ,joint.

Fatigue   tests were also performed on the mild steel specimens
while controlling tensile deformations. Figures 3-6 and 3-7
present test results for the 0.25 in. and 0.63 in. specimens, re-
spectively. Tests were run on five different configurations ranging
from a machined piece with no weld to the 0.6T misaligned welded
joint. As expected, the fatigue lives of the specimens decrease
with increase in misalignment. This decrease in fatigue life is
clearly related to the increased stress caused by stress
concentrations at the weld toe and by the eccentricity of the
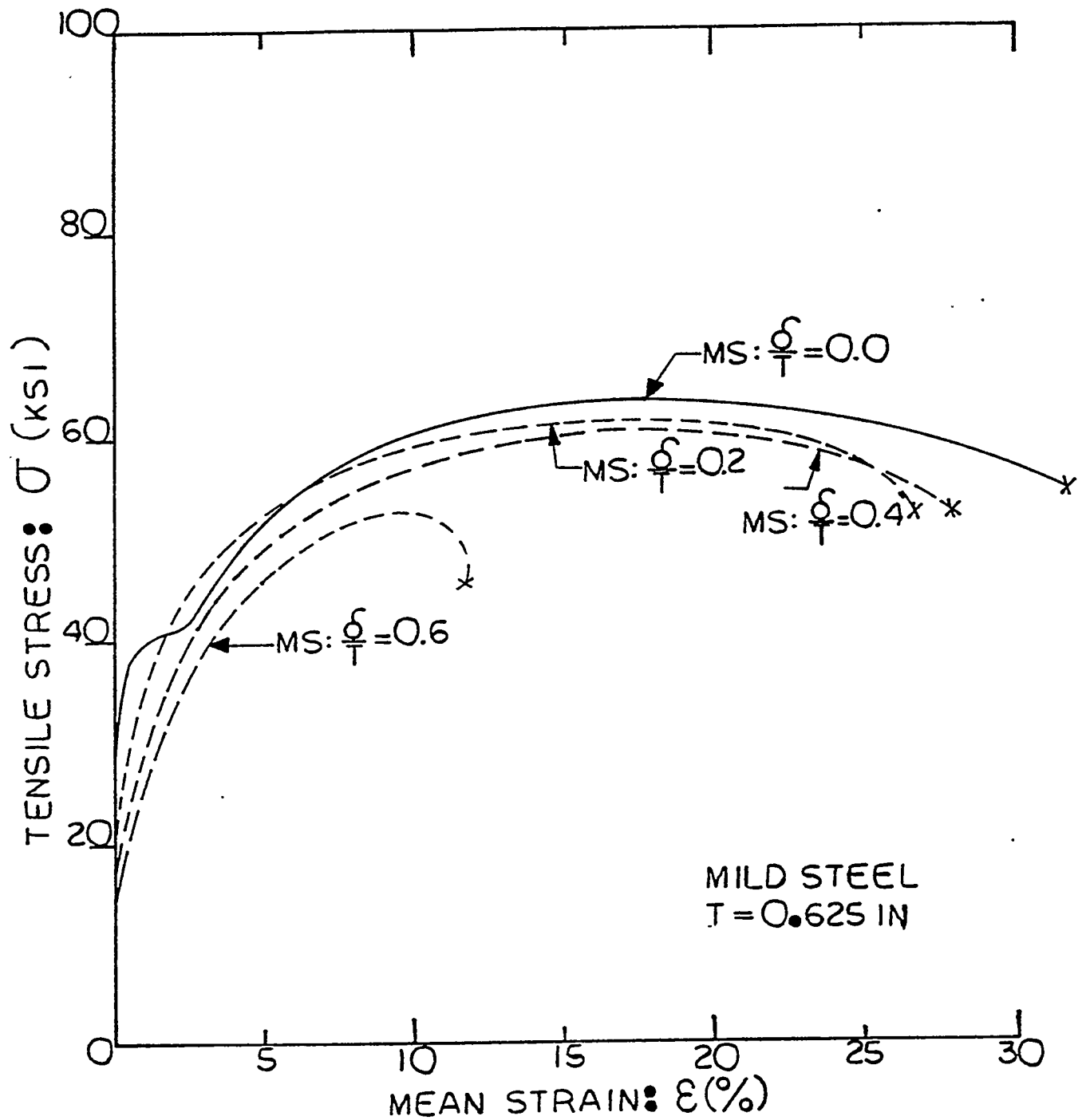
FIGURE 3-3

RESULTS OF STATIC TENSION TEST
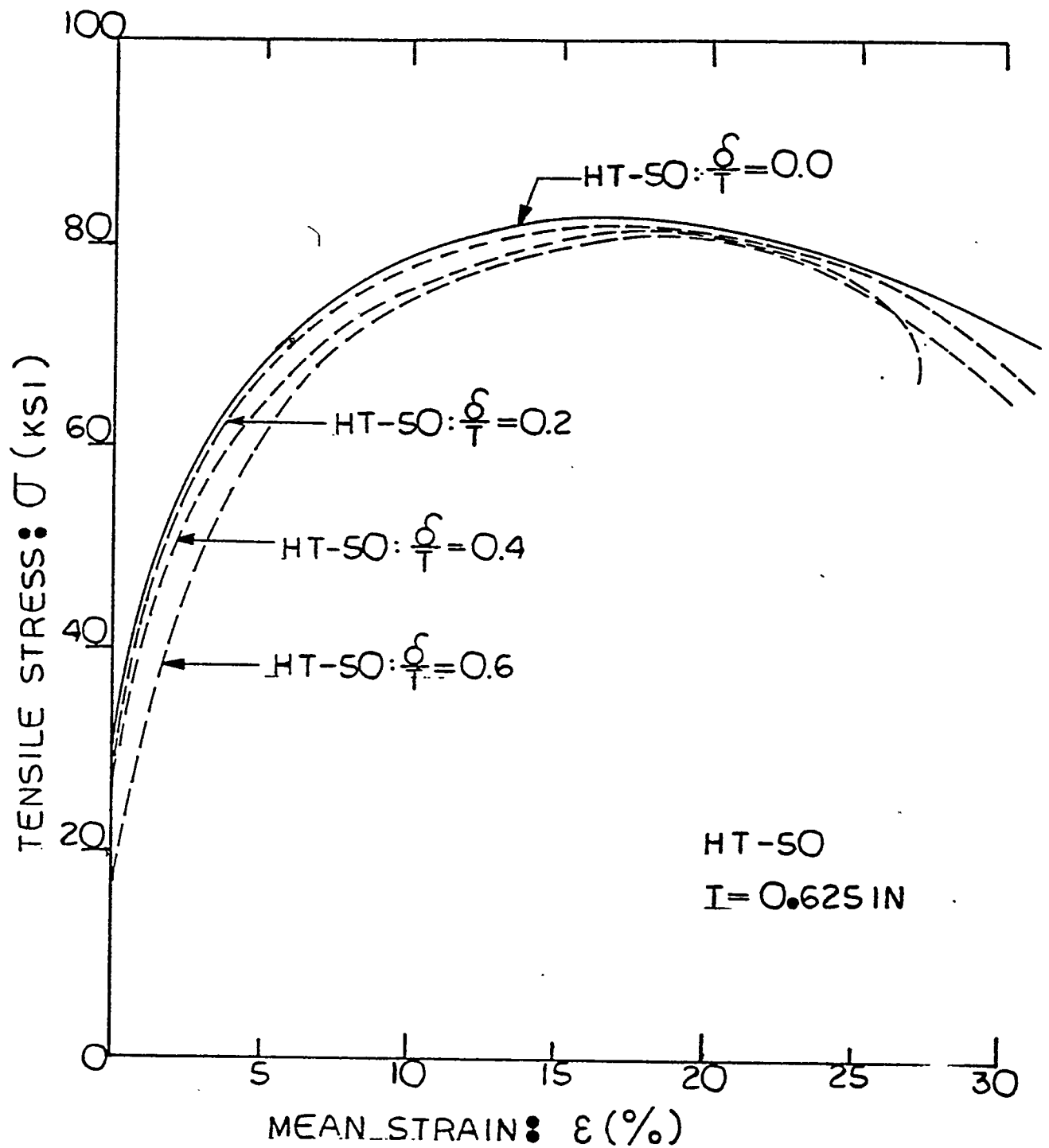
(REFERENCE 12)

FIGURE   3-4

RESULTS OF STATIC TENSION TEST

(REFERENCE 12)

3-7
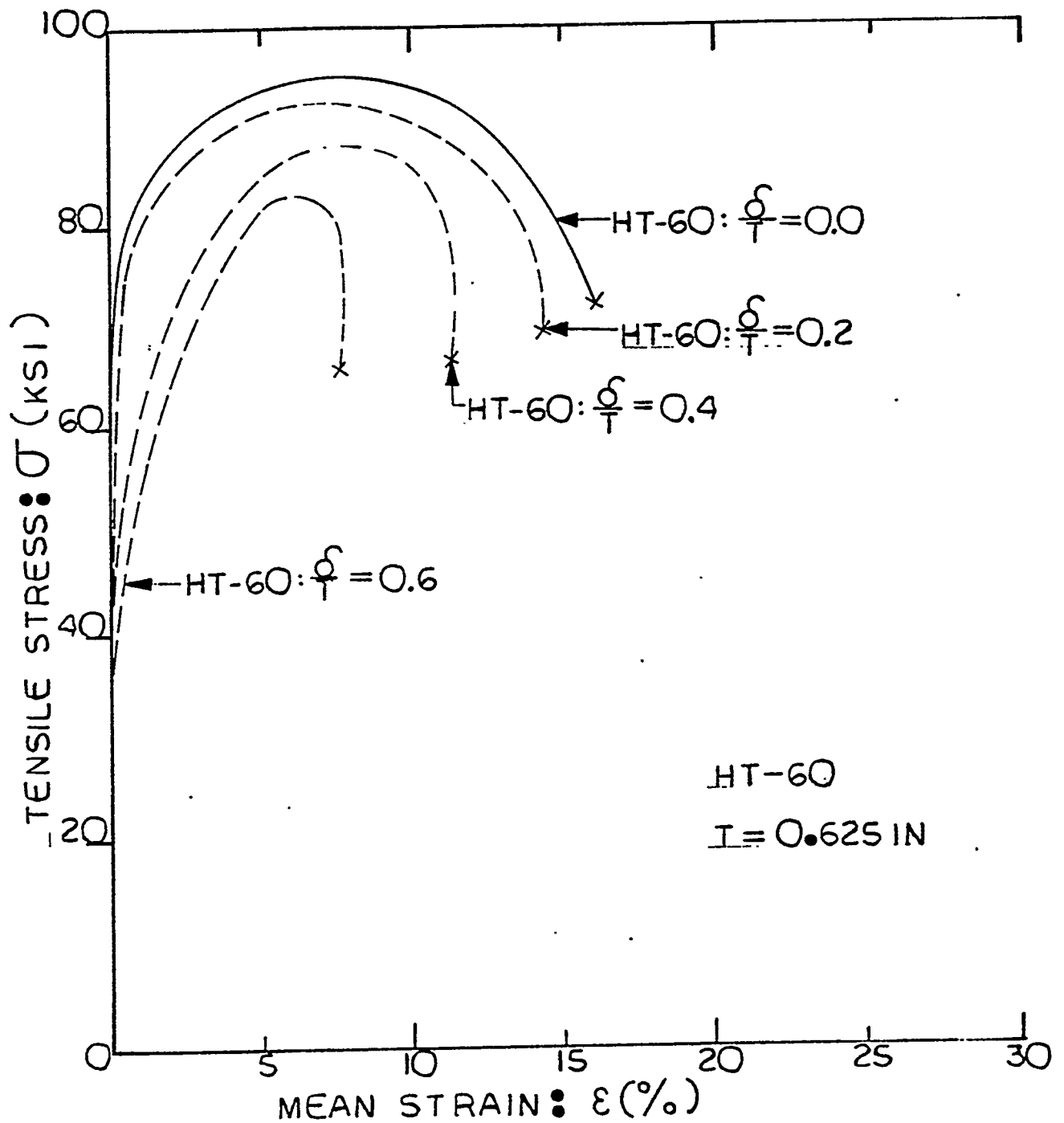
FIGURE 3-5

RESULTS OF STATIC TENSION TEST
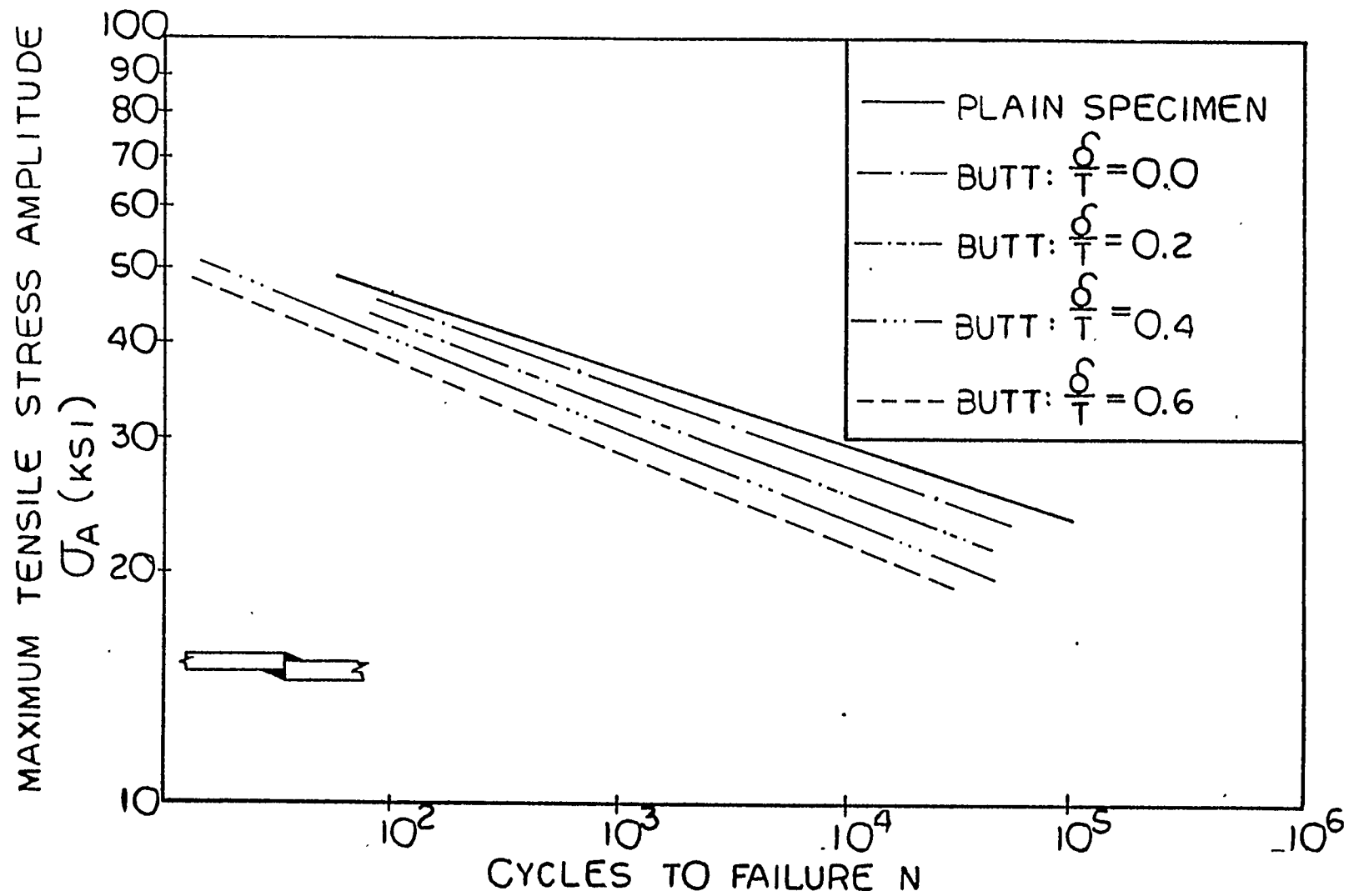
(REFERENCE 12)

FIGURE 3-6

S-N DIAGRAM FOR BUTT WELD: MILD STEEL: T = 0.25 IN

(REFERENCE 12)

3-9
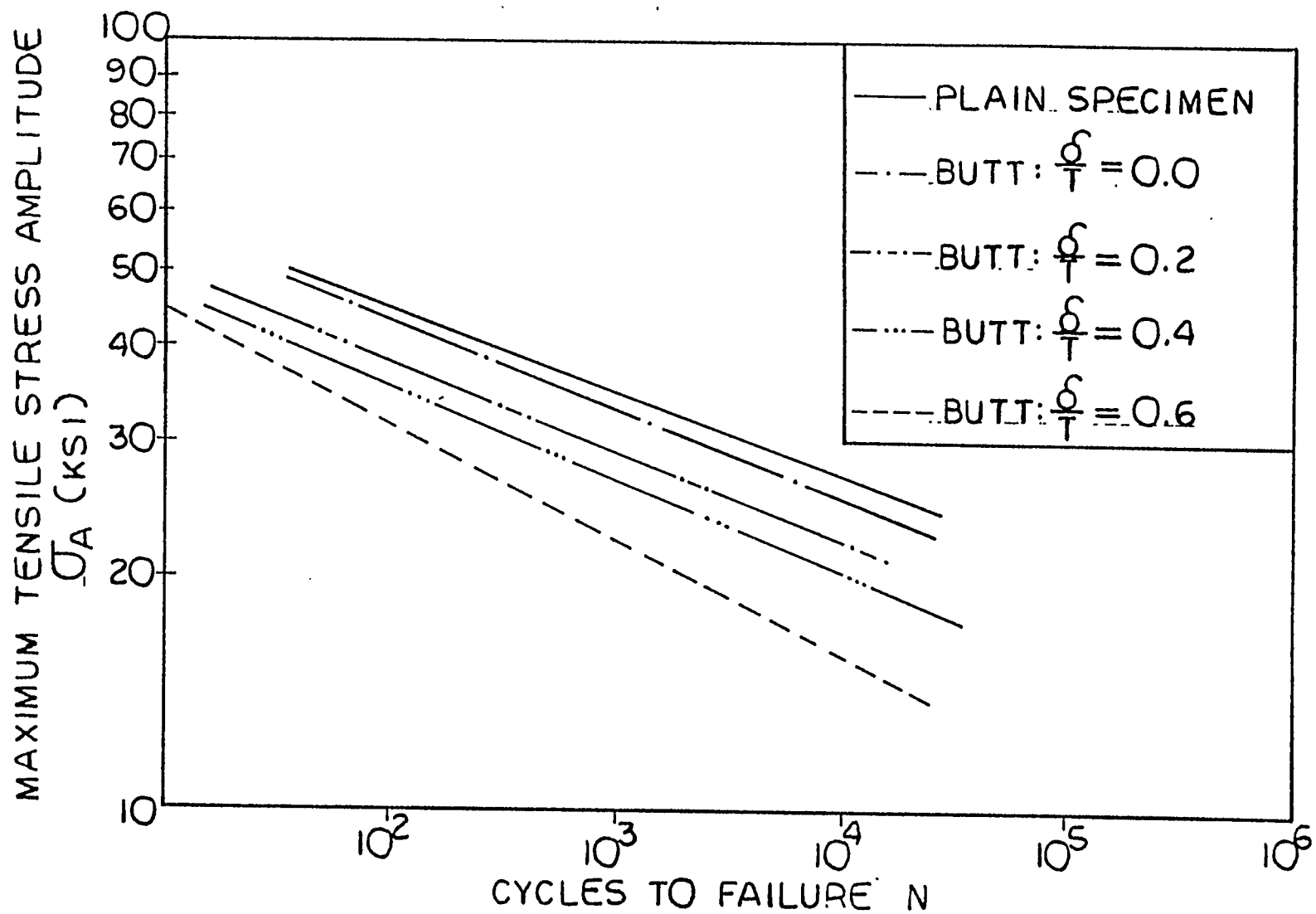
FIGURE 3-7

S-N DIAGRAM FOR BUTT WELDS: MS: T=0.625 IN

(REFERENCE 12)

misaligned plates. Although the effect of the misaligned plates
cannot easily be correted, the severity of the stress concen-
tration factor can be lessened by dressing the weld.

B.   "An Experimental Study On Reduction Of Fatigue Strength
Due To Discrepancy At Welded Joints" (Reference 13)

This study investigated the effect that misalignment has on the
fatigue strength of a cruciform joint. The test specimens used
are shown in Figure 3-8.   All specimens were of SS-41 steel,
whose mechanical properties are presented in Table 3-1. .

The specimens modeled misalignment equal to O.OT, 0.25T, O.5OT,
1.OT and 2.OT. Each specimen was tested to failure under cyclic
loading. Figure 3-9 presents the results of these tests.

Table 3-2 summarizes the effect of increasing the number of
cycles as a function of degree of misalignment. The influence
of misalignment is more significant in the high cycle range
(N = $10^3 \sim 10^5$) than in static tests.

3.3   QUALITY CONTROL AND ASSURANCE

Two references are summarized in this section. Each describes a
separate approach to the problem of evaluating the acceptability
of structural imperfections and construction errors.

A.   "The Acceptability Of Weld Defects" (Reference 16)
Although this paper deals exclusively with weld defects, the
suggestions made and methods described could be adapted to mis-
alignment. What follows a general discussion of the paper
with specific refercnce to modifications that would encompass
misalignment and structural imperfections.

The expressions "fitness for purpose", "significance of defects",
"critical defect evaluation", and "engineering critical assessment"
have been introduced in recent years as an attempt to show

P

P

T=0.375 IN

P

T=0.25 IN

14.56 IN

δ

14.56"

P

P
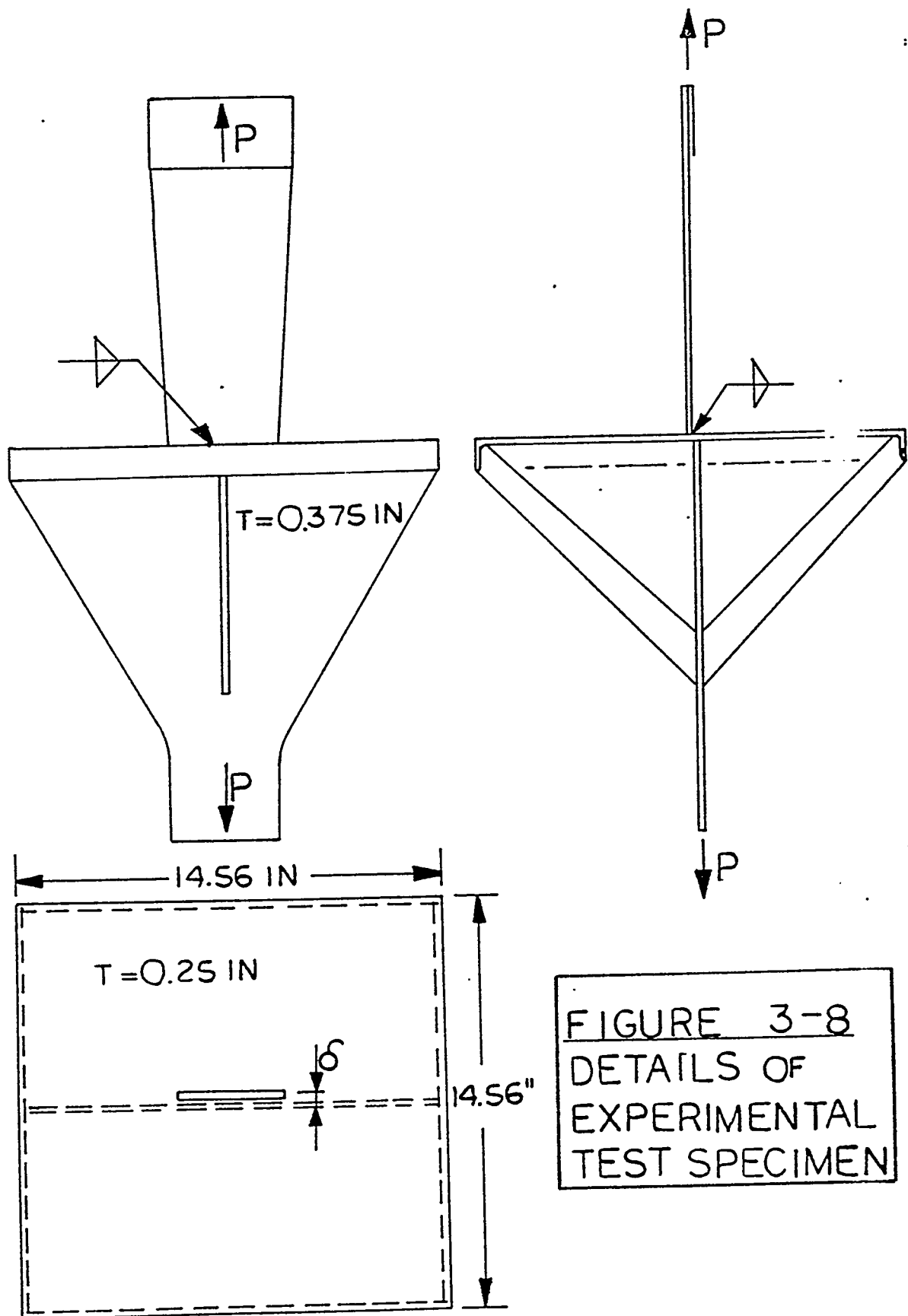
FIGURE 3-8
DETAILS OF
EXPERIMENTAL
TEST SPECIMEN

FIGURE 3-9

S-N DIAGRAM FOR CRUCIFORM JOINT

(REFERANCE 13)
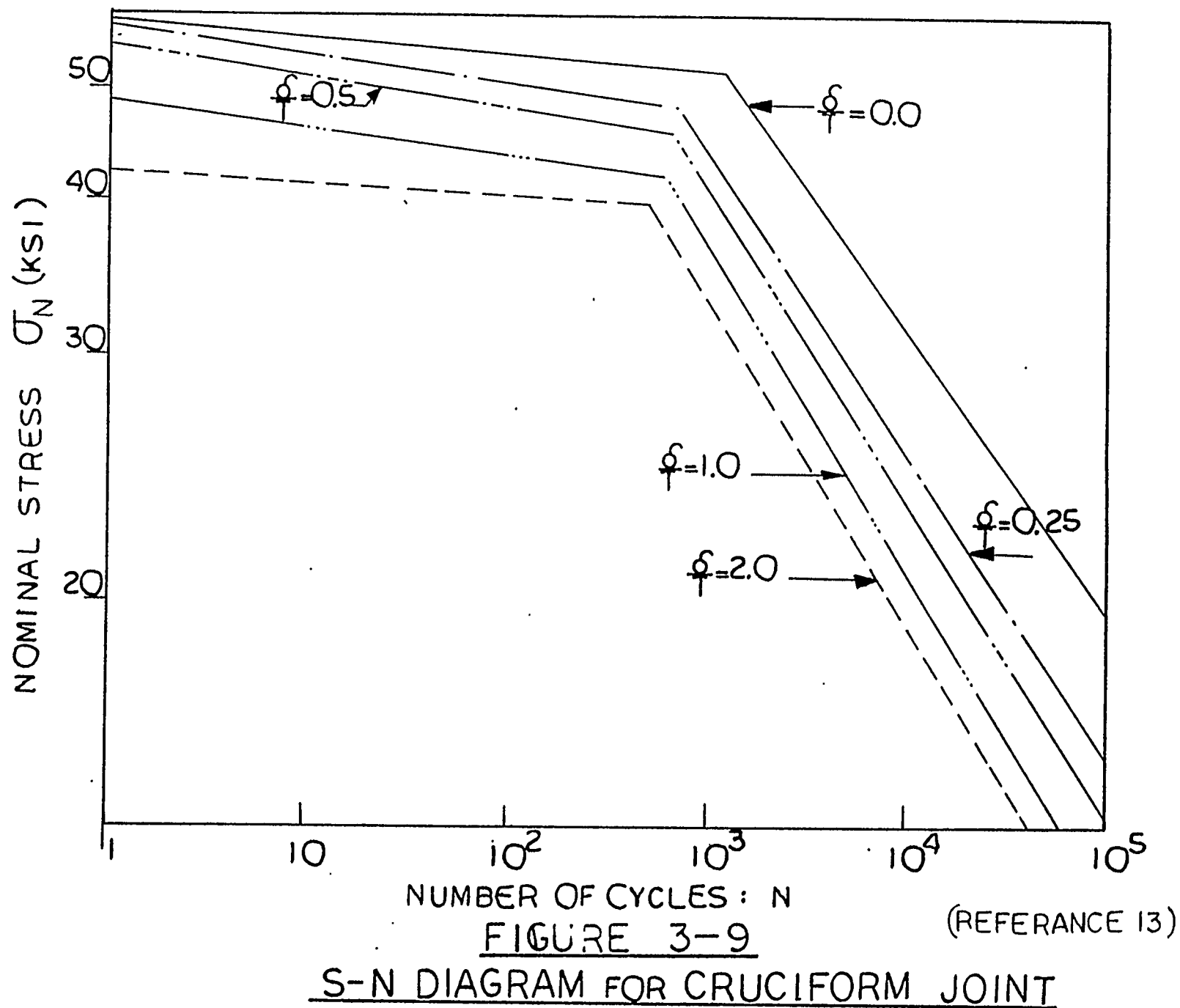
CYCLES \ δ	0MM	2MM $\left(\frac{T}{4}\right)$	4MM $\left(\frac{T}{2}\right)$	8MM (T)	16MM (2T)
$\frac{1}{2}$	100	97	93	86	78
10^2	100	96	92	83	79
10^3	100	89	85	79	72
10^4	100	85	79	73	64

TABLE 3-2

REDUCTION IN EFFECTIVENESS (PERCENT) AS A FUNCTION OF MISALIGNMENT AND NUMBER OF CYCLES

(REFERENCE 13)

justification for allowing structural imperfections to remain
and as an incentive to high quality workmanship.

Existing standards are sketchy and arbitrarily evolved. Each
classification society maintains their own set of informal
guidelines, generally not released for shipyard use.

Two strong arguments can be advanced for the adoption of
realistic acceptance standards:

1.   Economic: The labor cost involved in repairing, reinspecting
and re-repairing where necessary, while large, is probably
insignificant compared with cost of delays.

2.   Risk Factor: The danger that exists in repairing a harmless
and readily detectable defect is that a more harmful less detect-
able fault will be introduced.

The aim is not to impose standards that will result in a general
lowering of structural quality but rather to arrive at a set of
standards that are reasonable and allow the structure to perform
its intended purpose. Figure 3-10 depicts a proposal by the Inter-
national Institute of Welding Commission for Welding Standards.
Level B is the fitness for purpose quality fixed on the basis of
engineering assessment with a suitable factor of safety. Level
A is the quality level indicating good workmanship. Between
Levels A and B, no repairs are necessary but the reasons for the
loss of quality are investigated with a view to encouraging a
desirable trend towards improvement.

The following recommendations have been made for the shipbuilding
industry

1.   Each basic ship design should be divided into various areas
for the purposes of quality control and acceptance.

QUALITY ⟶

TREND TO BE ENCOURAGED

A: WORKMANSHIP STANDARD

TREND TC BE CORRECTED

NO REPAIR

B·FITNESS FOR PURPOSE STANDARC

REPAIR
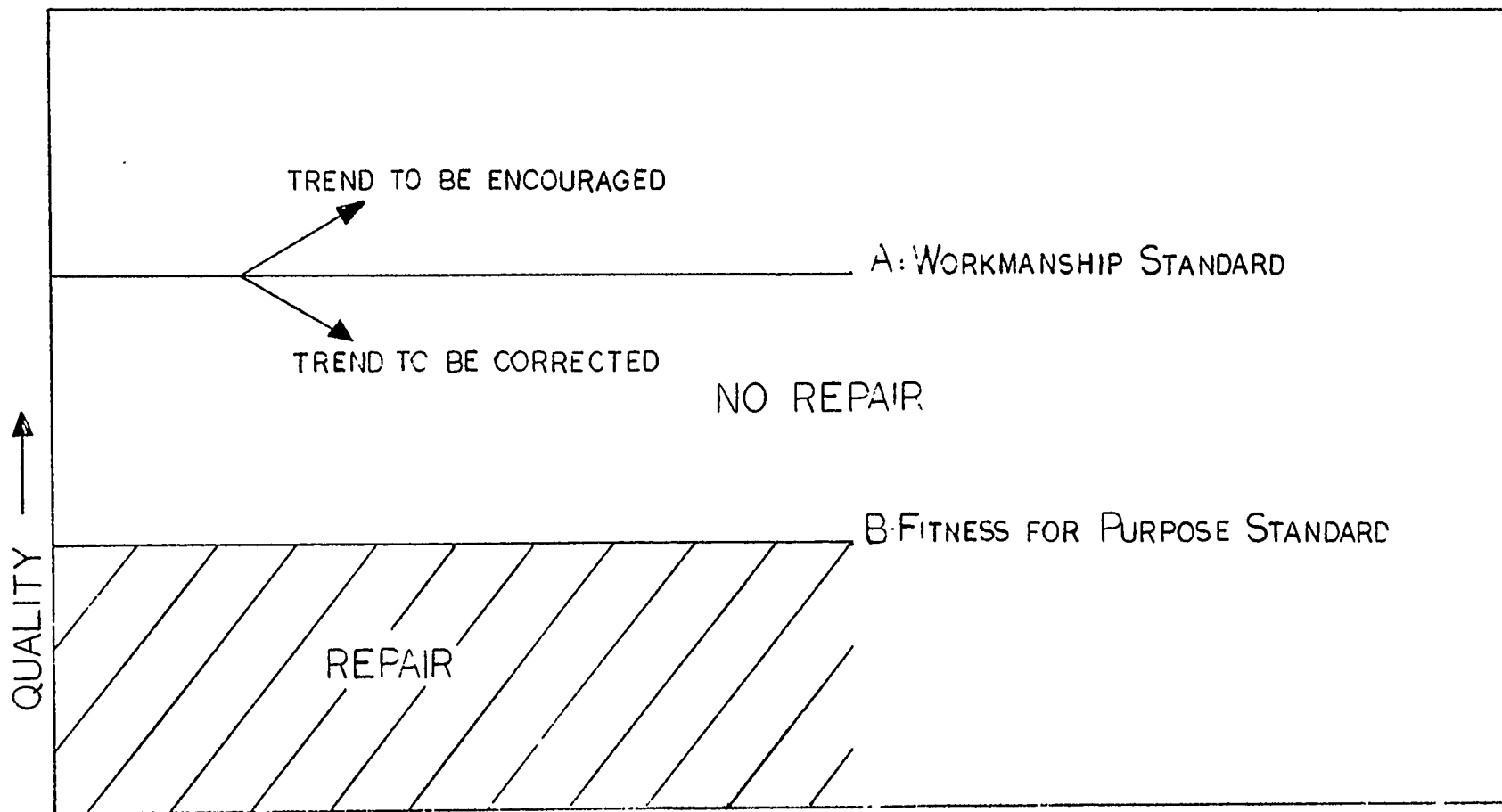
FIGURE 3-10

SCHEMATIC DIAGRAM OF QUALITY CONTROL AND ACCEPTANCE
LEVELS (REFERENCE ·16)

2.   Two sets of limits or standards should be developed for each area, one designated "Fitness For purpose" and the other known as the "Workmanship Standard".

B.   <u>"Assessment Of Imperfections In Ship Structural Design" (Reference 17)</u>

The main purpose of this paper is to describe a rational method of investigating the effect of changes in tolerance levels on structural design. Where tolerances are to be assessed it" should be possible to investigate in a rational way:

1.   The consequences of relaxing or tightening the tolerance.

2.   The consequences of varying the tolerance depending on location.

As far as structural design is concerned, the main effect of altering tolerance limits is to either increase or decrease the load carrying capacity of the structure, thus altering the safety and reliability of the structure. The areas that will affect the risk of failure of the structure are:

1.   Dimensional Control
2.   Misalignment
3.   Deformation
4.   Welding/Cutting Distortion

The importance of risk associated with these categories depends upon the consequences of failure. Too rigid a tolerance may be prohibitive in cost.

The reliability assessment system has been developed to study and determine the effects of variations around a mean value in the parameters which describe the load, response and capability of a struct,ure. This system may be used to assist in the appraised of quality control standards for geometrical varibles which, in addition to overall structural dimensions, includes imperfections and misalignment.

Structural reliability is defined as the probability that the structure will perform its intended functions for a specified time period when subjected to the operational loading conditions. A system designed to predict reliability would be used to determine acceptable tolerances.

The reliability assessment system is divided into four phases:

     Phase I: Data Base Input Stage
     Phase II: Capability Assessment
     Phase III: Loading Assessment
     Phase IV: Reliability Assessment

Phase I: Describes material scantlings, mechanical properties, construction data, and structural definition. It forms the permanent data base.

Phase II: Accurately identifies the design variables and determines type of distribution for each variable. In addition to these a capability distribution is established.

Phase III: Is a statistical definition of the wave induced
              and still water loads with necessary probability
              density functions.

Phase IV: This phase relates reliability to either damage
              or collapse.

This system could be used as a framework to help determine
permissible standards (tolerances). The shortcomings noted for
this system are that the locations of details are not considered
with respect to the overall structural configuration likewise
the consequence of failure of a detail or arrangement on the
overall behavior of the structure varies with the location of
the failure.

Section 4
RESULTS OF FINITE ELEMENT ANALYSES

4.1   GENERAL

The problem of misalignment has been discussed extensively,
but as shown in Section 3 actual data are meager. Some ship-
yards have performed finite element or other analyses on
specific alignment problems, when repair of such areas did
not appear practical or possible. However, the results of
these analyses have not been formally presented to the
industry.

For purposes of this study, finite element analyses have been
carried out. Three types of joints have been studied:
fillet welded cruciform, full penetration welded cruciform
and butt welded. In-plane loading has been investigated
for varying degrees of misalignment. The results obtained
from these analyses, while not complete, will with good
engineering judgement facilitate the development of criteria
for a variety of misalignment conditions. It is also hoped
that this information may be helpful in assessing cases not
covered in this study.

4.2   COMPUTER PROGRAM DESCRIPTION

All investigation and analysis has been performed utilizing
the Ices Strudl-II Computer Program.

Strudl uses a finite clement method where the element stiff-
ness malrix is computed from energy considerations, after
sc lecting a displacement or force expansion over the element,
and assuming that displacements or force quantities in the

interior of the element depend on nodal quantities.   The
stiffness analysis is a linear, elastic, static, small dis-
placement analysis where joint displacements are treated as
unknowns.   For elements the analytic procedure provides
stresses or stress resultants and couples, principal stresses,
strains, and principal strains, usually computed at the
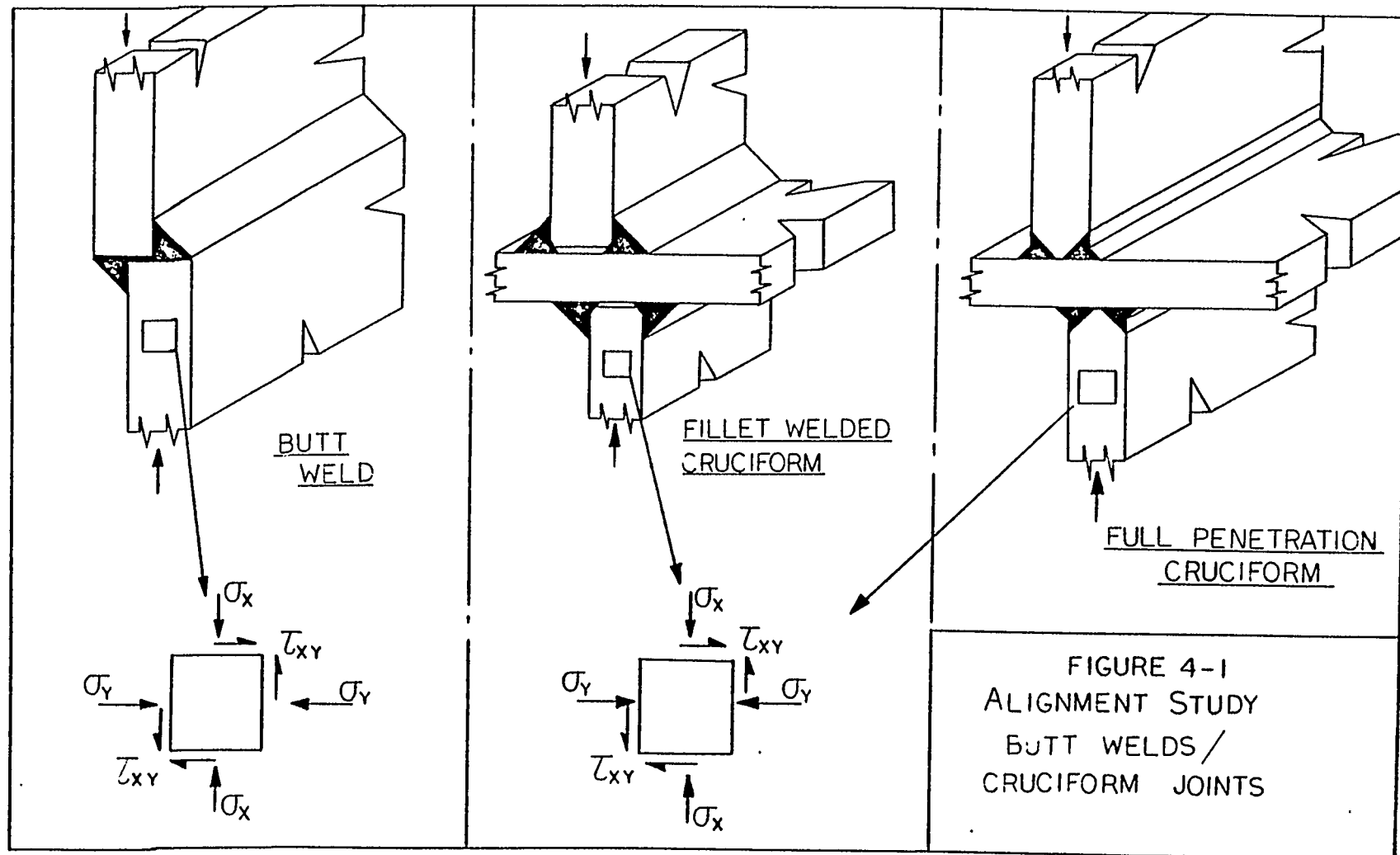centroid of each element.

For additional program documentation and the description of
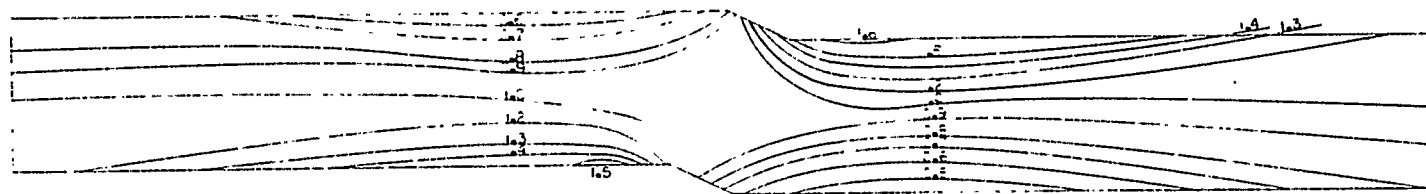plane strain methodology see References 18 and 19.

4.3   FINITE ELEMENT RESULTS

4.3.1 Elastic Analysis of Butt Welded Joints

The basic form of the butt welded joint used in this investi-
gation is shown in Figure 4-l.   Figures 4-2 through 4-6
present the finite element models used in the analysis.
Misalignment of 6   = 0.20T to   = 1.00T in increments
of 0.20T was investigated.   Plane strain elements have been
used because the plate is assumed to be long in the Z-direction
with a uniformly distributed in-plane load.   The deformation of
the body at some distance from the ends is independent of the
Z-coordinates and the displacements are functions of X and Y
only.   If the ends of the plate are prevented from moving in
the Z-direction, then **W** is zero there.   At the midsection of
the plate, by symmetry W must also be zero.   Thus the assump-
tion that W is zero at every cross section of the plate.   In
such a case, the strain components:

$$\varepsilon_x = \frac{\partial u}{\partial x} \qquad \varepsilon_Y = \frac{\partial v}{\partial Y} \qquad \gamma_{XY} = \frac{\partial u}{\partial Y} + \frac{\partial v}{\partial x}$$

BUTT
WELD

σ_X

τ_{XY}

σ_Y σ_Y

τ_{XY}

σ_X

FILLET WELDED
CRUCIFORM

σ_X

τ_{XY}

σ_Y σ_Y

τ_{XY}

σ_X

FULL PENETRATION
CRUCIFORM

FIGURE 4-1
ALIGNMENT STUDY
BUTT WELDS /
CRUCIFORM JOINTS

CASE 2
FINITE ELEMENT MODEL
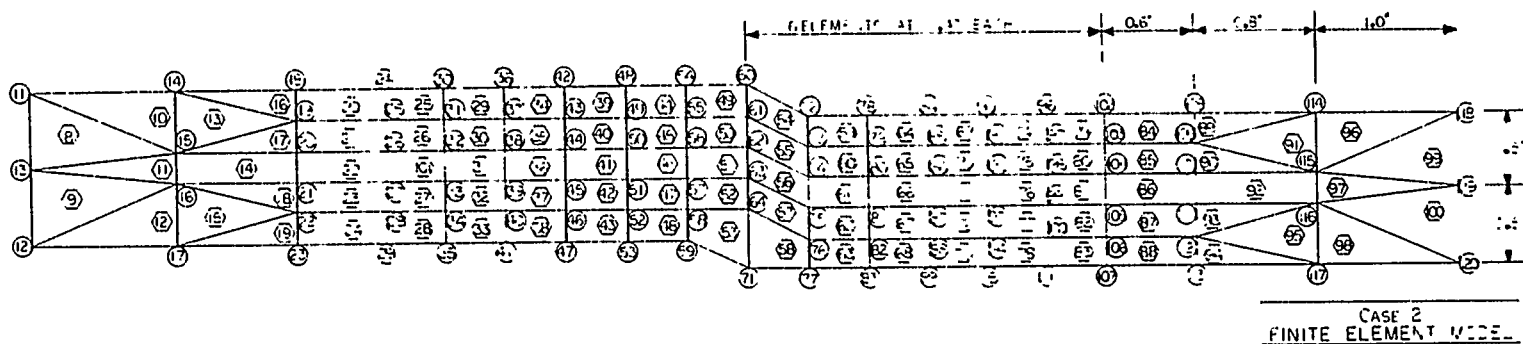
CASE 2
STRESS INTENSITY PLOT

FIGURE 4-3

ALIGNMENT STEPS

CATEGORY 18 BUTTS AND SEAMS

IN PLATING

CASE 28 0.2T MISALIGNMENT

O - NODE NUMBERS
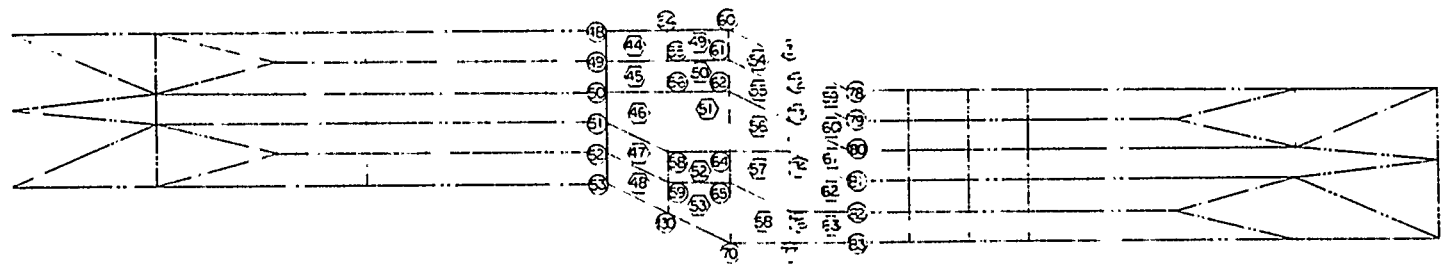
O - ELEMENT NUMBERS

CASE 3
FINITE ELEMENT MODEL
FOR ADDITIONAL DETAILS SEE CASE 2
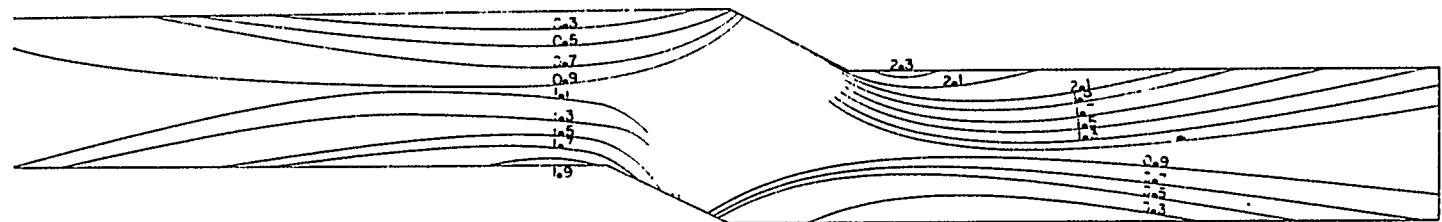
CASE 3
STRESS INTENSITY PLOT

FIGURE 4-3

ALIGNMENT STUDY
CATEGORY I: BUTTS AND SEAMS
IN PLATING
CASE 3: 0.4T MISALIGNMENT

O - NODE NUMBERS
⬡ - ELEMENT NUMBERS

4-5
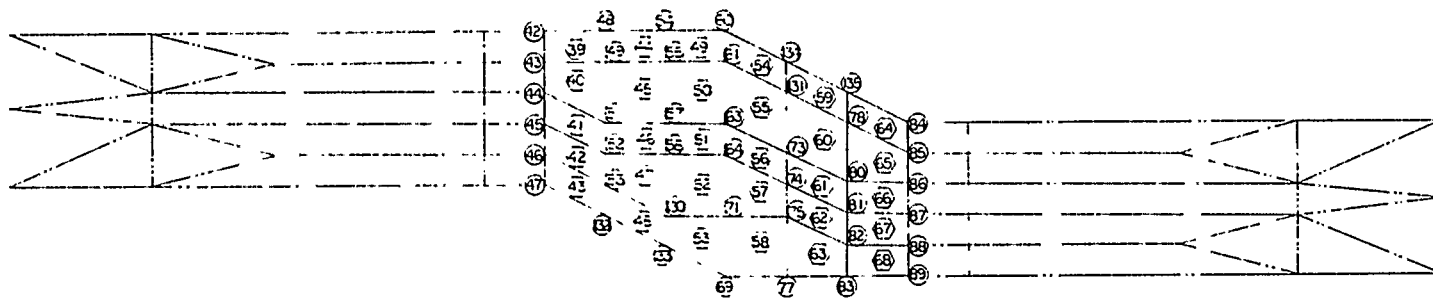
CASE 4
PLATE ELEMENT MODEL
FOR ADDITIONAL DETAILS SEE CASE 2
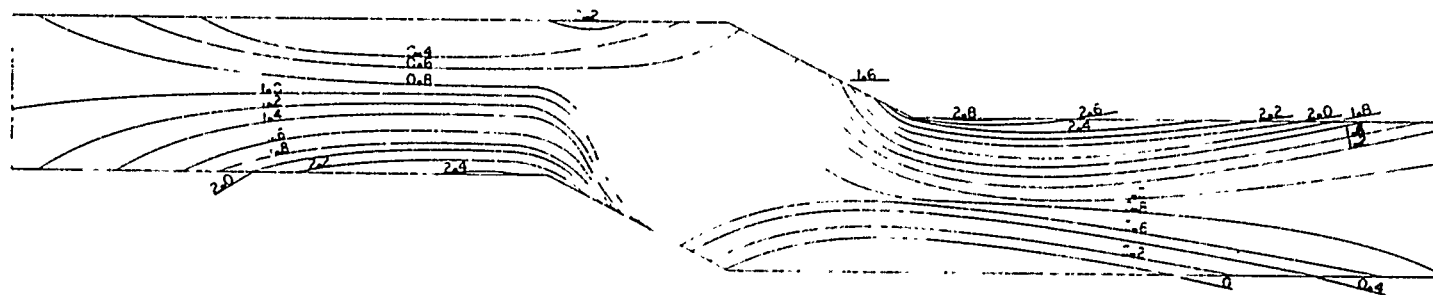
CASE 4
STRESS INTENSITY PLOT

FIGURE 4-4
ALIGNMENT STUDY
CATEGORY I: BUTTS AND SEAMS
IN PLATING
CASE 4: 0.6 MISALIGNMENT

○ — NODE NUMBERS
⬡ — ELEMENT NUMBERS
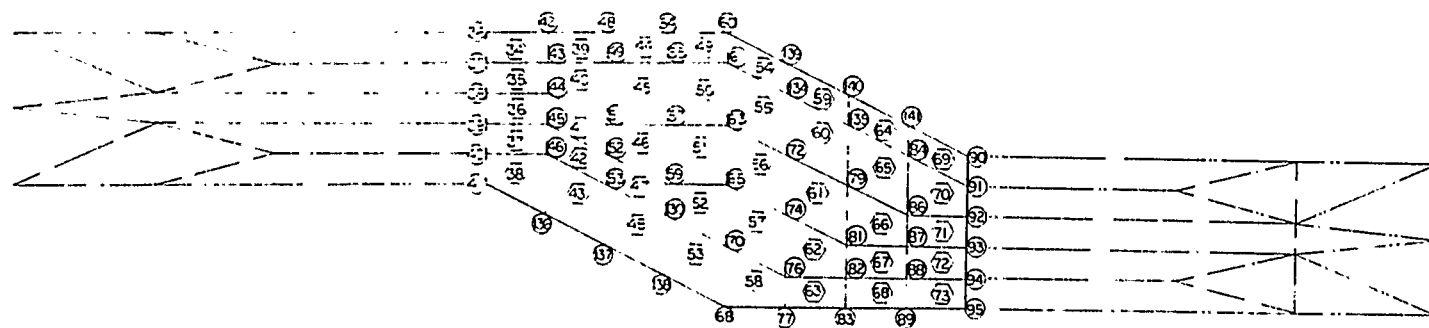
CASE 5
FINITE ELEMENT MODEL
FOR ADDITIONAL DETAILS SEE CASE 2
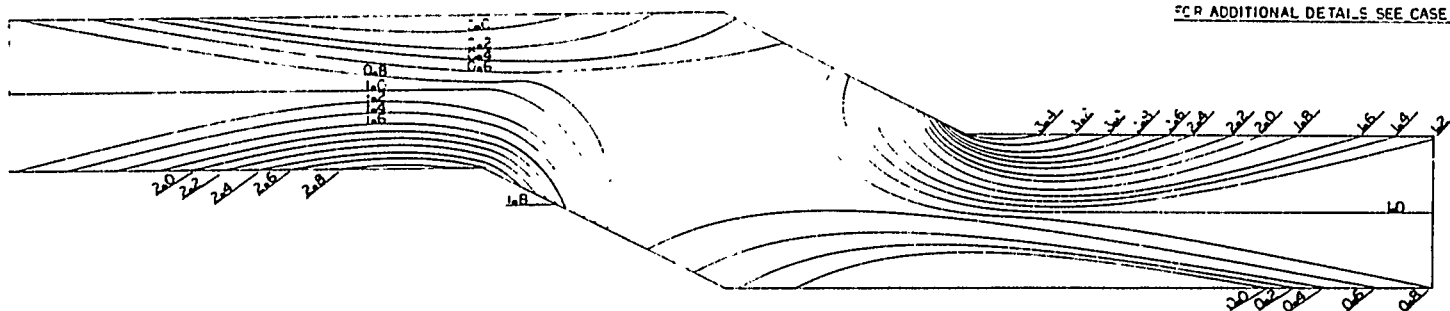
CASE 5
STRESS INTENSITY PLOT

FIGURE 4-5
ALIGNMENT STUDY
CATEGORY I: BUTTS AND SEAMS
IN PLATING
CASE 5: C₆8T MISALIGNMENT
○ - NODE NUMBERS
○ - ELEMENT NUMBERS

CASE 6
PLATE ELEMENT MODEL
FOR ADDITIONAL DETAILS SEE CASE 2

CASE 6
STRESS INTENSITY PLOT

FIGURE 4-6
ALIGNMENT STUDY
CATEGORY I BUTTS AND SEAMS
IN PLATING
CASE 6 JOT MISALIGNMENT
◯ - NODE NUMBERS
□ - ELEMENT NUMBERS

are functions of X and Y only and the strain components:

$$\epsilon_z = \frac{\partial w}{\partial z} \qquad \gamma_{xz} = \frac{\partial w}{\partial x} + \frac{\partial u}{\partial z} \qquad \gamma_{yz} = \frac{\partial w}{\partial y} + \frac{\partial v}{\partial z}$$

are equal to zero.
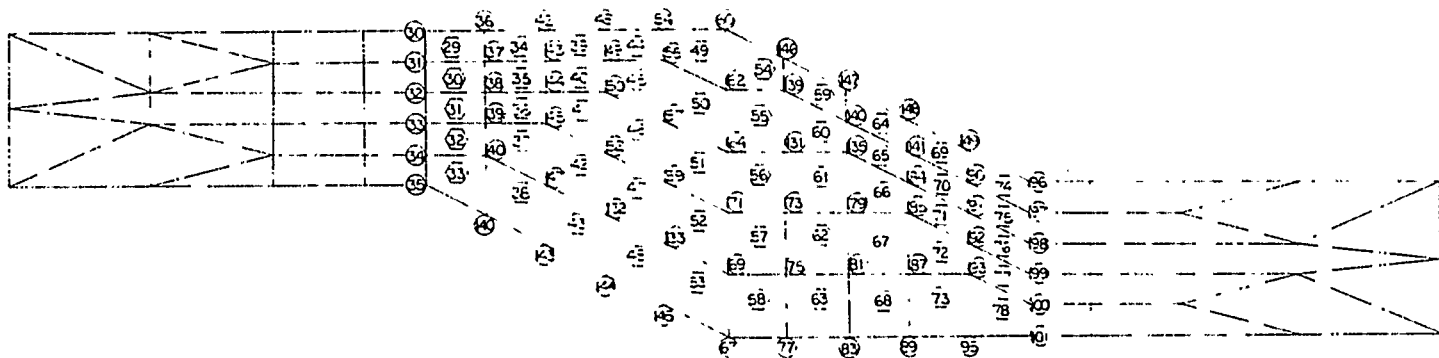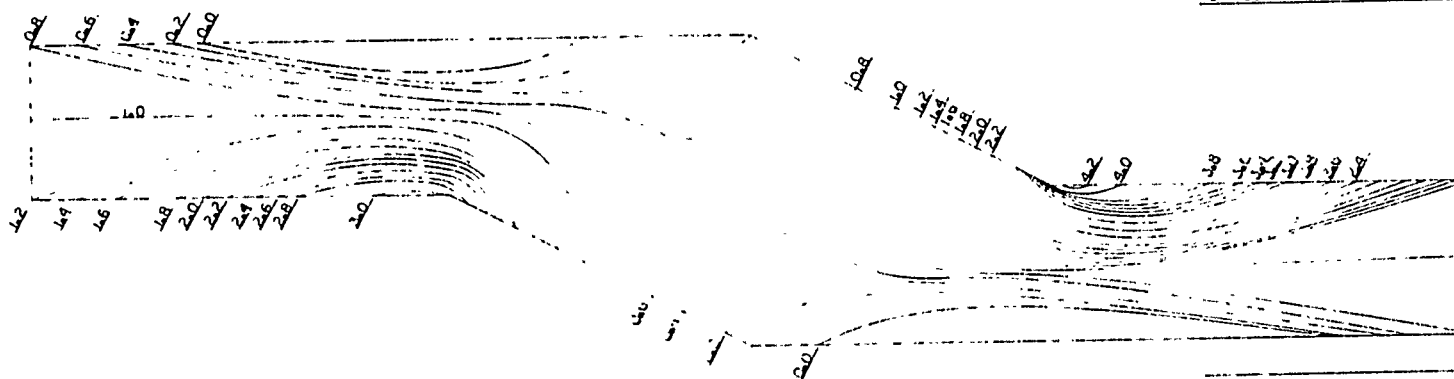
A uniaxial compressive load was applied with a magnitude equal to P (^{LB}/IN.)acting over a cross-sectional area equal to A (IN.^{2}/IN.l,such that in the aligned case, the axial . stress (σ_x) was uniform and equal to:

$$\sigma_x = \frac{P}{A}$$

The compressive load does not detract from generality, since linearity of response assures equal absolute stress magnitudes for an applied tensile load.

Stress intensity factors, i.e. stress amplification of the mean stress for the misaligned butt welds have been plotted in Figures 4-2 through 4-6. A stress intensity factor of 1.0 is the ideal design condition.

The stress intensity plots indicate maximum stress concentrations at the toes of the welds. Gurney in Reference 20 has investigated and reported on the effect and magnitude of these stress concentrations.

The stress intensity plots for the welded butt joints have **been constructed from the** σ_x (axial) stresses since these are the dominant stress components.

Table 4-1 presents a synopsis of the stress intensity plots with corresponding maxima for each case of misalignment.

MISALIGNMENT δ: T-THICKNESS	MAXIMUM STRESS INTENSITY FACTOR	$\dfrac{\sigma_{ALL.}}{\sigma_{ACTUAL}}$
0.2 T = 0.2 IN.	1.67	0.60
0.4 T = 0.4 IN.	2.35	0.43
0.6 T = 0.6 IN.	2.90	0.34
0.8 T = 0.8 IN.	3.50	0.29
1.0 T = 1.0 IN.	3.90	0.26

TABLE 4-1

FINITE ELEMENT ANALYSIS RESULTS

FOR WELDED BUTT JOINTS

The stress intensity factor, as stated earlier, is the factor by which the peak stress exceeds the mean or P/A stress across the section. The third column in Table 4-1, σ All/σ Actual, is the inverse of column 2, namely the ratio of mean section stress to maximum acceptable stress. The elongation for the total length of the model, i.e., 9.6 inch, For $\frac{e}{T}=0.0$ is 0.0064 inch.

Figure 4-7 represents a modified plot of data in Table 4-1. The abscissa indicates percent misalignment with respect to plate thickness; the ordinate represents the ratio of average stress to allowable stress, where the allowable stress is established by the designer. Three possible values of allowable stress are assumed: $0.6\sigma_Y$, incipient yield, and total yielding.

The curves are drawn against individual ordinates to provide a visual measure of permissible load amplitudes. Zone 1 is limited by a peak stress of $0.6\sigma_Y$ Zone 2 is limited by σ_{YIELD}, i.e. yield at some point in the structure, and Zone 3 by $\sigma_{ULTIMATE}$, where the latter is defined not as tensile failure but as the level at which the entire cross-section reaches yield.

The applicability of this data is essentially limited to statically loaded members, where the attainment of partial yielding is generally accepted. Consequently a design guideline would most likely use the curve for $\sigma_{ALL} = \sigma_{YIELD}$. For example, For- $\sigma_{ALL} = \sigma_{YIELD}$ the average static stress with $\frac{e}{T}$ = 0.5 could be approximately $0.45\sigma_Y$, i.e. 15 KSI for a steel with σ_Y = 33 KSI.
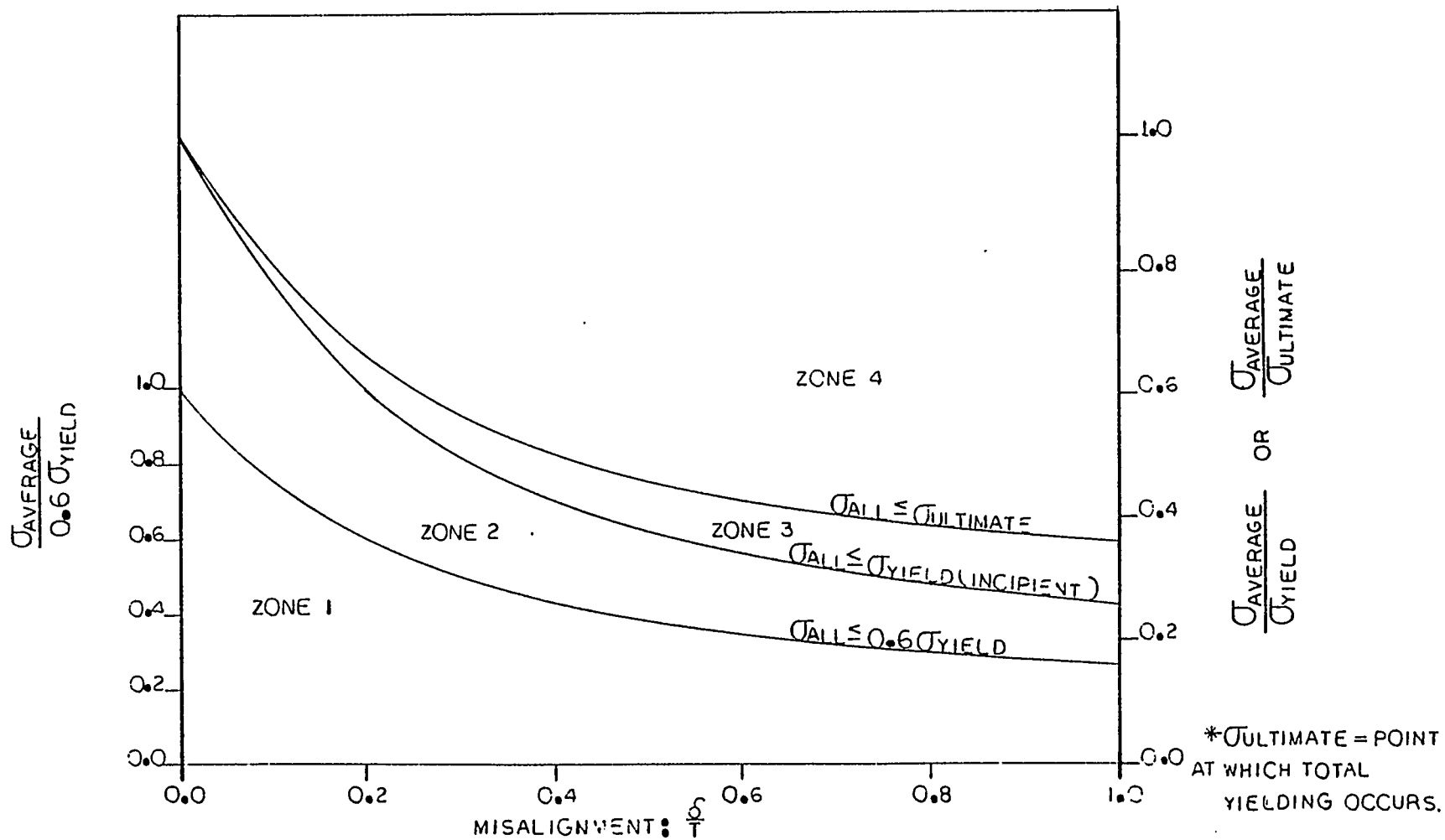
4-11

FIGURE 4-7: WELDED BUTT JOINTS/MISALIGNMENT VERSUS STRESS RATIO

4.3.2 Plastic Analysis of Butt Welded Joints

Generally, localized yielding will not be detrimental to the
structural integrity of the ship. Therefore some structural
elements may be stressed above the elastic limit. This
section discusses how the finite element method has been
used to determine the elasto-plastic response of structural
configurations considered in this study.

The elastic response of a structure for any given load
condition can be checked against the capability of the
structure. By this process the adequacy of the design can
be evaluated. The designer often performs a sophisticated
elastic analysis of the structure and is then forced to make
a series of simplifying assumptions when determining the
capability, thus negating the value of the analysis.

The finite element method has been used in this investigation
of the elasto-plastic behavior of plate structures. The
approach is a linear step-wise procedure. The method assumes
the structure behaves linearly and that the total stiffness
matrix can be formed by considering the geometry and material
properties associated with the individual elements at that
particular step. The analysis is accomplished in the follow-
ing manner:

1.   An initial load is chosen within the elastic range.

2.   The Stiffness matrix for the structure is formed
     based on the element material properties.

3.   Load is increased until at least one element nodal
     stress reaches σ_{YIELD}.

4.   Elements that indicate yielding are replaced with an
      artificial force system, which is equilibrated to
      the resistive body forces at yield.

5.   Combined elastic Properties and the artificial load
      system are used to continue the analysis.

6.   The process is repeated until a transverse section of
      the structure experiences total yielding.

(For additional details see Reference 21.)

The case of 1.OT misalignment is the only condition investi-
gated in this analysis, and the data have been used to
extrapolate from the incipient yield curve to provide results
for all intermediate cases of misalignment.

The extrapolation is made by reducing the ratio of σ_{Ult}/σ
Yield at $\frac{\delta}{T}$ **= 1.00 by the value of** $\frac{\delta}{T}$ **, thus accounting for**
the fact that at $\frac{\delta}{T}$ = 0 initial and total yielding occur
simultaneously.

Figure 4-8 represents the process of progressive yielding of
elements and Figure 4-7 shows the extrapolated curve for
σ_{ALL} = $\sigma_{ULTIMATE}$. Appendix A discusses the calculations
necessary for replacing the yielded element with the resis-
tive force system. Results of this analysis reveal that the
total yield load is forty percent greater than the incipient
yield load at $\frac{\delta}{T}$ = 1.0.

4.3.3 <u>Elastic Analysis of Fillet Welded Cruciform Joints</u>
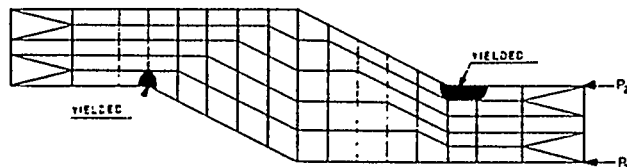
The basic form of the joint and of the finite element model
used in this investigation of the fillet welded cruciform
joints is shown in Figures 4-9 to 4-13. Misalignment from
 6 = 0.0T to 6 = L.OT in increments of $\frac{\delta}{T}$ = 0.20 was
investigated. Plane strain elements with a thickness equal
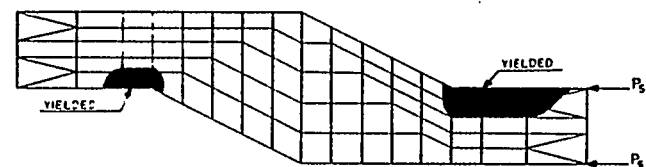to 1 inch for the misaligned members and 1/2 inch and 1 inch for

4-14
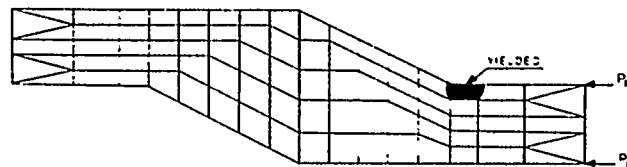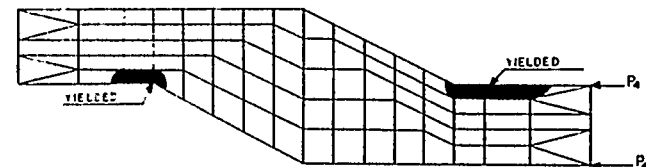
DETAIL A

DETAIL D

DETAIL B

DETAIL E
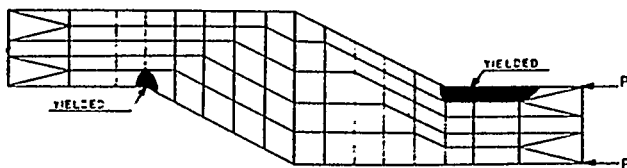
DETAIL C

FIGURE 4-8

WELDED BUTT JOINTS
MISALIGNMENT = 1.0 T
RESULTS OF INCREMENTAL
PLASTIC ANALYSIS
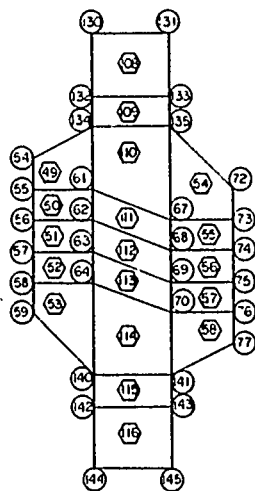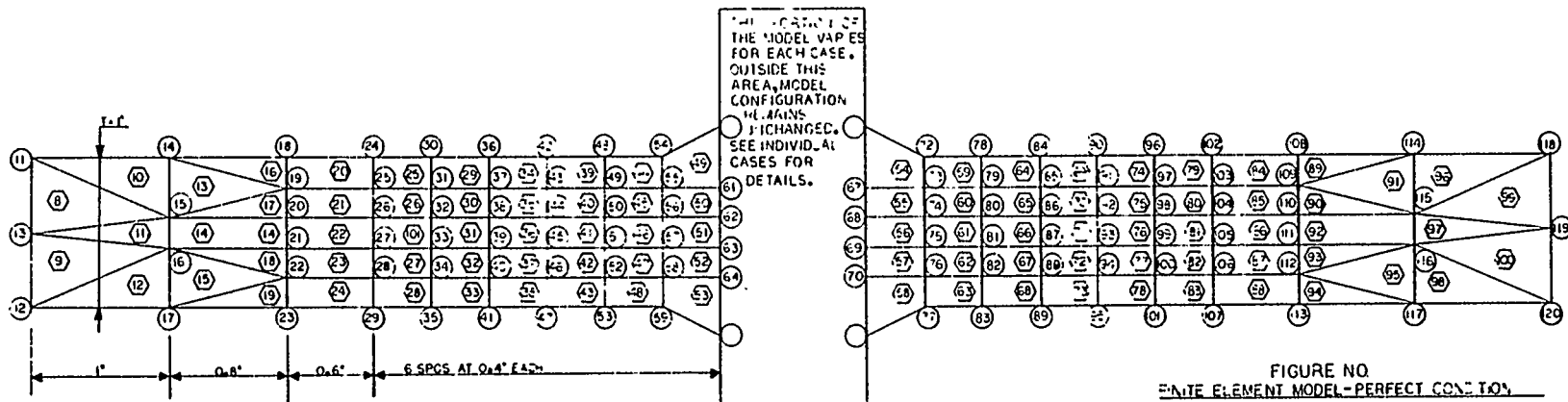
FIGURE NO.
FINITE ELEMENT MODEL-PERFECT CONDITION

CASE 1: 0.2T MISALIGNMENT
FULL PENETRATION WELD
THROUGH PLATE THICKNESS
=0.5T

CASE 2: 0.2T MISALIGNMENT
FILLET WELD
THROUGH PLATE THICKNESS
=0.5T

CASE 3: 0.2T MISALIGNMENT
FULL PENETRATION WELD
THROUGH PLATE THICKNESS
=1.0T

CASE 4: 0.2T MISALIGNMENT
FILLET WELD
THROUGH PLATE THICKNESS
=1.0T

FIGURE 4-9
ALIGNMENT STUDY
CATEGORY 2: CRUCIFORM WELDS
FINITE ELEMENT MODELS
O - NODE NUMBERS
O - ELEMENT NUMBERS

4-16
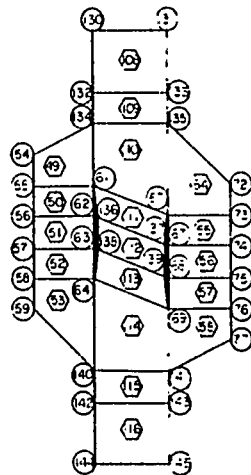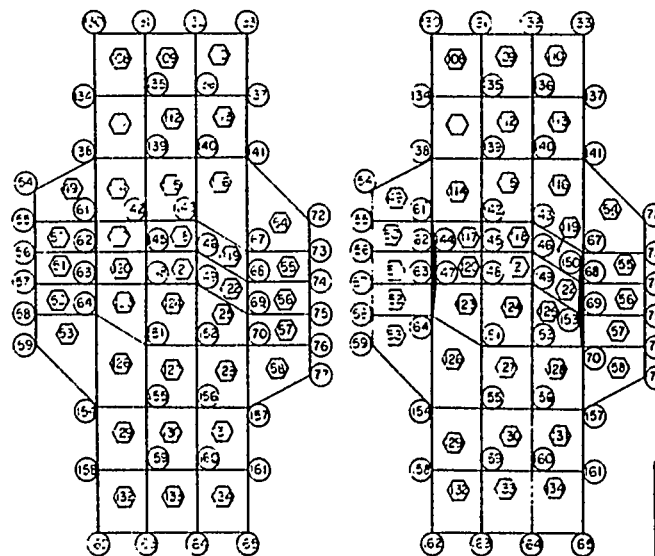
CASE 5: 0.4T MISALIGNMENT
FULL PENETRATION WELD
THROUGH PLATE THICKNESS
= 0.4T

CASE 6: 0.4T MISALIGNMENT
FILLET WELD
THROUGH PLATE THICKNESS
= 0.4T

FOR ADDITIONAL DETAILS
SEE CASE 5

CASE 7: 0.4T MISALIGNMENT
FULL PENETRATION WELD
THROUGH PLATE THICKNESS
= 1.0T

CASE 8: 0.4T MISALIGNMENT
FILLET WELD
THROUGH PLATE THICKNESS
= 1.0T

FOR ADDITIONAL DETAILS
SEE CASE 6

FIGURE 4-10
ALIGNMENT STUDY
CATEGORY 2: CRUCIFORM WELDS
FINITE ELEMENT MODELS

◯ — NODE NUMBERS
⬡ — ELEMENT NUMBERS

CASE 10: 0.6T MISALIGNMENT
PENETRATION WELD   FILLET WELD
THROUGH PLATE THICKNESS   THROUGH PLATE THICKNESS
= 0.5T   = 0.5T
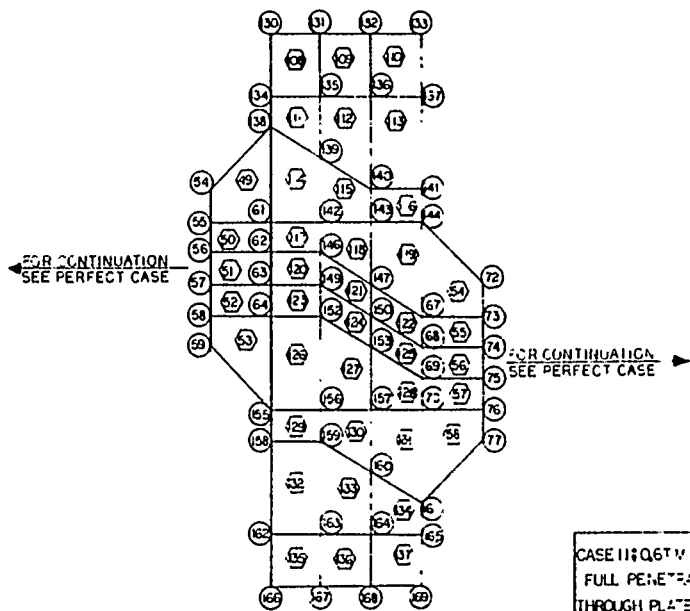
CASE 11: 0.6T MISALIGNMENT   CASE 12: 0.6T MISALIGNMENT
FULL PENETRATION WELD   FILLET WELD
THROUGH PLATE THICKNESS   THROUGH PLATE THICKNESS

FIGURE 4-11
COMPONENT STUDY
CATEGORY 2 LARGE PORT
WELDS
FINITE ELEMENT MODELS

○ - NODE NUMBERS
○ - ELEMENT NUMBERS

FOR CONTINUATION
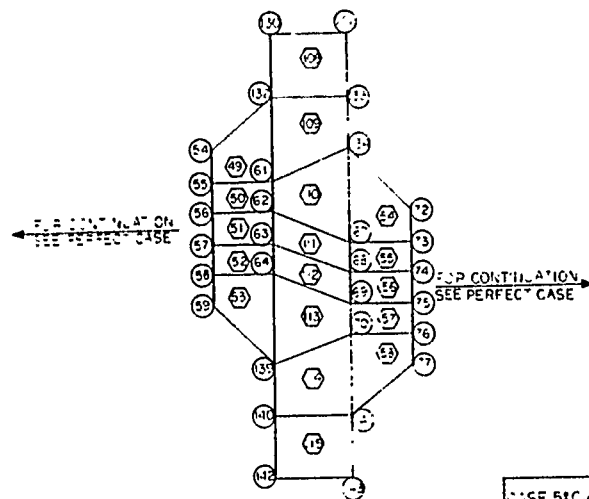SEE PERFECT CASE

FOR CONTINUATION
SEE PERFECT CASE

CASE 13: 0.8T MISALIGNMENT
FULL PENETRATION WELD
THROUGH PLATE THICKNESS
-0.5T

CASE 14: 0.8T MISALIGNMENT
FILLET WELD
THROUGH PLATE THICKNESS
-0.5T

FOR ADDITIONAL
DETAILS SEE CASE 13

FOR CONTINUATION
SEE PERFECT CASE

FOR CONTINUATION
SEE PERFECT CASE

CASE 15: 0.8T MISALIGNMENT
FULL PENETRATION WELD
THROUGH PLATE THICKNESS
-1.0 T

CASE 16: 0.8T MISALIGNMENT
FILLET WELD
THROUGH PLATE THICKNESS
-1.0 T

FOR ADDITIONAL
DETAILS SEE CASE 15

FIGURE 4-12
ALIGNMENT STUDY
CATEGORY 2: CRUCIFORM
WELDS
FINITE ELEMENT MODELS
◯ - NODE NUMBERS
◯ - ELEMENT NUMBERS
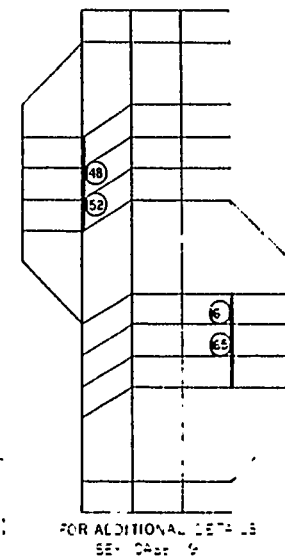
FIGURE 4-13
ALIGNMENT STUDY
CATEGORY 2: CRUCIFORM WELDS
FINITE ELEMENT MODELS
◯ - NODE NUMBERS
◇ - ELEMENT NUMBERS

CASE 17: I.0 T MISALIGNMENT
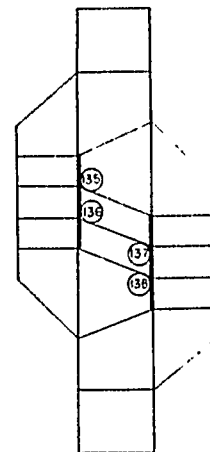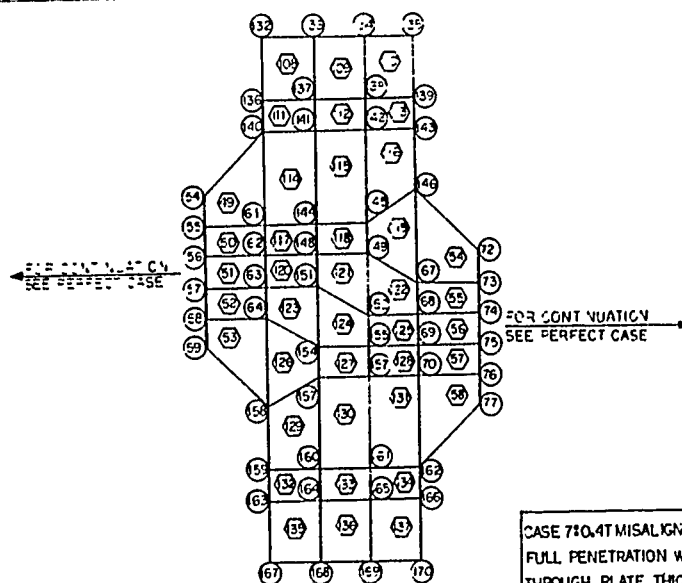FULL PENETRATION WELD
THROUGH PLATE THICKNESS
= 0.5 T

CASE 18: I.0 T MISALIGNMENT
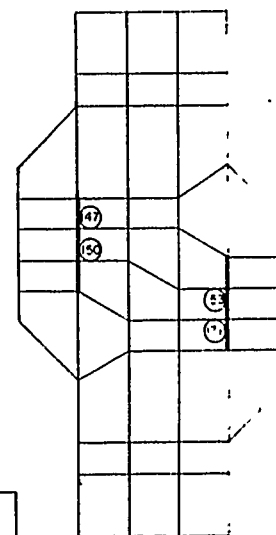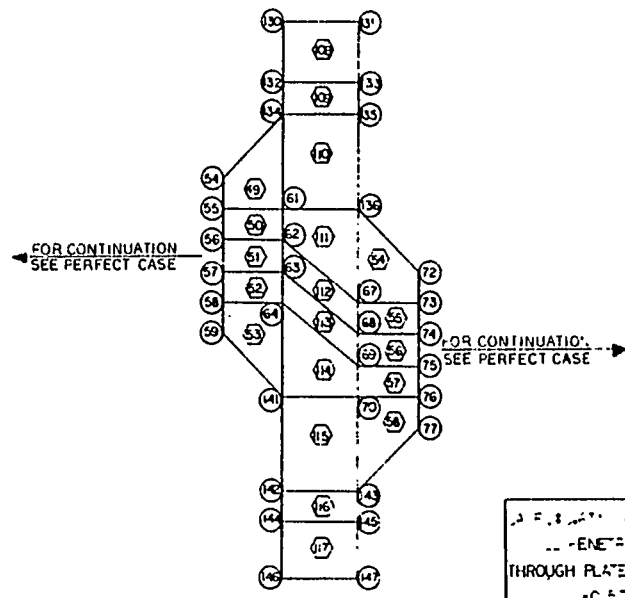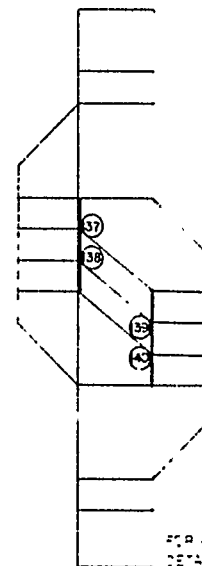FILLET WELD
THROUGH PLATE THICKNESS
= 0.5 T

CASE 19: I.0 T MISALIGNMENT
FULL PENETRATION WELD
THROUGH PLATE THICKNESS
= 1.0 T

CASE 20: I.0 T MISALIGNMENT
FILLET WELD
THROUGH PLATE THICKNESS
= 1.0 T

FOR CONTINUATION
SEE PERFECT CASE

FOR CONTINUATION
SEE PERFECT CASE

FOR ADDITIONAL DETAILS
SEE CASE 9

the continuous through plate were used. A root gap of
approximately l/16 inch has been included in the model.

A uniaxial compressive load was applied. Stress intensity
factors for the misaligned cruciform joints have been
plotted in Figures 4-14 to 4-23.

The stress intensity factors indicate large stress concen-
trations at the toes of the fillets and at the corners of
the root gap. This is consistent with work done by Gurney
 (Reference 20), and Sotah (Reference 22).

The stress intensity plots for the welded cruciform joints
have been constructed from calculated Von Mises stress
where:

$$\sigma_{VON} = \sqrt{\sigma_X^2 + \sigma_Y^2 - \sigma_X \sigma_Y + 3\tau_{XY}^2} = \sigma_{ACTUAL} \quad .$$

(See Figure 4-1 for explanation of terms.) .

Tables 4-2 and 4-3 present the stress intensity factors
with corresponding maxima for each case of misalignment.
The maximum stress intensity factor occurs at the toe of the
fillet weld.

Figures 4-24 and 4-25 present a series of curves based on
Tables 4-2 and 4-3. The abscissa indicates percent mis-
alignment with respect to plate thickness; the ordinate
represents the ratio of average stress to allowable stress.
Figure 4-24 depicts three curves and four designated zones
for the fillet welded cruciform joints with a through plate
thickness of O.5T. Figure 4-25 presents similar data for a
through plate thickness of 1.OT. The $\tau_{ULTIMATE}$ curve has
been approximated by use of results reported in the following
section.

CASE 1

CASE 2

FIGURE 4-1A
ALIGNMENT STUDY
CATEGORY 2: CRUCIFORM
JOINTS
STRESS INTENSITY PLOTS
0.2T MISALIGNMENT
0.5T THRU PLT THICKNESS

4-22

CASE 3

CASE 4

FIGURE 4-15

ALIGNMENT STUDY
CATEGORY 2: CRUCIFORM
JOINTS
STRESS INTENSITY PLOTS
0.2T MISALIGNMENT
1.0T THRU PLATE THICKNESS
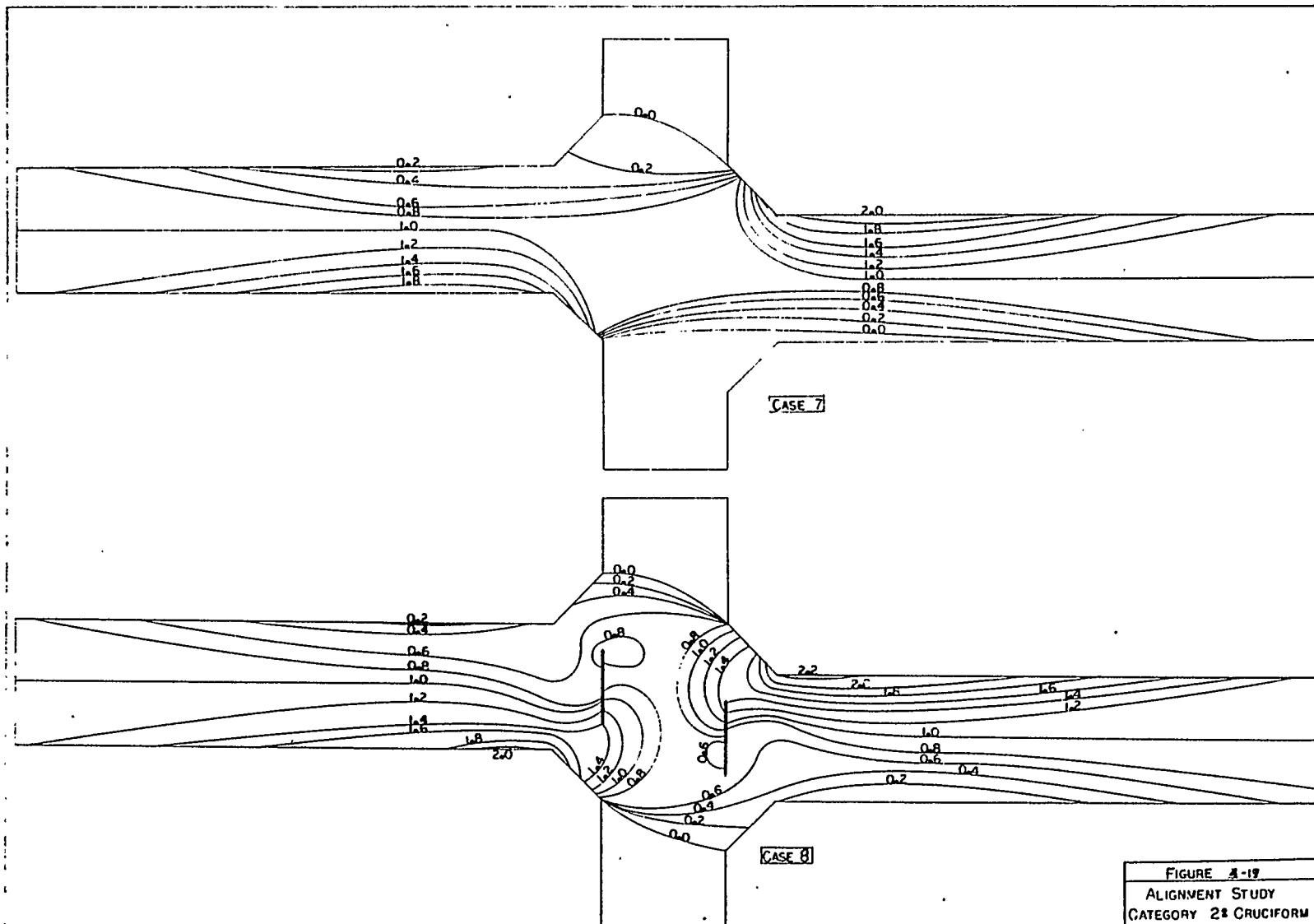
Case 5

Case 6

FIGURE 4-6

ALIGNMENT STUDY
CATEGORY 2 & CRUCIFORM
JOINTS
STRESS INTENSITY PLOTS
0.4T MISALIGNMENT
0.5T THRU PLATE THICKNESS

CASE 7

CASE 8

FIGURE 4-19
ALIGNMENT STUDY
CATEGORY 2: CRUCIFORM
JOINTS
STRESS INTENSITY PLOTS
0.4T MISALIGNMENT
1.0T THRU PLATE THICKNESS

CASE 9

CASE 10
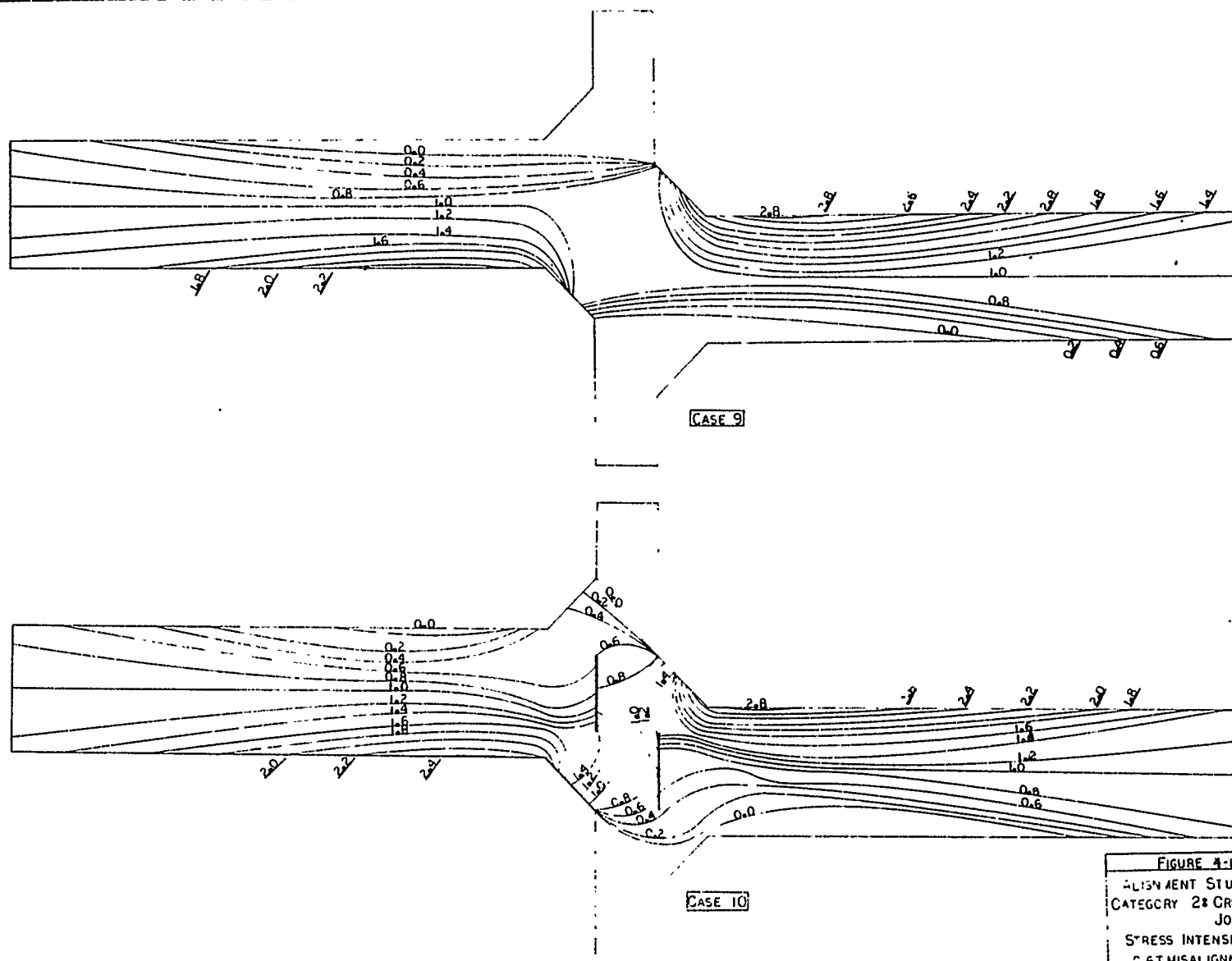
FIGURE 4-18

ALIGNMENT STUDY
CATEGORY 2 CRUCIFORM
JOINTS
STRESS INTENSITY PLOTS
0.6T MISALIGNMENT
0.5T THRU PLATE THICKNESS

CASE 11

CASE 12

FIGURE 4-19

ALIGNMENT STUDY
CATEGORY 2: CRUCIFORM
JOINTS
STRESS INTENSITY PLOTS
0.6T MISALIGNMENT
1.0T THRU PLATE THICKNESS

CASE 13

CASE 14

FIGURE 4-20
ALIGNMENT STUDY
CATEGORY 2: CRUCIFORM
JOINTS
STRESS INTENSITY PLOTS
0.6T MISALIGNMENT
0.5T THRU PLATE THICKNESS

CASE 15

CASE 16

FIGURE 4-21
ALIGNMENT STUDY
CATEGORY 2: CRUCIFORM
JOINTS
STRESS INTENSITY PLOTS
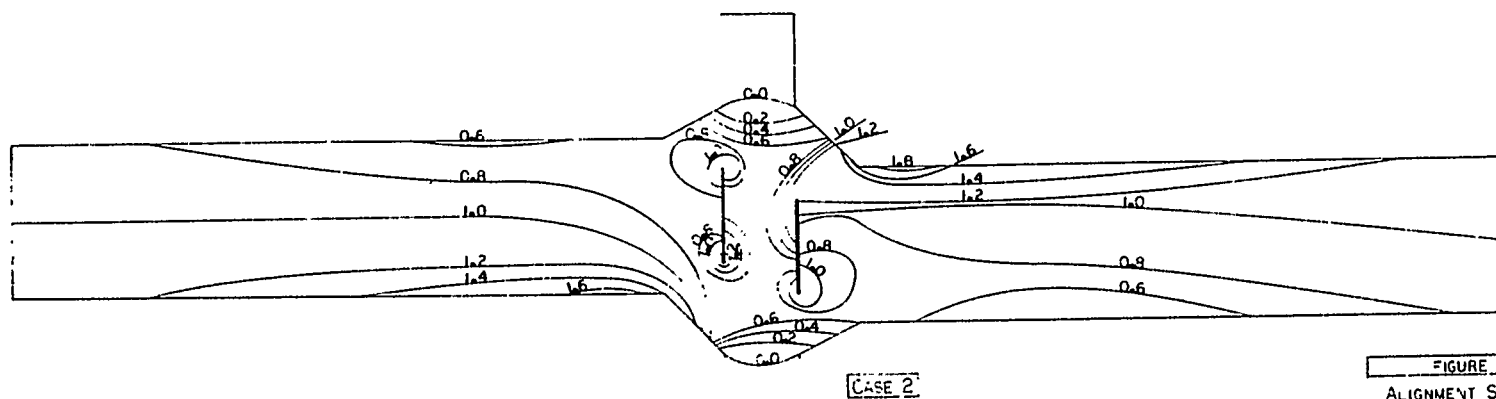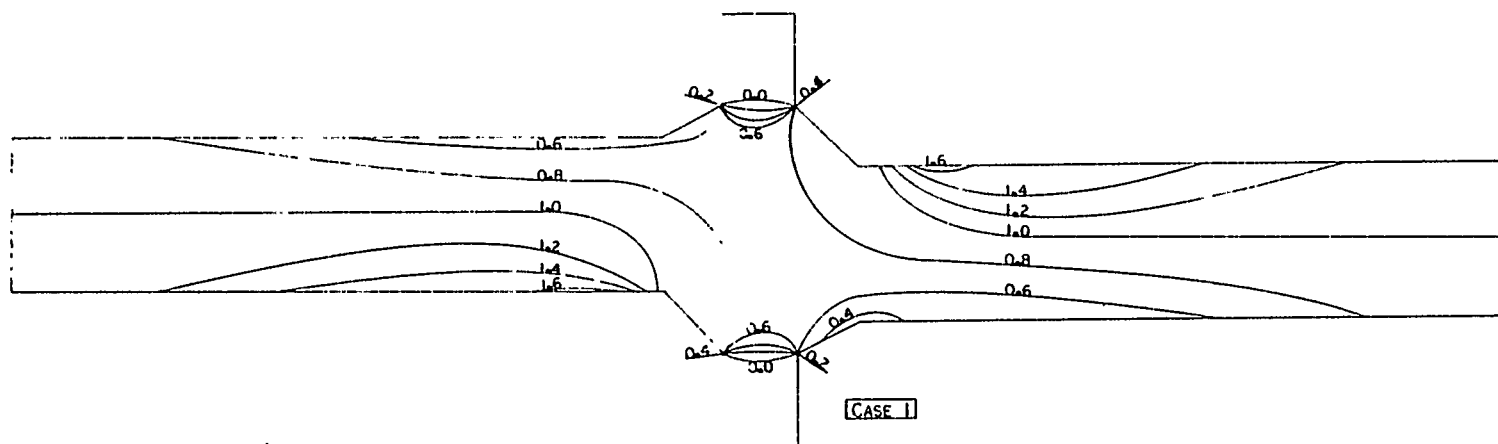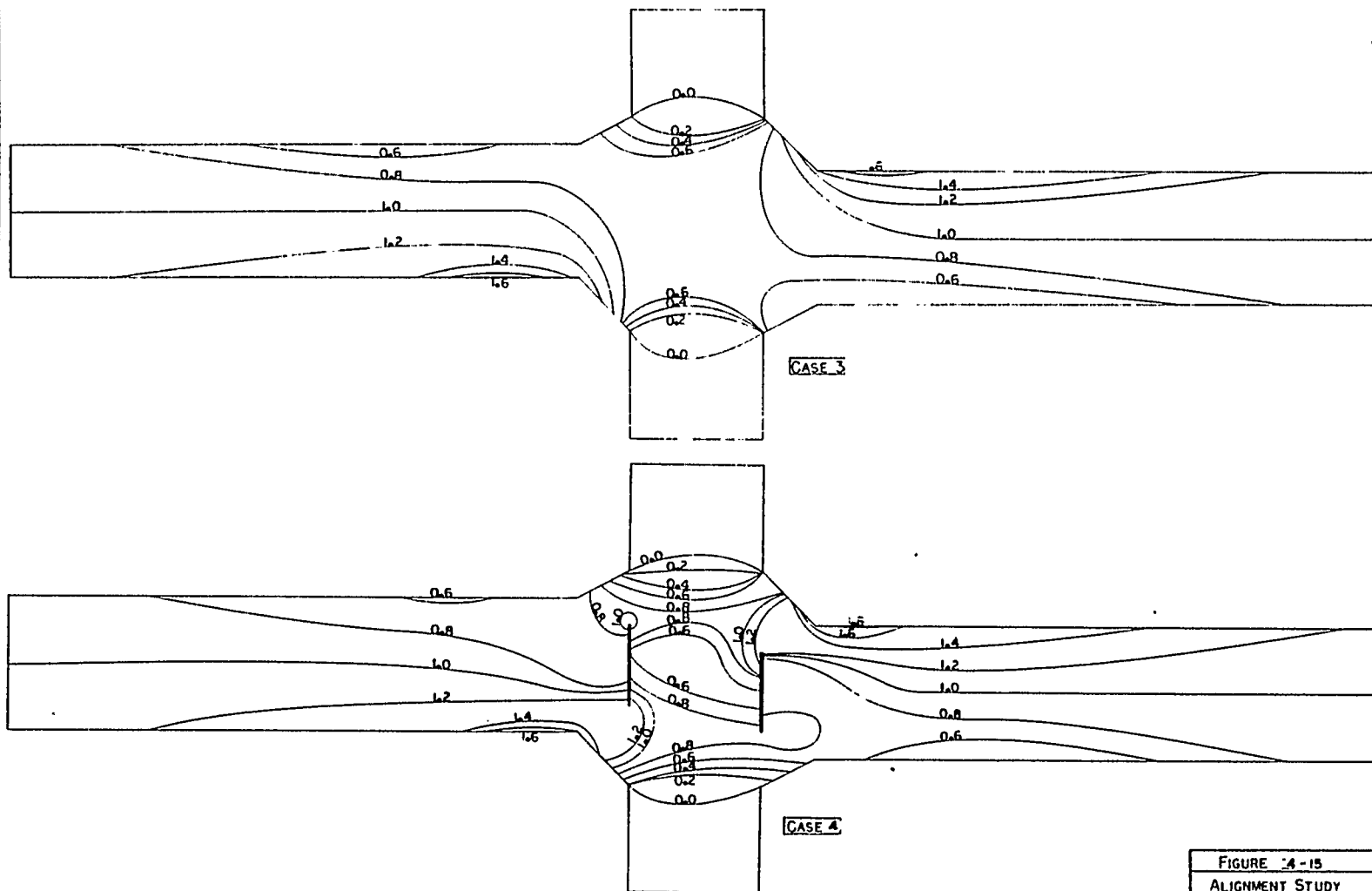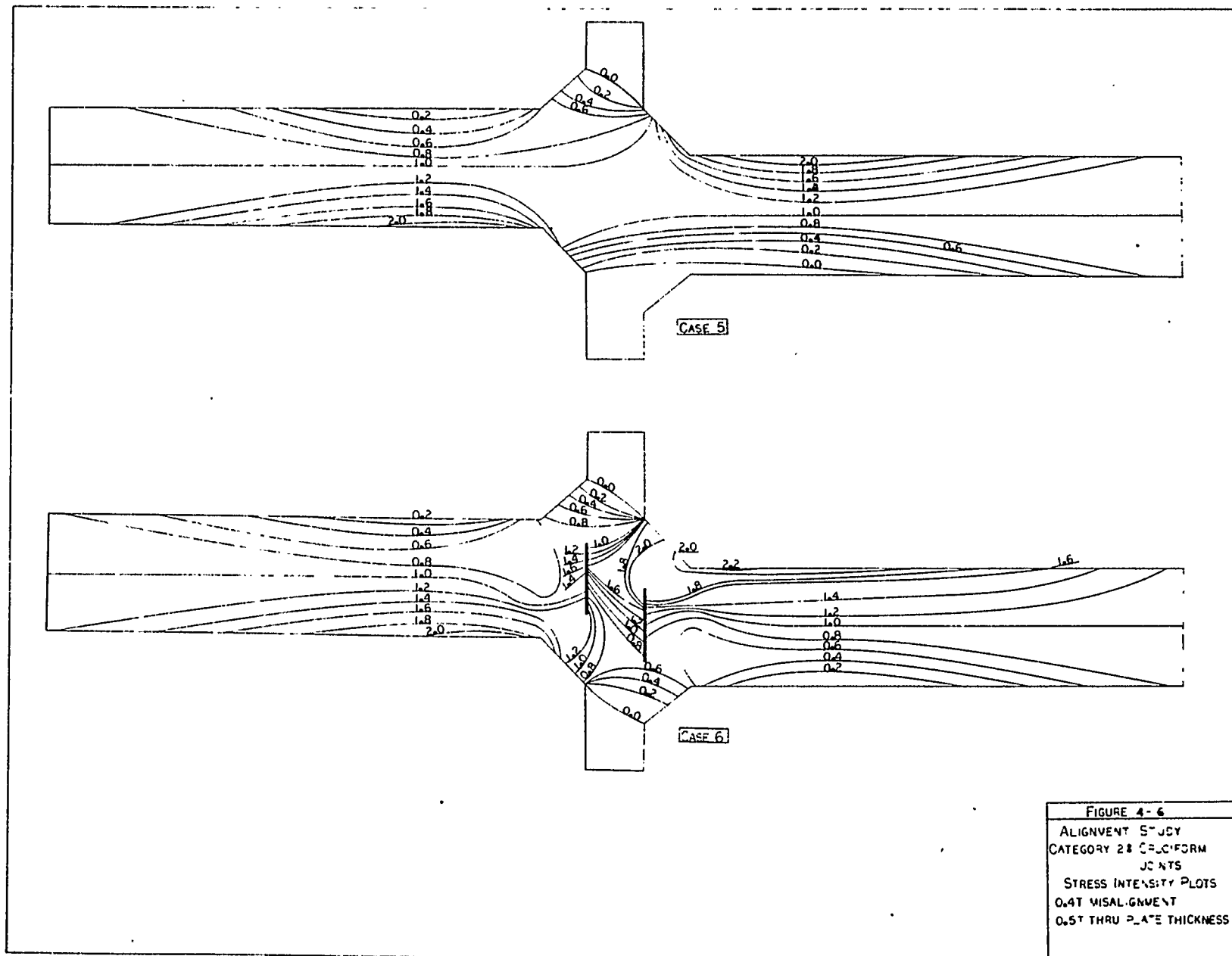0.8 T MISALIGNMENT
1.0 T THRU PLATE THICKNESS

CASE 17

CASE 18

FIGURE 4-22
ALIGNMENT STUDY
CATEGORY 2: CRUCIFORM
JOINTS
STRESS INTENSITY PLOTS
1.0T MISALIGNMENT
0.5T THRU PLATE THICKNESS

FIGURE 4-33
ALIGNMENT STUDY
CATEGORY

MISALIGNMENT δ: T – THICKNESS	MAXIMUM STRESS INTENSITY FACTOR	$\dfrac{\sigma_{ALL.}}{\sigma_{ACTUAL}}$
$0.2T = 0.2$ IN.	1.67	0.60
$0.4T = 0.4$ IN.	2.05	0.49
$0.6T = 0.6$ IN.	2.73	0.37
$0.8T = 0.8$ IN.	3.24	0.31
$1.0T = 1.0$ IN.	4.06	0.25

TABLE 4-2

FINITE ELEMENT ANALYSIS RESULTS

FOR FILLET WELDED CRUCIFORM JOINTS

W/ THROUGH PLATE THICKNESS = 0.50T

MISALIGNMENT δ: T-THICKNESS	MAXIMUM STRESS INTENSITY FACTOR	$\dfrac{\sigma_{ALL.}}{\sigma_{ACTUAL}}$
0.2T = 0.2 IN.	1.67	0.60
0.4T = 0.4 IN.	2.29	0.44
0.6T = 0.6 IN.	2.81	0.36
0.8T = 0.8 IN.	3.41	0.29
1.0T = 1.0 IN.	4.07	0.25

TABLE 4-3

FINITE ELEMENT ANALYSIS RESULTS

FOR FILLET WELDED CRUCIFORM JOINTS

W/ THROUGH PLATE THICKNESS = 1.0 T

FIGURE 4-24: FILLET WELDED CRUCIFORM JOINTS MISALIGNMENT VERSUS STRESS RATIO W/THROUGH PLATE THICKNESS = 0.50T

$\dfrac{\sigma_{AVERAGE}}{0.6\,\sigma_{YIELD}}$

1.0

C.8

C.6

C.4

C.2

0.0

ZONE 4

$\sigma_{ALL} = \sigma_{ULTIMATE}$

ZONE 3

$\sigma_{ALL} \leq \sigma_{YIELD}(INCIPIENT)$

ZONE 2

$\sigma_{ALL} \leq 0.6\,\sigma_{YIELD}$

ZONE 1

0.0   0.2   0.4   0.6   0.8   1.0

MISALIGNMENT: $\dfrac{\delta}{T}$

$\dfrac{\sigma_{AVERAGE}}{\sigma_{ULTIMATE}}$ OR $\dfrac{\sigma_{AVERAGE}}{\sigma_{YIELD}}$

$\dfrac{\sigma_{AVERAGE}}{\sigma_{YIELD}}$

1.0

0.8

C.6

C.4

C.2

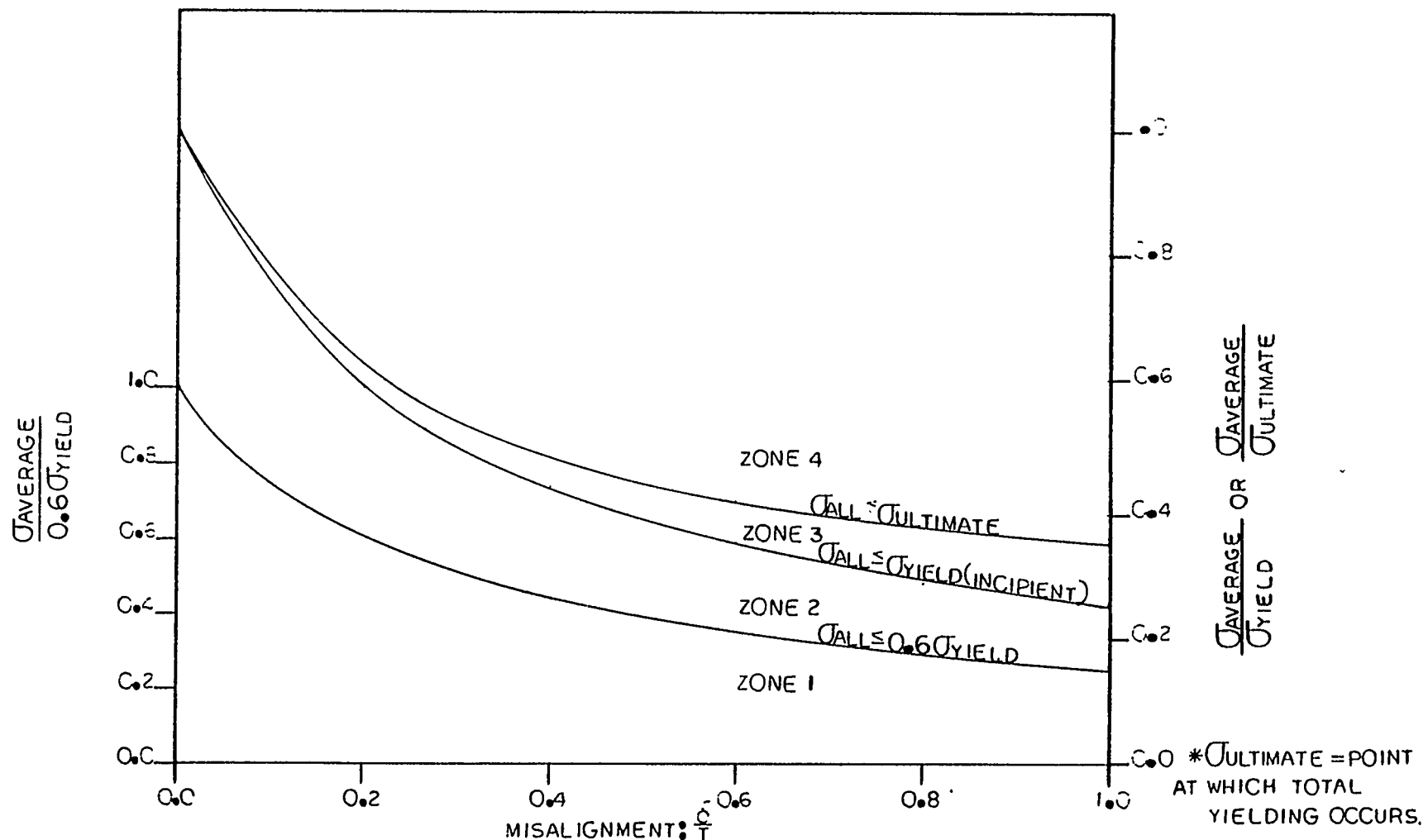C.0   *$\sigma_{ULTIMATE}$ = POINT AT WHICH TOTAL YIELDING OCCURS.
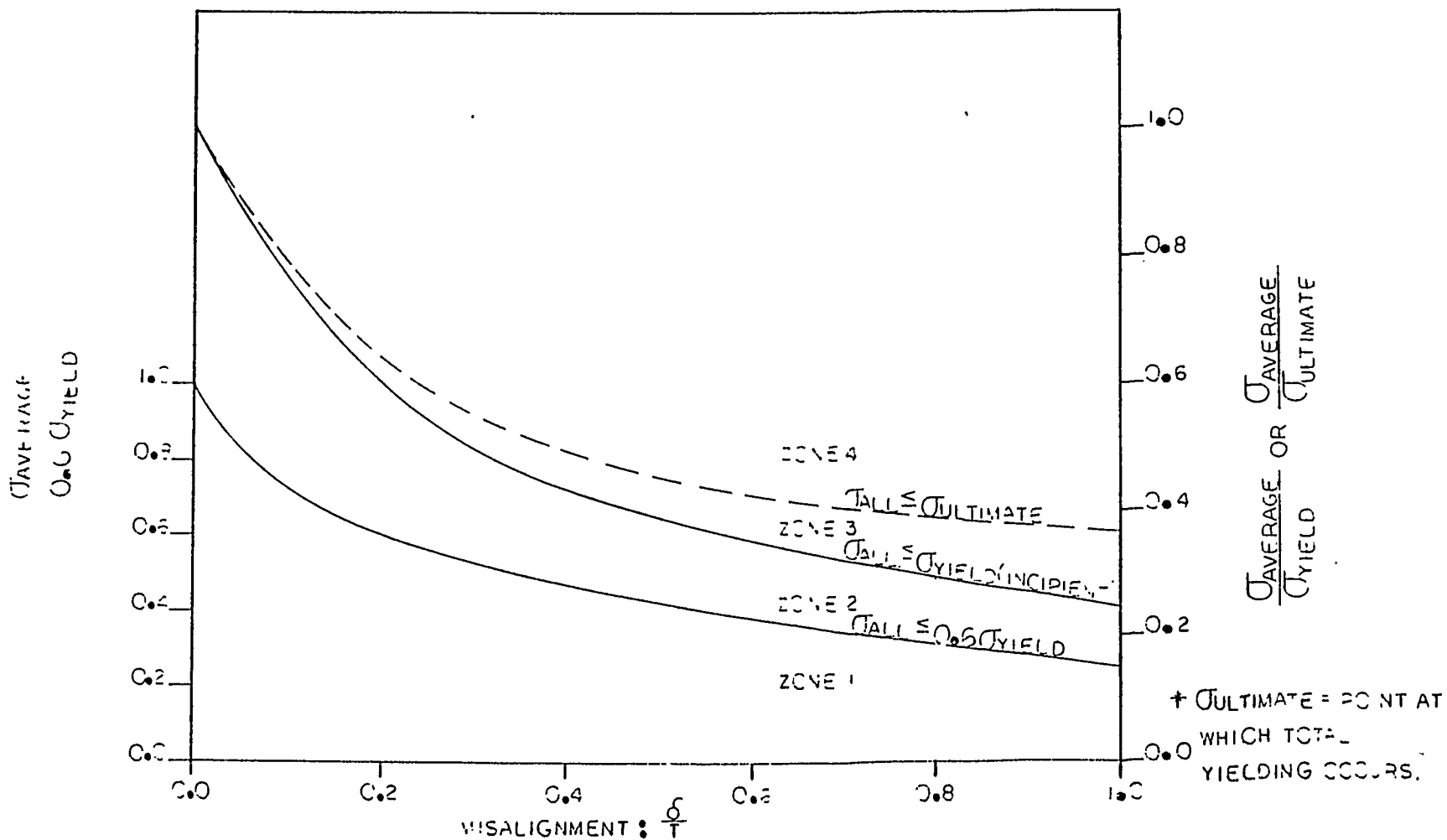
FIGURE 4-25: FILLET WELDED CRUCIFORM JOINTS MISALIGNMENT VERSUS STRESS RATIO w/ THROUGH PLATE THICKNESS = 1.0T

4.3.4 Plastic Analysis of Fillet Welded Cruciform Joints

Plastic analysis for the cruciform joint has been performed only for the case of 0.6T misalignment. Results of this analysis are recorded in Appendix A and have been used to develop the curve ($\sigma_{ULTIMATE}$) **shown on Figures 4-24 and** 4-25. Figure 4-26 illustrates the progressive yielding as calculated for the finite element model.

4.3.5 Elastic Analysis of Full Penetration Cruciform Joints

The basic form of the joint used in this investigation of the full penetration cruciform joints is shown in Figures 4-7 to 4-11, which describe the finite element models used in this analysis. Misalignment of 8 = O.OT to 8 = 1.OT in incre-ments of $ = 0.20 were investigated. Plane strain elements with a thickness equal to 1 inch for the misaligned members and 1/2 and 1 inch for the continuous through plate were used in the analysis. A root gap of O inch has been included in the model.

A uniaxial compressive load was applied as previously des-cribed in Section 4.3.3 stress intensity factors for the misaligned cruciform joints have been plotted in Figures 4-12 to) 4-22. These stress intcnsity plot do not exhibit the large internal stress concentration that were evident for the fillet welds with root gap. The maximum stress intensity factor occurs at the toe of the reinforcing fillet. The plots have been developed using the dominant σ_x stresses.

Tables 4-4 and 4-5 present the stress intensity factors with corresponding maxima for each case of misalignment.
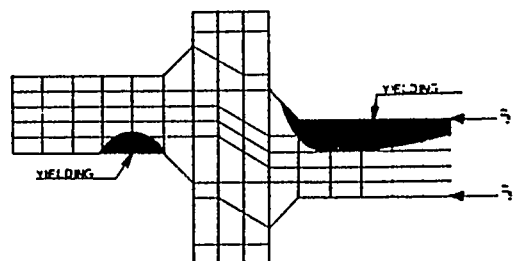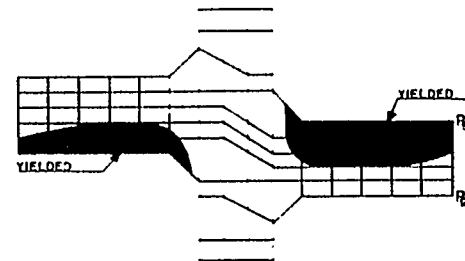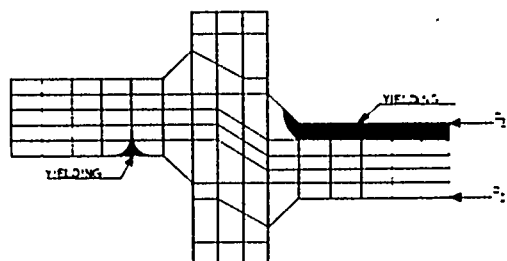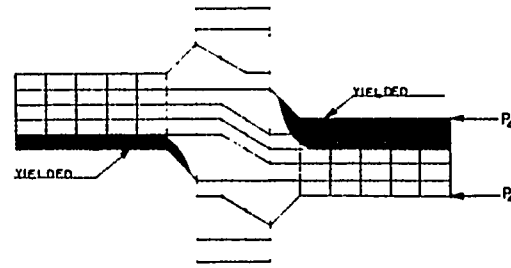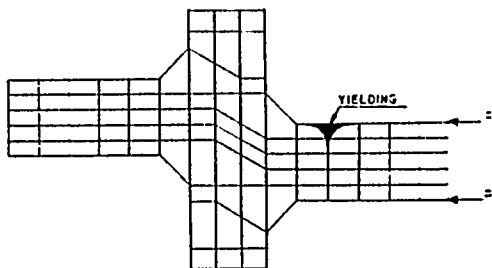
FIGURE 4-26
FILLET WELDED CRUCIFORM
JOINT
MISALIGNMENT = 0.6 T
RESULTS OF INCREMENTAL
PLASTIC ANALYSIS

4-37

MISALIGNMENT δ: T-THICKNESS	MAXIMUM STRESS INTENSITY FACTOR	$\dfrac{\sigma_{ALL.}}{\sigma_{ACTUAL}}$
0.2 T = 0.2 IN.	1.34	0.74
0.4 T = 0.4 IN.	1.78	0.56
0.6 T = 0.6 IN.	2.51	0.40
0.8 T = 0.8 IN.	3.21	0.31
1.0 T = 1.0 IN.	4.21	0.24

TABLE 4-4

FINITE ELEMENT ANALYSIS RESULTS

FULL PENETRATION CRUCIFORM JOINTS

w/THROUGH PLATE THICKNESS = 0.50 T

MISALIGNMENT δ: T-THICKNESS	MAXIMUM STRESS INTENSITY FACTOR	$\dfrac{\sigma_{ALL.}}{\sigma_{ACTUAL}}$
0.2T = 0.2 IN	1.47	0.68
0.4T = 0.4 IN	2.10	0.48
0.6T = 0.6 IN	2.67	0.37
0.8T = 0.8 IN	3.32	0.30
1.0T = 1.0 IN	4.02	0.25

TABLE 4-5

FINITE ELEMENT ANALYSIS RESULTS

FULL PENETRATION CRUCIFORM JOINTS

W/THROUGH PLATE THICKNESS = 1.0T

Figures 4-27 and 4-28 represent plots of the above data
Each depicts three curves and four dcsignated zones for the
full penetration cruci form joints with a through plate
thickness of 0.5T and 1.OT, respectively. No elasto-plastic
analysis was performed on these joints: Instead, the
information presented for the fillet welded cruciform joint
has been used to construct a set of extrapolated JULTIMATE
curves.

FIGURE 4-27: FULL PENETRATION CRUCIFORM JOINTS MISALIGNMENT VERSUS STRESS RATIO W/THROUGH PLATE THICKNESS = 0.50T

$\dfrac{\sigma_{AVERAGE}}{0.6\,\sigma_{YIELD}}$

$\dfrac{\sigma_{AVERAGE}}{\sigma_{YIELD}}$ OR $\dfrac{\sigma_{AVERAGE}}{\sigma_{ULTIMATE}}$

$\dfrac{\sigma_{AVERAGE}}{\sigma_{YIELD}}$

$\sigma_{ALL} \leq \sigma_{ULTIMATE}$

$\sigma_{ALL} \leq \sigma_{YIELD}(\text{INCIPIENT})$

$\sigma_{ALL} \leq 0.6\,\sigma_{YIELD}$

ZONE 4

ZONE 3

ZONE 2

ZONE 1

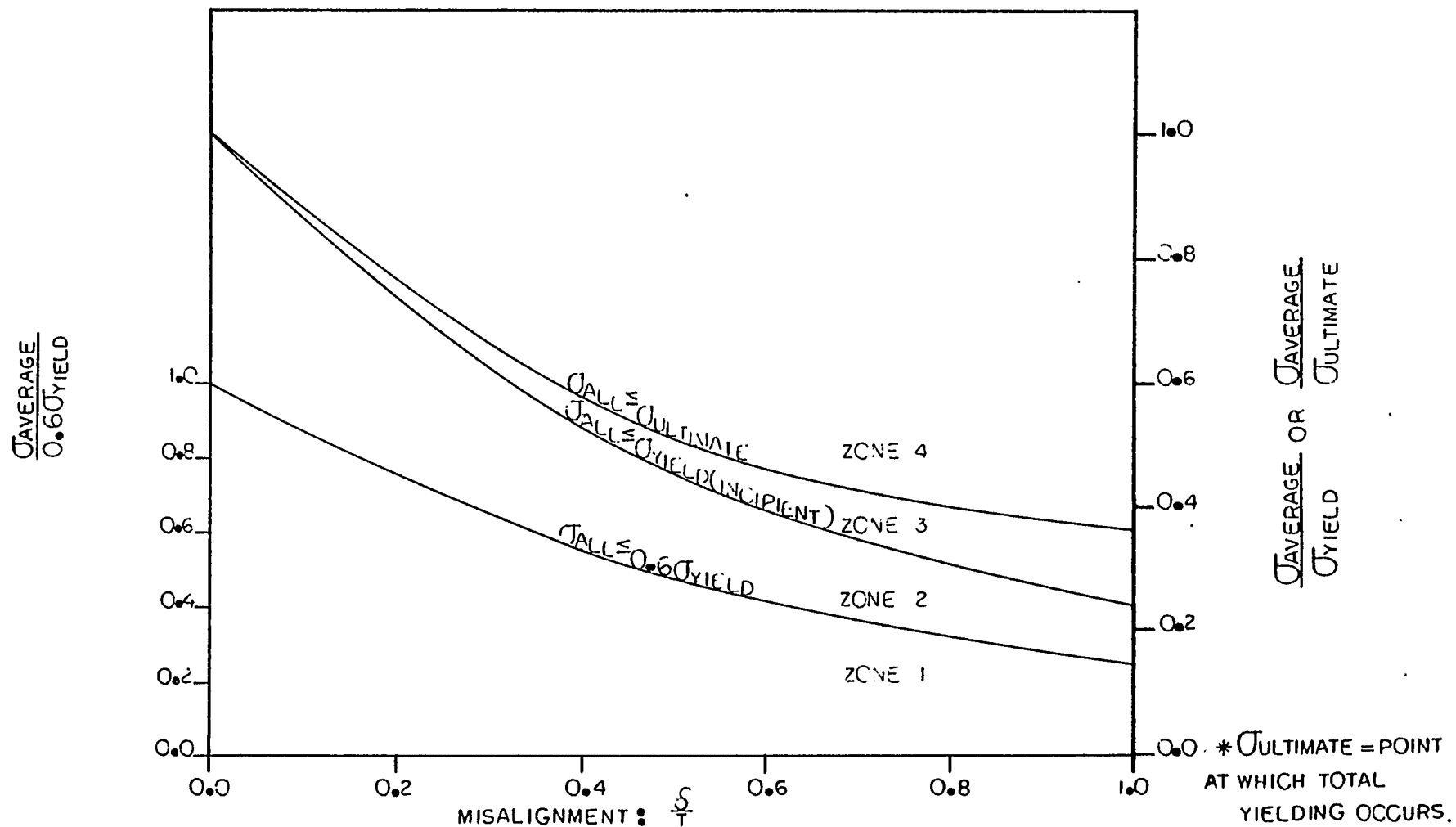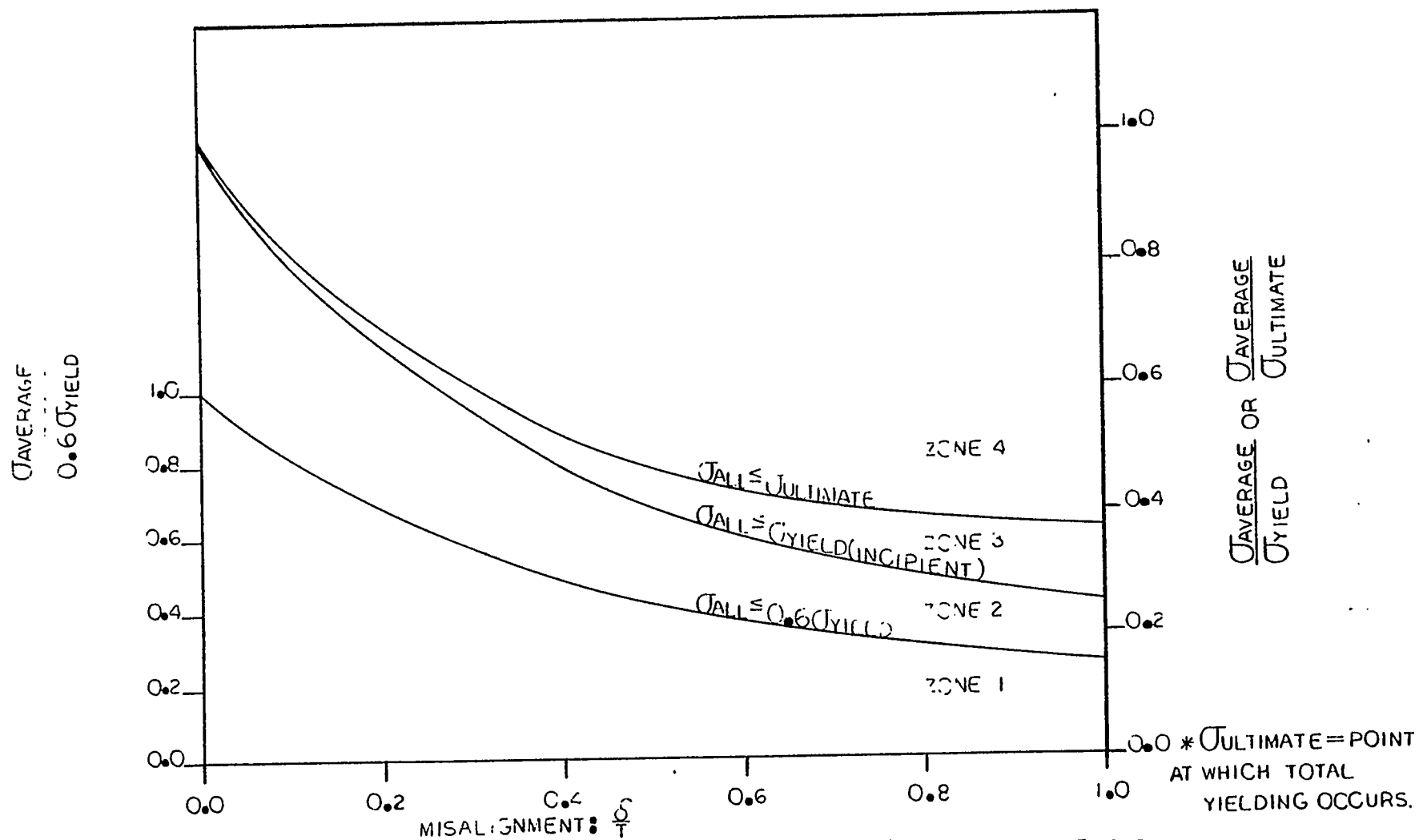$*\ \sigma_{ULTIMATE} =$ POINT AT WHICH TOTAL YIELDING OCCURS.

MISALIGNMENT: $\dfrac{\delta}{T}$

FIGURE 4-28: FULL PENETRATION CRUCIFORM JOINTS MISALIGNMENT VERSUS STRESS RATIO w/THROUGH PLATE THICKNESS = 1.0 T

Section 5
FATIGUE STRENGTH OF MISALIGNED JOINTS

5.1 <u>GENERAL</u>

The most critical ship structural elements are generally
subjected to cyclic or fatigue type of loading. For such
elements the guidance to be obtained from the results of the
preceding static finite element analysis is not sufficient.

Reference 12 and 13, discussed in detail in Section 3, provide
experimental fatigue data related to misaligned butt welded and
cruciform joints. Although these data by themselves provide
little guidance to the designer, they form an adequate basis
for-extrapolated and generalized data to be derived and
discussed in the following paragraph.

5.2 <u>METHODOLOGY</u>

The available experimental data are for a stress ratio R = 0
 (R is the algebraic ratio of minimum to maximum stress).
Although it is becoming generally recognized that stress range
is more relevant to the true fatigue performance of welded
elements than is stress ratio (Reference 23), these experimental
values have nonetheless been extrapolated to a stress ratio
R = -1 (full stress reversal). That stress ratio is more
typical of ship structural behavior, more conservative for
design and as will be seen, simplifies the response analysis.

 Extrapolation is performed by using a factor corresponding
to design fatigue stress values for mild steel taken from Table
10.4 of Reference 24. The experimental data are limited to
tests up to 105 cycles, whereas a twenty year ship life
corresponds to about 108 wave encounters or cycles.
Extrapolation to the higher range is made by using ratios of
higher cycle fatigue strength, i.e., 6 $x10^5$ and 2 $x10^6$
to strength at 10^5 cycles, again taken from Reference 24.
The final extrapolation to 10^8 cycles is made graphically.

The expressions used to form the above ratios are:

No. of Cycles	Allowable Stress

$$2,000,000 \qquad F_A = \frac{19000}{(1 - 0.73R)}$$

$$600,000 \qquad F_A = \frac{24000}{(1 - 0.60R)}$$

$$100,000 \qquad F_A = \frac{28000}{(1 - 0.75R)}$$

Where:

F_A = Allowable unit fatigue stress, psi

R = Algebraic ratio of minimum to maximum stress.

The fatigue curves for butt and cruciform joints, discussed and shown in Sections 5.3 and 5.4, are then used to calculate (by an iterative process) the maximum permissible stress range for a stress histogram of a ship structural element over 10^8 cycles.

A sample histogram is shown in Figure 5-1. Note that with number of cycles plotted on a logarithmic abcissa, straight line elements join maximum and zero stress levels. This is an approximation justified by a generally similar measured pattern of probability distribution for linearized ship responses to a long term sea spectrum.

Maximum values of stress used in constructing the histogram can be approximated by the calculated response to bending moment, shear or pressure corresponding to peak quasistatic design wave height, such as L/20 or $1.1\sqrt{L}$.

The Palmgren-Miner cumulative fatigue damage theory is used in conjunction with a finite subdivision of the histogram.
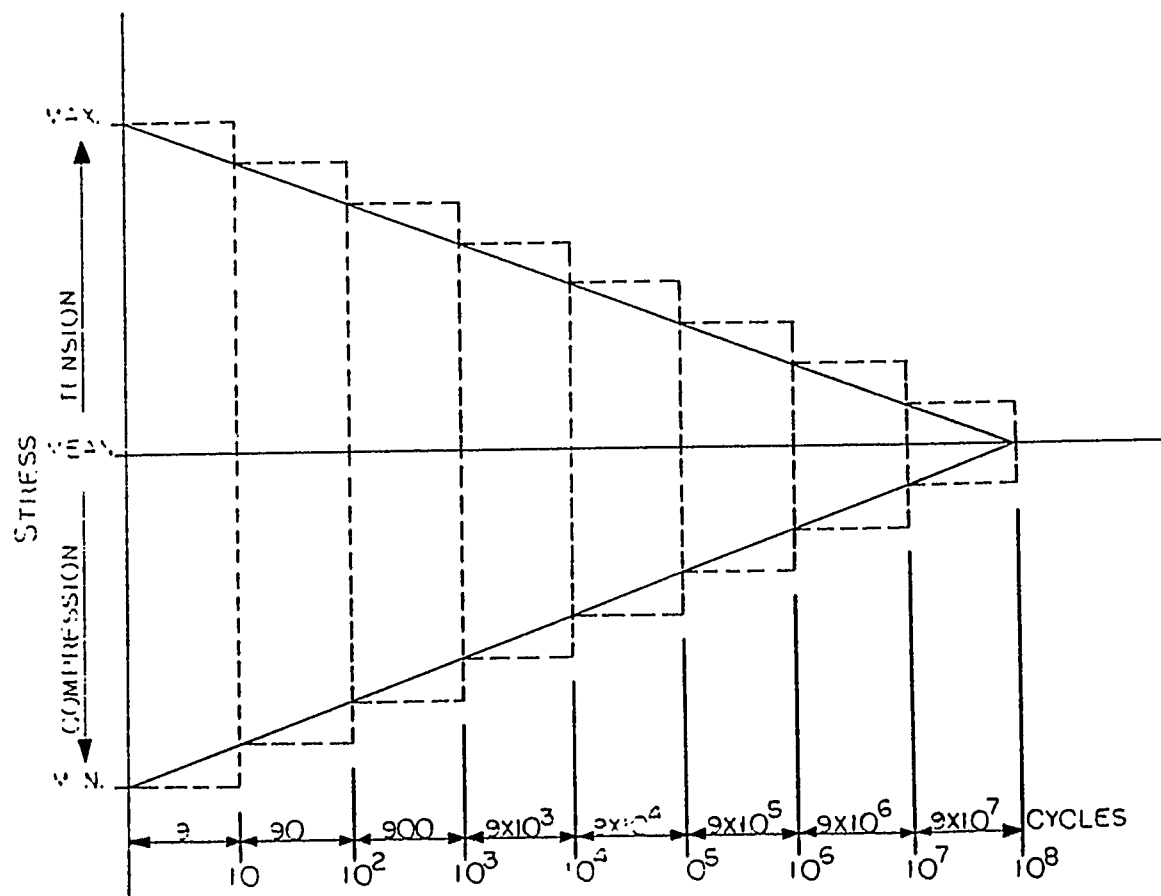
FIGURE 5-1
SIMPLIFIED
STRESS HISTOGRAM

The expression

$$\sum \frac{n_i}{N_i} \leq 0.5$$

Where n_i = number of cycles at stress σ_i

            N_i = number of cycles to failure at σ_i

implies a two-fold margin on service lite.

By using R = -1 the stress ratio is equal for every block in the histogram, which simplifies the calculation and greatly reduces the quantity of required experimental data.

As an example, the final iterative cycle to establish the extreme permissible stress range corresponding to the S-N diagram in Figure 5-5 is outlined below:

Step 1.   The maximum stress is divided into eight equal increments and these are plotted on the ordinate.

           Stress increment = 1 ksi

           Values plotted: (8, 7, 6, 5, 4, 3, 2, 1)

Step 2.   Extend lines parallel to abscissa until they cross the respective S-N curve.

           Points of intersection are to be used as N values.

Step 3.   Calculate cumulative damage factor:

$$\sum_{i=1}^{8} \frac{n_i}{N_i} = \frac{2}{26000} + \frac{90}{74000} + \frac{900}{600000} + \frac{9000}{2000000} +$$

$$\frac{90000}{6000000} + \frac{900000}{100000000} + \frac{9000000}{250000000} +$$

$$.\frac{9000000}{(?)} \quad \cdots 0.52$$

$$\sum \frac{n}{N} \cong 0.50$$

5.3 FATIGUE DATA FOR SEAMS AND BUTTS

Figures 5-2 to 5-5 are the S-N diagrams for butt welded plates with misalignment varying from 0.0 to 0.6T. The R = O curves are shown only as reference.

Calculating maximum permissible stress range for R = -1 by the method of Paragraph 5.2 leads to the summary in Table 5-1. The tabulated values can be very useful in the evaluation of functional adequacy of misaligned joints subject to cyclic loading.
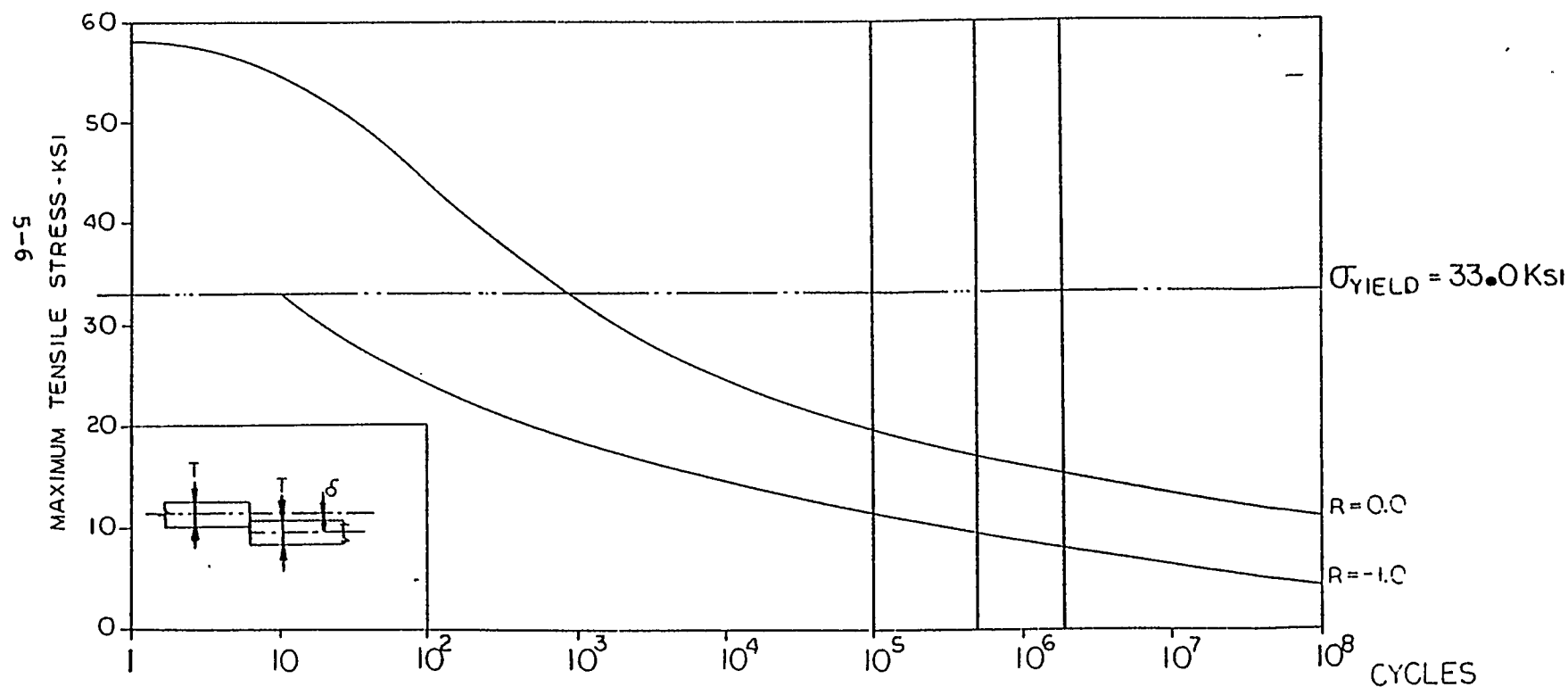
FIGURE 5-2
S-N DIAGRAM FOR
BUTT WELDS
MILD STEEL: $\frac{\delta}{T}$ =0.0

σ_{YIELD} = 33.0 KSI

R=0.0

R=-1.0

MAXIMUM TENSILE STRESS - KSI

CYCLES

5-6

FIGURE 5-3
S-N DIAGRAM FOR
BUTT WELDS
MILD STEEL: $\frac{\delta}{T} = 0.2$

$\sigma_{YIELD} = 33.0$ Ksi

R = 0.0
R = -1.0

MAXIMUM TENSILE STRESS - KSI

CYCLES

5-7
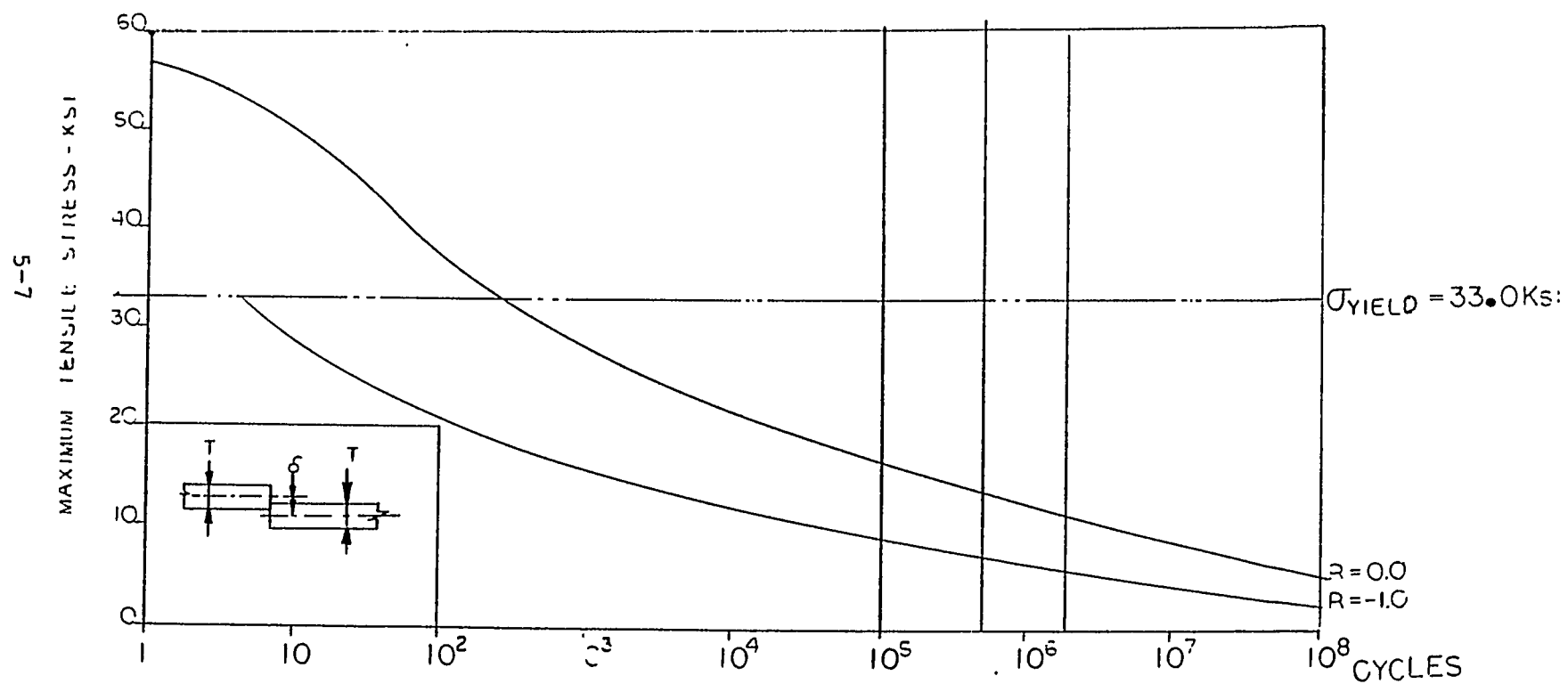
FIGURE 5-4
S-N DIAGRAM FOR
BUTT WELDS
MILD STEEL: $\frac{\delta}{T}$=0.4

σ_{YIELD}=33.0 KSI

R = 0.0
R = -1.0

CYCLES
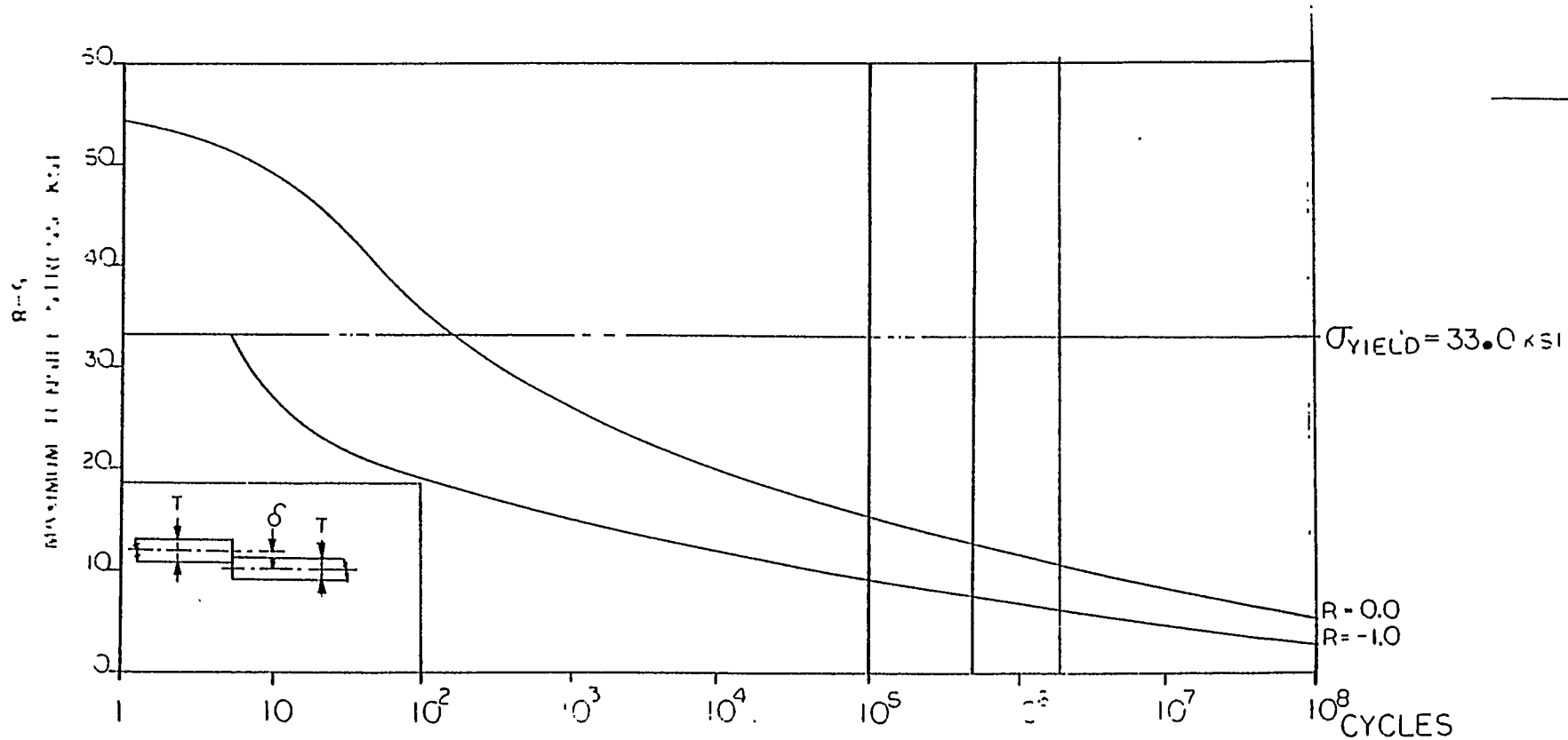
FIGURE 5- 5
S-N DIAGRAM FOR
BUTT WELDS
MILD STEEL: $\frac{\delta}{T}=0.6$

$\sigma_{YIELD}=33.0$ KSI

MAXIMUM TENSILE STRESS - KSI

R=0.0
R=-1.0

CYCLES
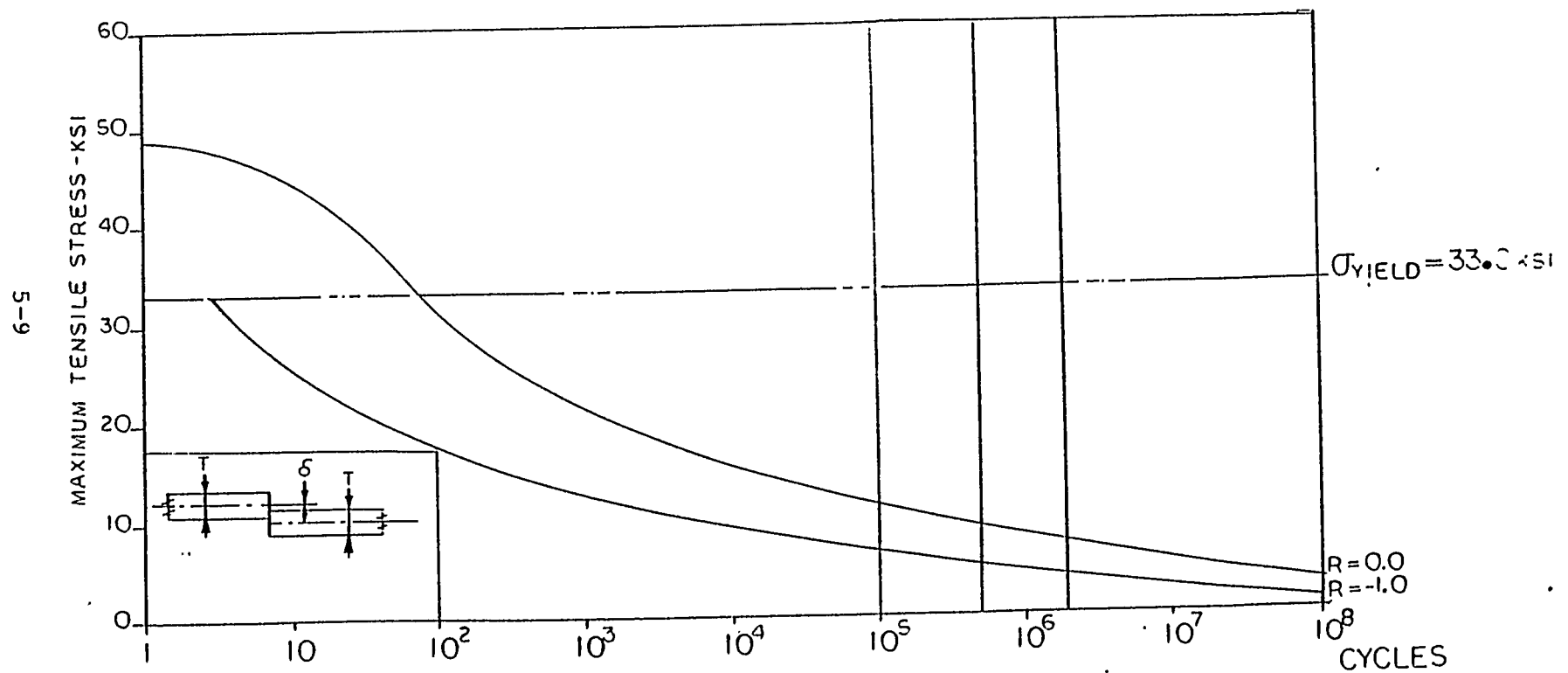
TABLE 5-1

MISALIGNED BUTT WELDS	
δ/T	MAXIMUM STRESS RANGE $^{(R=-1)}$
0.0	37200 PSI
0.2	29200 PSI
0.4	26000 PSI
0.6	15600 PSI
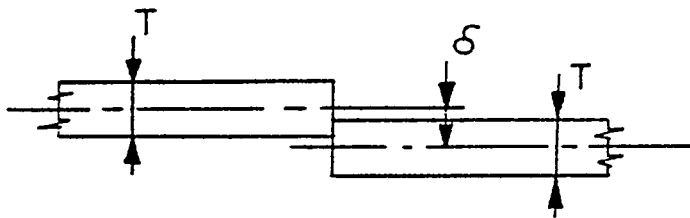
MAXIMUM CALCULATED STRESS
RANGES FOR MISALIGNED BUTT
WELDS EXPERIENCING CYCLIC LOADING

5.4 FATIGUE DATA FOR CRUCIFORM JOINTS

Figures 5-6 to 5-9 are the S-N diagrams for cruciform welded plates with misalignment ratio $\frac{e}{t}$ varying from 0.0 to 1.0. Again the curves for R = O are shown only as reference.

Calculated maximum permissible stress ranges for R = -1 are listed in Table 5-2.

FIGURE 5-6
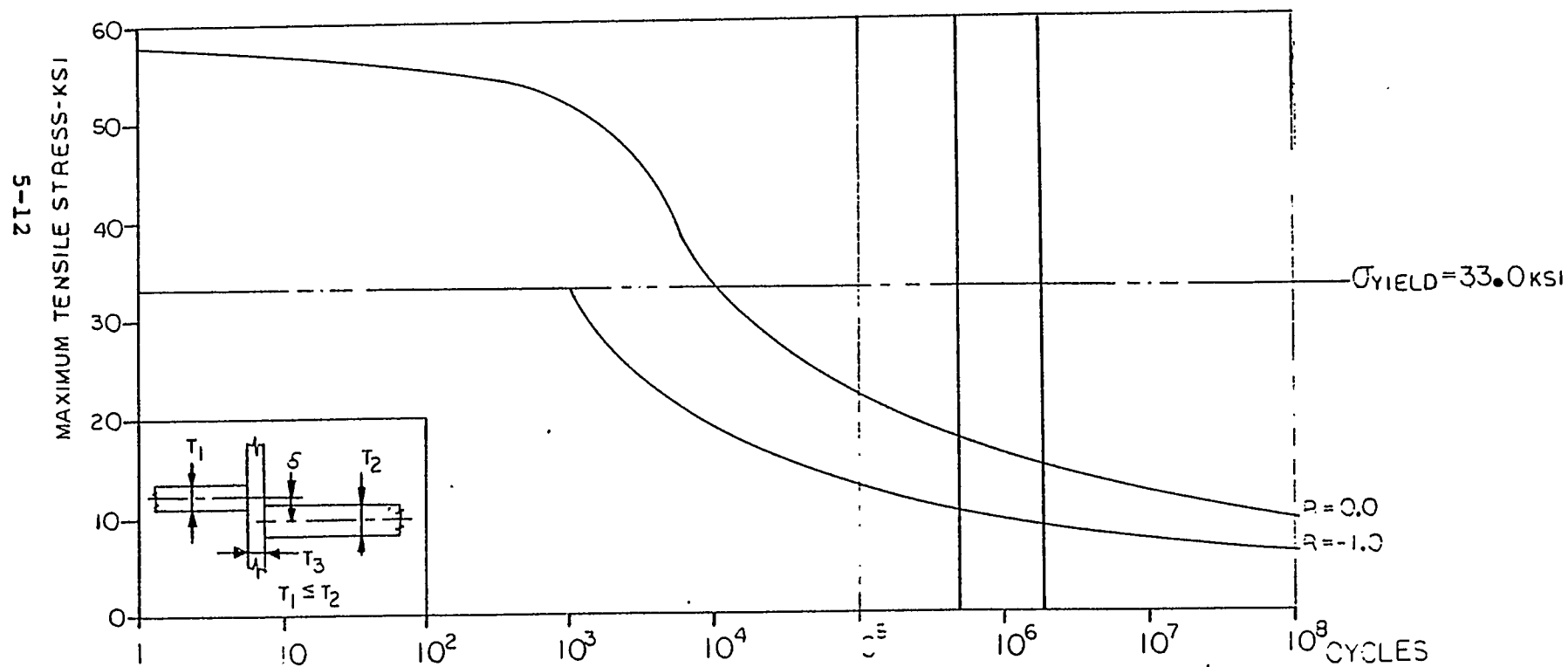S-N DIAGRAM FOR
CRUCIFORM JOINTS
MILD STEEL: $\frac{S}{T_1} = 0.0$

$\sigma_{YIELD} = 33.0$ KSI

MAXIMUM TENSILE STRESS-KSI

$T_1 \leq T_2$

$R = 0.0$

$R = -1.0$

CYCLES

FIGURE 5-7
S-N DIAGRAM FOR
CRUCIFORM JOINTS
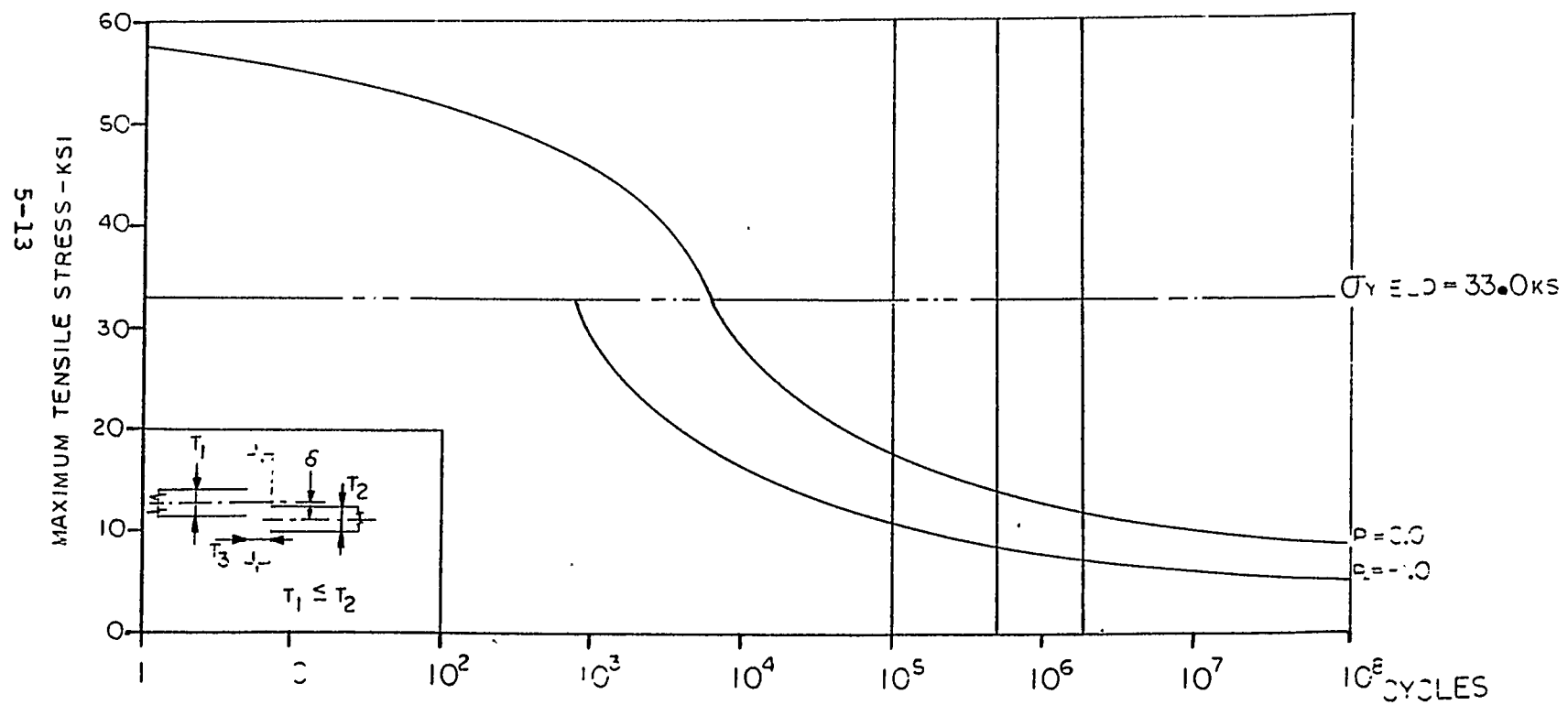MILD STEEL $\frac{e}{T}=0.25$

5-13

FIGURE 5-8
S-N DIAGRAM FOR
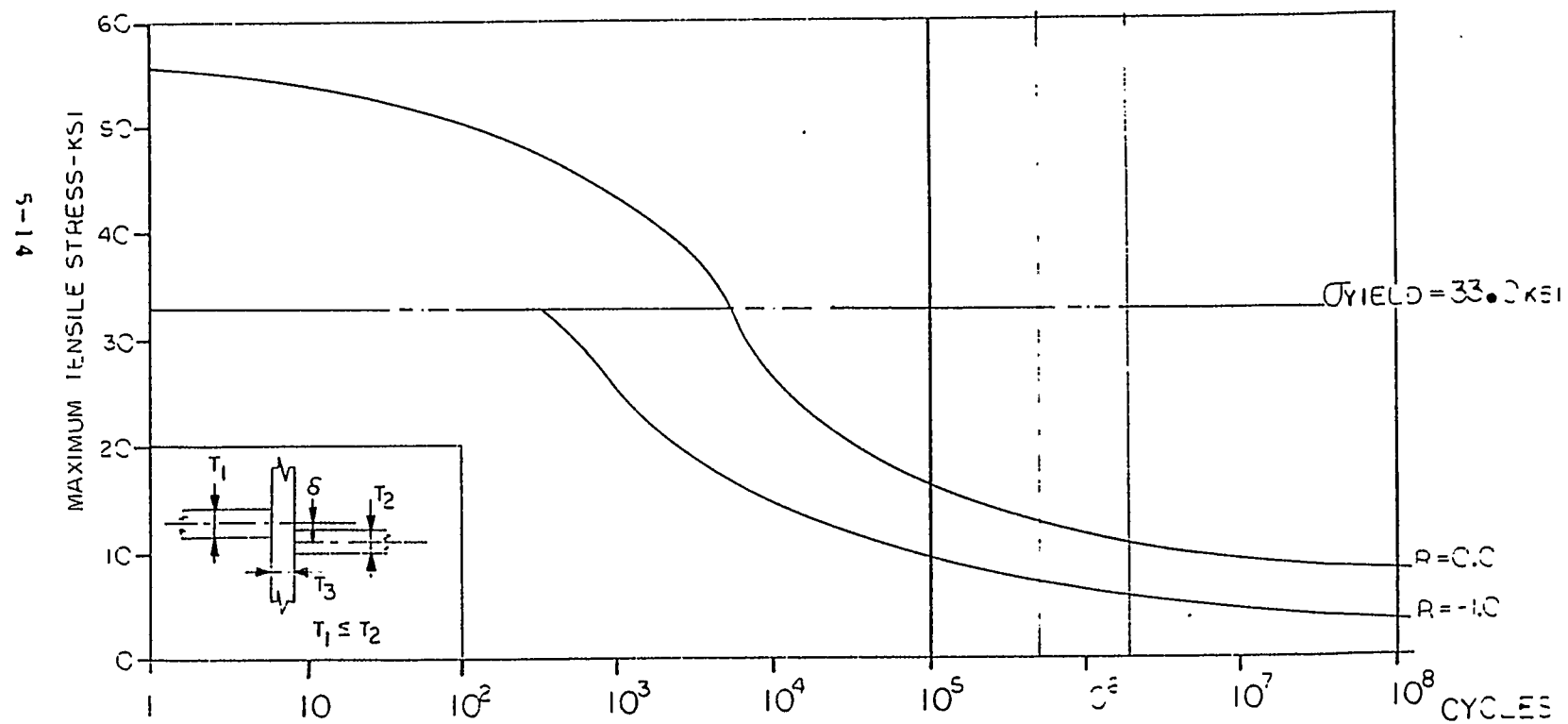CRUCIFORM JOINTS
MILD STEEL: $\frac{\delta}{T_1} = 0.50$

5-14

FIGURE 5-9
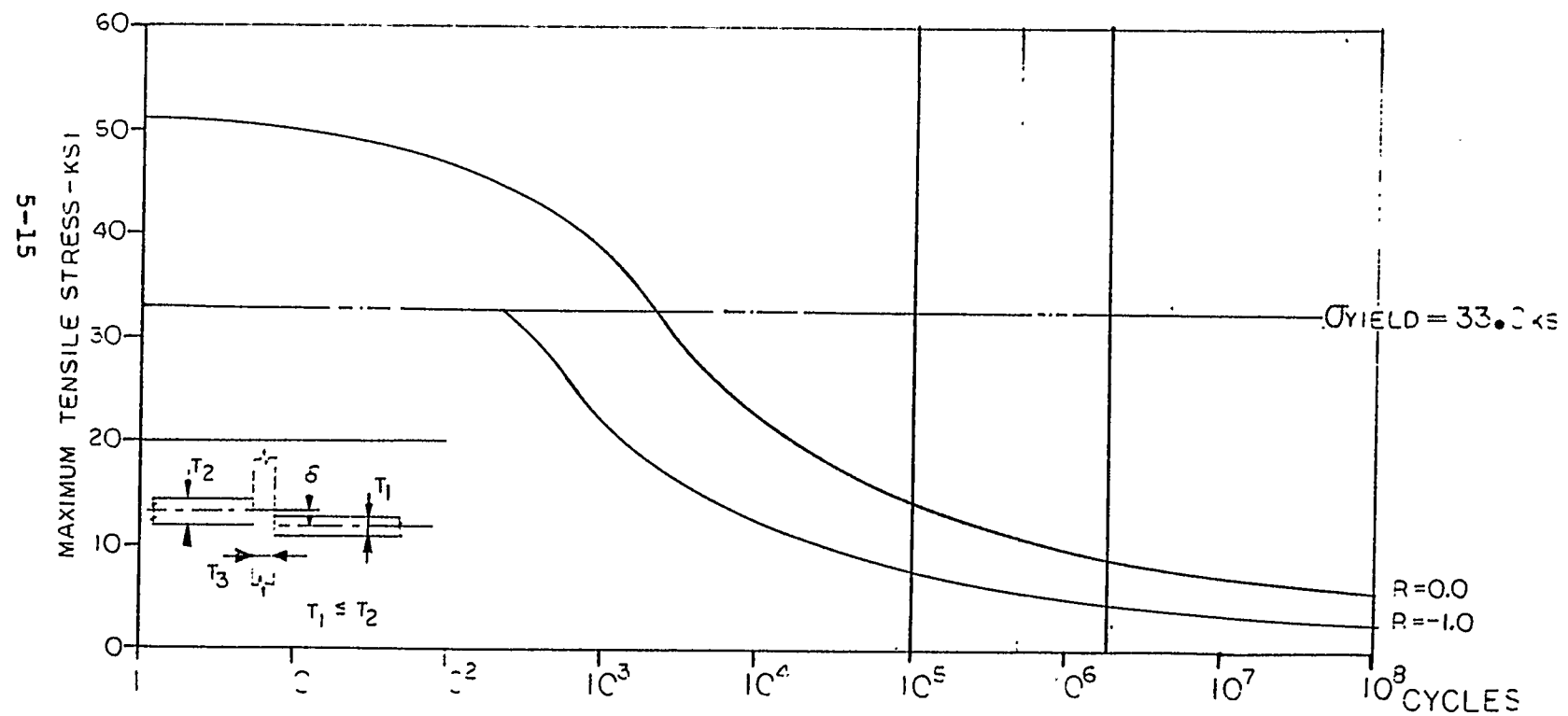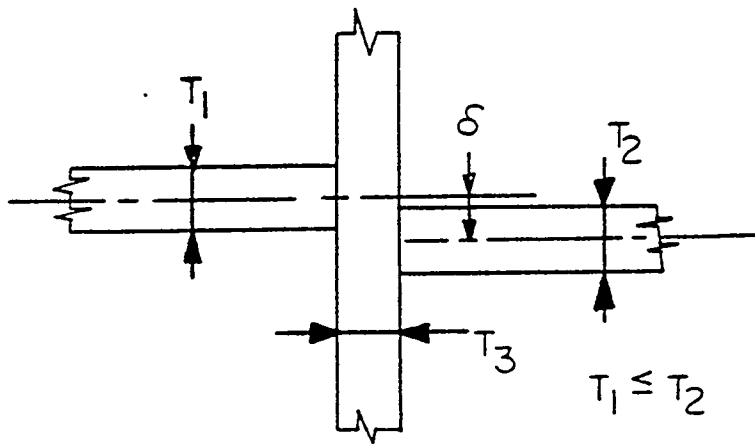S-N DIAGRAM FOR
CRUCIFORM JOINTS
MILD STEEL: $\frac{\delta}{T_1}$ = .0

TABLE 5-2

MISALIGNED CRUCIFORM JOINTS	
δ/T_1	MAXIMUM STRESS RANGE $(R=-1)$
0.0	38400 PSI
0.25	32800 PSI
0.50	28000 PSI
1.0	24000 PSI

$T_1 \leq T_2$

MAXIMUM CALCULATED STRESS
RANGES FOR MISALIGNED CRUCIFORM
JOINTS EXPERIENCING CYCLIC LOADING

Section 6

DATA FOR MISALIGNMENT ACCEPTABILITY GUIDELINES

6.1   GENERAL

This section summarizes the results of static and fatigue
analysis of butt welded and cruciform joints discussed in
Sections 4 and 5.   The relevant plots and tables from those
sections are reproduced here for easy reference.   The
limitations inherent in their potential use can best be .
understood by reading earlier sections.

6.2   STATIC LOADING GUIDELINES

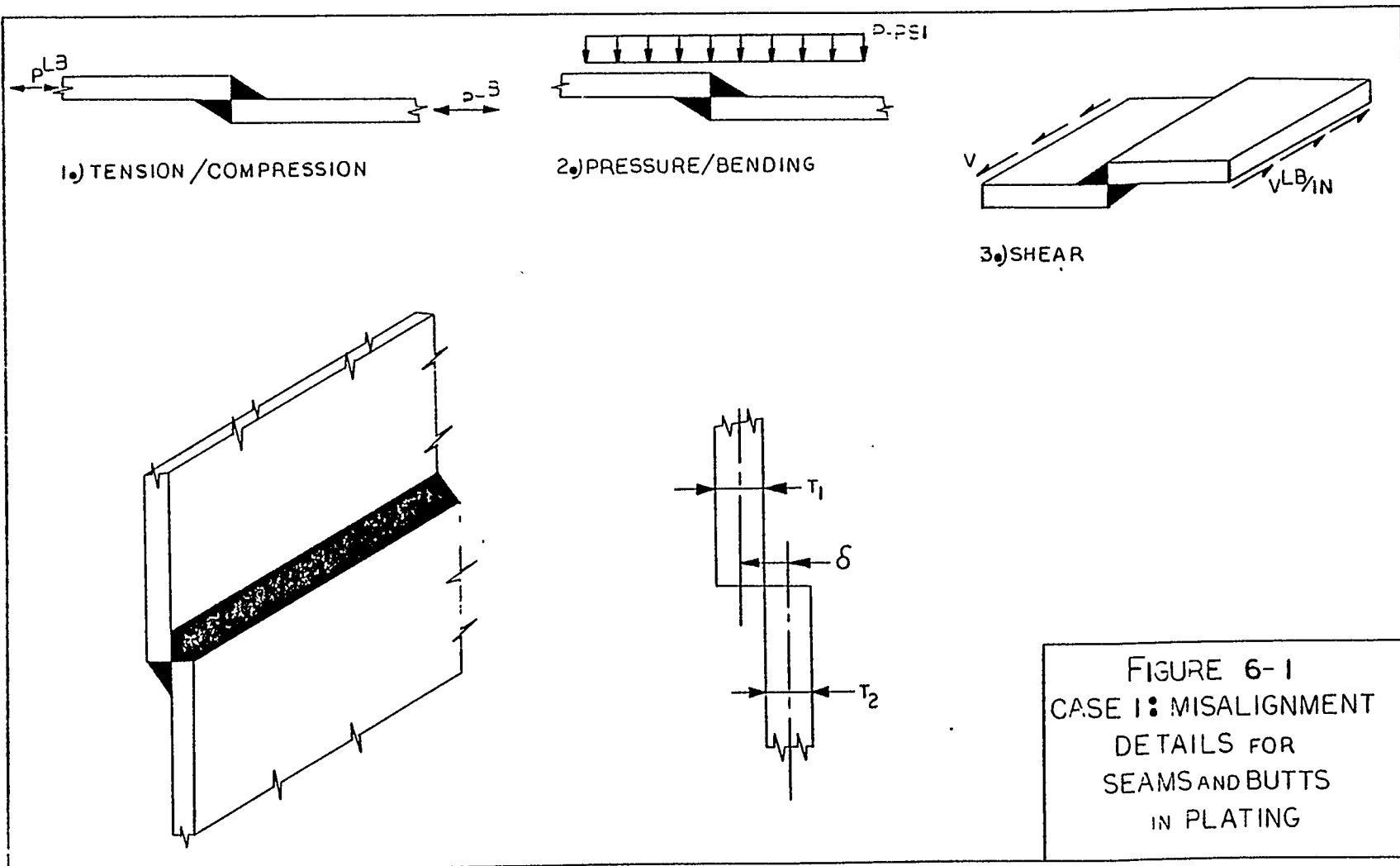6.2.1 Seams and Butts In Plating

Although the title of this section implies seams and butts
in continuous plating, it is not the intent of this section
to exclude butts in web plates, flanges, etc.

Figure 6-1 depicts basic butt misalignment conditions as a
function of type of loading.

The loadings presented in Figure 6-1 can be described as
follows:

Loading 1 Describes a tensile or compressive load which
this and other studies have found to create the most severe
stress condition resulting from the eccentricity of the
reactive or resistive forces, and the stress concentrations
developed at the toe of the weld.   Results indicate that
initial yielding occurs in this area.

Loading 2 Indicates a pressure loading or some form of
bending load.   The effect of this loading on the joint is
limited to the stress concentration occurring at the toe of.

1.) TENSION / COMPRESSION

2.) PRESSURE / BENDING

3.) SHEAR

FIGURE 6-1
CASE I: MISALIGNMENT
DETAILS FOR
SEAMS AND BUTTS
IN PLATING

the weld. As long as an adequate section modulus is main-
tained through the joint, its strength will depend on the
magnitude of the stress concentration factor and not on
the degree of misalignment. The stress concentration may
be reduced by tapering the weld.

Loading 3 Depicts shear loading on the joint. For this
case, the degree of misalignment is not a factor as long as
the cross-sectional area in the weld is equivalent to that
of the plate.

Figure 6-2 presents a set of curves that could be used to
determine the misalignment limit for a butt joint. Four
zones are shown which can be used to determine the ratio of
average stress to allowable stress. Average stress is that
at a distance from the joint and allowable stress is a limit-
ing value based on judgment and experience.

Zone 4 is definitely unacceptable since it implies large
plastic deformation and potential failure. Similarly Zone 1
is too conservative: An allowable stress of $0.6\sigma_Y$ is
acceptable as an average value, with the tacit understanding
that some local increase in acceptable.

Acceptability criteria would be expected to center about the
incipient yield line that separates Zones 2 and 3. In a
potential application, static strength should be checked
whether or not fatigue loading is a consideration.

Suitability for purpose must be considered: Primary hull
structure such as deck or bottom plating should be designed
and built to stricter alignment tolerances than deckhouse
fronts or tween decks, for example.

FIGURE 6-2

EFFECT OF MISALIGNMENT
WELDED BUTT JOINTS
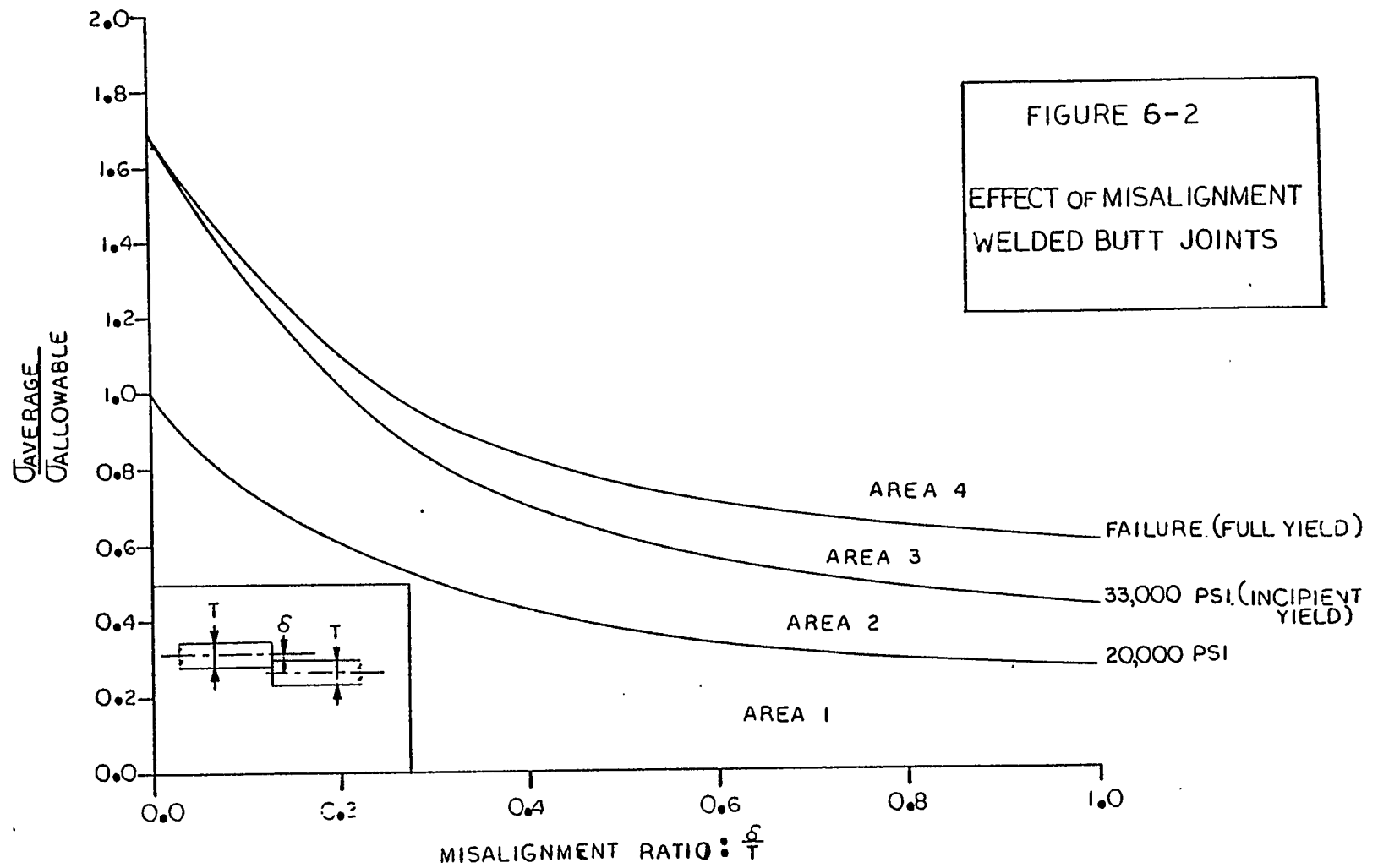
6.2.2 Cruciform Joints In Plating

Figure 6-3 depicts the basic misaligned loading conditions corresponding to cruciform joints. As discussed in Section 6.2.1, load type No. 1 is the most severe and the only one specifically considered in this study.

Figure 6-4 presents curves similar to those in Figure 6-2. These curves can provide misalignment guidelines for fillet welded and full penetration welded joints with ratios of intercostal to through plate thickness of 1.0 and 2.0.

Potential application of data for the four zones in Figure 6-4 is guided by the same criteria of suitability for purpose discussed in Section 6.2.1.

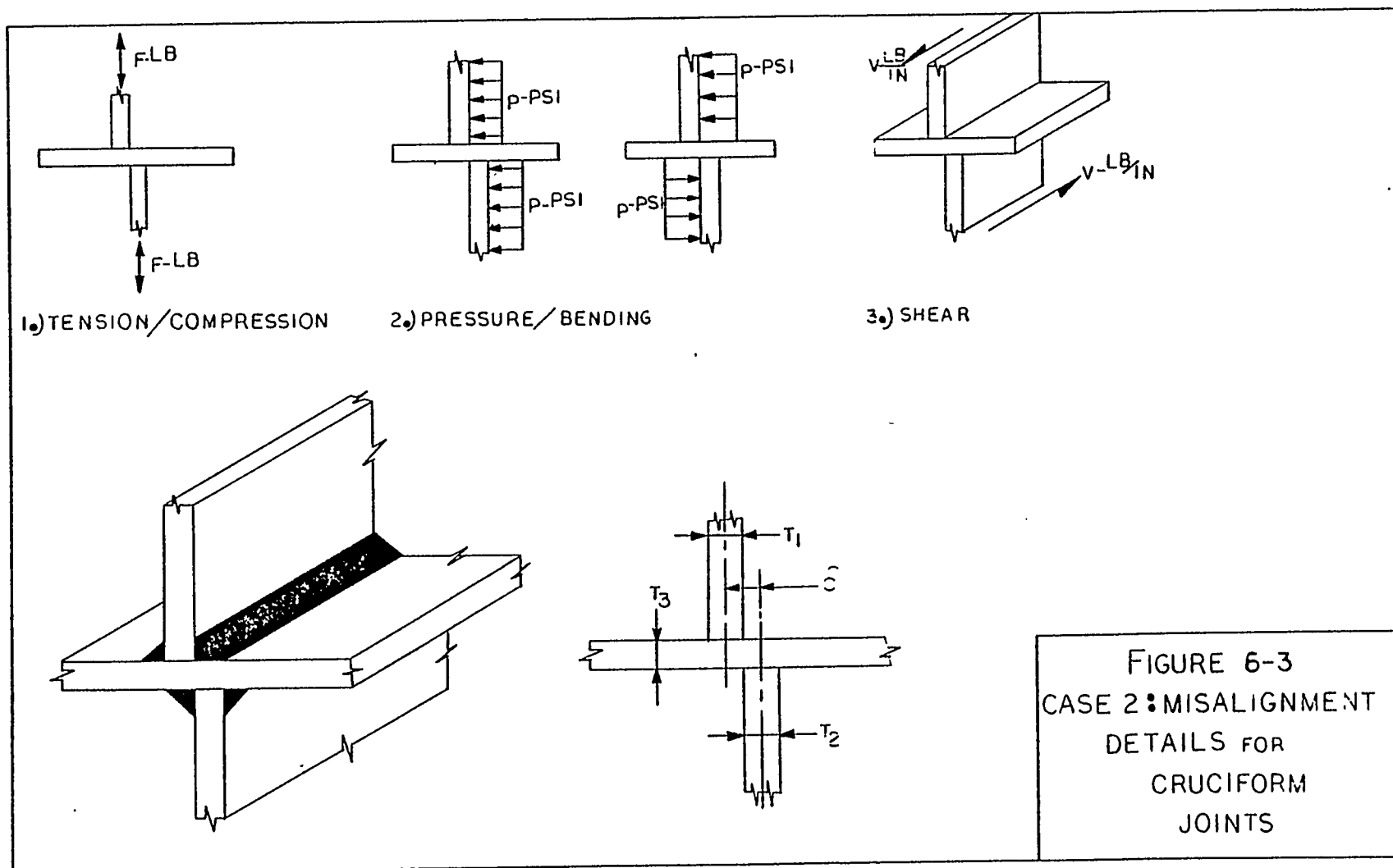### 6.2.3 Modified Cruciform Joints In Continuous Plating

A modified cruciform joint has one or both of its intercostal members entering the joint at an angle other than 90 degrees (Figure 6-5).
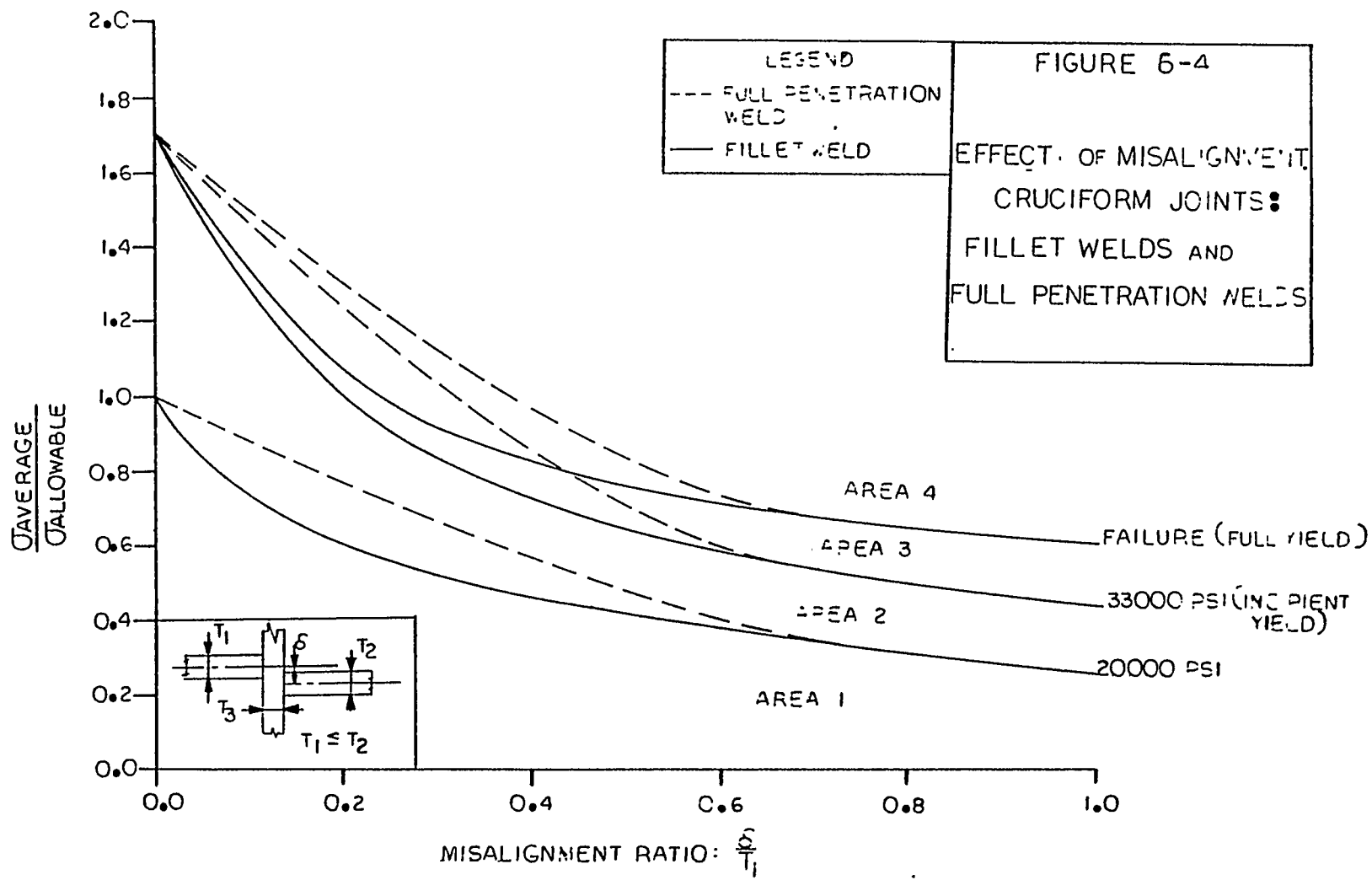
Figure 6-6 describes the perfect alignment case, where all plate centerlines are coincident.
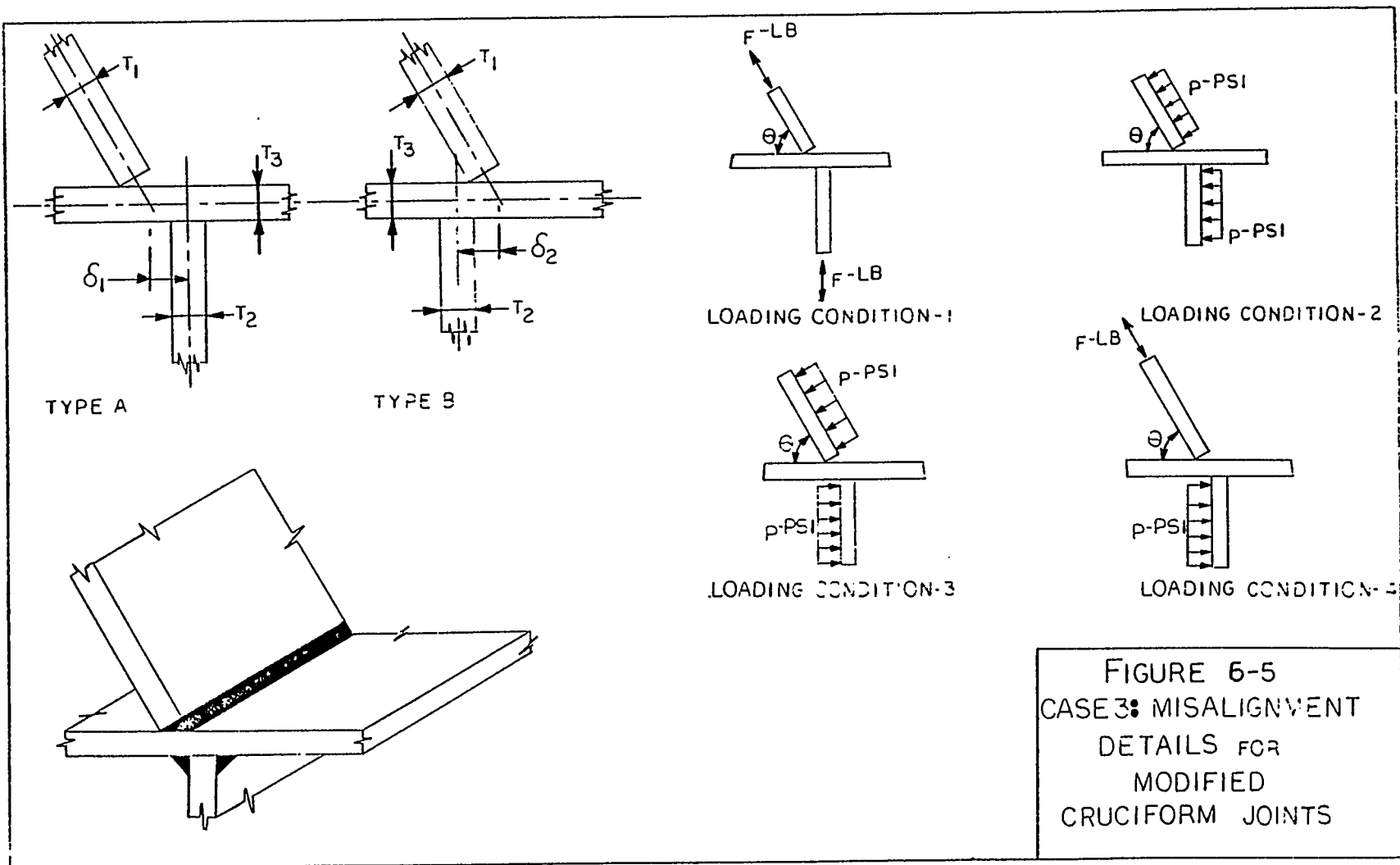
Since the force F can be broken down into components, it is evident that the modified cruciform joint can then be related back to the cruciform joint described in Section 6.2.2.
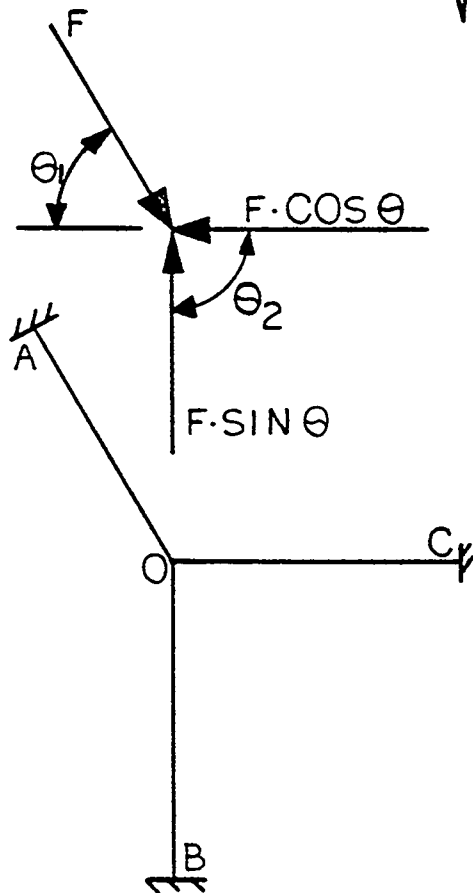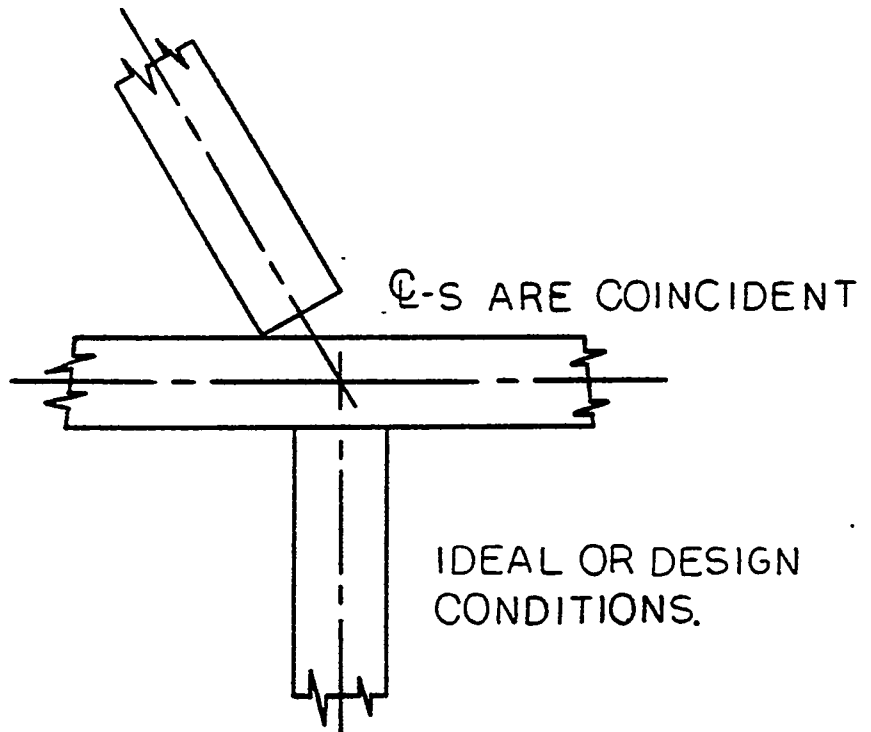
6.2.4 General Categories

The potential for misalignment exists for any welded joint, including chocks, stanchions, bulkhead and deck stiffeners, etc. Evaluation of a misaligned joint may permit assignment to either of the basic categories treated earlier.

1.) TENSION/COMPRESSION   2.) PRESSURE/BENDING   3.) SHEAR

FIGURE 6-3
CASE 2: MISALIGNMENT
DETAILS FOR
CRUCIFORM
JOINTS

FIGURE 6-4

EFFECT OF MISALIGNMENT
CRUCIFORM JOINTS:
FILLET WELDS AND
FULL PENETRATION WELDS

TYPE A

TYPE B

LOADING CONDITION-1

LOADING CONDITION-2

LOADING CONDITION-3

LOADING CONDITION-4

FIGURE 6-5
CASE 3: MISALIGNMENT
DETAILS FOR
MODIFIED
CRUCIFORM JOINTS

℄-S ARE COINCIDENT

IDEAL OR DESIGN
CONDITIONS.

$\theta_1 = 90°$: CASE 2

$$\sigma_{AO} = F/A_X$$
$$\sigma_{BO} = FSIN\theta/A_X$$
$$\sigma_{CO} = FCOS\theta/A_X$$

FIGURE 6-6
IDEAL CONDITION FOR
MODIFIED CRUCIFORM
JOINTS

Figures 6-7 and 6-8 depict a few examples of joints with potential misalignment which are common in ship structure.

If a misaligned member is a component of a larger structural system it may deserve special consideration. For example, a single misaligned stiffener in a transverse bulkhead will cause a load redistribution to adjacent members which implies a less severe condition than if several stiffeners were misaligned.

6.3   CYCLIC LOADING GUIDELINES

Ship bottom, side shell and deck structural elements are subject to cyclic loading as a result of pressure, shear and bending moment variation resulting from passage through waves.
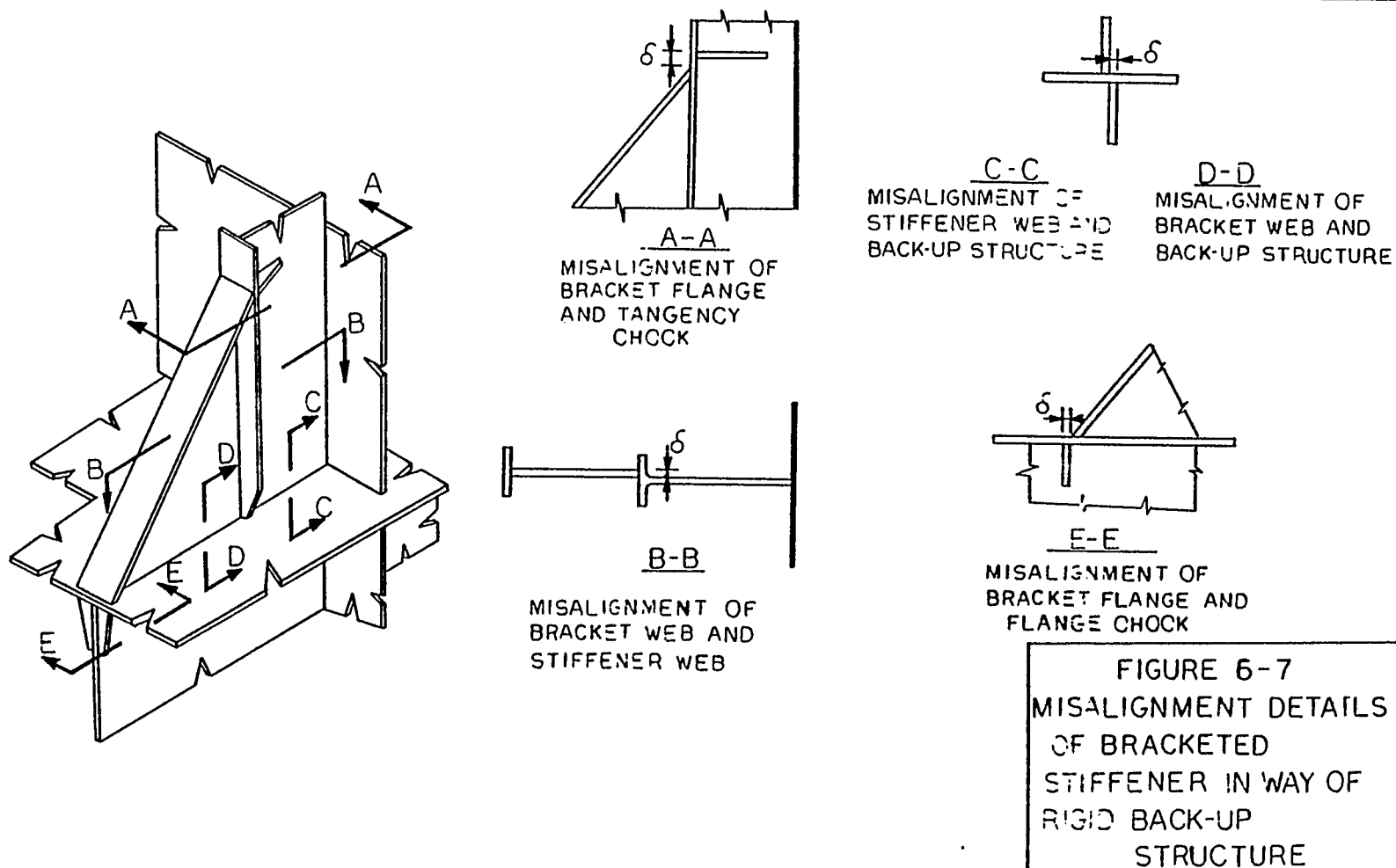
Limited experimental data on fatigue strength of misaligned joints have been empirically extended to provide a basis for acceptability guidelines.
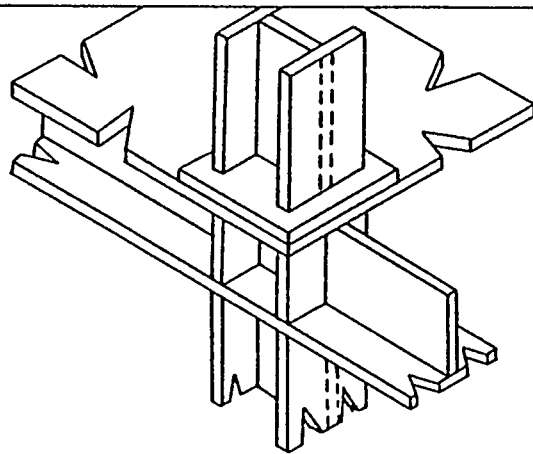
6.3.1 Butts and Seams In Plating

Figure 6-9 presents extrapolated S-N curves for a stress ratio * R = -1 for butt welds with misalignment ratio $\frac{e}{t}$ of 0.0, 0.2, 0.4 and 0.6.
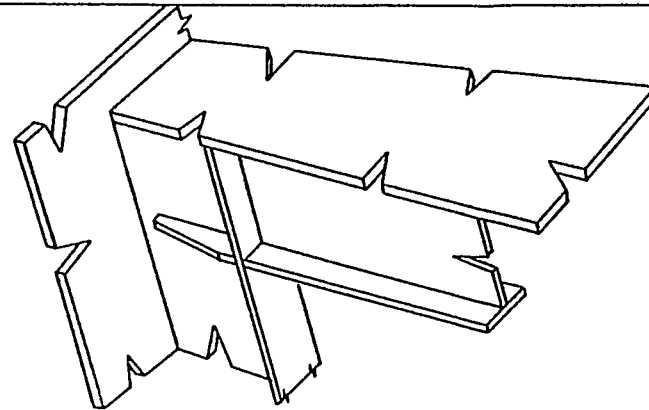
The load spectrum for a ship element is generally made up of a few cycles at large stress amplitude with ever increasing cycles at progressively lower stress amplitudes. By using the Palmgren-Miner cumulative fatigue damage criterion with a factor of safety of about 2.0, it is possible to establish the maximum permissible stress range (difference between maximum and minimum stress in a load cycle) for a given degree of misalignment. Those data are presented in Table 6-1.

_____

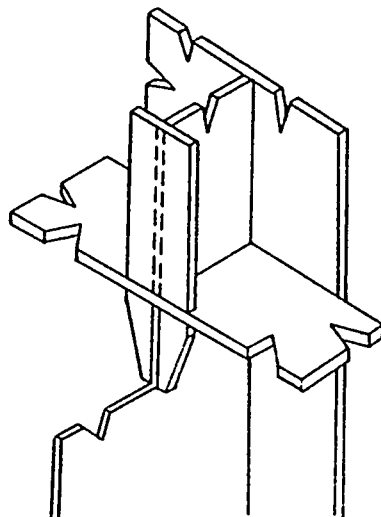* stress Ratio R = algebraic ratio of minimum to maximum stress in a load cycle.

δ

C-C
MISALIGNMENT OF
STIFFENER WEB AND
BACK-UP STRUCTURE

D-D
MISALIGNMENT OF
BRACKET WEB AND
BACK-UP STRUCTURE

δ

A-A
MISALIGNMENT OF
BRACKET FLANGE
AND TANGENCY
CHOCK

δ

B-B
MISALIGNMENT OF
BRACKET WEB AND
STIFFENER WEB

δ

E-E
MISALIGNMENT OF
BRACKET FLANGE AND
FLANGE CHOCK

FIGURE 6-7
MISALIGNMENT DETAILS
OF BRACKETED
STIFFENER IN WAY OF
RIGID BACK-UP
STRUCTURE

MISALIGNMENT OF STANCHIONS

MISALIGNMENT OF DECK GIRDERS
WITH SHELL FRAMES

MISALIGNMENT OF BULKHEAD
GIRDERS AND BACK-UP
STRUCTURE

FIGURE 6-8
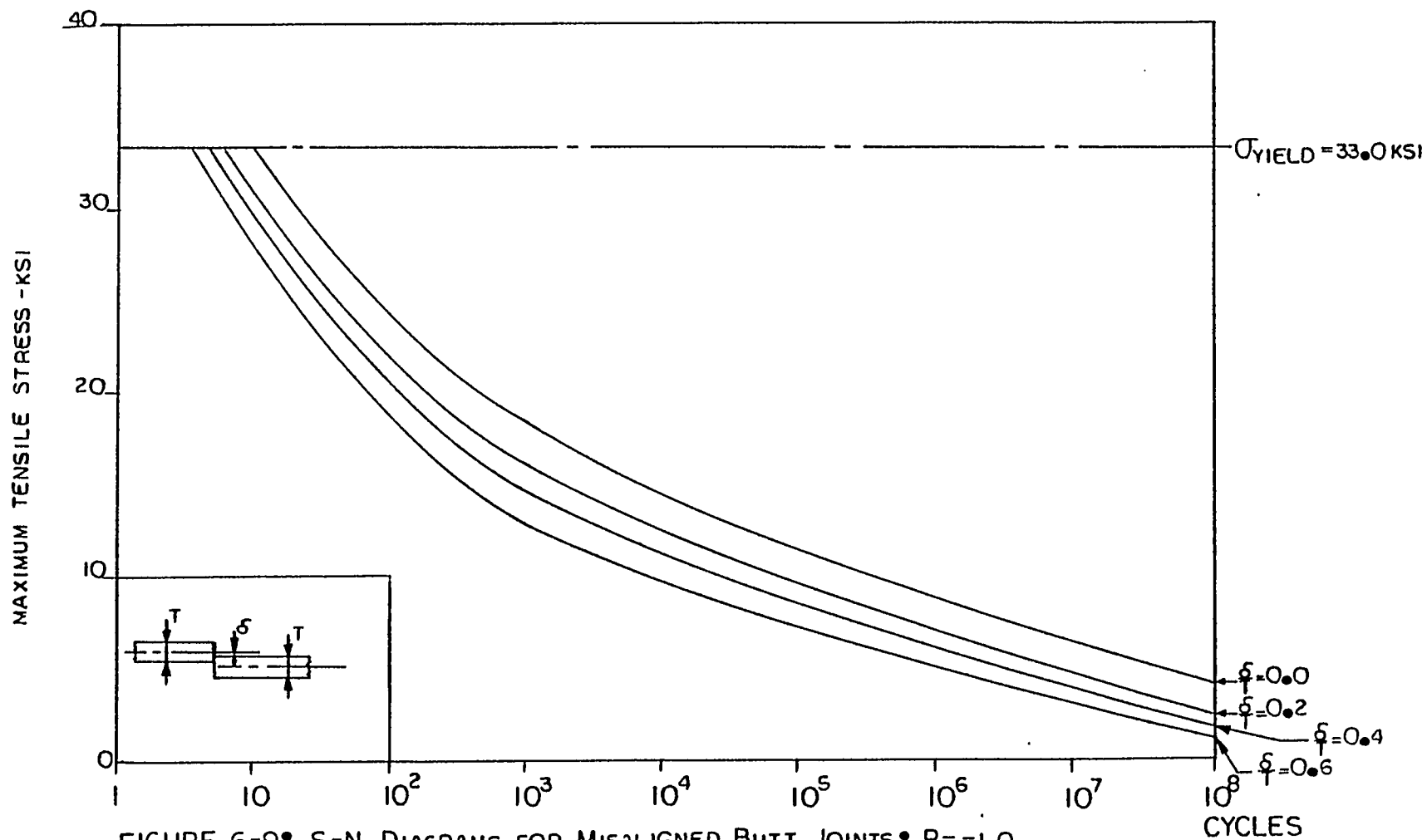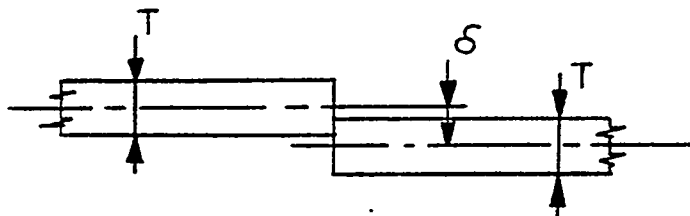MISALIGNMENT
DETAILS OF TYPICAL
SHIPBOARD
STRUCTURE

FIGURE 6-9: S-N DIAGRAMS FOR MISALIGNED BUTT JOINTS: R=-1.0

6-13

TABLE 6-1

MISALIGNED BUTT WELDS	
δ/T	MAXIMUM STRESS RANGE$^{(R=-1)}$
0.0	37200 PSI
0.2	29200 PSI
0.4	26000 PSI
0.6	15600 PSI

MAXIMUM CALCULATED STRESS
RANGES FOR MISALIGNED BUTT
WELDS EXPERIENCING CYCLIC LOADING

The maximum stress range can be approximated during design
evaluation by calculating maximum and minimum stresses due
to pressure, shear or bending moment based on any established
quasistatic extreme wave height criterium, such as L/20 or
$1.1\sqrt{L}$. Cyclic distributions other than those due to long
term exposure to waves should be calculated by direct
reference to the S-N diagrams of Figure 6-9, using the
methodology discussed in Section 5.

6.3.2 Cruciform Joints

Figure 6-10 presents extrapolated S-N curves for a stress
ratio R = -1 for cruciform joints with $\frac{e}{t}$ misalignment
ratios of 0.00, 0.25, 0.50 and 1.00.

By the method discussed in Section 6.3.1, maximum calculated
stress ranges for cruciform joints subject to long term
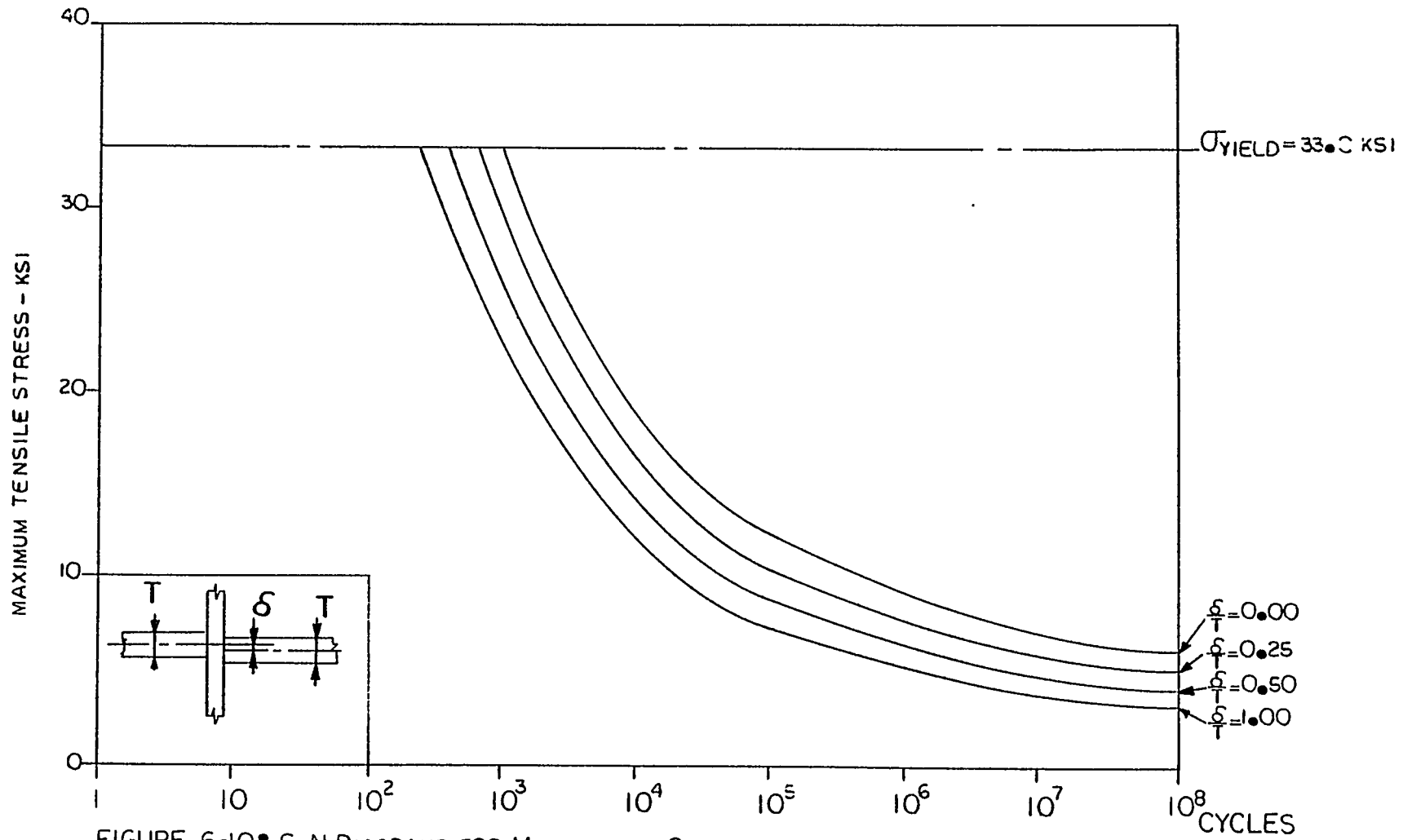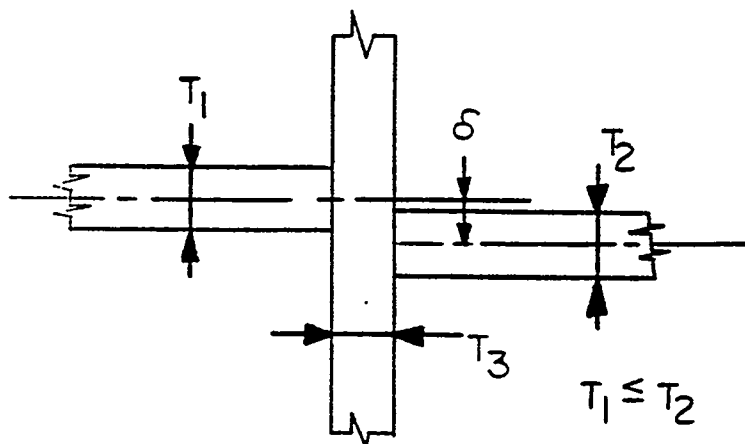wave load distributions are shown in Table 6-2.

FIGURE 6-10: S-N DIAGRAMS FOR MISALIGNED CRUCIFORM JOINTS: R=-1.0

TABLE 6-2

MISALIGNED CRUCIFORM JOINTS	
δ/T_1	MAXIMUM STRESS RANGE$^{(R=-1)}$
0.0	38400 PSI
0.25	32800 PSI
0.50	28000 PSI
1.0	24000 PSI

MAXIMUM CALCULATED STRESS RANGES FOR MISALIGNED CRUCIFORM JOINTS EXPERIENCING CYCLIC LOADING

Saction 7
SURVEY OF STRUCTURAL ALTERATIONS TO
CORRECT MISALIGNMENT

7.1 GENERAL

During ship construction structural alterations are sometimes
required to correct construction errors and to accommodate
design modifications made during the manufacturing process.
These may include addition or deletion of temporary and
permanent openings, reduction in scantlings, misalignment,
unfairness, etc. These alterations and corrections must be .
made in a manner that meets the physical and operational
objectives of the specification and the requirements of the
regulatory agencies. It is in the best interests of the
shipbuilder and the owner that these alterations be accom-
plished in a timely manner, using the most economical
combination of material, labor and facilities, to produce a
product that meets the above requirements.

The following sections provide the designer with a collection
of corrective methods for misalignment errors that have
exceeded permissible limits. No recommendations accompany
this review.

7.2 MISALIGNMENT OF BUTTED MEMBERS

Misalignment of butted members may range from very large
 (200-ton) units to single flat bar stiffeners. When plating
misalignment is to be corrected, the most often used method
is to force the two plates into acceptable alignment by the
use of jacks, wedges and weights and then weld the joint.
To reduce the effect of stress concentrations, the weld is
tapered or "buttered" so that the toe angle is small. Mis-
alignment of butts or seams in plating is generally allowed
only over a small portion of the total joint length.

7.2.1 Flanges

Figure 7-1 depicts a misalignment condition between member flanges. Five methods for correcting this misalignment are presented. Methods 1, 2 and 3 involve the removal of a section of the web plate and possibly of the flange and the rewelding of a tailored section which provides a continuous load path for the flanges. Methods 4 and 5 show the inclusion of a flange reinforcing member which requires less work but conversely will introduce higher stress concentrations.

7.2.2 Web Plates

Figure 7-2 indicates three methods for correcting misalignment of butted web plates. These methods may be applied to tees, angles and flat bars. When misalignment between web plates occurs, the most common correction method is to cut the web plate free of the supporting member and force the webs into alignment. Method 2 presents an example of the correction with a recommended disengagement length of 50T where T = web plate thickness. When the misalignment is too great to force the webs into alignment it may be necessary to replace a portion of the member. Method 1 depicts the introduction of a skewed filler piece while Method 3 shows the addition of a web splice and a flange doubler plate. When the misaligned members carry large lateral loads and are skewed, knuckled *or* bent, it is recommended that a support member be installed as close to the knuckle as possible, see Figure 7-3 for details.

### 7.3 MISALIGNMENT OF CRUCIFORM JOINTS

Cruciform joints are the most susceptible to misalignment. This form of misalignment would appear to be a direct result of inaccuracies in fit-up and the inability of the shipfitter to properly locate back-up structure. This problem may range in severity from the single misaligned bulkhead stiffener to the complete misalignment of the machinery casing with its back-up structure.
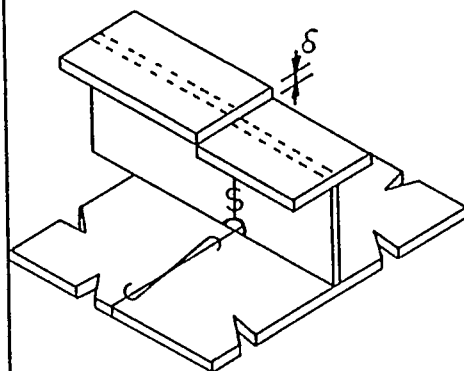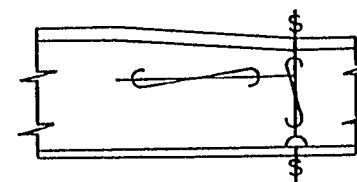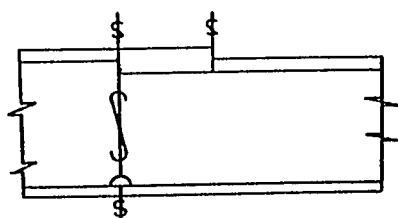
MISALIGNMENT EXAMPLE
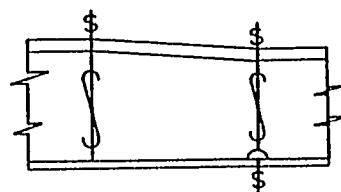
METHOD-1:
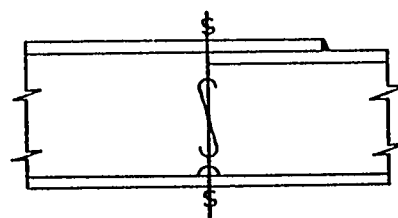REMOVE SECTION OF
GIRDER, REPLACE WITH
TAILORED SECTION.
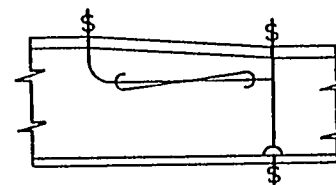
METHOD-2:
COPE OUT A SECTION
OF ONE OF THE MEMBERS,
REPLACE WITH A
TAILORED SECTION.

METHOD-3:
REMOVE A WEDGE-
SHAPED PIECE OF WEB
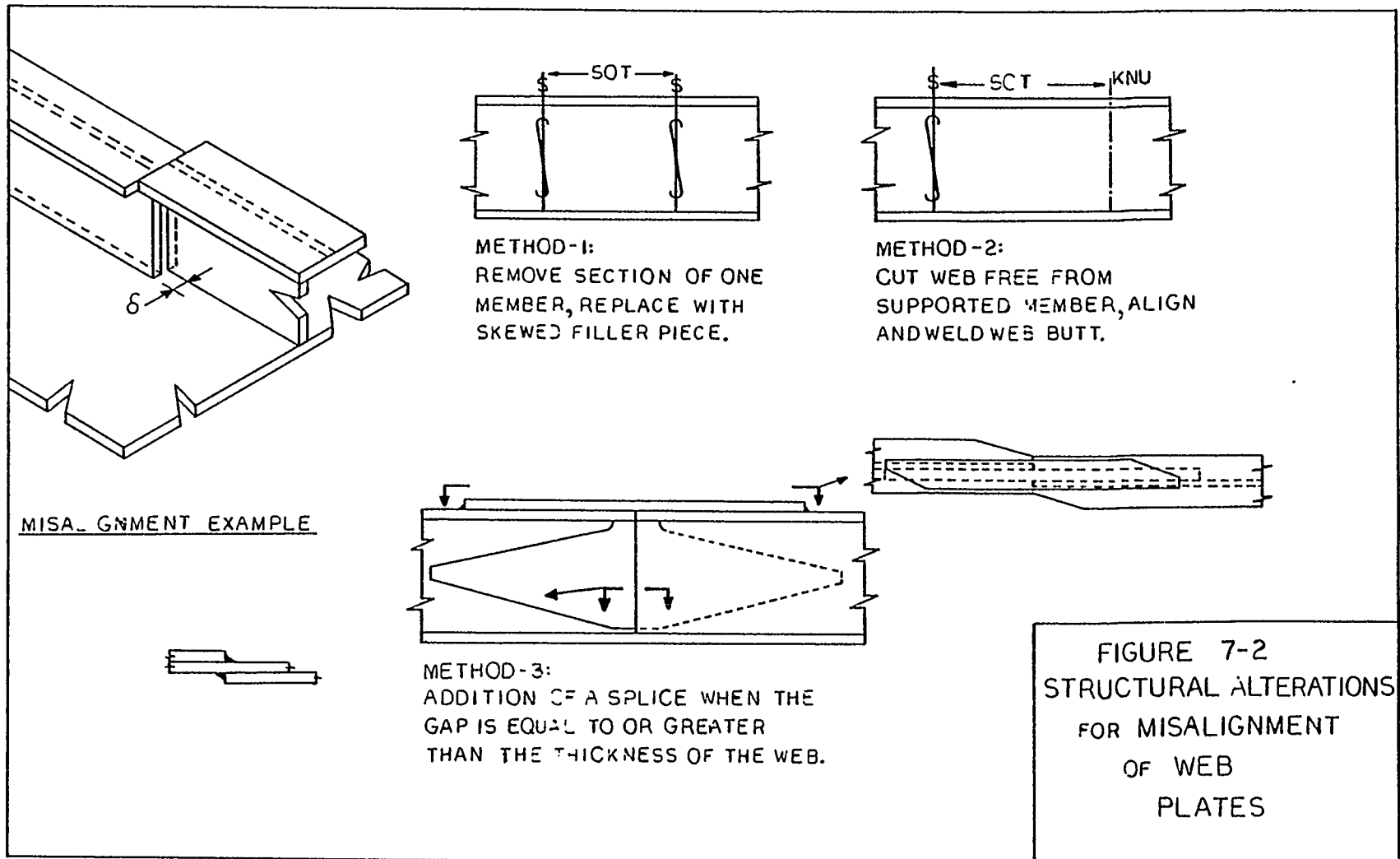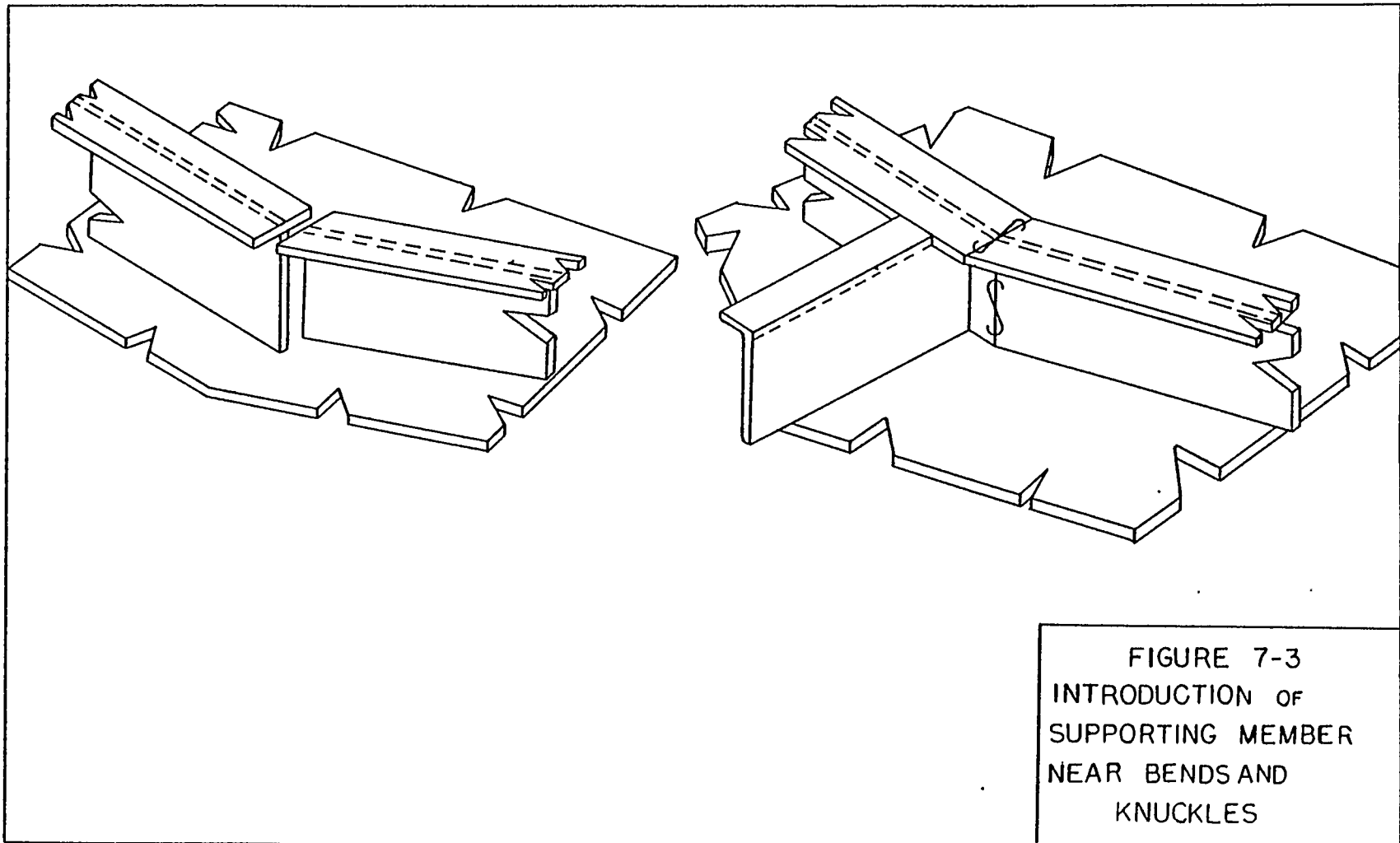BEND FLANGE DOWN
REWELD.

METHOD-4:
REMOVE SECT·ON OF
FLANGE, REPLACE WITH
INSERT PLATE.

METHOD-5:
ADD NEW CHOCK TO
FLANGES.

FIGURE 7-1
STRUCTURAL ALTERATIONS
FOR
MISALIGNMENT OF
BUTTED FLANGES

MISALGNMENT EXAMPLE

METHOD-1:
REMOVE SECTION OF ONE
MEMBER, REPLACE WITH
SKEWED FILLER PIECE.

METHOD-2:
CUT WEB FREE FROM
SUPPORTED MEMBER, ALIGN
AND WELD WEB BUTT.

METHOD-3:
ADDITION OF A SPLICE WHEN THE
GAP IS EQUAL TO OR GREATER
THAN THE THICKNESS OF THE WEB.

FIGURE 7-2
STRUCTURAL ALTERATIONS
FOR MISALIGNMENT
OF WEB
PLATES

FIGURE 7-3
INTRODUCTION OF
SUPPORTING MEMBER
NEAR BENDS AND
KNUCKLES

7.3.1 Continuous Plating

Misaligned cruciform joints are normally corrected by increasing the leg of the fillet weld or by adding doubler plates. Figure 7-4 presents three methods by which mis-alignment may be corrected. Method 1 shows a weld increase, however this method is limited to small values of & since the larger the weld size the greater the opportunity for a poor weld and for excessive deformation.

Methods 2 and 3 employ doublers or sole plates to improve the error in alignment. An evaluation of the adequacy of these methods is not attempted.

7.3.2 Stiffeners, Beams and Stanchions

Figure 7-5 shows common methods for correcting alignment errors in the above structural elements.

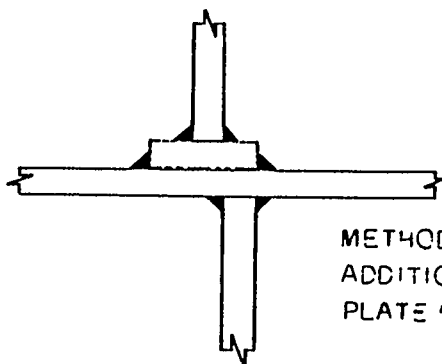**7.4** MISALIGNMENT OF MODIFIED CRUCIFORM JOINTS

Figure 7-6 depicts a misaligned modified cruciform joint with a set of common corrective methods. Methods 1 through 3 have been discussed in Section 7.3.1, Methods 4 through 6 are similar with some degree of modification. This type of detail is used for foundations, miscellaneous bulkheads and where structure is added on and common reference points do not exist.
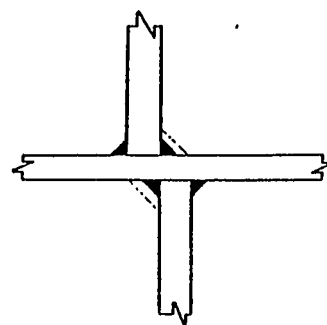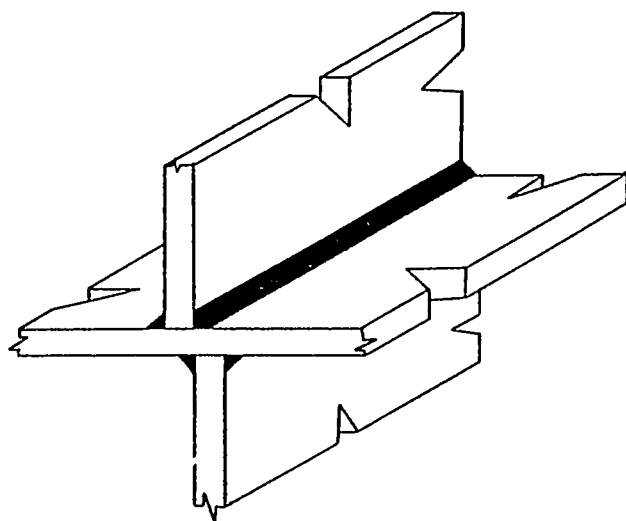
METHOD 1:
INCREASE LEG OF FILLET
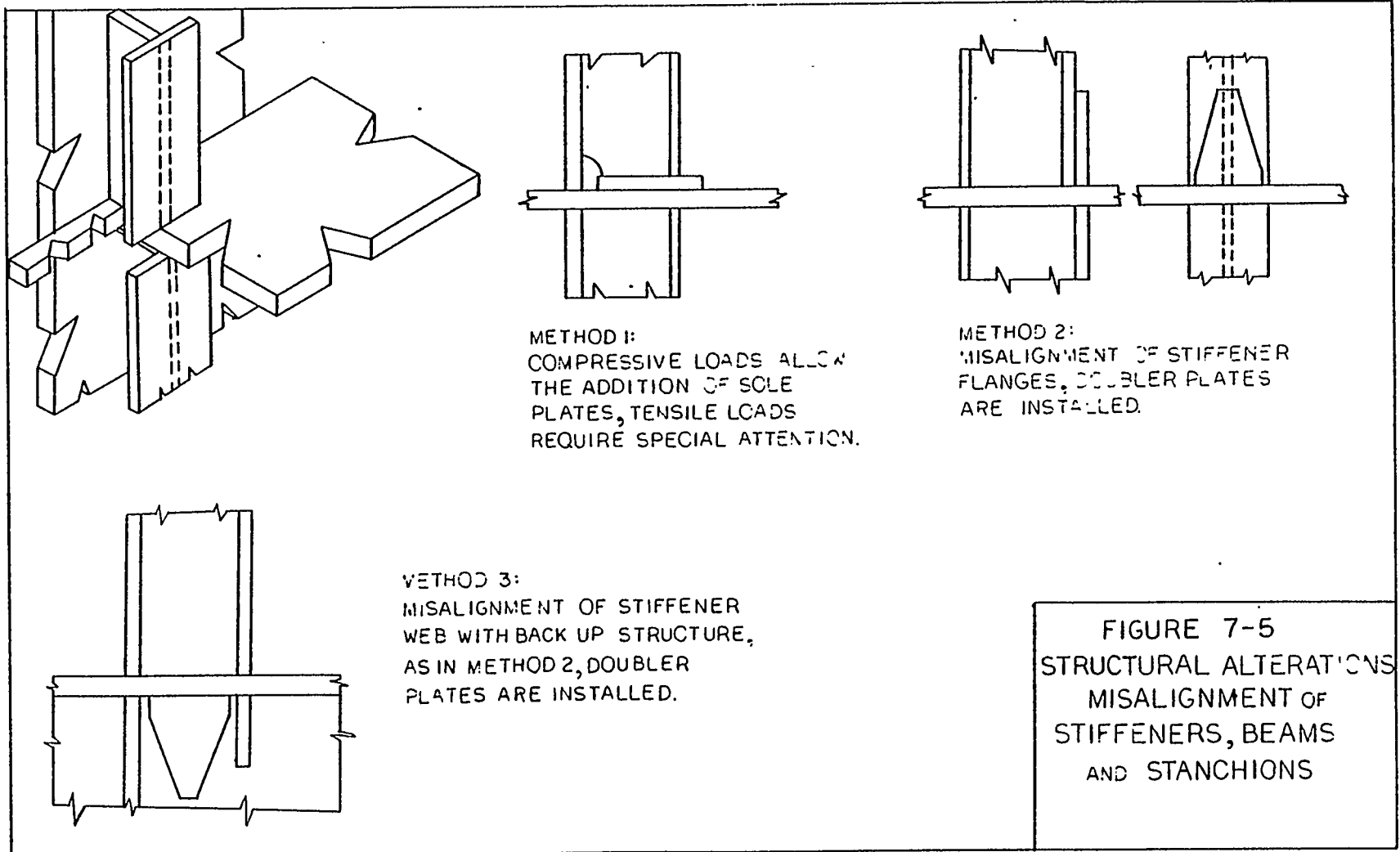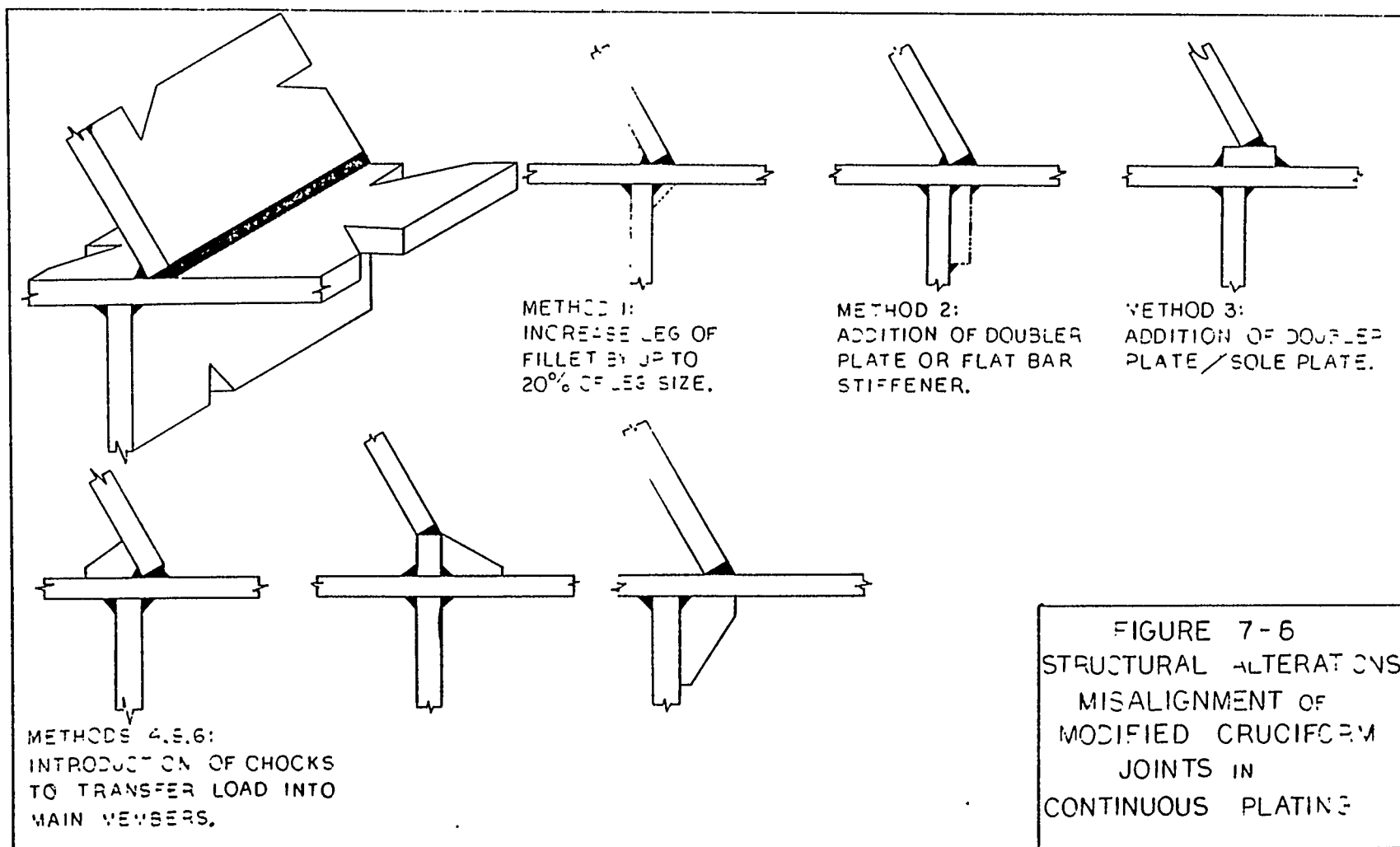WELD BY UP TO 20% OF
LEG SIZE.
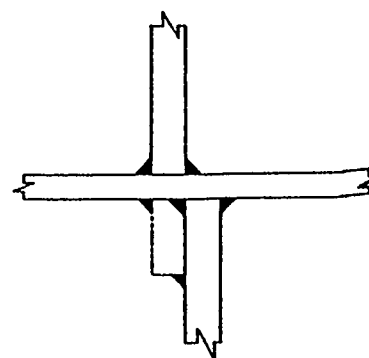
METHOD 2:
ADDITION OF DOUBLER
PLATE OR FLAT BAR.

METHOD 3:
ADDITION OF DOUBLER
PLATE OR SOLE PLATE.

FIGURE 7-4
STRUCTURAL ALTERATIONS
MISALIGNMENT OF
CRUCIFORM
JOINTS
CONTINUOUS PLATING

METHOD I:
COMPRESSIVE LOADS ALLOW
THE ADDITION OF SOLE
PLATES, TENSILE LOADS
REQUIRE SPECIAL ATTENTION.

METHOD 2:
MISALIGNMENT OF STIFFENER
FLANGES, DOUBLER PLATES
ARE INSTALLED.

METHOD 3:
MISALIGNMENT OF STIFFENER
WEB WITH BACK UP STRUCTURE,
AS IN METHOD 2, DOUBLER
PLATES ARE INSTALLED.

FIGURE 7-5
STRUCTURAL ALTERATIONS
MISALIGNMENT OF
STIFFENERS, BEAMS
AND STANCHIONS

METHOD 1:
INCREASE LEG OF
FILLET BY UP TO
20% OF LEG SIZE.

METHOD 2:
ADDITION OF DOUBLER
PLATE OR FLAT BAR
STIFFENER.

METHOD 3:
ADDITION OF DOUBLER
PLATE / SOLE PLATE.

METHODS 4,5,6:
INTRODUCTION OF CHOCKS
TO TRANSFER LOAD INTO
MAIN MEMBERS.

FIGURE 7-6
STRUCTURAL ALTERATIONS
MISALIGNMENT OF
MODIFIED CRUCIFORM
JOINTS IN
CONTINUOUS PLATING

Section 8

LIST OF REFERENCES

1. Basar, N. S. and Stanley, R. F., "Survey of Structural Tolerances in the United States Commercial Shipbuilding Industry", Navships No. 0935-00-042-6010.

2. Swedish Shipbuilding Standards Institute, "Accuracy in Hull Construction", Report No. VIS 530, January 1976.

3. "Japanese Shipbuilding Quality Standards" (J.S.Q.S.) (Hull Part) SNAJ Publication 8-2, Tokyo, 1975.

4. "Production Standard of the German Shipbuilding Industry", Association of the German Shipbuilding Industry, Hamburg, November 1974.

5. "IHI SPAIS-The Shipbuilding and Process and Inspection Standard", Ikawajima-Harima Heavy Industries Co., Ltd., November 1973.

6. "Rules for the Building and Classing Steel Vessels", American Bureau of Shipping, New York 1976.

7. "Rules and Regulations for the Construction and Classification of Steel Vessels", Bureau Veritas, Paris, 1975.

8. "Rules for the Construction and Classification of Steel Ships", Det Norske Veritas, Oslo, 1975.

9. "Rules for the Classification and Construction of Seagoing Steel Ships", Germanischer Lloyd, Hamburg, 1973.

10. "Rules and Regulations for the Construction and Classification of Steel Ships", Lloyd's Register of Shipping, London, 1975.

LIST OF REFERENCES (Cont'd)

11. "Rules and Regulations for the Construction and
     Classification of Ships", Nippon Kaiji Kyokai,
     Tokyo, 1975.

12. Nishimaki, K., "Fatigue Strength of Butt Joints With
     Misalignment", SNAJ Publication, Tokyo.

13. Hagiwara, K., "An Experimental Study on Reduction of
     Fatigue Strength Due to Discrepancy at Welded Joints",
     SNAJ Publication, Tokyo.

14. Not Used

15. Not Used

16. Harrison, J. D. and Young, J. G., "The Acceptability
     of Weld Defects", The Royal Institution of Naval
     Architects, London, 1974.

17. Goodman, R. A. and Mowatt, G. A., "Assessment of
     Imperfections in Ship Structural Design", Lloyd's
     Register of Shipping, London, 1976.

18. Logcher, R. D., Et. Al., "The Structural Design
     Language Engineering User's Manual" – Volume 1 and
     2, Massachusetts Institute of Technology, Cambridge,
     1968.

19. Connor, J. and Will, G., "Computer-Aided Teaching of
     The Finite Element Displacement Method", Massachusetts
     Institute of Technology, Cambridge, 1969.

20. Gurney, T. R., "Finite Element Analyses of Some Joints
     With the Welds Transverse to the Direction of Stress",
     The Welding Institute, 1975.

21. Mowatt, G. A., "The Strength of Ship Structural
     Elements", Transactions of North East Coast
     Institution of Engineers and Shipbuilders, December
     1974.

LIST OF REFERENCES (Cont'd)

22. Satoh, K. and Others, "Treatment of Misfit in Tee and
     Cruciform Weld Connections", Journal of the society
     of Naval Arch of Japan, Vol. 136.

23. Glasfeld, R. D., and others, "Review of Ship structural
     Details", Ship Structure Committee Report SSC-266, 1977.

24. Brockenbrough, R. L. and Johnston, B. G., "USS Steel
     Design Manual - Chapter 10: Design for Repeated Loads",
     ADUSS 27-3400-01, July 1968.

APPENDIX A

CALCULATIONS FOR ELASTO-PLASTIC
ANALYSIS OF MISALIGNED JOINTS

This Appendix Contains Computations Relative to
Section 4 - Results of Finite Element Analysis

Appendix A

Part A:

THIS APPENDIX CONTAINS THE COMPUTATIONS NECESSARY TO PERFORM THE PLASTIC ANALYSIS FOR THE BUTT WELDED JOINT WITH A 1.0T MISALIGNMENT. SEE FIGURE 4-6 FOR CORRESPONDING DETAILS:

Load Case 1:

$P = 4000^{LB}$

ELEMENT 74 & 79:
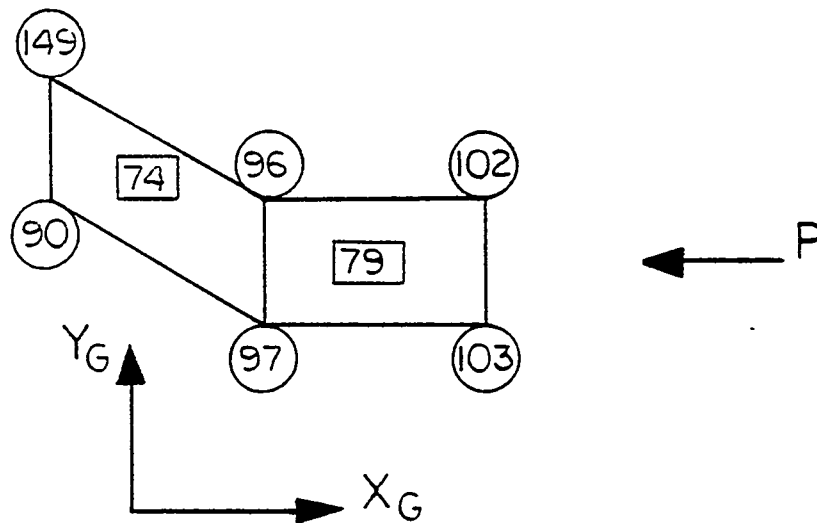
S_{xx}	S_{yy}	S_{xy}:
149: −21441 PSI	−6034	8470
90: −8924 PSI	−6694	7400
96: −32754 PSI	−4768	4430
97: −18365 PSI	+1409	3794
102: −31714 PSI	−3049	640
103: −17854 PSI	+2751	−3049

A-1

$$\sigma_T = \sqrt{S_{XX}^2 + S_{YY}^2 - S_{XX}S_{YY} + 3S_{XY}^2}$$

149: -24124 PSI

90: 15132 PSI

96: 31600 PSI

97: 19234 PSI

102: 30325 PSI

103: 20083 PSI

NODE 96:

$$\sigma_T = 31600 \text{ PSI} < \sigma_{YIELD}$$

$P = 4000^{LB}$ — ELASTIC RANGE:

YIELD LOAD:

$$P_Y = \frac{4000 \times \sigma_T}{31600} = 4177^{LB}$$

YIELDING OF NODE 96:

NODE 102:

YIELD LOAD: $P_Y = 4353^{LB}$

ELEMENT 79 MUST THUS BE MODIFIED TO REFLECT ARTIFICIAL MATERIAL PROPERTIES.
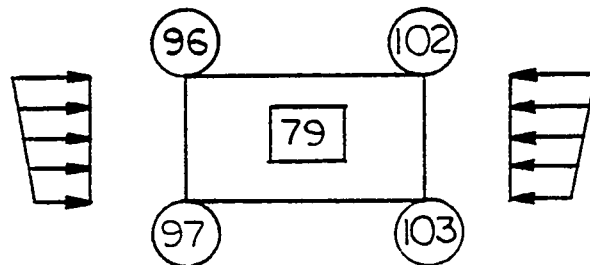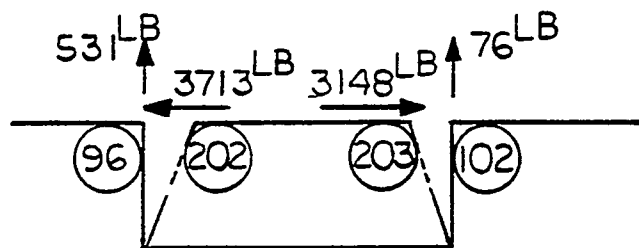
ELEMENT 79 YIELDS SEE DETAIL A, FIGURE 4-8 ,
P = 4200^{LB}

ELEMENT 24,28,33:
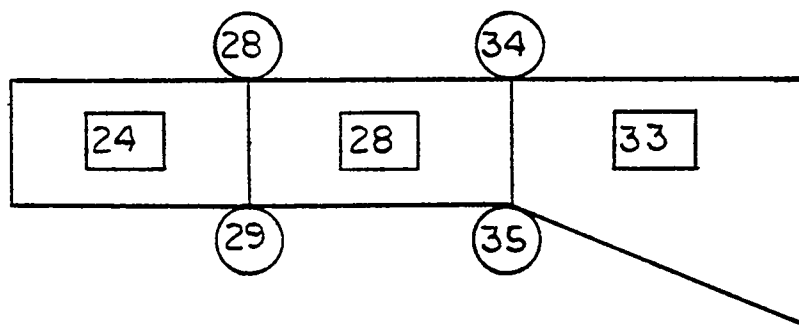
S$_{XX}$:	S$_{YY}$	S$_{XY}$
28:-16080 PSI	2070 PSI	482 PSI
29:-27288 PSI	-2505 PSI	530 PSI
34:-13782 PSI	2063 PSI	3184 PSI
35:-28000 PSI	3739 PSI	3881 PSI

σ_T:

17229 PSI

26141 PSI

15907 PSI

30787 PSI

YIELD LOAD: NODE 35:
$$P_Y = \frac{4200 \times \sigma_Y}{30787} = 4500^{LB}$$

YIELD LOAD: NODE 29: $P_Y = 5300^{LB}$

ELEMENT 28 & 33: NODE 35 YIELDS AT $P = 4500^{LB}$
SEE DETAIL B, FIGURE 4 - 8.

ELEMENT 28,33: NODE 35
ARTIFICIAL MATERIAL PROPERTIES:
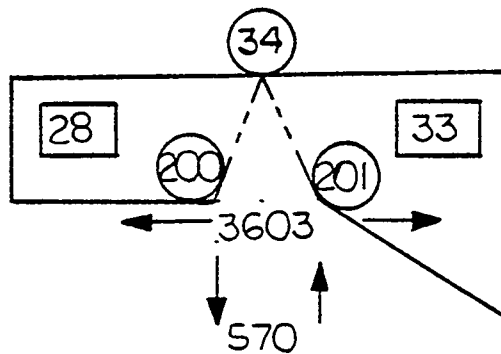
ELEMENTS: 74,75,79,80,84,85:
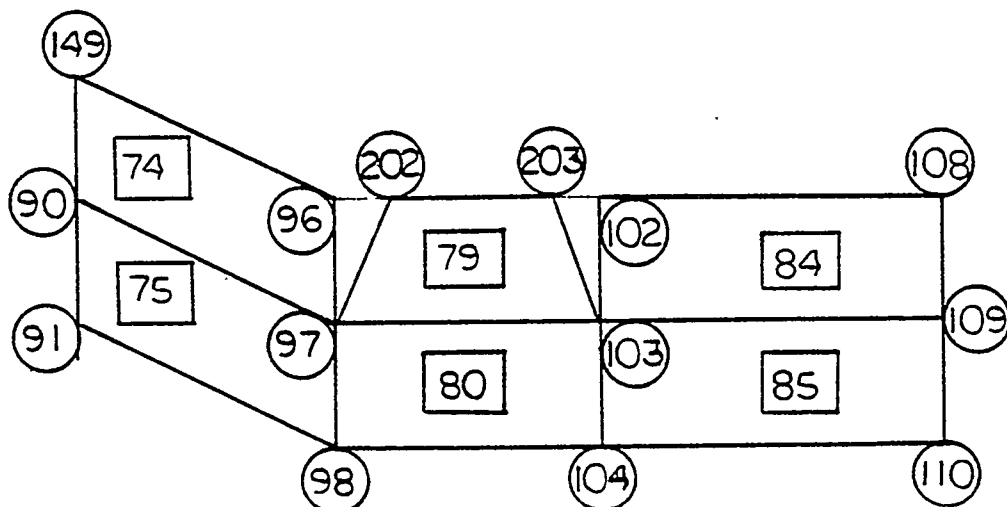
	Sxx: PSI	Syy: PSI	Sxy: PSI	σ_T: PSI
90	−14875	−1787	4468	16055
91	−13940	−1520	−272	13253
96	−32145	−4773	3201	30664
97	−23691	−2614	2223	22825
98	−15778	−2901	−103	14547
102	−31882	−2124	4350	31780
103	−21991	−462	1973	22032
104	−12381	−300	1219	12415
108	−32261	−3008	−5563	32336
109	−22031	−1170	−4965	23128
110	−12164	−400	2885	12970
149	−18808	−4356	6881	20805

P_Y − NODE 108 = 4600^{LB}

ELEMENT 84,89: NODE 108: SEE DETAIL C, FIGURE 4−8

REMOVE NODE 108:
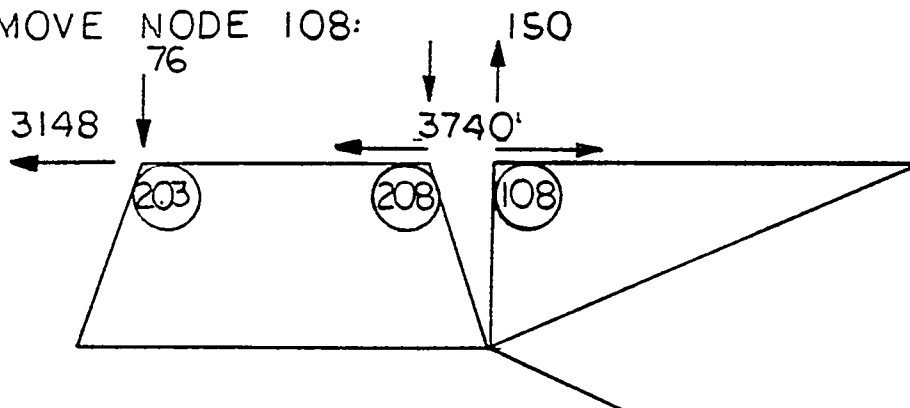
LOAD CASE 3:

P = 4600^{LB} + INCREMENTAL LOADING

P = 5300^{LB}/NODE 29 YIELDS.

	Sxx: PSI	SYY: PSI	SXY: PSI	σ_T: PSI
90	−18056	−1930	5663	19776
91	−13600	902	1707	14380
97	−30604	−5032	2568	28780
98	−20222	−3727	−11	18680
103	−28584	−1491	1251	27592
109	−27620	−2037	−4803	27928
149	−20721	−4003	7870	23415

PYIELD:

NODE 97: 6077^{LB}

" 103: 6337^{LB}

" 109: 6263^{LB}

REMOVE NODE 29:
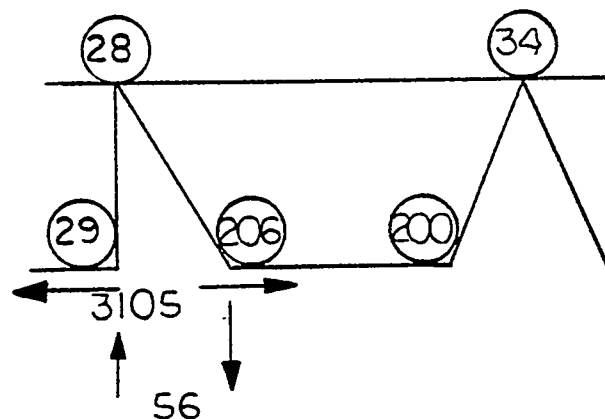
SEE DETAIL D, FIGURE 4−8.

A−6

LOAD CASE 4:

P= 5300^{LB}+INCREMENTAL LOADING

AT P= 6000^{LB}

	Sxx: PSI	Syy: PSI	Sxy: PSI	σ_T: PSI
97	−36623	−7158	2886	33990
98	−24188	−4696	76	22216
103	−34729	−2367	1333	33687
104	−18303	+ 53	1550	18500
109	−33382	−3399	− 4520	32767
110	−18478	− 231	4592	20010

YIELD LOADS:

$P_{Y-97} = 5825^{LB}$

$P_{Y-103} = 5877^{LB}$

$P_{Y-109} = 6042^{LB}$
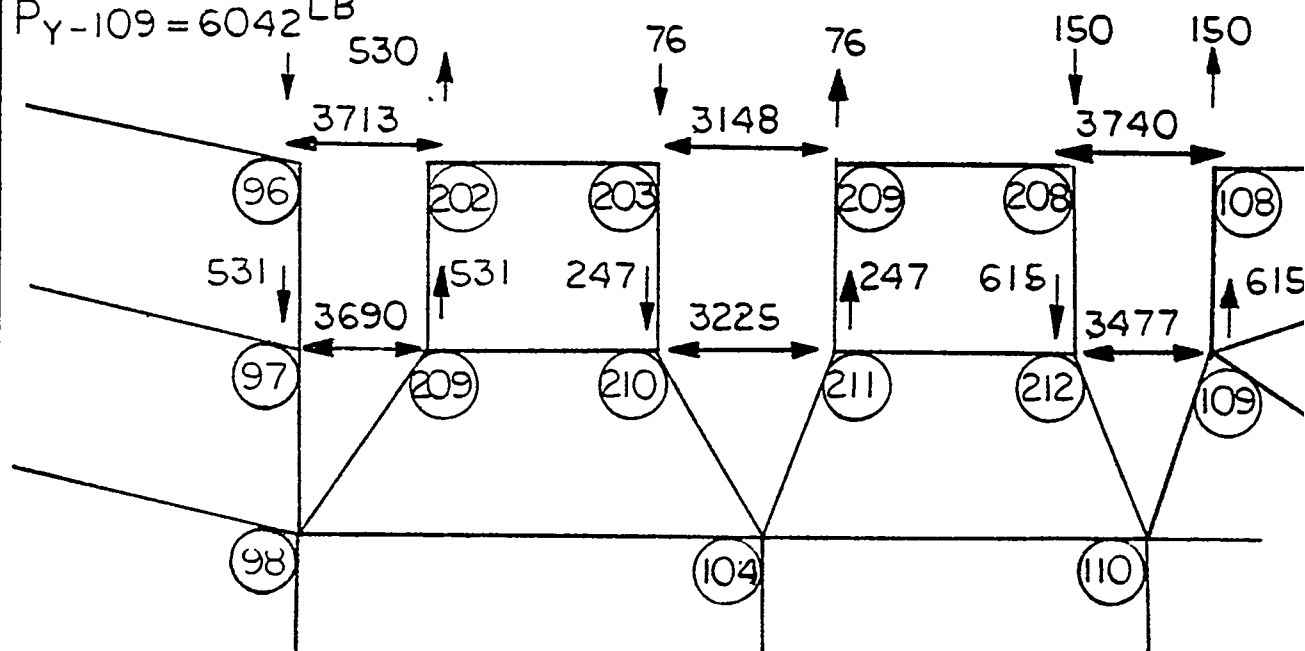
SEE DETAIL E, FIGURE 4 − 8.

LOAD CASE. 5:
P = 5800^{LB} + INCREMENTAL LOADING

FAILURE OF SECTION AT 5875^{LB}.

SUBSTITUTE ARTIFICIAL LOADINGS TO MODEL
YIELDED ELEMENTS.
SEE DETAIL FIGURE 4-26 FOR LOAD CASE 2
RESPONSE.

NODE 72:
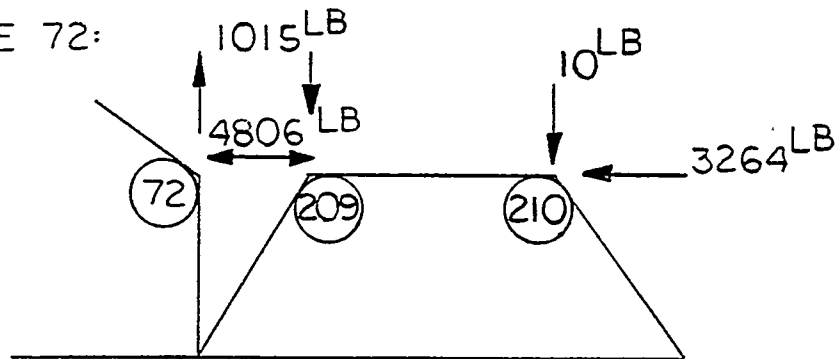
NODE: 84,90:
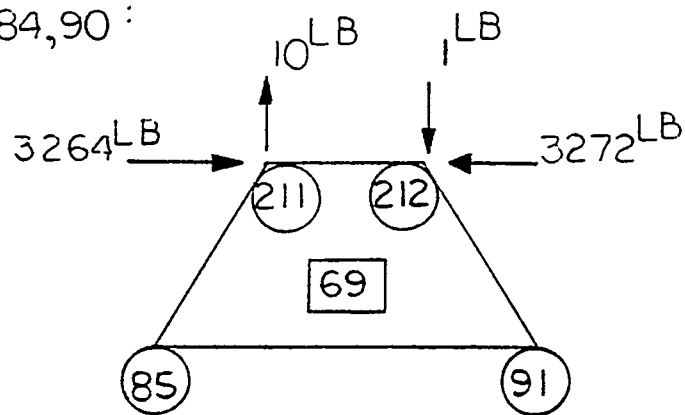
NODE:90,96,102:

NODE: 102,108 :

45^{LB}

110^{LB}

3180^{LB}

3380^{LB}

216

217

84

103

109
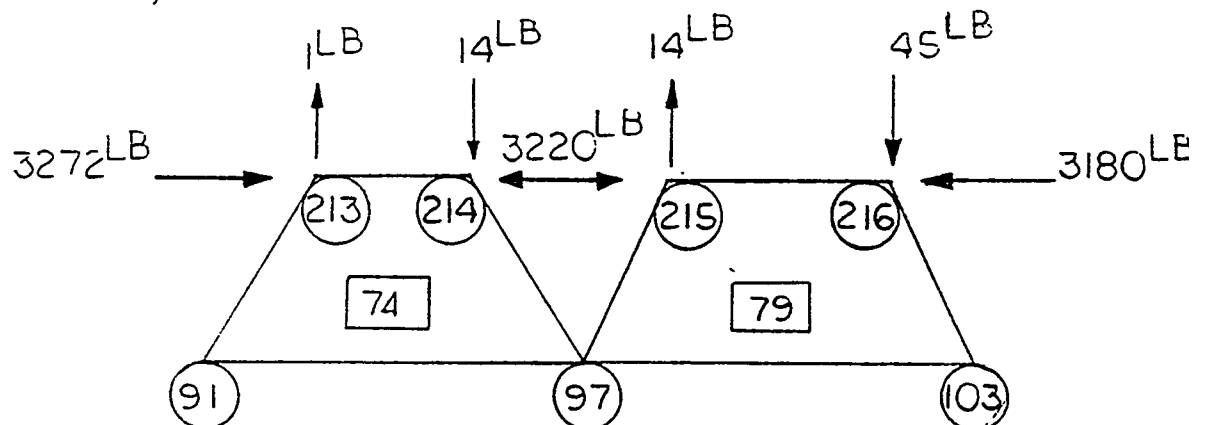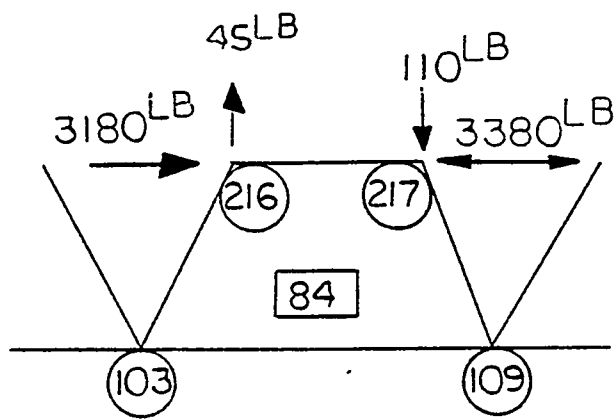
LOAD CASE 3:
P=6350^{LB}

PART B:

THIS SECTION CONTAINS THE COMPUTATIONS NECESSARY TO PERFORM THE PLASTIC ANALYSIS FOR THE FILLET WELDED CRUCIFORM JOINT WITH A 0.6T MISALIGNMENT.

SEE FIGURE 4-11 FOR CORRESPONDING DETAILS.

LOAD CASE 1:

$P = 5430^{LB}$

ELEMENTS: 54,59,64,69,74,79,84:

	S_{XX}	S_{YY}	S_{XY}	σ
72	-28625	-3172	8028	30528
78	-34655	-3700	170	32962
84	-29637	-1938	118	28718
90	-29115	-1767	-73	28273
96	-28710	-1746	-71	27878
102	-27976	-1927	926	27111
108	-27522	-2211	4026	27388

YIELD LOAD: $P_Y = {}^{33000}\!/\!\sigma \times 5430$

72	$P_Y = 5870^{LB}$
78	$P_Y = 5436^{LB}$
84	$P_Y = 6240^{LB}$
90	$P_Y = 6338^{LB}$
96	$P_Y = 6428^{LB}$
102	$P_Y = 6611^{LB}$
108	$P_Y = 6543^{LB}$

A-9

NODE 78:

SEE DETAIL , FIGURE 4-26 FOR INITIAL YIELDING.
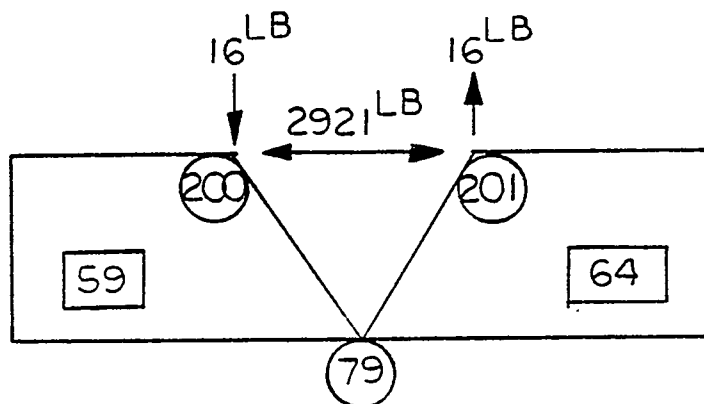
LOAD CASE 2:

$P = 5800^{LB}$

ELEMENTS: 54, 59, 64, 69, 74, 79, 84:

	S_{XX}	S_{YY}	S_{XY}	σ
72	−30283	−3476	8586	32327
84	−31030	−1798	187	30173
90	−31013	−1858	71	30127
96	−30662	−1868	74	29844
102	−29862	−2060	495	28900
108	−29374	−2357	4295	29232

YIELD LOAD: $P_Y = 33000 \times 5800 / \sigma$

72	$P_Y = 5920^{LB}$
84	$P_Y = 6343^{LB}$
90	$P_Y = 6353^{LB}$
96	$P_Y = 6413^{LB}$
102	$P_Y = 6623^{LB}$
108	$P_Y = 6548^{LB}$

PART 2

FINAL TECHNICAL REPORT

ON

POTENTIAL SHIP STRUCTURE
TRIPPING BRACKET
GUIDELINES

PART NO. 2 OF

STANDARD
STRUCTURAL ARRANGEMENTS
TASK S-11
OF THE
SHIP PRODUCIBILITY PROGRAM

GENERAL DYNAMICS
QUINCY SHIPBUILDING DIVISION

TABLE OF CONTENTS

TABLE OF CONTENTS (Cont'd)

Section 1
INTRODUCTION AND SUMMARY

Differentiated from the unrestrained lateral-torsional buckling of beams, the lateral-torsional buckling failure mode of plate-stiffeners is by laying-over **or** tripping about an enforced axis of rotation (the stiffener-to-plate line of attachment). Like Euler buckling, tripping is a possible primary mode of failure which must be prevented. There are three basic design procedures to prevent tripping failure:

1. Use sections having sufficient torsional rigidity for unbraced span length.
2. Use intermediate lateral supports to reduce unbraced span lengths.
3. Use tripping brackets to reduce unbraced span lengths.

The objective of this study was to provide guidelines to establish the need for tripping brackets, their spacing and their configuration. Motivation for the study was a consensus among shipyard designers that this guidance was lacking, and that the costs incurred by arbitrary placement of large tripping brackets are excessive.

The guidelines are presented in summary form in Section 2, with application examples in Section 3. Tripping bracket configuration is briefly discussed in Section 4. Although the design guidelines are self-contained, maximum benefit and understanding will be obtained by reading the outline of analytical techniques employed in the study, which are presented in Section 5.

Review of the literature leads to the conclusion that researchers have preferred to reformulate existing solutions rather than build on the background of others. The compilation

in this study should help focus attention on those areas Of the tripping phenomenon most needing attention: a) behavior of asymmetrical stiffeners under lateral load (bending), and b) experimental verification of all formulations. Not only is the tripping problem for asymmetrical sections in bending unsolved, but there appears to be no accurate method for calculating the stress distribution in such a member other than finite element analysis. The latter is unacceptable for routine design work.

Section 2
TRIPPING INSTABILITY DESIGN GUIDELINES

2.1 AXIAL COMPRESSION

2.1.1 Symmetric Sections

Flat Bars

$$F_{T\alpha} = 0.38 E \left(t/d \right)_w^2$$

(2-1)

Tees

$F_{T\alpha}$ is the larger value of Equation (2-2) or (2-3)

$$F_{T\alpha} = \frac{0.35 A_f E}{I_{po}} \sqrt{\frac{b_f^2 d_w^2}{A_f \left(s_p/t_p^3 + 2 d_w/t_w^3 \right)}}$$

(2-2)

$$F_{T\alpha} = \frac{0.80 A_f E}{I_{po}} \left(\frac{b_f d_w}{\ell} \right)^2$$

(2-3)

2.1.2 Asymmetric Sections

Angles

$F_{T\alpha}$ is the larger value of Equation (2-4) or (2-5)

$$F_{T\alpha} = \frac{0.50 A_f E}{I_{po}} \sqrt{\frac{b_f^2 d_w^2}{A_f \left(s_p/t_p^3 + 2 d_w/t_w^3 \right)}}$$

(2-4)

$$F_{T\alpha} = \frac{2.5 A_f E}{I_{po}} \left(\frac{b_f^2 d_w^2}{\ell} \right)$$

(2-5)

2.2 LATERAL BENDING

2.2.1 Symmetric Sections

Flat Bars

$$F_{Tb} = \frac{0.13 E t_w}{S_x}$$

(2-6)

Tees

F_{Tb} is the larger value of Equation (2-7) or (2-8)

$$F_{Tb} = \frac{0.17 A_f E}{d_w S_x} \sqrt{\frac{b_f^2 d_w^2}{A_f \left(S_p/t_p^3 + 2 d_w/t_w^3 \right)}} \qquad (2-7)$$

$$F_{Tb} = \frac{0.40 A_f E}{d_w S_x} \left(\frac{b_f d_w}{l} \right)^2 \qquad (2-8)$$

2.3 FLANGES

$$F_{TF} = 0.60 E \sqrt{(b/t)_f \cdot (t/d_w)^3} \qquad (2-9)$$

2.4 TRIPPING IN THE INELASTIC RANGE $(F_T > \frac{1}{2} F_Y)$

$$F_{Ti} = F_Y \left(1 - \frac{F_Y}{4 F_{Te}} \right) \qquad (2-10)$$

2.5 COMBINED AXIAL COMPRESSION AND LATERAL BENDING

Symmetric Sections

$$\frac{f_a}{F_{Ta}} + \frac{f_b}{F_{Tb}} \leq 1.0 \qquad (2-11)$$

2.6 TRIPPING BRACKET STIFFNESS AND STRENGTH

2.6.1 Required Stiffness

$$K_{REQ'D} = \frac{C_i F_T A}{l} \qquad (2-12)$$

2.6.2 Required Strength

$$P_{BRKT} = \frac{C_i F_T A}{250} \qquad (2-13)$$

Number of Spans	2	3	4	8	≥ 10
C_i	4.00	6.00	6.82	7.80	8.00

2.7 DESIGN FACTOR OF SAFETY

The tripping stresses calculated by using the design guidelines have a factor of safety of 1, i.e, they are the theoretical critical values. Rather than apply an arbitrary factor of safety, it is recommended to equate tripping stress to 1.00 to 1.15 times the proportional limit. Below the proportional limit the full strength of the section is not being utilized, while above the proportional limit the strength drops off rapidly.

2.8 NOMENCLATURE OF DESIGN GUIDELINES

The following definitions of symbols and terms are to be understood, in the absence of other specifications, where they appear in the design guideline.

A Cross sectional area of stiffener

A_f Cross sectional area of stiffener flange

$(b/t)_f$ Stiffener flange width to thickness ratio

b_f Flange width

C_1 Span dependent constant

d_w Stiffener depth

E Young's modulus

f_0 Axial stress

f_b Bending stress

F_{TQ} Axial tripping stress

F_{Tb} Bending tripping stress

F_{Te} Elastic tripping stress

F_{Ti} Inelastic tripping stress

F_{TF} Flange tripping stress

I_{PO} Stiffener polar moment of inertia about toe

J Length between lateral supports

S_p Stiffener spacing

S_x Section modulus of plate-stiffener combination to flange

t_p- Plate thickness

tw   Web thickness

(t/d)w Stiffener web thickness to depth ratio

Section 3
APPLICATION EXAMPLES OF DESIGN GUIDELINES

EXAMPLE 1

Determine the axial compressive tripping stress, F_{Ta} , for the flat bar shown in Figure 3-1. The unbraced span length is 172 inches and the material EH-36 steel, F_Y = 51 ksi.
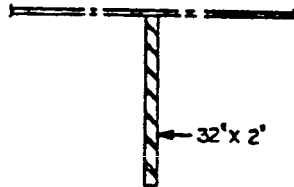
<u>Solution</u>

$$F_{Ta} = 0.38 E \left(\frac{t}{d} \right)^2_w \qquad (2-1)$$

$$F_{Ta} = 0.38 (29.5 \times 10^3) \left(\frac{2}{32} \right)^2 = 43.8 \text{ KSI}$$

$F_{Ta} > \frac{1}{2} F_Y \therefore$ Correct for inelasticity

$$F_{Ti} = F_Y \left(1 - \frac{F_Y}{4 F_{Ta}} \right) \qquad (2-10)$$

$$F_{Ti} = 51 \left(1 - \frac{51}{4(43.8)} \right) = 36.2 \text{ ksi (Answer)}$$

Figure 3-1

$-32' \times 2'$

EXAMPLE 2

Determine the axial compression tripping stress, F_{Ta} for the tee shown in Figure 3-2. The unbraced span length is 48 in. and the material mild steel, F_Y = 33 ksi

0.30°   24°
0.28°   6°
0.56°
3°
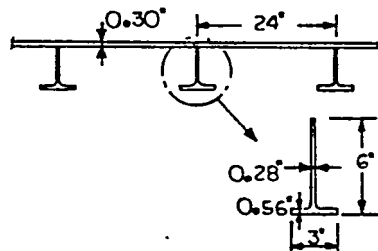
Figure 3-2

Solution

$$F_{Ta} = \frac{0.35 A_f E}{I_{po}} \sqrt{\frac{b_f^2 \, d_w^2}{A_f \left(\frac{Sp}{t_p^3} + \frac{2d_w}{t_w^3} \right)}} \qquad (2\text{-}2)$$

$$F_{Ta} = \frac{0.35(1.68)(29.5 \times 10^3)}{79.3} \sqrt{\frac{(3)^2(5.87)^2}{1.68\left(\frac{24}{1.3^3} + \frac{2(5.87)}{0.28^3}\right)}} = 78.8 \text{ KSI}$$

$$F_{Ta} = \frac{0.80 A_f E}{I_{po}} \left(\frac{b_f \, d_w}{\ell} \right)^2 \qquad (2\text{-}3)$$

$$F_{Ta} = \frac{0.80(1.68)(29.5 \times 10^3)}{79.3} \left(\frac{3(5.87)}{48} \right)^2 = 67.3 \text{ KSI}$$

$$F_{Ta}(78.8 \text{ KSI}) > \tfrac{1}{2} F_Y \quad \therefore$$

$$F_{Ti} = F_Y \left(1 - \frac{F_Y}{4 F_{Ta}} \right) \qquad (2\text{-}10)$$

$$F_{Ti} = 33 \left(1 - \frac{33}{4(78.8)} \right) = 29.5 \text{ KSI} \qquad \text{(Answer)}$$

(During Testing [1] this grillage failed by stiffener tripping at 27.3 ksi.)

EXAMPLE 3

Determine the Axial Compression tripping stress, F_{Ta}, for the tee shown in Figure 3-3. The unbraced span length is 48 in. and the material mild steel, F_Y = 33 ksi.
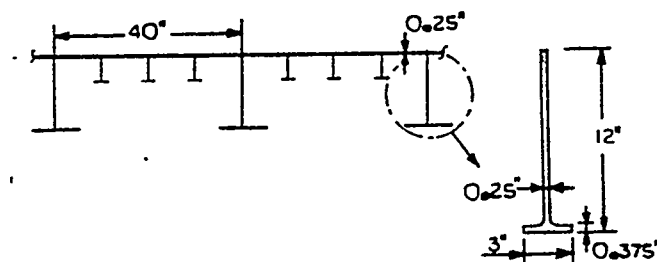
Figure 3-3

[1] Smith, "Compressive Strength of Welded Steel Ship Grillages", RINA, 1975

Solution

$$F_{Ta} = \frac{0.80 A_f E}{I_{po}} \left(\frac{b_f d_w}{\ell} \right)^2 \tag{2-3}$$

$$F_{Ta} = \frac{0.80 (1.13)(29.5 \times 10^3)}{292} \left(\frac{3(11.94)}{48} \right)^2 = 50.8 \text{ KSI}$$

Since Equation (2-3) is always conservative and $F_{Ta} > F_Y$
Equation (2-2) need not be used.

$$F_{Ta}(50.8) > \tfrac{1}{2} F_Y \quad \therefore \qquad \text{Correct for inelasticity}$$

$$F_{Ti} = F_Y \left(1 - \frac{F_Y}{4 F_{Ta}} \right) \tag{2-10}$$

$$F_{Ti} = 33 \left(1 - \frac{33}{4(50.8)} \right) = 27.6 \text{ KSI} \qquad \textbf{(Answer)}$$

(During testing [1] this grillage.failed by stiffener
tripping at 31.3 ksi.)

---

[1] Smith, "Compressive Strength of Welded Steel Ship
Grillages", RINA, 1975

Section 4
TRIPPING BRACKET DETAILS

Figure 4-1 illustrates some common and uncommon tripping brackets used by the shipbuilding industry. A more comprehensive review is to be found in Reference [1].

The single best guideline to tripping bracket design is that their effectiveness is no better than that of the structure to which it is attached. Tripping brackets are best when anchored against intersecting structural shapes and are least efficient when welded to an unstiffened plate field.

1	2
Not very effective: bracket maintains stiffener crossectional shape but does not prevent plate-stiffener rotation.	Bracket at heel or bossom of stiffener is fairly effective, but detail is poor due to hardspot at base of flat bar.
3	**4**
Effective if panel stiffener meets requirements of Section 2.6	Effective
5	**6**
Effective, but flange on bracket is probably not required	Effective

Figure 4-1   Tripping Bracket Details

7	8
Better than No. 1, but still ineffective: plate would rotate with stiffener.	Marginally effective

Figure 4-1 Tripping Bracket Details (Cont'd)

Section 5
OUTLINE OF TECHNIQUES USED IN DEVELOPMENT OF GUIDELINES

5.1 INTRODUCTION AND GENERAL COMMENTS

This section is presented in the belief that the Designer/
Engineer will benefit more from the design guidelines if he
understands the methods used to derive them.

Section 5.2 is based on theoretical background presented in
numerous elementary texts on instability. It is not felt
necessary to repeat this information here. The assumption that
the stiffener ends are simply supported, prevented from twist-
ing, and free to warp is realistic for most ship structure.

Furthermore, for structure such as transverse web frames which
are elastically restrained at their base it is possible that
the buckle wave length is less than the span length. Thus the
interior portion definitely behaves as if it were simply
supported.

To avoid using a value of rotational restraint which would
cause excessive bending of the stiffener web, $K\emptyset$ is modified
to include the bending stiffness of the stiffener web. Although
this approach is not theoretically correct, it is felt to be
better than placing an arbitrary upper limit on $K\emptyset$ (plate.)

A plot of equation (5-1) is shown in Figure 5-1. As can be
seen for span lengths less than l_{CR}, Equation (5-11) can
underestimate F_{Ta} because it assumes the number of buckled half
waves is a continuous instead of discrete function. In this
event Equation (5-1) with $K\emptyset=0$ may give a better estimate.
In any case, Equation (5-13) is always the minimum value of F_{Ta} .
(Assuming $K\emptyset=0$ is equivalent to assuming the toe of the
stiffener is pinned.)
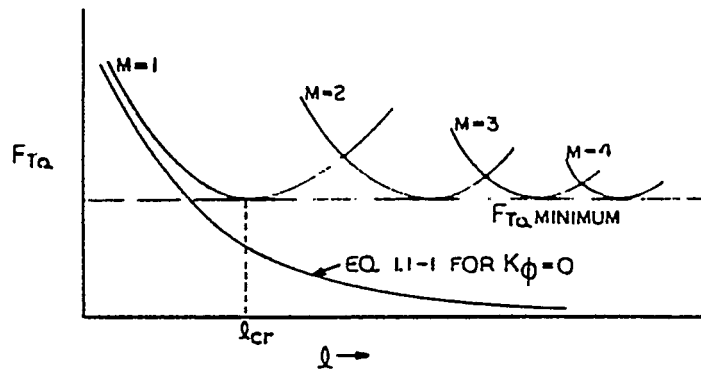
Figure 5-1

The comments made for Section 5.2 similarly apply to Section 5.3. The potential energy function is presented in case a more accurate analysis is wanted when the moment is nonuniform, i.e., the transverse lateral load is not zero or the end moments are unequal. These conditions (variable coellicients) can be solved using the Raleigh-Rite method. A method is not presented to calculate F_{Tb} for asymmetric shapes. Their use as inner bottom longitudinal and shell longitudinal in ballast tanks indicates the coupling effect is probably very slight.

A stiffener will not trip unless its flange is in compression. The unbraced compression length is considered to be the length of flange between inflection points.

Lateral buckling of flanges (Section 5.4) can not strictly be considered tripping. However, it is felt that when using the rotation restraint available at the stiffener toe this is a prudent check which should be made for deep sections having heavy flanges.

Although material presented in Section 5.5 is based on work done entirely on beams and columns, Equation (5-35) has been widely used on other structures, from spacecraft to ships. It is cautioned that no initial imperfection is explicitly accounted for by Equation (5-35).

Section 5.7 is based on the Euler buckling of columns. Its use should be very conservative when applied to bracing for stiffener tripping. The term $F_T.A$ represents the total force acting on the stiffener cross section (not including plate). The stiffness required is measured at the flange.

5.2 TRIPPING DUE TO AXIAL COMPRESSION

5.2.1 Symmetric Stiffeners

The basic equation for tripping of a symmetric stiffener about an enforced axis of rotation is (Reference 2, p 140): .

$$F_{Ta} = \frac{E}{I_{po}}\left[\frac{J}{2.6} + \frac{\pi^2 M^2}{\ell^2}\Gamma_o + \frac{\ell^2}{\pi^2 m^2}\frac{K\phi}{E}\right] \tag{5-1}$$

Where

F_{Ta} = Axial compression tripping stress

E = Young's modulus

I_{po} = Stiffener polar moment of inertia about toe

J = Torsional constant

M = number of buckled half-waves

Γ_o = warping constant

Q = unbraced span length

$k\phi$ = rotational restraint

The derivation of Equation (5-1) assumes the stiffener ends are simply supported and prevented from twisting, but the flange is free to warp. Local deformations of the stiffener are not considered, see Figure 5-2.

(a)
TRIPPING

(b)
LOCAL DEFORMATIONS

Figure 5-2

In Equation (5-1) the axial tripping stress F_{Ta} is a function of the number of buckled half-waves m. F_{T_a} is minimized if m is minimized, or:

$$\frac{\partial F_{Ta}}{\partial M} = 0$$

(5-2)

Applying Equation (5-2) to Equation (5-1), the critical wave number is:

$$M = \sqrt[4]{\frac{K_\phi \, \ell^4}{\pi^4 E T_o^3}}$$

(5-3)

Substituting Equation (5-3) into Equation (5-1) gives:

$$F_{Ta} = \frac{E}{I_{po}}\left[\frac{J}{2.6} + \sqrt{\frac{\Gamma_o K_\phi}{E}}\right]$$

(5-4)

Equation (5-4) is valid only if   is treated as a continuous function. This assumption is accurate enough for $m \geq 3$.
If $m < 3$, Equation (5-1) should be used to determine F_{Ta} where m is the lower adjoining integer of Equation (5-3). The minimum value of m is 1.

The terms in Equation (5-1), except for the rotational restraint, are propertion of the stiffener cross-section, Sec Figure 5-3. The only terms which require further explanation are T_o and K_ϕ .
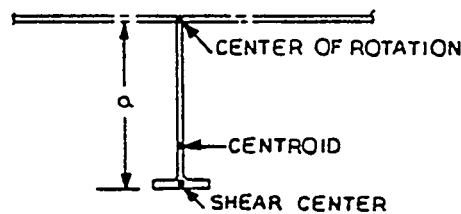
Figure 5-3

The warping constant T_0 is a property of the stiffener cross-section and of the location of the center of rotation relative to the shear center. It is analogous to the ordinary flexural and torsional constants, but has different dimensions. The equation for T_0 is:

$$T_0 = C_W + \alpha^2 I_Y \qquad (5-5)$$

C_W for various shapes can be determined from equations found in Reference 3. Since it is much smaller than the second term in Equation (5-5) for shipbuilding shapes, omitting it causes no appreciable error.

During tripping the rotation of the stiffener is resisted by the bending stiffness of the plate. If the plate is considered to be made up of beam strips, this restraint can be determined by the method shown in Figure 5-4. As can be seen from this Figure, the minimum restraint is for antisymmetric tripping.

$$K_m = \frac{M_T}{\varnothing} = \frac{12EI}{L} = \frac{E}{\cdot L^3} \cdot \frac{t_p^3}{L}$$

SYMMETRIC TRIPPING

$$K_\varnothing = \frac{M_T}{\varnothing} = \frac{4EI}{L} = \frac{E}{3(1-\nu^2)} \cdot \frac{t_p^3}{b_p}$$

ANTISYMMETRIC TRIPPING
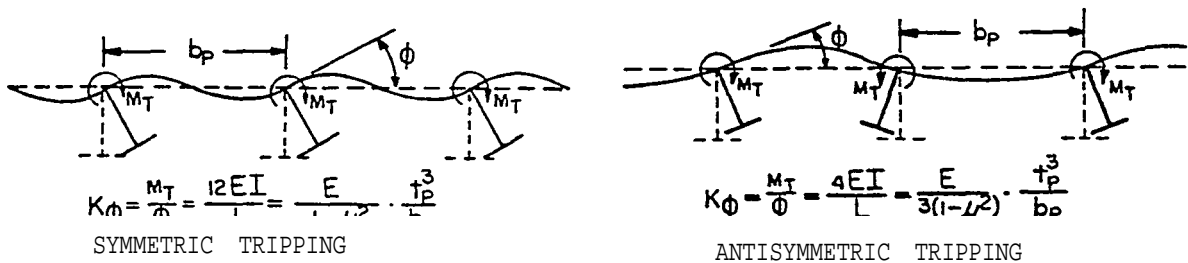
Figure 5-4

The above analysis gives an exaggerated value of $K_\varnothing$ since bending of the web will occur during tripping. This can be corrected if the bending stiffness of the stiffener web is included in the calculation of $K_\varnothing$.

$$\phi = \phi_P + \phi_W$$

$$\phi_P = \frac{M_T b_P}{4EI_P}$$

$$\phi_W = \frac{\delta}{d} = \frac{M_T d}{2t\, I_W}$$
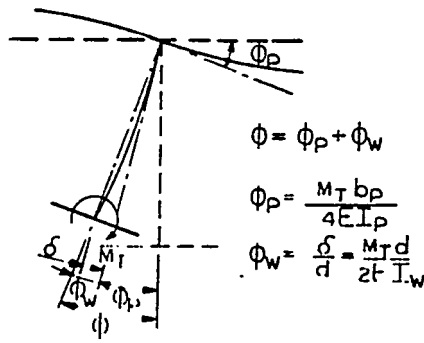
Figure 5-5

Refering to Figure 5-5, the equation for the rotational, restraint including the web stiffness is:

$$\frac{1}{K_\phi} = \frac{1}{K_P} + \frac{1}{K_W} \tag{5-6}$$

or in terms of the plate and stiffener web:

$$K_\phi = \frac{E}{3(1-\nu^2)} \left[\frac{1}{\frac{s_P}{t_P^3} + \frac{2d_W}{t_W^3}} \right] \tag{5-7}$$

For flat bars the term $\sqrt{I_0 K_\phi / F}$ is much smaller than $0.38J$. Thus , Equation (5-4) reduces to:

$$F_{T_a} = \frac{0.38\ EJ}{I_{po}} \tag{5.8}$$

or substituting the expressions for J and I_{po}

$$F_{T_a} = 0.38E \left(t/d \right)_W^2 \tag{5-9}$$

Equation (5-9) is Equation (2-1) of the design guideline. It is interesting to note that Equation (5-9) is the local plate buckling equation for an infinitely long $\left(\ell/d > s \right)$ uniformly compressed plate with one long edge simply sup

For tee's the term $\sqrt{\frac{T_o K_\phi}{E}}$ is much larger than 0.38J. Thus Equation (5-4) reduces to:

$$F_{Ta} = \frac{2E}{I_{po}} \sqrt{\frac{T_o K_\phi}{E}}$$

(5-10)

or substituting the expressions for T_o **and** K_ϕ :

$$F_{Ta} = \frac{0.35 A_f E}{I_{po}} \sqrt{\frac{b_f^c d_w^c}{A_f \left(\frac{s_p/3}{t_p} + \frac{2d_w/3}{t_w}\right)}}$$

(5-11)

Equation (5-11) is Equation (2-2) of the Design Guideline.

When m from Equation (5-3) is a noninteger less than 3, it is possible that Equation (5-11) significantly underestimates F_{Ta}. In this event a better estimate of F_{Ta} **may** sometimes be made using Equation (5-1) with m-1 and K_ϕ=0. The term 0.38J which is small compared to $\pi^2 I_o$ **may be neglected. Thus Equation** (5-1) reduces to:

$$F_{Ta} = \frac{\pi^2 E \Gamma_o}{I_{po} \ell^2}$$

(5-12)

or substituting the expression for T_o :

$$F_{Ta} = \frac{0.8 A_f E}{I_{po}} \left(\frac{b_f d_w}{\ell}\right)^2$$

(5-13)

Equation (5-13) is Equation (2-3) of the design guideline.

5.2.2 <u>Asymmetric Stiffeners</u>

Because asymmetric stiffeners such as angles lack an axis of symmetry perpendicular to the plate, flexure and torsion are coupled and therefore, the axial buckling and tripping stresses are coupled. The coupled axial buckling-tripping stress, which

is always smaller than either the individual axial buckling or tripping stress, can be calculated from the following equation (Reference 4):

$$F_{Ca} = \frac{F_E + F_{Ta}}{2(1 - \xi^2)} \left[1 - \sqrt{\frac{1 - 4 F_E F_{Ta}(1 - \xi^2)}{(F_E + F_{Ta})^2}} \right]$$ (5-14)

Where F_{Ca} =   Coupled axial buckling-tripping stress

F_E =   Euler plate stiffener buckling stress

F_{Ta} =   Axial compression tripping stress [Equation (5-1)]

ξ =   Coupling parameter $= \frac{X_o - X_3}{r_o}$

X_o =   Cordinate of plate stiffener shear center from stiffener web

X_3 =   Cordinate of plate stiffener centroid from stiffener web

r_o =   Polar radius of gyration $= \sqrt{\frac{I_{po}}{A_{p-s}}}$

I_{po} =   Polar momement of inertia of stiffener about toe

A_{p-s} =   Plate stiffener cross-sectional area

Provided Euler buckling of the plate stiffener does not govern, i.e. $F_E > F_{Ca}$ can conservatively be taken as 75 percent of F_{Ta}. Equation (2-4) and (2-5) of the design guideline are thus based on 75 percent of Equation (5-10) and (5-12) respectively, with **the appropriate expressions substituted for I_o** and K_ϕ. It should be noted that for the same size flange, an angle resists tripping due to axial compression better than a tee.

5.3 <u>TRIPPING DUE TO LATERAL LOADING</u>

5.3.1 <u>Symmetric Stiffeners</u>

The potential energy function for lateral buckling of a stiffener about an enforced axis of rotation is (Reference 2, p.164):

$$\Phi = \frac{1}{2} \int_0^l (E I_o \ddot{\phi}^2 + G J \dot{\phi}^2 + 2 a M \ddot{\phi} \phi - \bar{a} w_y \phi + K_\phi \phi^2) dz$$ (5-15)

The following differential equation is derived from Equation (5-15) by applying the calculus of variations:

$$0 = E\Gamma_0 \phi^{IV} - (GJ - 2\alpha M)\ddot{\phi} - (\alpha w_Y - K_\phi)\phi \qquad (5\text{-}16)$$

Where
- E = Young's modulus
- Γ_0 = Warping constant
- G = Shear modulus
- J = Torsional constant
- α = Distance from shear center to center of rotation
- M = Simple **beam moment** due to externally applied forces
- $\bar{\alpha}$ = Distance transverse load is applied above shear center
- w_Y = Transverse distributed load
- $K_\emptyset$ = Rotational restraint

If the stiffener is subjected to a uniform moment only, i.e., the lateral load is zero, the solution to Equation (5-16) is:

$$\phi = A_1 \sin \frac{n\pi z}{\ell} \qquad (5\text{-}17)$$

Substituting Equation (5-17) into Equation (5-16) and simplifying gives:

$$M_{CR} = \frac{1}{2\alpha}\left[E\Gamma_0 \frac{\pi^2 m^2}{\ell^2} + GJ + K_\phi \frac{\ell^2}{\pi^2 n^2}\right] \qquad (5\text{-}18)$$

Equation (5-18) can be expressed in terms of stress if it is assumed:

$$F_{Tb} = \frac{M_{CR}}{S_{FLG}}$$

$$(5\text{-}19)$$

Where S_{FLG} = section modulus to the flange of the stiffener plate combination.

Using the same minimization procedure outlined in Section 5.2.1, the equation for the critical wave number is

$$m = \sqrt[4]{\frac{K_\phi \ell^4}{E \Gamma_o \pi^4}}$$

substituting Equation (5-20) into Equation (5-19) gives:

$$F_{Tb} = \frac{E}{\alpha S_{FLG}} \left[\frac{J}{S_o 2} + \sqrt{\frac{\Gamma_o K_\phi}{E}} \right] \tag{5-21}$$

Similar to Equation (5-4), Equation (5-21) is valid for m ≥ s . . If m<3 , then the lower adjoining integer from Equation (5-20) should be used in Equation (5-19) to determine F_{Tb} .

Although Equation (5-21) was developed for uniform moment, it can conservatively be used for other loading conditions.

For flat bars the term $\sqrt{\frac{\Gamma_o K_\phi}{E}}$ is much smaller than 0.19J . Thus Equation (5.3) reduces to:

$$F_{Tb} = \frac{EJ}{S_o 2 \alpha S_{FLG}} \tag{5-22}$$

or substituting the expression for J and noting $\alpha = \frac{d_w}{2}$

$$F_{Tb} = \frac{0.13 E t_w^3}{S_{FLG}} \tag{5-23}$$

Equation 5.3 is Equation 2.1 of the design guideline.

For lee's the term $\sqrt{\dfrac{\Gamma_o K_\phi}{E}}$ is much larger than $0.19J$
Thus Equation 5-21 reduces to:

$$F_{Tb} = \frac{E}{a S_{FLG}} \sqrt{\frac{\Gamma_o K_\phi}{E}} \tag{5-24}$$

or substituting the expression for Γ_o and K_ϕ and noting
$a = d_w$

$$F_{Tb} = \frac{0.17 A_f E}{d_w S_{FLG}} \sqrt{\frac{b_f^2 \cdot d_w^2}{A_f \left(\dfrac{S_p}{t_p^3} + \dfrac{2 d_w}{t_w^3}\right)}} \tag{5-25}$$

Equation (5-25) is Equation (2-7) of the Design Guideline.

When m from Equation (5-20) is a noninteger less than 3, it
is possible that Equation (5-25) significantly underestimates
F_{Tb} . In that event, a better estimate of F_{Tb} may sometimes
be made by using Equation (5-18) with m=1 and $K_\phi=0$ The
term $0.19J$ **which is small compared to** $\pi^2 \Gamma_o$ **may be** neglected.
Thus Equation (5-18) reduces to:

$$F_{Tb} = \frac{\pi^2 E \Gamma_o}{2 a S_{FLG} \ell^2} \tag{5-26}$$

or substituting the expression for Γ_o and again noting
$a = d_w$

$$F_{Tb} = \frac{0.40 A_f E}{d_w S_{FLG}} \left/ \frac{b_f^2 d_w^2}{\ell^2} \right. \tag{5-27}$$

Equation (5-27) is Equation (2-8) of the design guideline.

5.3.2 Asymmetric Stiffeners

Tripping of asymmetric stiffeners due to lateral load is
analogous to axial buckling of an eccentrically loaded column.
The assymetric stiffener begins to twist (trip) as soon as
lateral load is applied due to the eccentricity of the shear
center to the web, See Figure 5-6. At first the twisting

increases slowly, but as f_b approaches F_{cb} (F_{cb} = the coupled lateral bending tripping stress) the twisting increases more and more rapidly until at f_b-f_{cb} the twist increases without bound. The larger the eccentricity of the shear center, the sooner infinite twisting is approached see Figure 5-7.

STIFFENER PROPERTIES

LATERAL LOAD INFORMATION

Figure 5-6

MID-SPAN TWIST
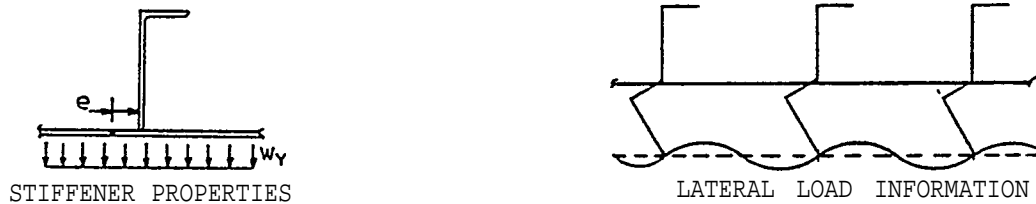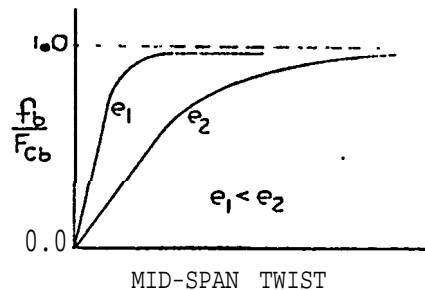
Figure 5-7

An analytical method has not yet been developed to calculate F_{cb} Reference 5 suggests using the Bryan plate buckling stress of the flange as a stability criteria. Reference 6 states that for the loading condition shown in Figure 5-8 the local buckling failure mode is dominant over the tripping failure mode.

FLANGE MOMENT
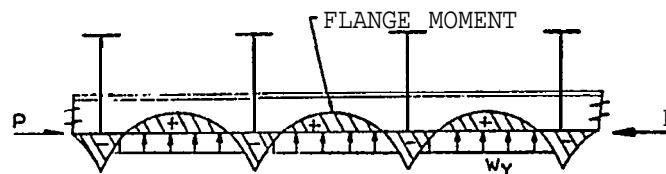
Figure 5-8

This report does not present a method to determine the tripping stability of asymmetric shapes under lateral load. It is recommended that pending further work in this area, the existing classification societies' rules be followed in this area.

Note that members requiring the application of large and costly tripping brackets, such as deep web frames, are generally symmetric sectionS for which guidelines have been formulated.

5.4 LATERAL BUCKLING OF FLANGES

Stiffeners having deep webs and heavy flanges may trip due to Euler buckling of the flange about its strong axis, See Figure 5-9. This behavior is similar to that of a beam on an elastic foundation where the flange is the beam and the web is the elastic foundation. The buckling equation is (Reference 7, p. 140):

$$F_T = \frac{m^2 \pi^2 E I_y}{A_f \ell^2} + \frac{K_w \ell^2}{m^2 \pi^2 A_f} \tag{5-28}$$
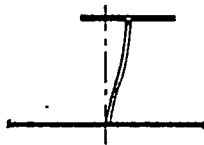
Figure 5-9)

where   m = Number of buckled half waves
        E = Young's modulus
        I_y = Flange moment of inertia about web
        A_f = Flange area
        l = Span
        K_w = Elastic spring constant

5-13

Using the same minimization procedure outlined in Section
5.2.1, the equation for the critical wave numer is:

$$m = \sqrt{\frac{K_W \ell^4}{\pi^4 E I_Y}}$$ (5-29)

Substituting Equation (5-29) into Equation (5-28) gives

$$F_T = 2E \sqrt{\frac{K_W I_Y}{E A_f^2}}$$ (5-30)

If the web is assumed to be a guided cantilever, the elastic .
spring constant is

$$K_W = \frac{E t_w^3}{0.91 \, d_w^3}$$ (5-31)

Substituting Equation (5-31) into Equation (5-30) and
simplifying gives

$$F_T = 0.6 E \sqrt{(b/t)_f \cdot (t/d)_w^3}$$ (5-32)

Equation (5-32) is Equation (2-9) of the Design Guidelines

5.5 <u>INELASTIC RANGE</u>

5.5.1 <u>Axial Compression</u>

The equations in Section 5.2 can be used to cover inelastic
range tripping by substituting the tangent modulus for Young's
Modulus when the calculated tripping stress is above the
proportional limit. This method requires trial and error to
find the calculated tripping stress which corresponds to the
assumed tripping stress used to select the tangent modulus.

To accomplish this procedure for steel columns in the inelastic range without iteration, Bleich proposed the following parabolic equation:

$$F_e' = F_Y - (F_Y - F_P)\frac{F_P}{F_e}$$ (5-33)

Where F_e' = Inelastic range column buckling stress
          F_Y = Material yield point
          F_p = Material proportional limit
          F_e = Euler column buckling stress

Column buckling tests have since shown the stress-strain curve departs from linearity below the proportional limit due to residual stresses. This led the Column Research Council (CRC} to replace F_p in Equation (5-33) by

$$F_P' = F_Y - F_R$$ (5-34)

Where F_P' = Shape proportional limit
          F_R = Residual stress

Although the maximum residual compressive stress in the flange of hot-rolled steel shapes is approximately $0.3 F_Y$, consideration of its effect on both weak and strong axis buckling caused the CRC to select F_R equal to $0.5 F_Y$ thus

$$F_e' = F_Y\left(1 - \frac{F_Y}{4F_e}\right)$$ (5-35)

In reference 8 Det Norske Veritas uses Equation (5-35) to calculate the inelastic range stability of ship plate stiffeners for both Euler buckling and tripping. Similarly, Equation (5-35) has been adopted by this report. It is cautioned, however, that if the residual stresses in the

stiffener flange are more adverse than the residual stresses
shown in Figure 5-10 for a hot-rolled shape, Equation (5-35)
will be unconservative.
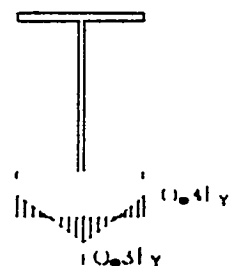
Figure 5-10

5.5.2 Lateral Bending

The stress due to lateral bending varies across the stiffener
cross-section. Thus if the tripping stress is in the inelastic
range, the tangent modulus will also vary across the stiffener
cross-section. This makes the analysis too complicated for a
rational solution. Fortunately, Equation (5-35) agrees with
test results for the lateral buckling of beams (Relerence 9).
Therefore, Equation (5-35) has also been adopted for inelastic
tripping due to lateral bending by this report.

5.6 COMBINED AXIAL COMPRESSION AND LATERAL BENDING

5.6.1 Symmetric Stiffeners

The interaction between axial and lateral tripping for
symmetric stiffeners is a very complex phenomenon. A
sufficient, although not necessary, condition of stability is
(Reference 10, p 739):

$$\frac{f_a}{F_{Ta}} + \frac{f_b}{F_{Tb}} \leq 1.0 \qquad\qquad (5\text{-}36)$$

Equation (5-36) is the Design Guideline interaction equation
for symmetric stiffeners.

5.6.2 Asymmetric Stiffeners

Pending development of F_{cb} no interaction equation is
proposed for asymmetric stiffeners.

5.7 BRACING

5.7.1 Required Stiffness

The following method for calculating the minimum stiffness
required for tripping brackets to be fully effective was first
suggested by Winter for the lateral bracing of columns. A
summary of Winter's work on lateral bracing requirements is
contained in Reference 11.
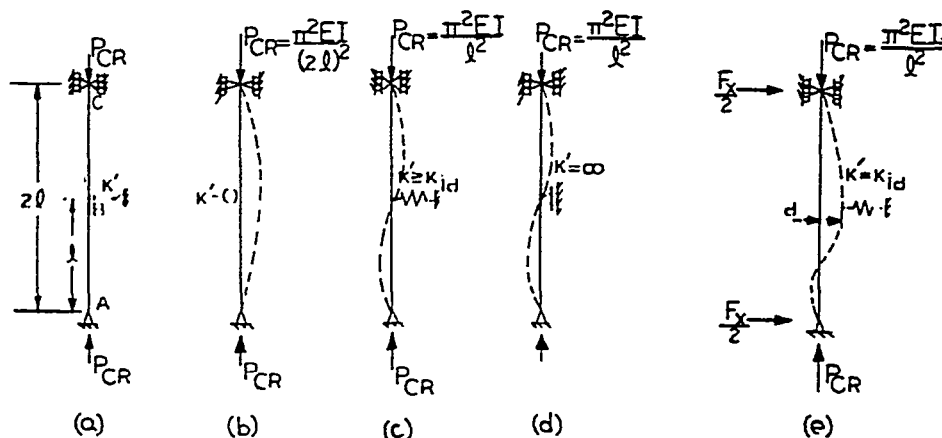
Figure 5-11

span shown in Figure 5-n(a). If the stiffness is initially
zero, the column will buckle in one half-wave when the load
reaches $\frac{EI}{(2\ell)^2}$, see Figure 5-n(b). As the lateral bracing
stiffness is increased, the load required to buckle the column
also increases until, at a certain stiffness, the load reaches

5-17

$$\frac{\pi^2 EI}{(\ell^2)}$$ and the column buckles in two half-waves, Figure 5-11(C). Increasing the lateral bracing stiffness beyond this value causes no further increase in critical load, Figure 5-n(d).The minimum lateral bracing stiffness necessary for the column to reach its maximum strength for the unbraced span length can be calculated by assuming an infinitesimally small lateral displacement is superimposed upon the antisymmetric buckled shape of Figure 5-11(c), see Figure 5-11(e). Summing moments about midspan (Point "B") for the upper half of the column (B C) gives

$$0 = \frac{F_x}{2} \cdot \ell - P_{CR} \cdot d \qquad (5\text{-}37)$$

Noting stiffness is force per unit displacement, Equation (5-37) can be rearranged to give

$$K'_{id} = \frac{2P_{CR}}{\ell} \qquad (5\text{-}38)$$

Equation (5-38) applies only for two spans. It can be made more general by introducing a span dependent coefficient. Thus

$$K'_{id} = \propto \cdot \frac{P_{CR}}{\ell} \qquad (5\text{-}39)$$

A curve for a presented in Reference 11 is shown in Figure 5-12.

Figure 5-12

5-18
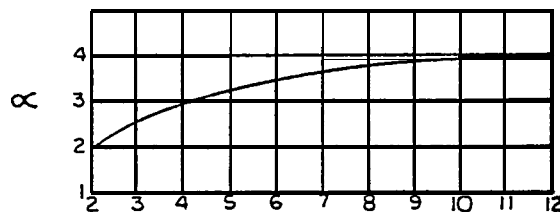
Because of imperfections, real columns begin deflecting at the onset of loading. The effect this has on required bracing stiffness can be determined by again considering the two span column shown in Figure 5-11(a). Now instead of being straight, assume the column has the initial imperfection form shown in Figure 5-13. The equilibrium equation at incipient buckling becomes

Figure 5-13

$$0 = \frac{F}{2}\ell - P_{CR}(d + d_o) \qquad (5\text{-}40)$$

or
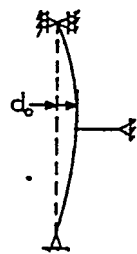
$$K_{ACT} = K'_{id}\left(1 + \frac{d_o}{d}\right) \qquad (5\text{-}41)$$

a more useful form of Equation (5-41) is

$$d = \frac{d_o}{\left(\dfrac{K_{ACT}}{K'_{id}} - 1\right)} \qquad (5\text{-}42)$$

Equation (5-42) shows that the actual bracing stiffness must be greater than the ideal bracing stiffness. If K_{ACT} equals K_{i_d} the deflection becomes infinite which is equivalent to buckling. Winter suggests K_{ACT} be twice K_{id} to keep the deflections prior to buckling acceptable.

The Design Guideline uses Equation (5-39) to determine the required bracing stiffness to prevent tripping. The values of $\propto$ have been doubled in the Design Guideline to account for imperfections.

5.7.2 <u>Required Strength</u>

The force exerted on the tripping bracket at buckling is

$K_{ACT} \cdot d$ **thus** from Equation (5-42)

$$F_{REQ'D} = d_o \left(\frac{K_{id}}{1 - \frac{K_{id}}{K_{ACT}}} \right)$$

(5-43)

and for K_{ACT} equal to $2K_{id}$

$$F_{REQ'D} = d_o \left(\frac{2 \alpha P_{CR}}{\ell} \right)$$

(5-44)

Assuming a maximum tolerance for d_o is $\frac{\ell}{250}$, Equation (5-44) becomes

$$F_{REQ'D} = \frac{2 \alpha P_{CR}}{250}$$

(5-45)

Equation (5-45) is used in the Design Guideline to determine .
tripping bracket strength. The factor of 2 is contained in the
design chart for α .

Section 6

REFERENCES

1. Glasfeld, R., et al, <u>Structural Details Design Review</u>, Ship Structure Committee Report SSC-266, 1977.

2. Bleich, <u>Buckling Strength of Metal Structures</u>, McGraw-Hill Book Company, Inc., 1952.

3. Timoshenko, and Gere, <u>Theory of Elastic Stability</u>, McGraw-Hill Book Company Inc., 1961.

4. Argyris, "Flexure-Torsion Failure of Panels," Aircraft Engineering, June 1954, V.26.

5. Shama, "Stress Analysis and Design of Fabricated Asymmetrical Sections", Schiffstechnik, Bd 23, 1967.

6. Geertsema, "Buckling Analysis of Ship Plate Structure", Report No. 207S, Netherlands Ship Research Centre.

7. Chajes, <u>Principles of Structural Stability</u>, Prentice-Hall, Inc., 1974.

8. Sigvaldsen, Sodal, and Johnsen, "Stability of Ship Profiles", DNV Report No. 68-60-0.

9. Johnston, <u>Guide to Design Criteria for Metal Compression Members</u>, John Wiley and Sons, Inc., 1967.

10. Evans, <u>Ship Structural Design Concepts</u>, Ship Structures Committee, 1974.

11. McGuire, <u>Steel Structures</u>, Prentice-Hall, 1968.

FINAL TECHNICAL REPORT

ON

POTENTIAL SHIP STRUCTURE
STRUCTURAL DETAILS
GUIDELINES

PART NO. 3 OF

STANDARD
STRUCTURAL ARRANGEMENTS
TASK S-11
OF THE
SHIP PRODUCIBILITY PROGRAM

GENERAL DYNAMICS
QUINCY SHIPBUILDING DIVISION

TABLE OF CONTENTS

Section 1
INTRODUCTION AND SUMMARY

In the last few years there has been a belated recognition
of the importance of structural details in the design and
performance of ship structure. At one end is an extensive
collection of commonly used details (Reference 1) , while at
the other there is a massive and very useful survey of in-
service performance of details (Reference 2) . Several
technical papers, for example References 3 and 4, discuss
experimental and analytical results for specific detail
configurations, and Committee 3a of the International Ship
Structures Congress was created in time for the 1976 session
with specific responsibility in this area.

The purpose of the present study is part of an effort to
formulate standards for ship construction in an attempt to
reduce building costs. Structural details, perhaps more
than any other component of hull structure, lend themselves
to standardization because attempts in that direction are
already made by many shipyards on an individual and on a
ship by ship basis.

Cost reduction due to eventual standardization of details is
less related to reduced cost of construction than to enhanced
ship performance, such as reduced scantlings of load carrying
members and decreased requirements for maintenance in repair.

The industry now lacks the background data for an unequivocal
selection of optimum details, but could use what information
is currently available in an attempt to reduce diversity.

Section 2 is a general critical discussion of structural
details that forms the basis for the tentative collection
of standard details in Section 4.

Section 3 presents data on finite element analysis of
clearance cuts with various collar and support arrangements
that are useful in providing guidance for the selection of
perhaps the most frequently used structural detail.

Reducing the incredible variety of any type of detail will
lead to clearer performance evaluation of specific design
details than is possible with today's proliferation.   The
feedback from such preliminary standardization would then
be directly applicable to focusing analytical and experimental
investigations, to providing numerical design guidelines,
and to promulgating more definitive standards.

Section 2
REVIEW OF STRUCTURAL DETAILS

2.1   <u>GENERAL</u>

The definition of requirements and the cooperation of the
United States shipbuilding industry was sought through
visits to most major United States shipyards (Reference 5).
The importance of attempts to standardize structural details .
was well recognized, and many shipyards generously assisted
by providing plans or booklets of their structural details.

All details were cut-out, numbered and attached, by category,
to "wallpaper". The "wallpaper" was discussed in sessions
attended by no less than two structural engineers and two
structural designers. The objective was to single out good
and bad individual features or complete details. Criteria
for the discussions were:

> 1.   Strength (potential for failure, history of
>   damage)
> 2.   Installation (ease of fitup)
> 3.   Complexity (cost)
> 4 .   Accessibility (welding, painting, maintenance)

Grouping of details was by commonly used categories. These
categories and the number of samples available for review
are listed below:

<u>Category</u>	<u>Number</u>
Cutouts and Collars	105
Miscellaneous Cutouts	96
Patches	7
Stanchion End Connections	57
Face Plates	18
Stiffener End Connections	64
Chocks	42

Category	Number
Panel Stiffeners	50
Beam Brackets	79

For discussion purposes these details have been grouped into the following more general categories:

Structural intersections (cutouts and collars)
Miscellaneous cutouts (snipes, limber holes, penetrations, patches, oil stops and water stops)
Brackets and chocks
Stiffener endings and transitions
Panel stiffeners
Stanchion end connections

In the following paragraphs the discussion is limited to broad general comments and to remarks on specific good and bad features of actual details encountered in the survey. The application of this discussion is made in the selection and design of those details to be found in Section 4.

2.2   STRUCTURAL INTERSECTIONS

The commonly used terminology for types of structural inter-sections is cutouts and collars, which would be better described as free and collared (or lugged) structural inter-sections. No such redefinition is attempted here for this or any other category of detail.

The necessary variety in this type of detail is great because of the shape variations in penetrating members (tees, angles, flat bars, bulb flats, etc.) and because of the degree of support required by the penetrating member.

Cutouts are provided to permit stiffeners or girders to
pass through deeper structural members such as webs, bulk-
heads and decks. They may also serve the secondary purpose
of providing drainage or venting openings in non-tight
members. Where necessary, these cutouts are partially or
fully collared to increase strength or restore tightness.

The simple clearance cut shown in Figure 2-1 is typical of
where the penetrated member, in this case a bulkhead, is
not a support point for the stiffeners.
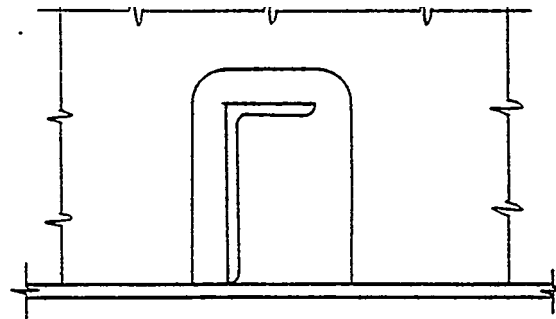
Figure 2-1

At the other extreme is Figure 2-2, representing a clearance
cut with a heavily loaded stiffener. Shear load is taken
out by lugs or collars to both the heel and the bosom of
the stiffener, and by a panel stiffener lapped over the web
of the stiffener.

Figure 2-2

2-3
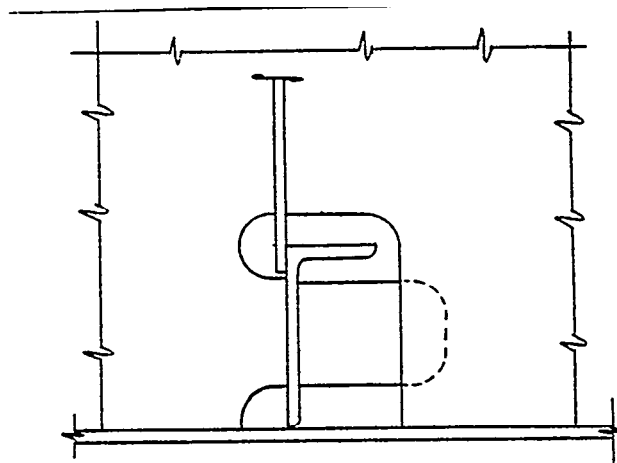
A modification of this detail is shown in Figure 2-3. Here the substitution of a lapped collar to the heel of the stiffener simplifies fitup of parts during assembly or erection.
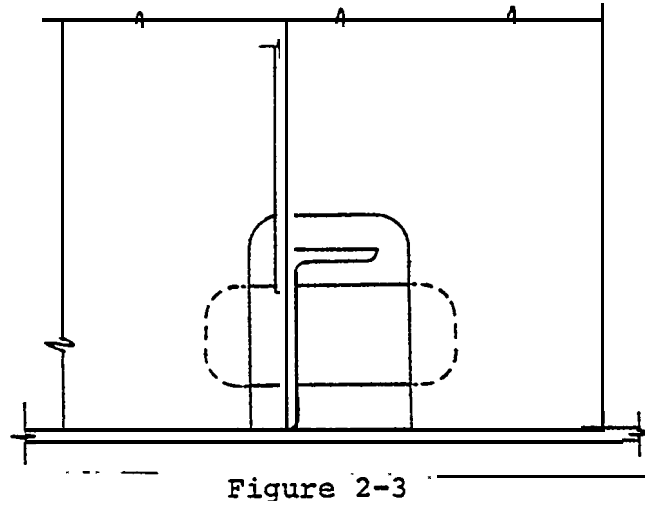
Figure 2-3

All the most commonly used poor features in clearance cuts are illustrated by Figure 2-4.

Figure 2-4
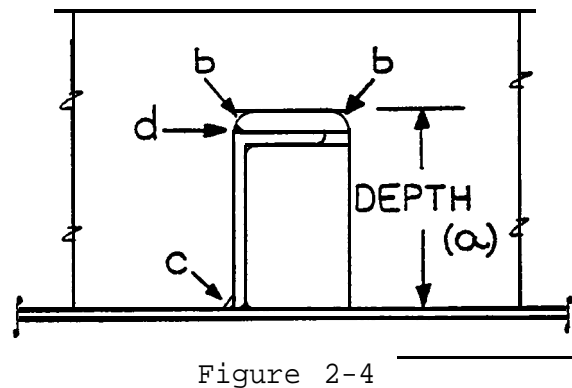
a.   If the stiffener exceeds the depth of the opening that opening must be trimmed, probably by hand, possibly introducing notches (stress risers) .

b.   The sharp radii in the cutout have produced service cracks.

c.   The small size of the snipe at the base of the penetrated member creates difficult access for welding and may introduce corrosion and maintenance problems.

2-4

d.   Welding past the web of the stiffener may introduce undercut at the edge of the stiffener, resulting in a notch effect at a highly stressed location.

Desirable features of cutouts are illustrated by Figure 2-5.
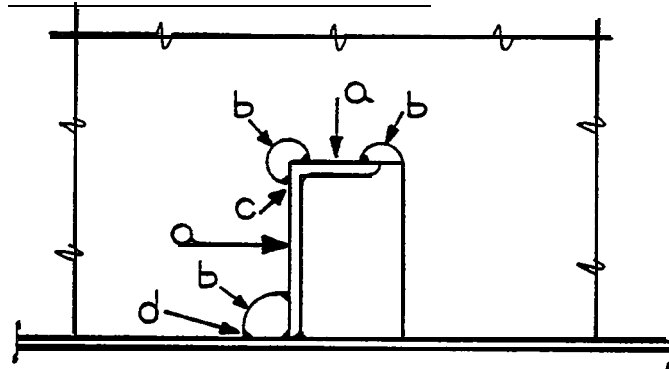
Figure 2-5

a.   Alignment or dimensional errors can be corrected with relative ease by straight line trimming of the tabs.

b.   Large radius of the snipe and flange cutouts provides better access for welding.

c.   Notches produced by welding of the tabs to the stiffener are more nearly in line with the direction of applied stress than normal to it, therefore reducing the possibility of crack initiation and propagation.

d.   Short tangency extensions to the snipe cut permit modest trimming without introducing acute angles or disturbing accessibility.

Additional comments relative to collars (tabs) and snipes will be found in the paragraphs on stiffener endings and miscellaneous cutouts. It should be noted that more complex yet favorable cutout geometries create little difficulty for the modern shipyard equipped with numerically controlled flame cutting. In fact, the complex cutout is somewhat of a guarantee that the correct tool will be used and that casual manual burning will be avoided.

2.3   MISCELLANEOUS CUTOUTS

2.3.1   Penetrations

The one-sided pipe coaming in Figure 2-6 is commonly used
in the machinery space.   The inability to seal weld the
interior permits trapping moisture and can lead to corrosion.
Although a penetrating coaming is preferred, it is recognized
that the advanced planning it requires is not always practical.
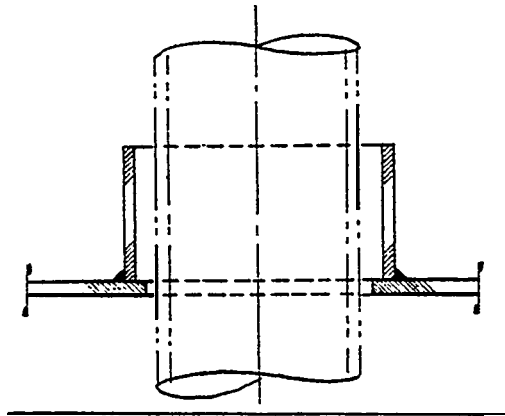
Figure 2-6

2.3.2   Temporary Openings and Patches

It is good shipyard practice to minimize temporary openings.
Provision for access should be provided in the design stage
by optimum use of lightening holes, with special attention
to the position of structural units during subassembly.

Round openings are preferred, with oval openings sized to
OSHA requirements used when required for personnel access.

Lapped patches over temporary openings should be used only
in areas of low stress.   Their use generally requires
approval by the resident inspector.   Flush patches with an
integral backing bar (Figure 2-7) must be used when only one
side is accessible for welding.   The unwelded backing bar
edge is susceptible to corrosion.

Figure 2-7
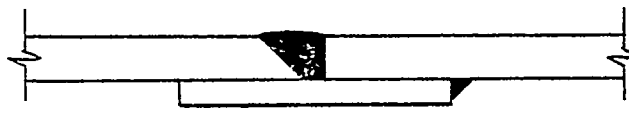
2.3.3   Miscellaneous openings

There is great diversity in the configuration of snipes drain holes, etc. , and it is difficult to rank one detail over another without specific consideration of purpose and location.

Round holes are generally preferred over half-round and oval holes, i.e. Figure 2-8a is favored over Figure 2-8b.   Small radius cutouts as illustrated by Figure 2-9 should be avoided: coating and maintenance is difficult, and they obviously produce higher stress concentration.   To minimize the effects of stress concentration, small radius tits are better drilled than burned.   Figure 2-10 shows an opening close to a structural intersection that should generally be avoided.
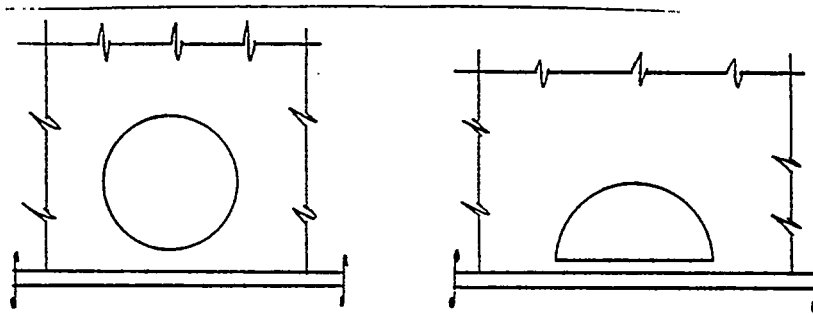
Figure 2-8a   **Figure 2-8b**
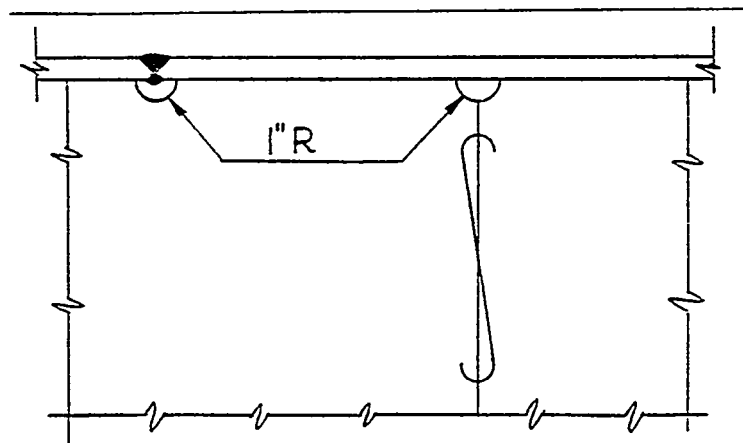
Figure 2-9
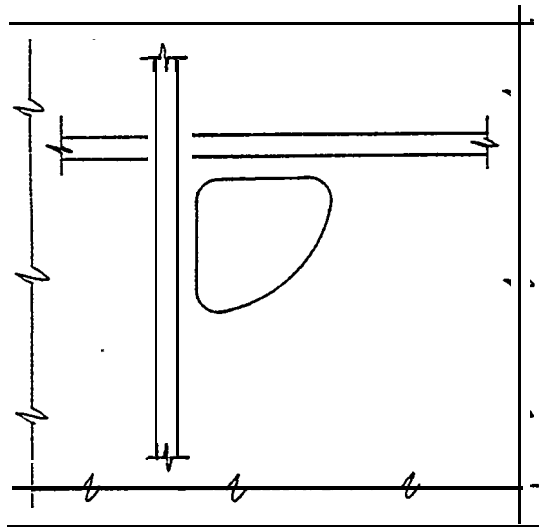
Figure 2-10

The elliptical cutout in Figure 2-11 provides greater drain-age area, a lower "drain" and less stress concentration than that in Figure 2-12.

Figure 2-11
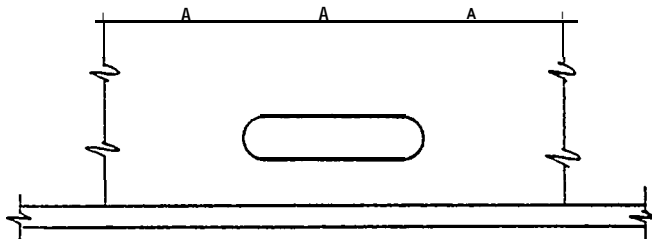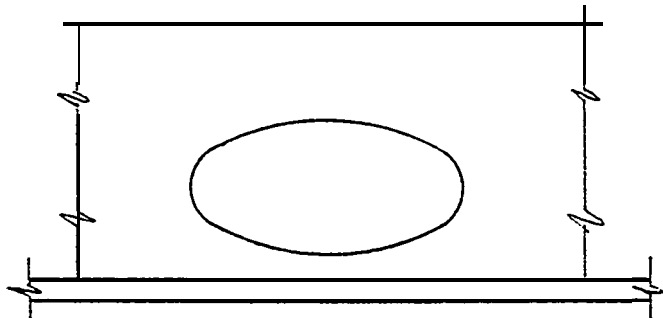
Figure 2-12

Straight snipes as shown in Figure 2-13 are very common but less desirable than rounded cuts . Welding at the edges, particularly if a weld wrap is required, does not lead to a very sound weld.

Figure 2-13.
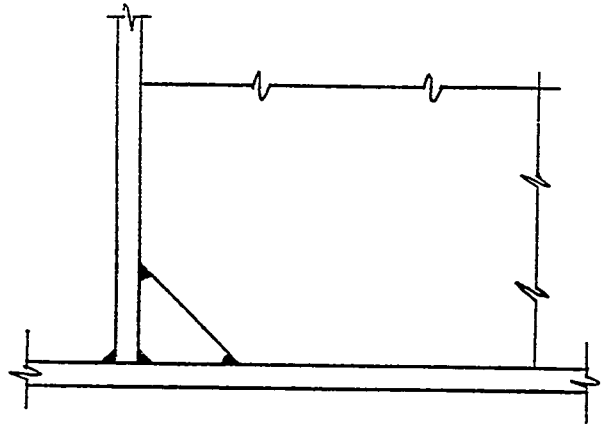
Figure 2-14 shows the extension of a snipe to accommodate
an adjacent seam or butt. Partial collars (Figure 2-15) or
full collars (Figure 2-16) may be necessary to restore
strength in heavily loaded areas.

6" MAX

Figure 2-14

OVER 6"
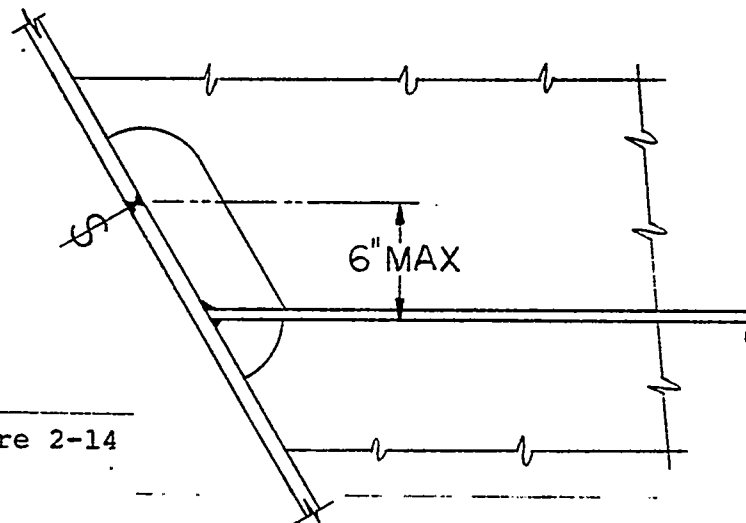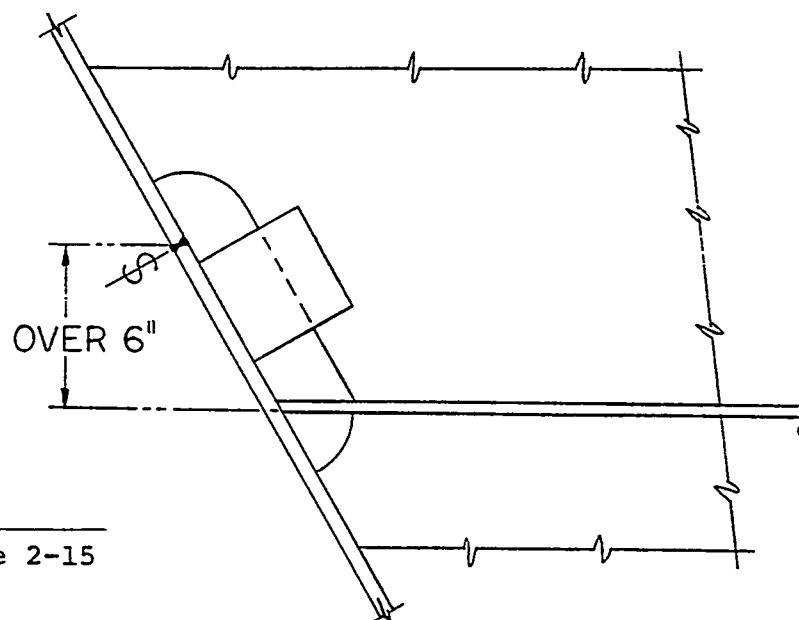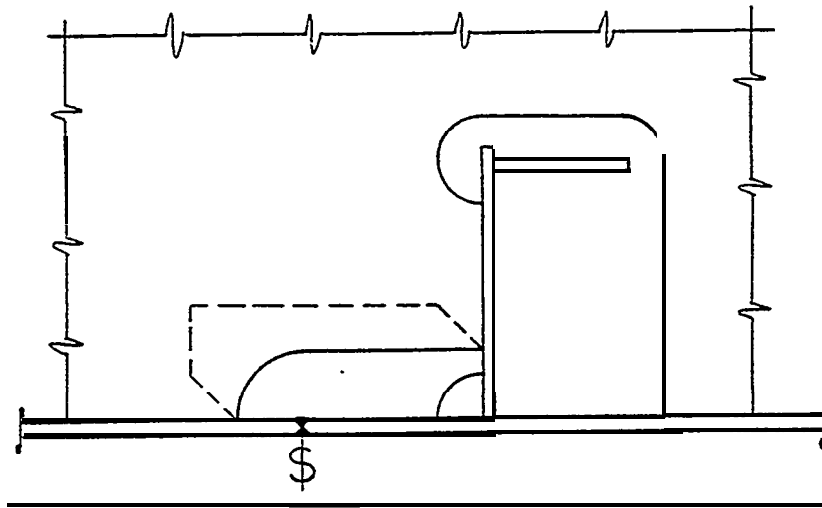
Figure 2-15

Figure 2-16

2.4   BRACKETS AND CHOCKS

2.4.1   Beam Brackets

Beam brackets, not knee brackets, are generally treated as
structural details. These brackets serve to transfer end
moments and shear into adjacent structure, and to reduce the
unsupported span of a beam.

The standardization of beam brackets is nearly impossible
because of the diversity their function calls for. An
extreme case is mentioned in Reference 2, where 81 geometrical
forms of beam brackets were observed on a single ship.

For coplanar angle or flat bar stiffeners, a lapped bracket
is preferred to a butted bracket. Brackets with sniped flange
are used where the bracket edge is long and where loads are
relatively high. When higher loading requires a continuous
bracket (Figure 2-17), tangency and flange chocks should be
fitted to the intersecting structural members. Without these
chocks the knife-edge arrangement can result in cracks.
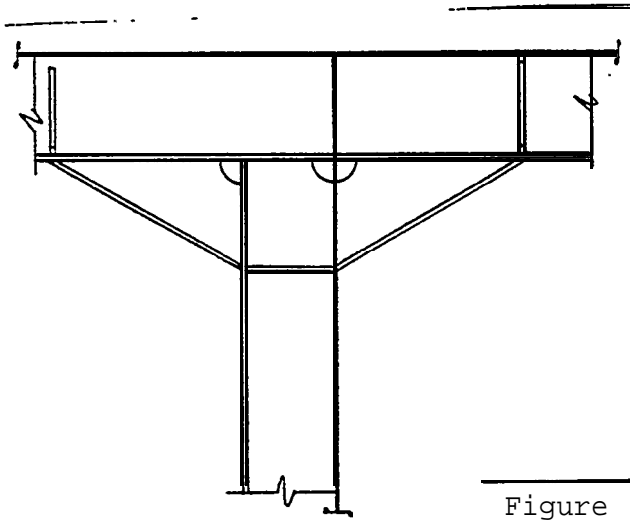
Figure 2-17

2.4.2   Chocks

Chocks are used as reinforcement or backup in areas of con-
centrated force; as intermediate load carriers in areas of
structural discontinuity and as a means of stabilizing flanges
in structural elements. Tangency chocks are generally the
same thickness as the web of the girder to which they are
attached, and flange chocks are of similar thickness to that
of the flange to which they are welded.

Sniping the corner of a chock is a good design feature which
allows the weld to be easily wrapped. If the angle of the
chock edge is steep enough (e.g.   60 degrees) sniped corners
are not necessary. The snipe should be about 1/2 inch.
Some snipes of smaller dimensions (Figures 2-18a and 2-18b)
do not provide enough material for a good weld wrap and tend
to "burn up".

Small interior snipes as shown in Figure 2-19 simplify fit-
up of the chock, but make welding more difficult and create
a difficult area to access for cleaning, painting and main-
tenance. Interior snipes should provide enough of a cut-
away to reduce these difficulties or be eliminated altogether.
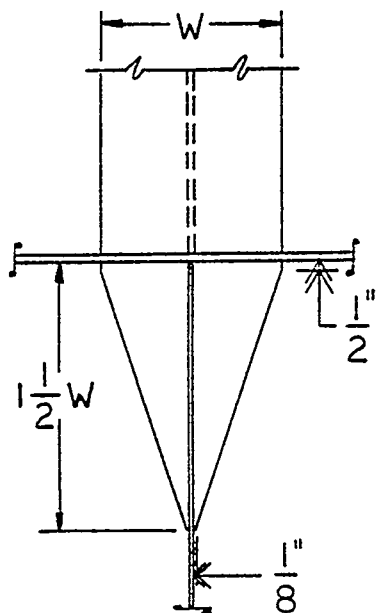
Figure 2-18a
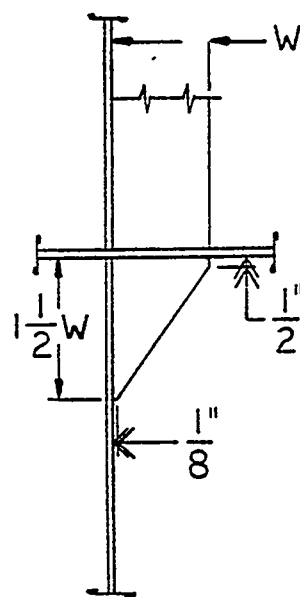
Figure 2-18b
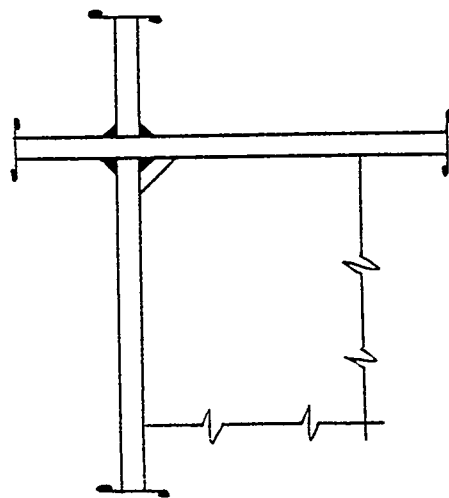
Figure 2-19

2.5   STIFFENER ENDINGS AND TRANSITIONS

Three degrees of stiffener end fixity are recognized by
the American Bureau of Shipping in establishing section
modulus requirements. Efficient brackets provide fixed end
support, clips provide intermediate support, and no end
attachment corresponds to a pinned connection.

Fixed end connections are typically attempted with angles
or tees as stiffeners, and free ended stiffeners are often
flat bars.

When web and flange of a stiffener are butted against adjacent
structure to create a fixed end condition, it is common to
use flange chocks, as shown in Figure 2-20, to reduce stress
concentration.

(A)

(B)
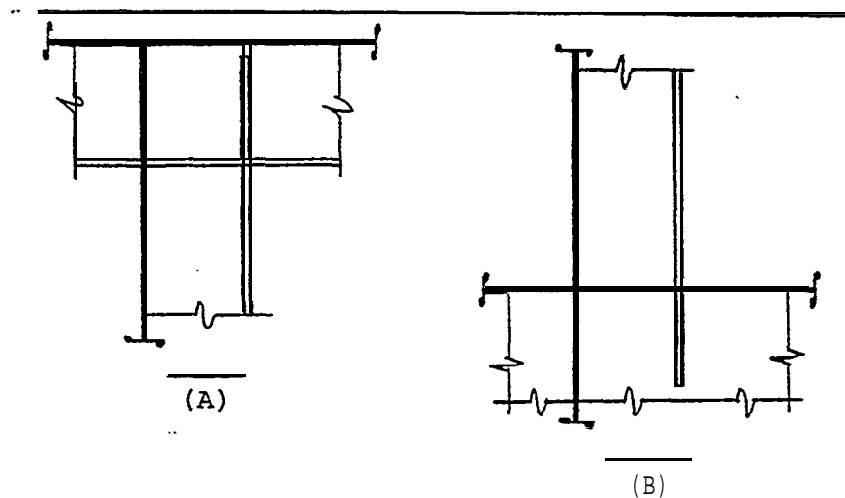
Figure 2-20

Lapped end connections and clips are credited with similar
end fixity. The lapped connection provides greater lateral
stability, but requires stiffeners on opposite sides of the
molded trace. Typical overlaps are in the range of 2-2 1/2
inches, and are illustrated in Figure 2-21. The snipe detail
shown in Figure 2-21b allows better weld access and continuity
than that in Figure 2-21a.
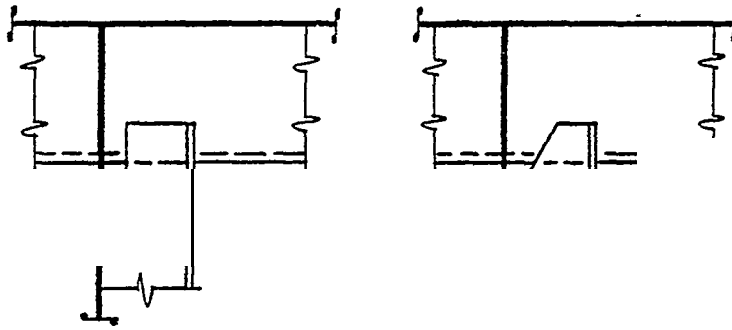
Figure 2-21a   Figure 2-21b

Clips are generally made at least as thick as the web of the
stiffener to which they are attached. Increasing the clip
scantlings allows it to carry the full stiffener-induced
load.

A clipped connection should allow a gap between stiffener
end and adjacent structure large enough to permit good
welding and painting access.

Stiffener endings assumed to be free ended may have much of
their section cut away (Figure 2-22) or have no end attachment
 (Figures 2-23, 2-24 and 2-25). A free stiffener end cut
square is more difficult to weld than one that is sniped and
introduces larger end stress concentrations. The gap for an
unattached stiffener end should be large enough to allow
access for welding. Figure 2-25 illustrates a better arrange-
ment than Figure 2-24, although the snipe in the former is
considered too complex for *commercial* practice. The
corner of Figure 2-25 should be sniped to a depth greater
than 1/8 inch for satisfactory welding. One-half inch is a
reasonable minimum.

Figure 2-26 illustrates a producibility problem when it is
required to wrap the weld against the angle bosom.

Figure 2-22

Figure 2-23

ABT 2"
CLEAR

Figure 2-24

$1\frac{1}{4}$"

30°

ABT
2"

$\frac{1}{8}$"

Figure 2-25

$\frac{5}{8}$"
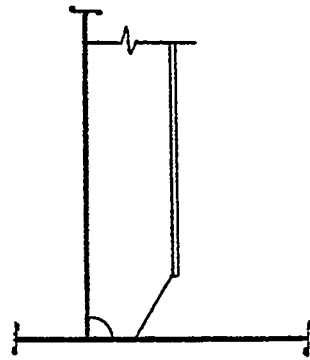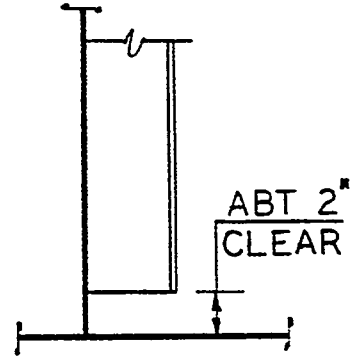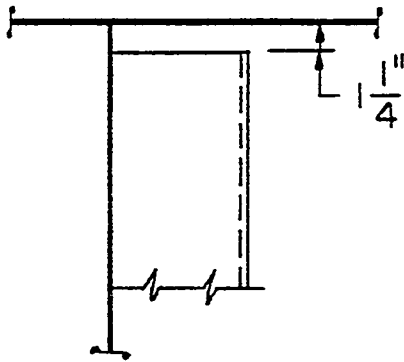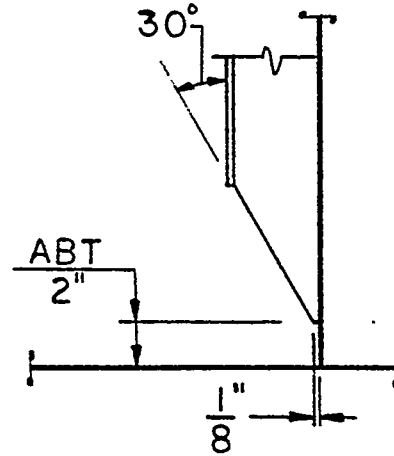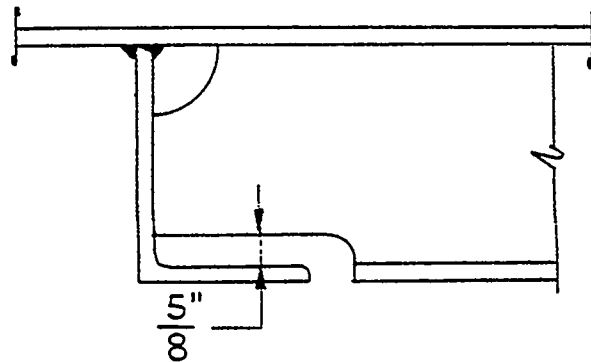
Figure 2-26

Clip ended stiffeners as shown in Figure 2-27 are often
used without backup structure, giving rise to potential
"punch through". The clip on the angle stiffener in
Figure 2-27a overlaps the flange, and because of greater
resulting eccentricity reduces the reaction force on the
plating. On occasion the hardspot is relieved by fitting
a sole plate as shown in Figure 2-28.
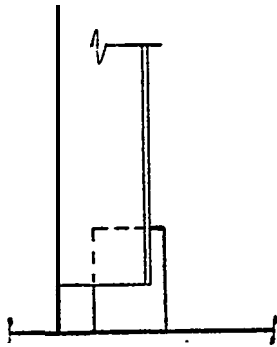
Figure 2-27a
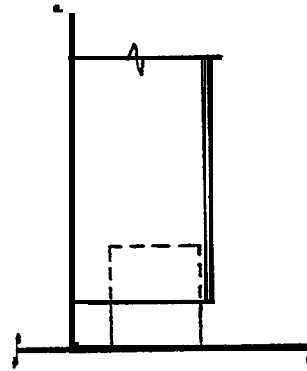
Figure 2-27b
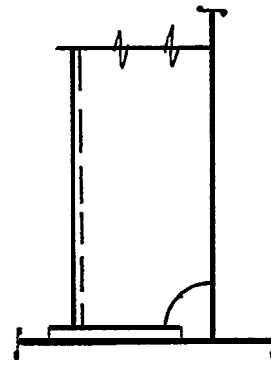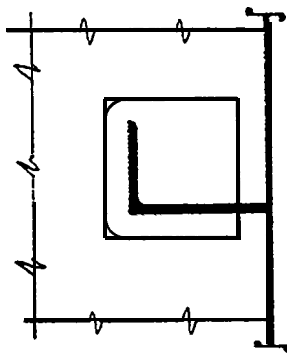
Figure 2-28

Transition pieces can also fall into the category of face
plates. Their purpose is to provide gradual transition
between structural members of different width (Figure 2-29)
and depth, or to run out stiffeners, say longitudinal at
the ends of the ship (Figure 2-30).
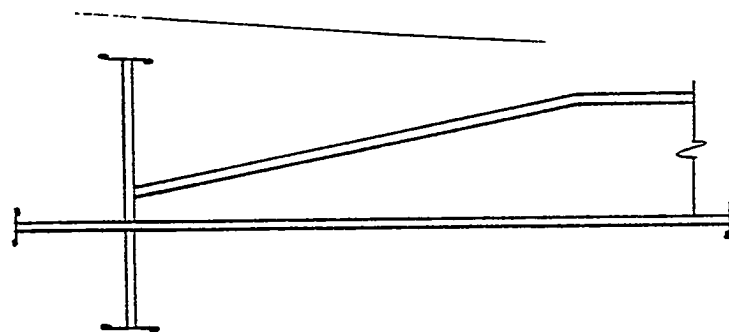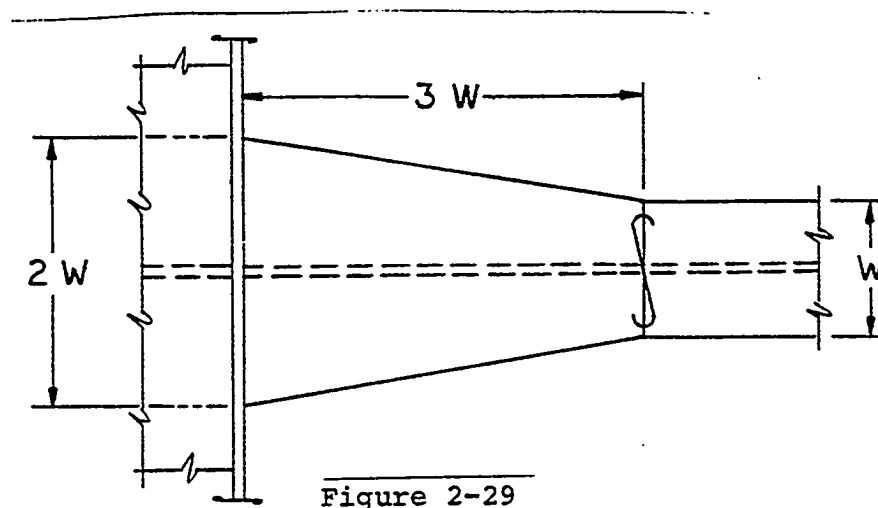
Figure 2-29

Figure 2-30

2.6   PANEL STIFFENERS

Panel stiffeners are used as local or intermediate deck
structural reinforcement, as stiffeners intended to prevent
buckling of deep webs, and as support to members penetrating
these webs.   Panel stiffeners are generally rolled angles or
flat bars, whose section properties are specified by the
Classification Societies for any given application.

The distinguishing features of types of panel stiffeners are
their method of end connection, generally discussed in
Section 2-5.   Sniped corners, particularly for flat bar panel
stiffeners as shown in Figure 2-31, allow better material
utilization and better access for welding.   The desirability
of about a 1/2 inch land for better wrapping was discussed
earlier.

2-17

Angle or tee panel stiffeners not connected to intersecting structure are commonly cut square as shown in Figure 2-32. In the presence of a lateral load this arrangement results in high stresses at the end connection. If lateral load is present, the panel stiffeners can be lapped as shown in Figure 2-33b, where the cutaway at the left clears the weld of the intersecting member. That weld will interfere with the detail as shown in Figure 2-33a.
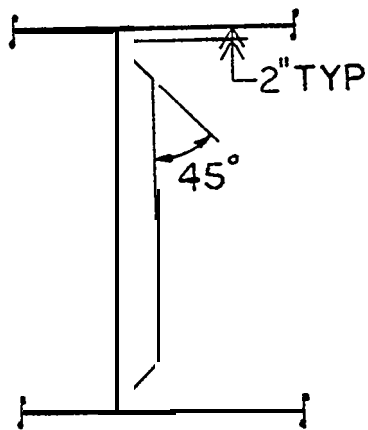
Figure 2-31
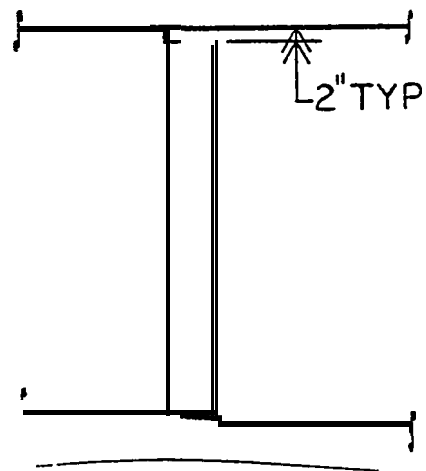
Figure 2-32
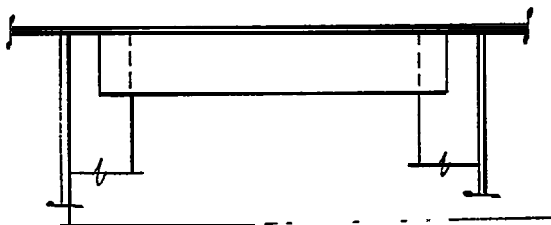
Figure 2-33a
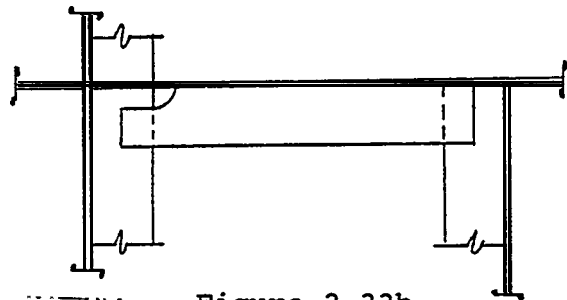
Figure 2-33b

2.7   STANCHION END CONNECTIONS

Stanchion end connections provide for transition between generally dissimilar structural members.

Although stanchions are normally viewed as compressive members (columns), they may also be loaded in tension, particularly at the ship's bow. This results from section deformation due to large lateral pressures. Therefore the stanchion end connection should have the cross sectional area and section properties required by its function. Generally those properties should be equivalent to those of the stanchion itself.

It is simpler to design end connections for an H or I-beam stanchion than for a pipe stanchion, although the required orientation of the former in a particular application may make alignment with deck girders difficult.

It is common practice to provide a sole piece for pipe stanchions whose wall thickness exceeds the thickness of the plate to which they are attached. A particularly effective, although admittedly complex, connection for pipe stanchions is shown in Figure 2-34. It has high tensile capability **and is very compact.**
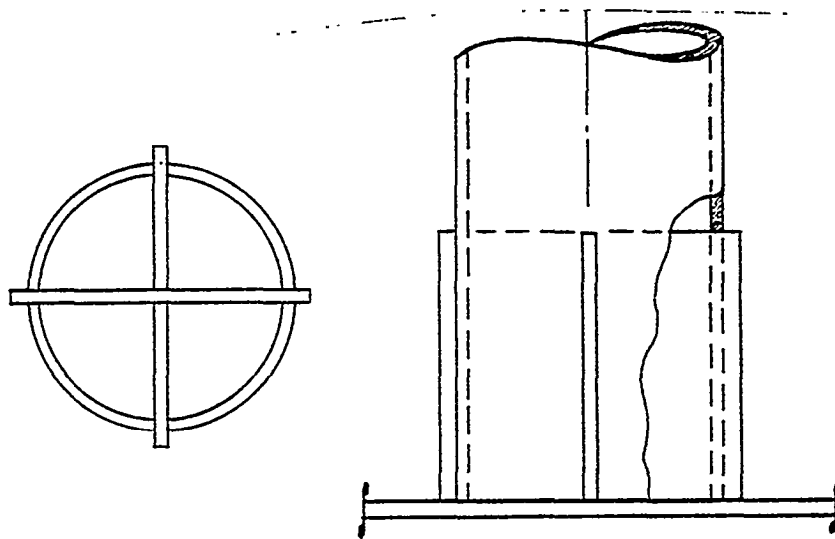
Figure 2-34

The I-beam connection in Figure 2-35 provides good alignment
with two intersecting members, and is therefore better than
that shown in Figure 2-36 which requires additional chocks.
The load capacity of supporting girders must be considered.
Clearance cuts in close proximity to stanchion end connec-
tions are often provided with a flush full collar to increase
strength. Figure 2-37 illustrates a connection that is
difficult to fabricate. The detail in Figure 2-38 could be
improved if a 90 degree rotation of the stanchion were
permissible.
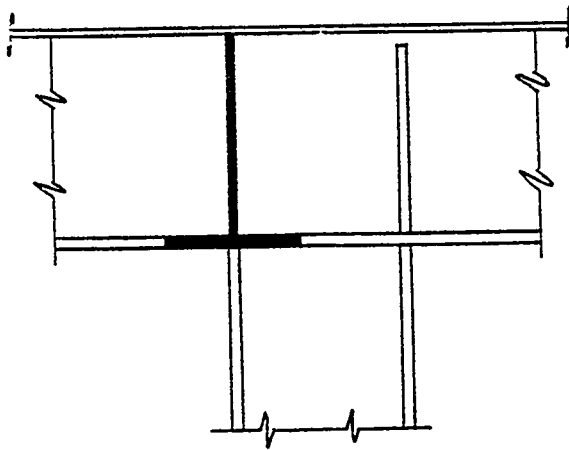
Figure 2-35
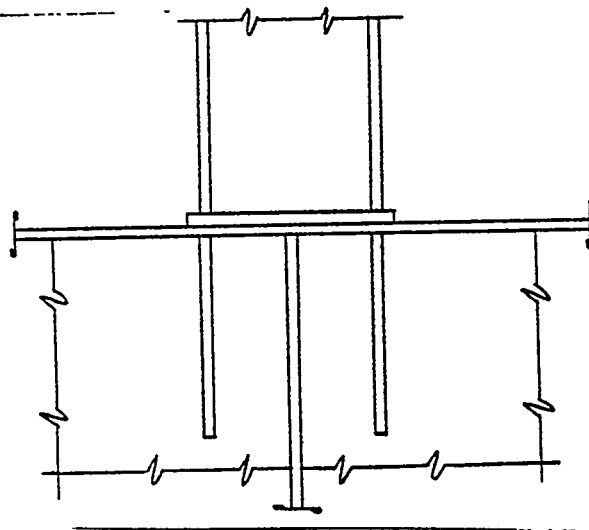
Figure 2-36
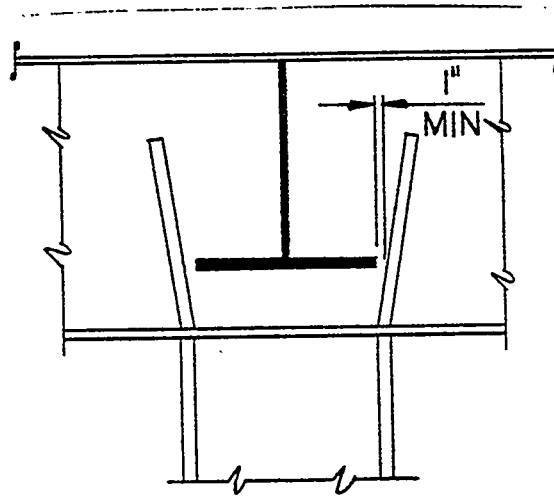
Figure 2-37
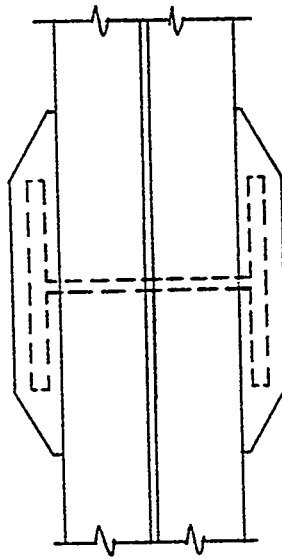
Figure 2-38

Section 3
ANALYSIS OF STRUCTURAL INTERSECTIONS

3.1   <u>GENERAL</u>

Specific attention was focused on structural intersections
because for any given ship they generally constitute the
largest single group of details and because many structural
failures have been attributed to stress concentrations due
to unfavorable geometry.

The analysis was undertaken in two parts: one to investigate
the effect of cutout geometry and type of loading on stress
distribution, and the second to establish the effect of type
of stiffener connection on stress level and joint efficiency.

Only a static analysis has been attempted, consequently the
results are primarily useful for comparing alternative con-
figurations, rather than for definitive evaluation of the
load carrying capacity of the detail.

The finite element analysis was performed with the ICES
"STRUDL II" computer program, specifically the IUG version
V3MO of June 1976.

3.2   <u>CLEARANCE CUTS</u>

3.2.1   <u>Clearance Cuts - Elliptic</u>

The analytical model employed represents a beam with a
29 inch x 1/2 inch web and 12-1/2 inch x 1 inch flange with
a length of 10 feet. The girder is attached to a plate with
an equivalent section area of 30 square inches. Three cutouts
are modeled: coarse ones at the ends and one with a fine mesh
at the center, which is the one analyzed. The details of the
model are shown in Figures 3-1, 3-2, 3-3 and 3-4. Elliptical
and flat-topped clearance cuts were studied under three

FIXED END

FINITE ELEMENT ANALYSIS MODEL

ELLIPTICAL CUTOUT
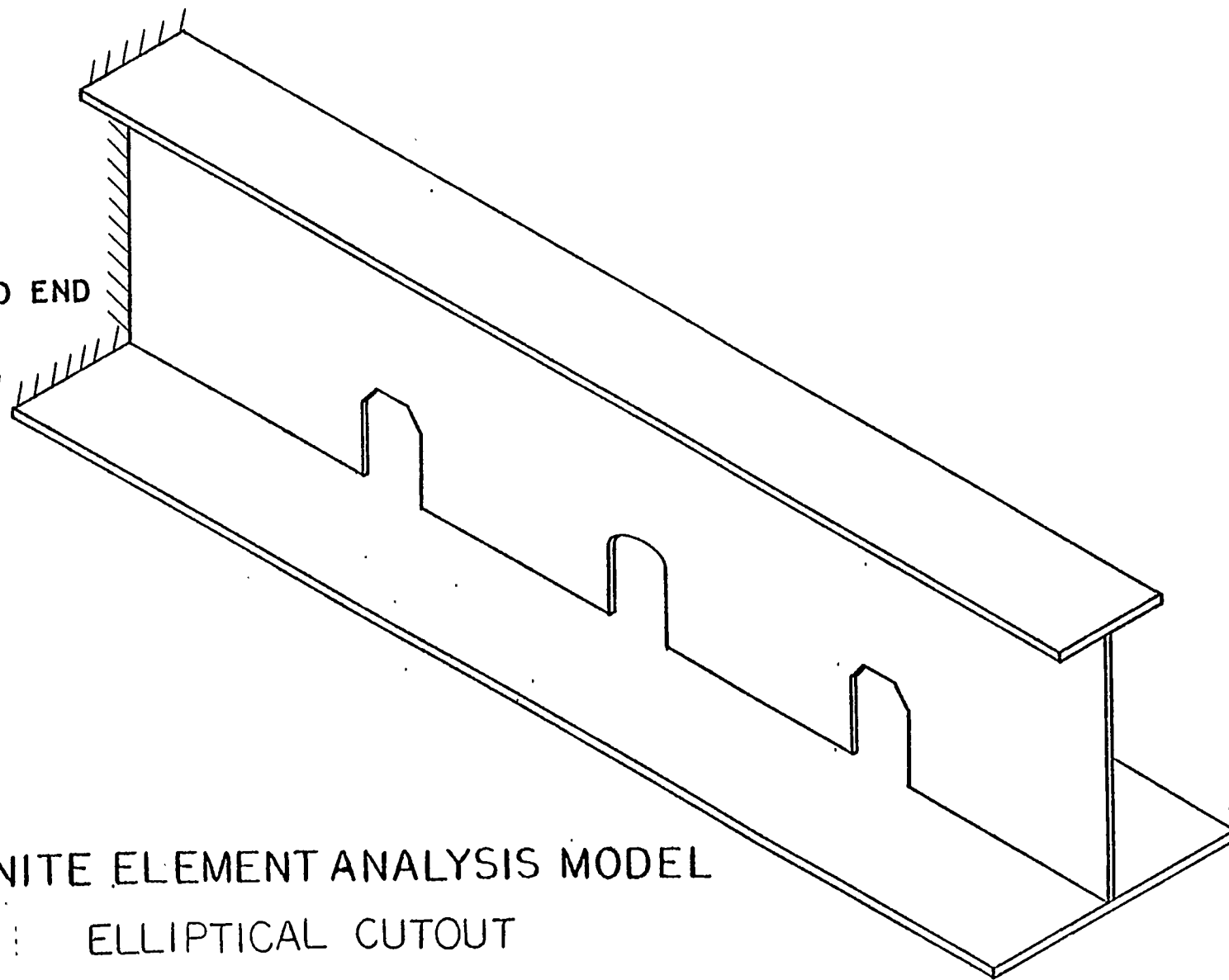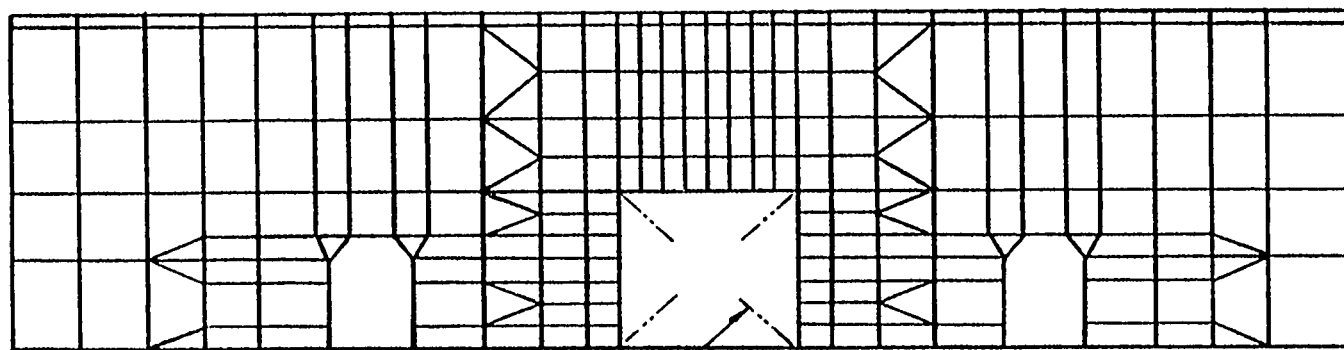
Figure 3-1

FOR MODEL
OF THIS AREA
SEE FIG.3-4

FINITE ELEMENT ANALYSIS MODEL
ELLIPTICAL CUTOUT

Figure 3-2

ELLIPSE 2:1 RATIO OF MAJOR TO MINOR AXIS

$1\frac{1}{2}"$

$1\frac{1}{2}"$
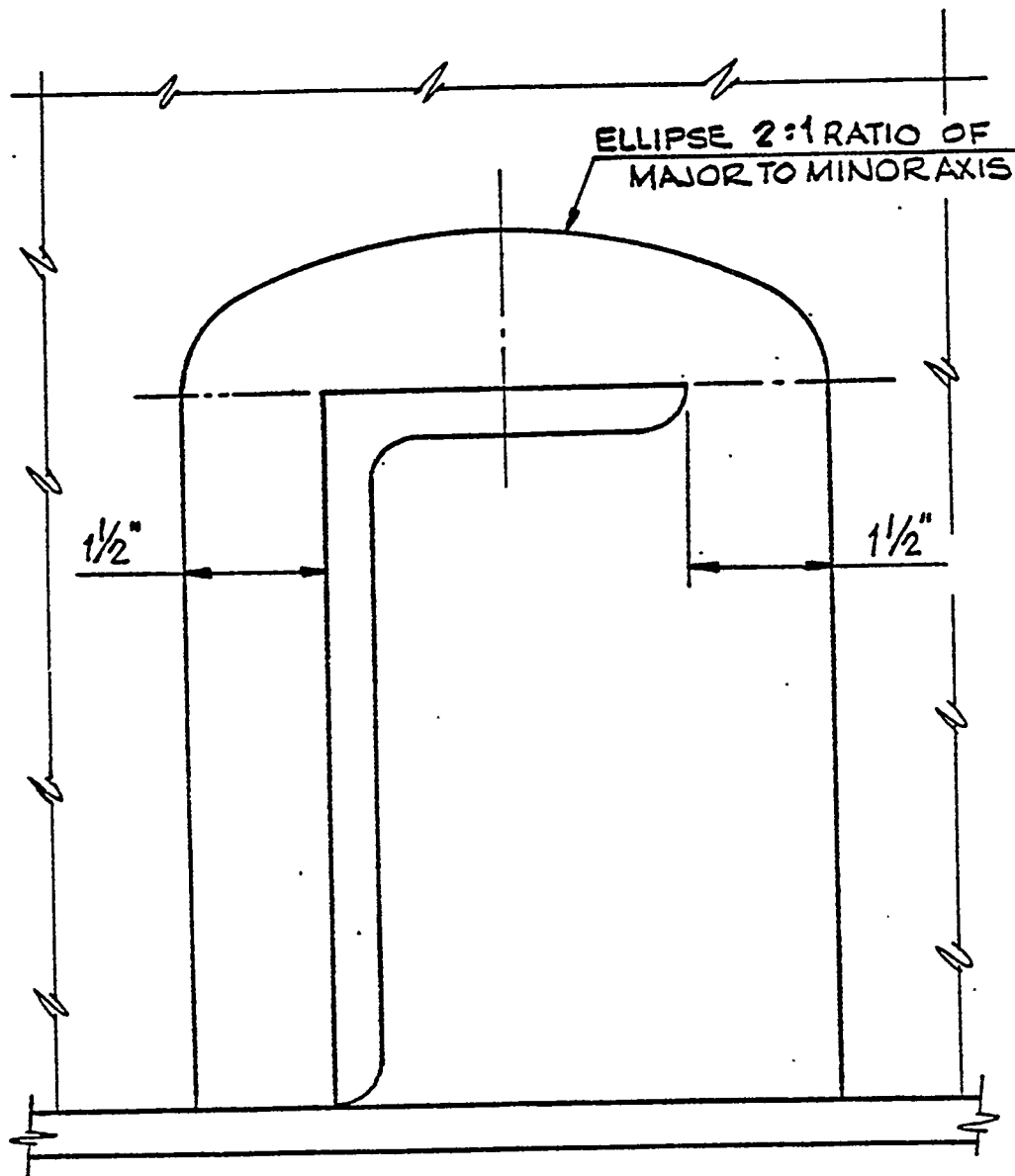
ELLIPTICAL CUTOUT
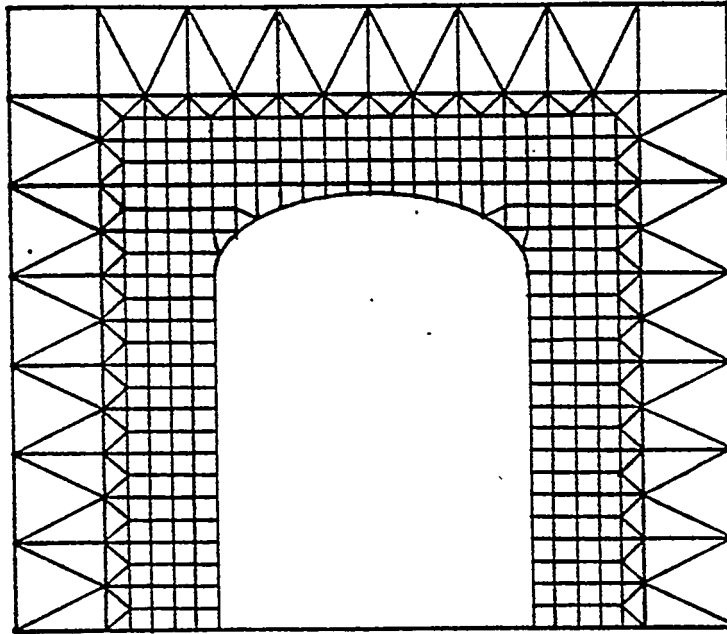
Figure 3-3

DETAILED MODEL OF CUTOUT AREA

ELLIPTICAL CUTOUT

Figure 3-4

loading conditions:

       Case 1 - Axial
       Case 2 - Bending
       Case 3 - Shear

The analysis of the flat-topped cutout was simplified by applying the displacements of the elliptic fine mesh segment boundary to the modified fine mesh segment.

3.2.2   Elliptic-Results

For each loading case the stress amplification in way of the clearance cut centerline was calculated and plotted. For example Figure 3-5 indicates a maximum amplification factor of 2.53 at the cutout. This means that the maximum axial stress is 2.53 times the average stress calculated for the

FLG
12½" x 1"

WEB
29" x ½"

EQUIVALENT RTG
AREA = 30 IN² = A

LOAD CASE NO.1: AXIAL LOAD

0.97

Von Mises Stress
DISTRIBUTION @
CUT-OUT

2.53

1.13

STRESS @ "A-A"
(WITH CUT-OUT)

1.00

$\sigma = \dfrac{P}{A}$
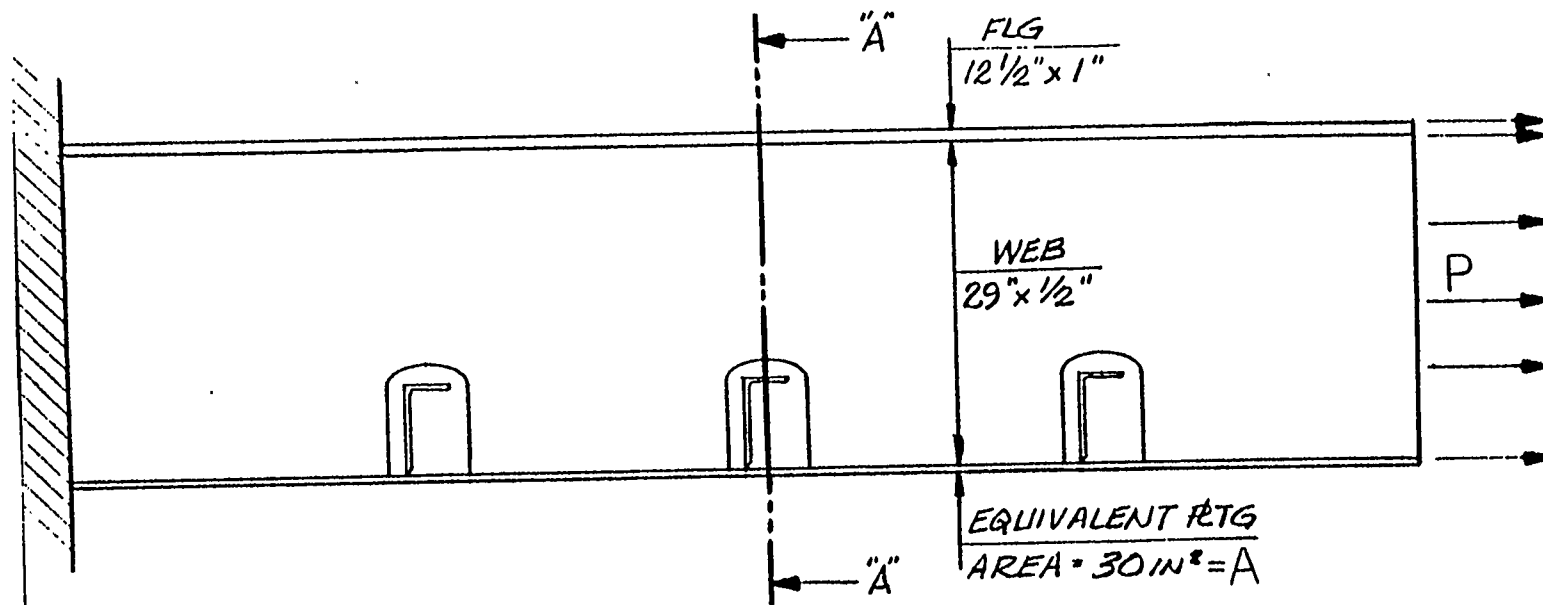
STRESS @ "A-A"
(WITH NO CUT-OUT)
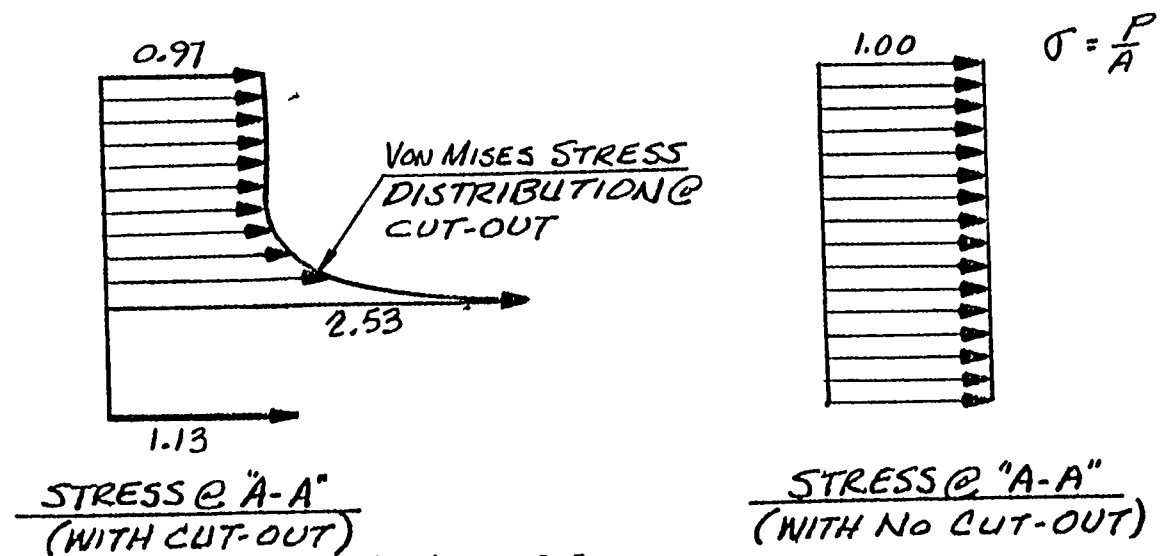
Figure 3-5

intact section. Overall and local plots of stress magnifi-
cation were prepared (Figures 3-6 and 3-7) , where the values
shown are the ratios of von Mises equivalent stress of the
cutout to those of the intact section. Von Mises equivalent
stresses were used because they provide a generally accepted
yielding criterion that takes all plane stress components
into account.

Load distribution and section stress magnification factors.
for the case of pure bending are shown in Figure 3-8. Note
that essentially no section amplification occurs due to
bending.

The stress amplification plots in Figures 3-9 and 3-10
represent ratios with respect to the maximum intact section
stress, i.e. at the flange of the girder.

Pure section shear (Figure 3-11) is developed by applying a
shear and a moment at the free end that induce canceling
moments at the central cutout (Section A-A). Stress ampli-
fication due to shear is 1.95, or about a similar order of
magnitude as that due to axial load.

Stress magnification factor plots in Figures 3-12 and 3-13
indicate that the highest concentration occurs at the upper
corners of the cutout and is in the order of 4.4. A plot
of stress magnification factor along the periphery of the
cutout loaded in shear is presented in Figure 3-14.

Since axial loads on girders are generally small, it can
be concluded that section shear is the most important factor
to be considered in the design of cutouts. Future fatigue
studies could be guided by this conclusion.
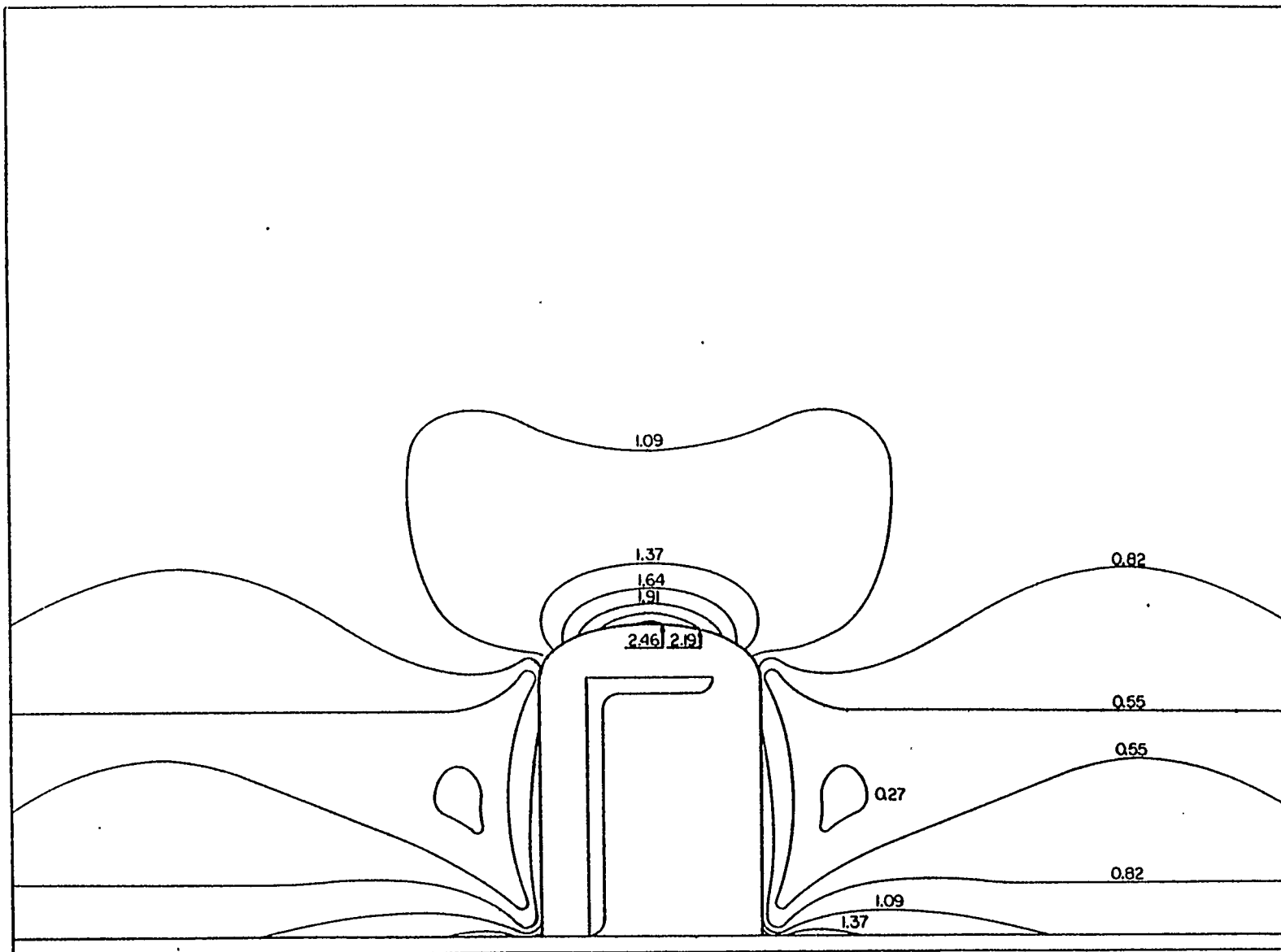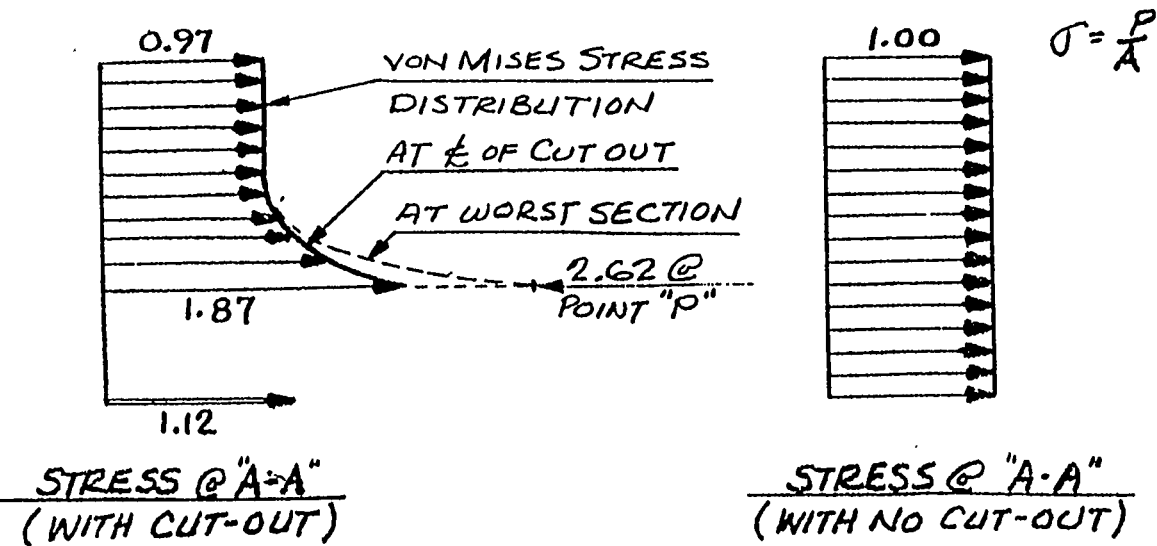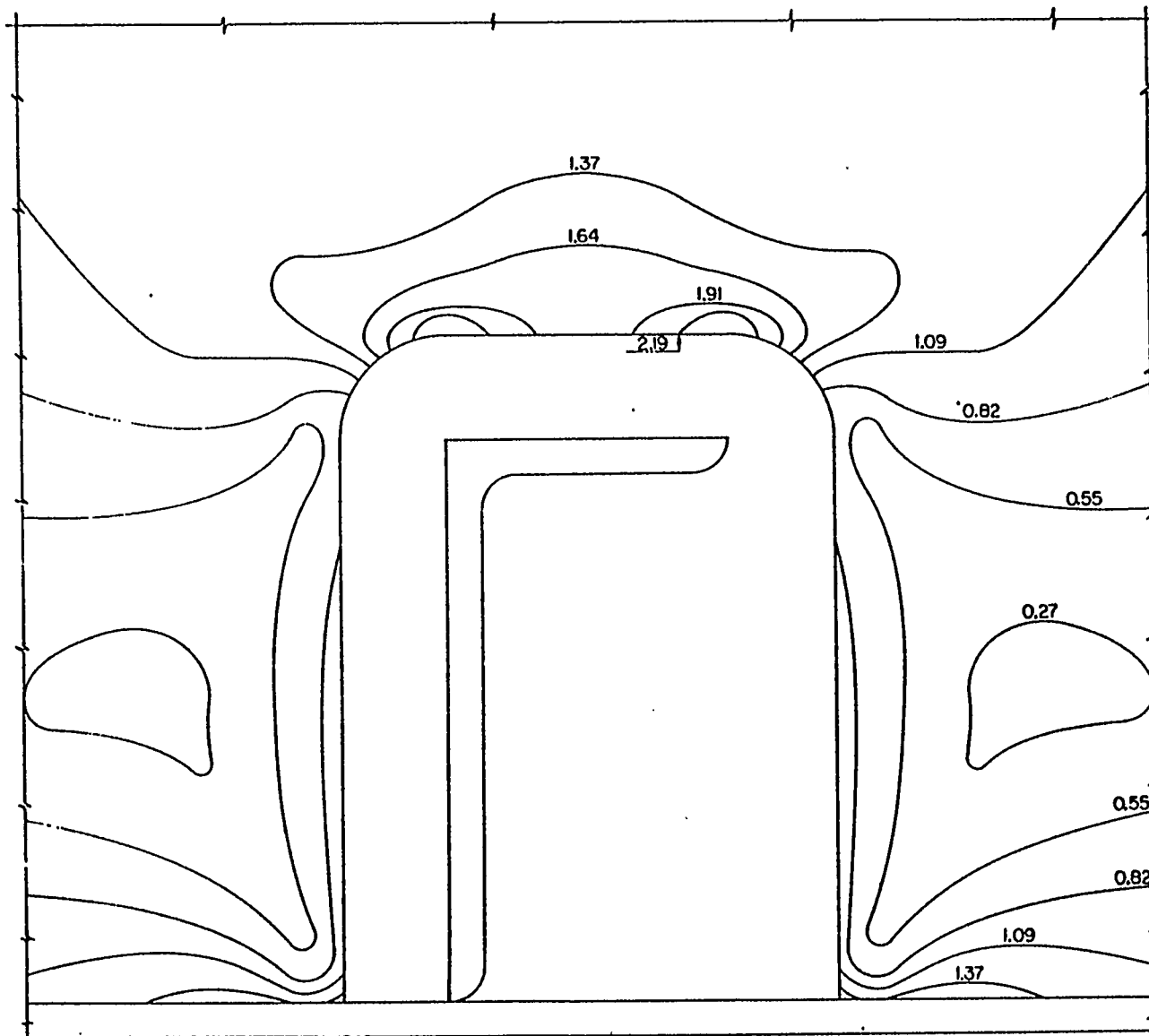
LOAD CASE NO. 1 : AXIAL LOAD STRESS MAGNIFICATION FACTOR

Figure 3-6
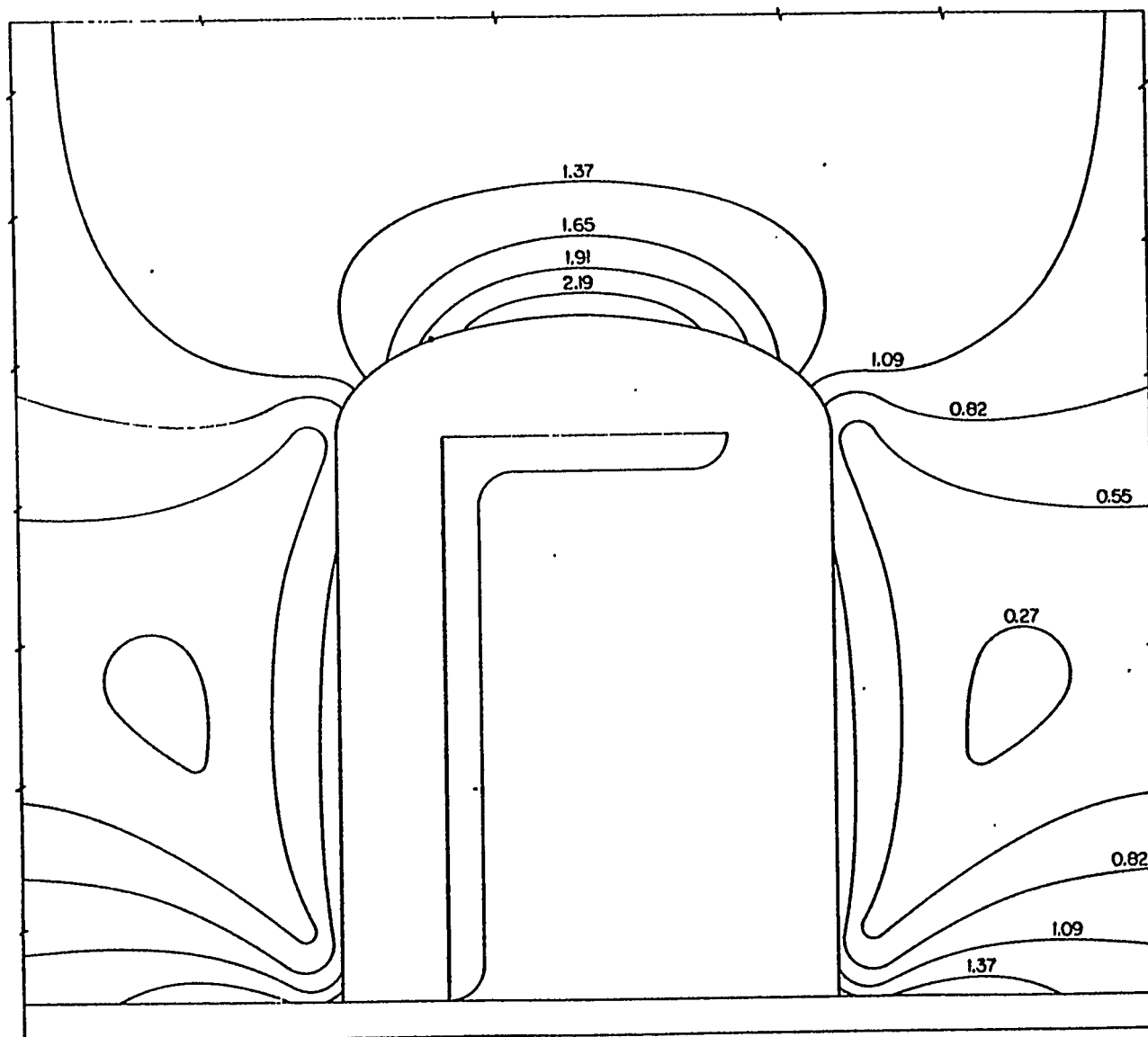
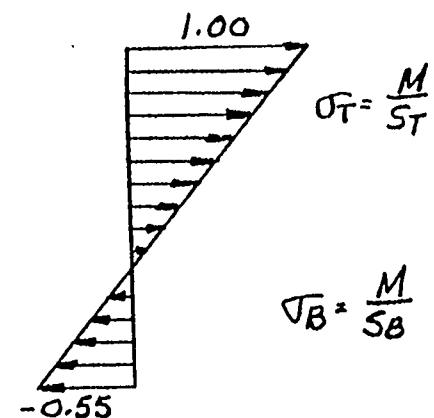LOAD CASE NO.1: AXIAL LOAD STRESS MAGNIFICATION FACTOR

DETAIL @ CUTOUT

Figure 3-7

FLG
$12\frac{1}{2}"\times1"$

"A"

WEB
$29"\times\frac{1}{2}"$

NEUTRAL AXIS

$10.89"$

EQUIVALENT RTG
AREA = 30 IN²

"A"

LOAD CASE NO. 2 : BENDING
(SHEAR = O)

1.02

VON MISES STRESS
DISTRIBUTION @
CUT-OUT

-0.19

-0.54

__STRESS @ "A-A"__
(WITH CUT-OUT)

1.00

$\sigma_T = \dfrac{M}{S_T}$

$\sigma_B = \dfrac{M}{S_B}$

0.55

__CALCULATED STRESS DISTRIBUTION__
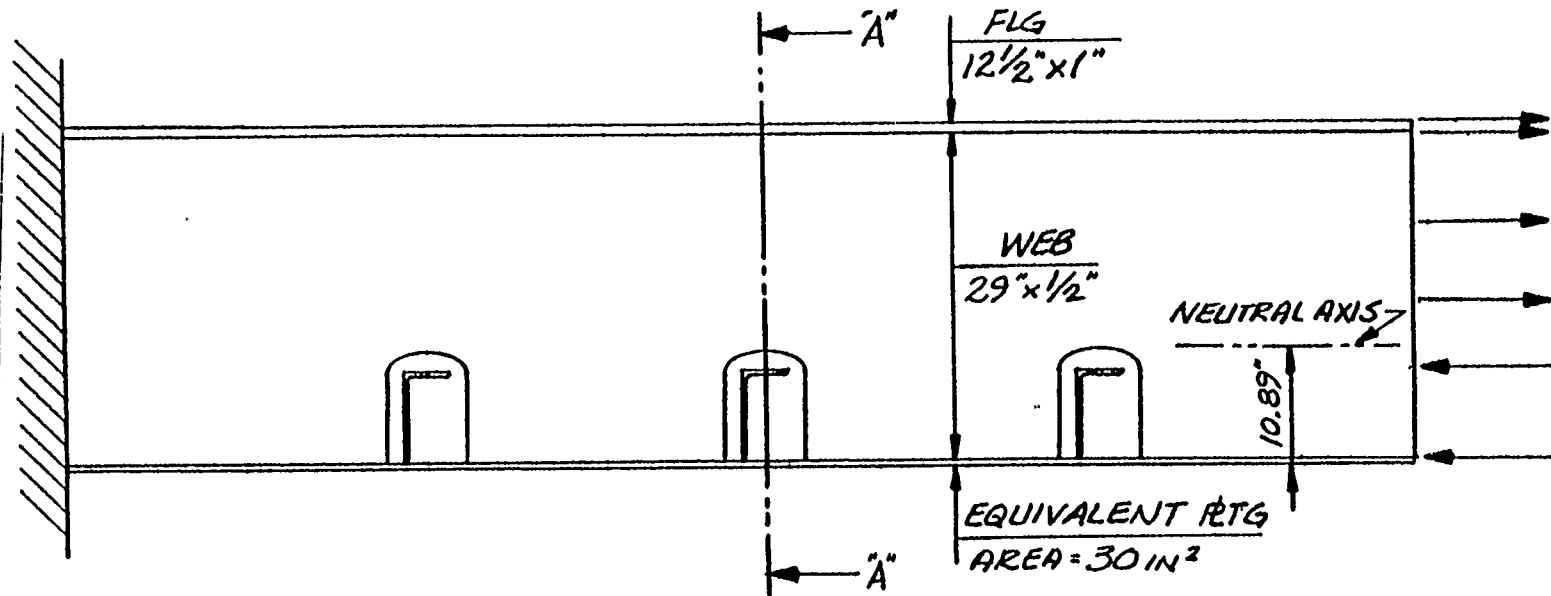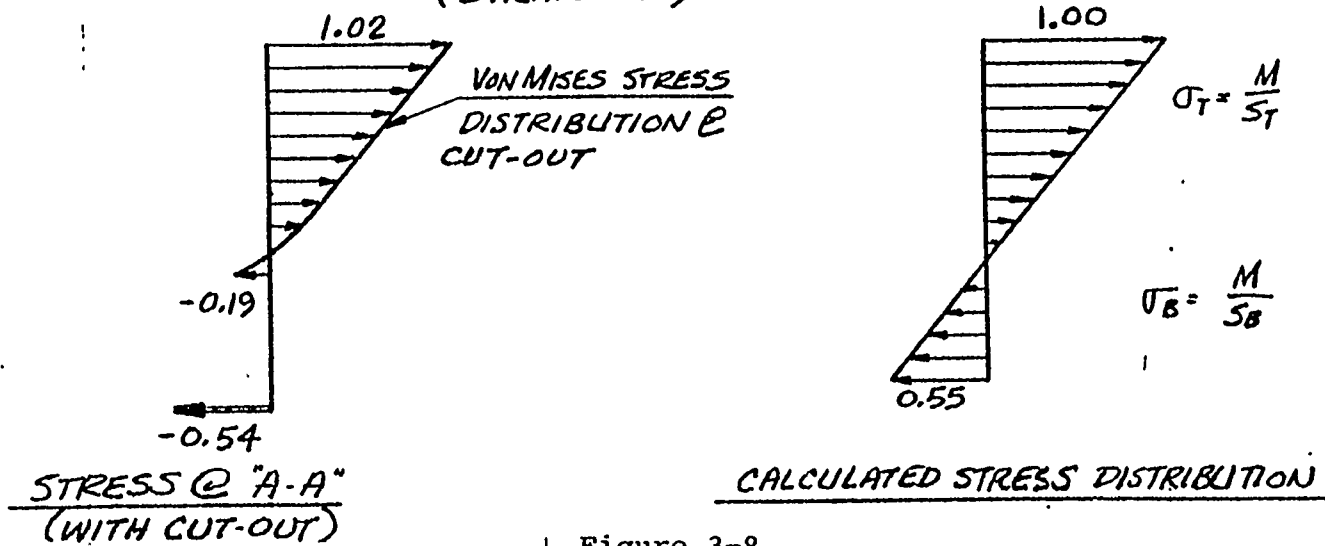
Figure 3-8

LOAD CASE NO. 2: BENDING STRESS MAGNIFICATION FACTOR
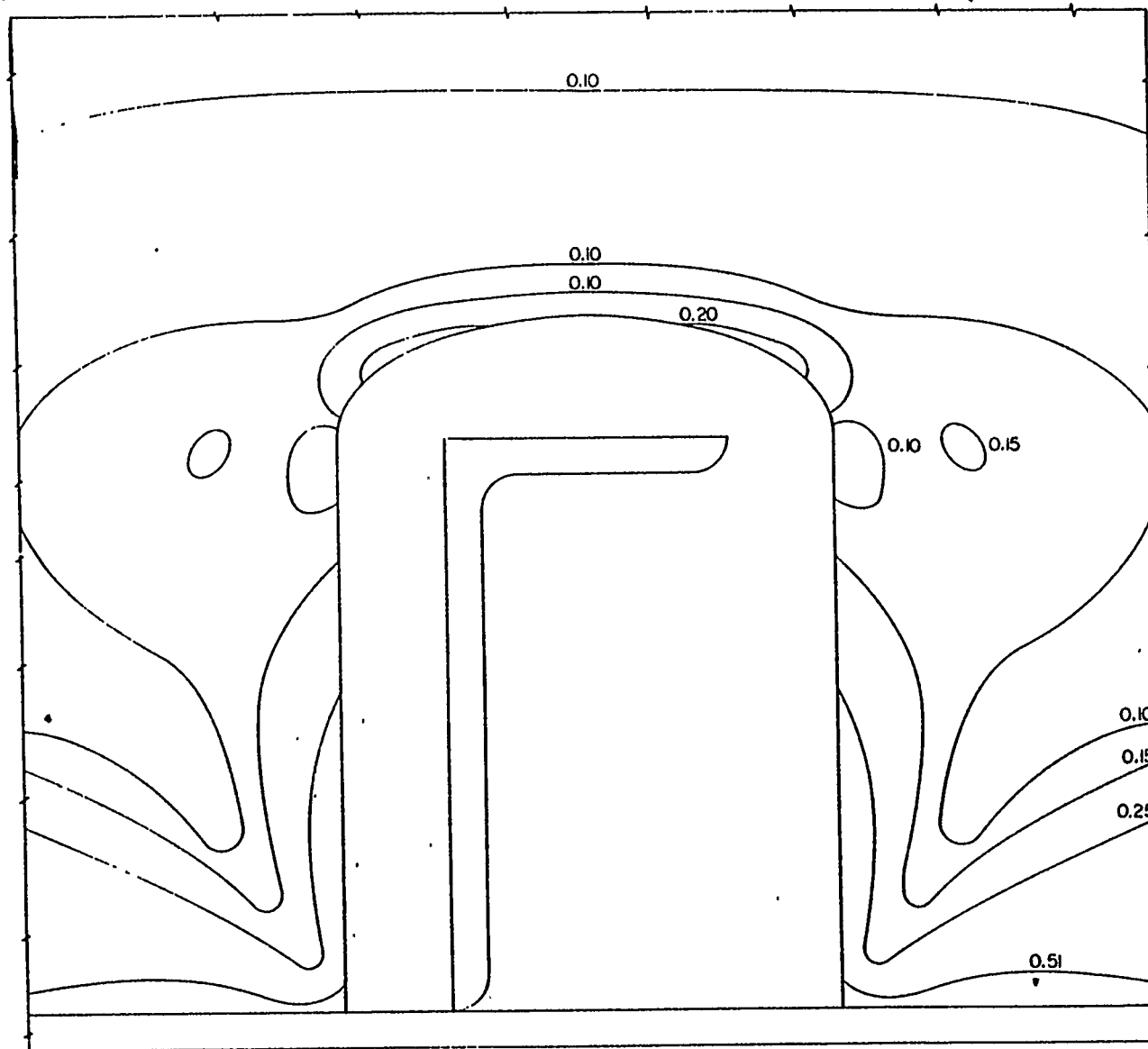
Figure 3-9

LOAD CASE NO. 2 : BENDING STRESS MAGNIFICATION FACTOR
DETAIL 9 CUTOUT

Figure 3-10
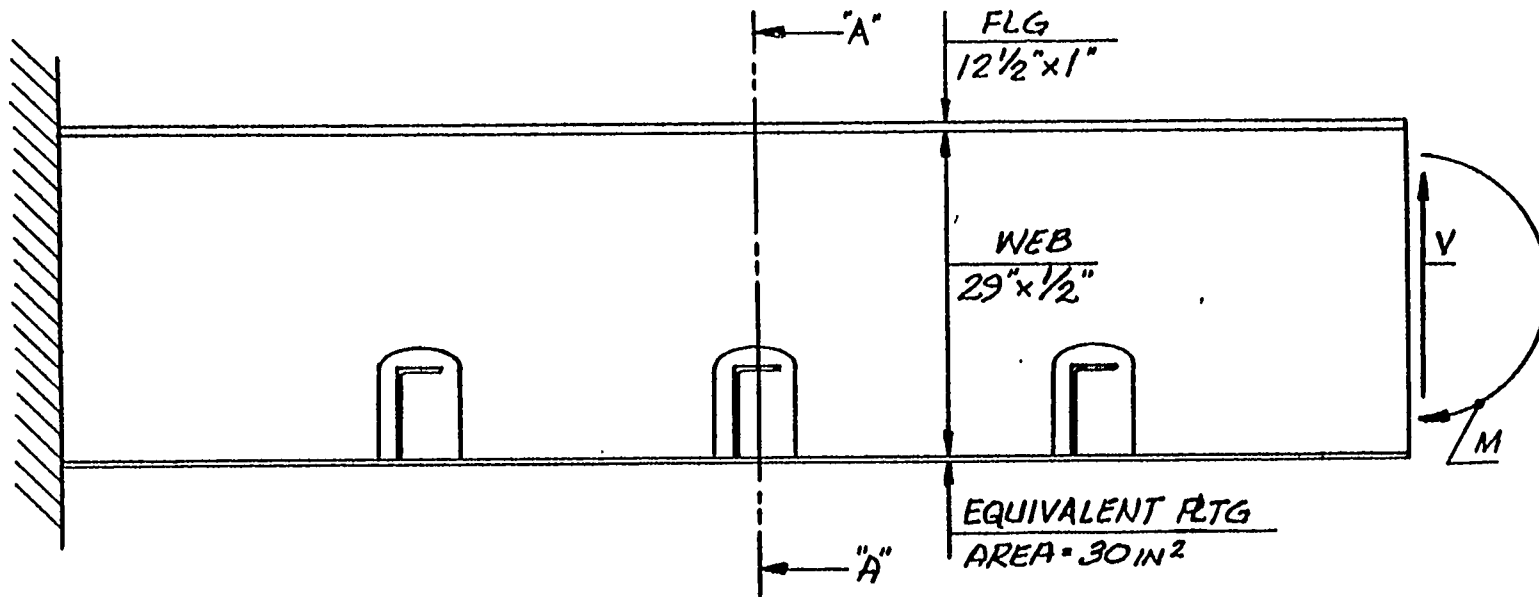
"A"

FLG
12½"×1"

WEB
29"×½"

V

M

EQUIVALENT RTG
AREA = 30 IN²

"A"

LOAD CASE NO.3: SHEAR
(MOMENT = 0 @ CUT-OUT)

SHEAR STRESS
DISTRIBUTION
VON MISES STRESS
DISTRIBUTION @
CUT-OUT

0.90

3.38

0.36

1.95

0.03

NOTE: VON MISES STRESS =
1.73 × SHEAR STRESS

STRESS @ "A·A"
(WITH CUT-OUT)

0.73

$\sigma_{xy} = \dfrac{VQ}{Ib}$

$\sigma_{VON\ MISES}$

$\nabla_{xy} = 1.00$
Max @ N.A.

0.93

CALCULATED STRESS DISTRIBUTION
@ A·A (WITHOUT CUT-OUT)

Figure 3-11

1.31
1.74
2.18
2.62
3.05
3.05
2.18
3.49
4.36
2.18
1.74
1.31
0.87
0.44
2.62
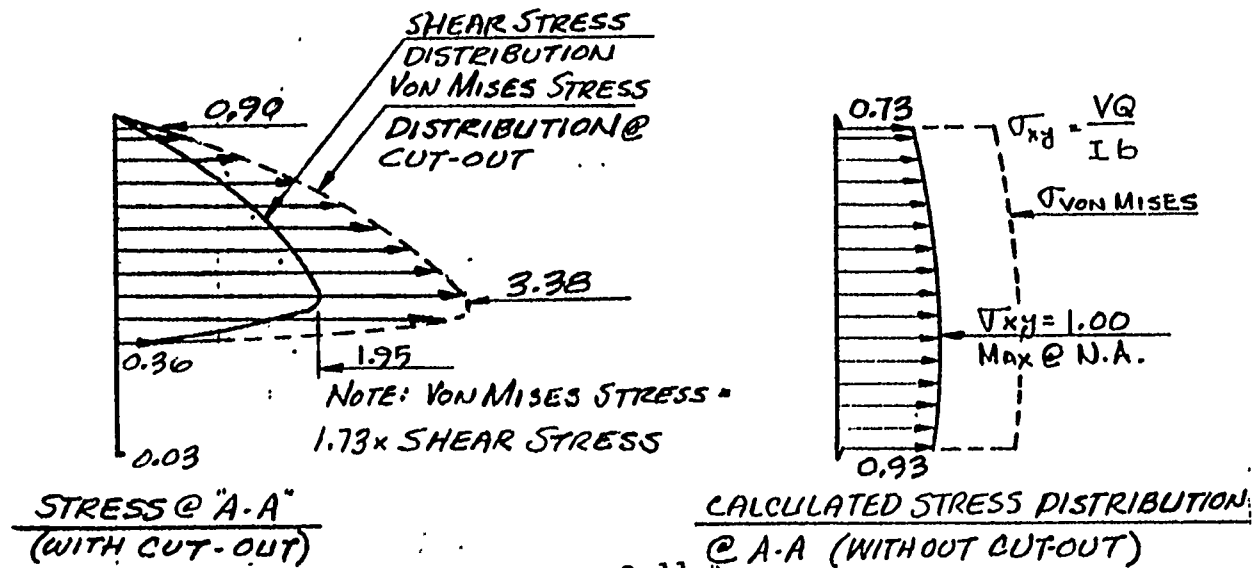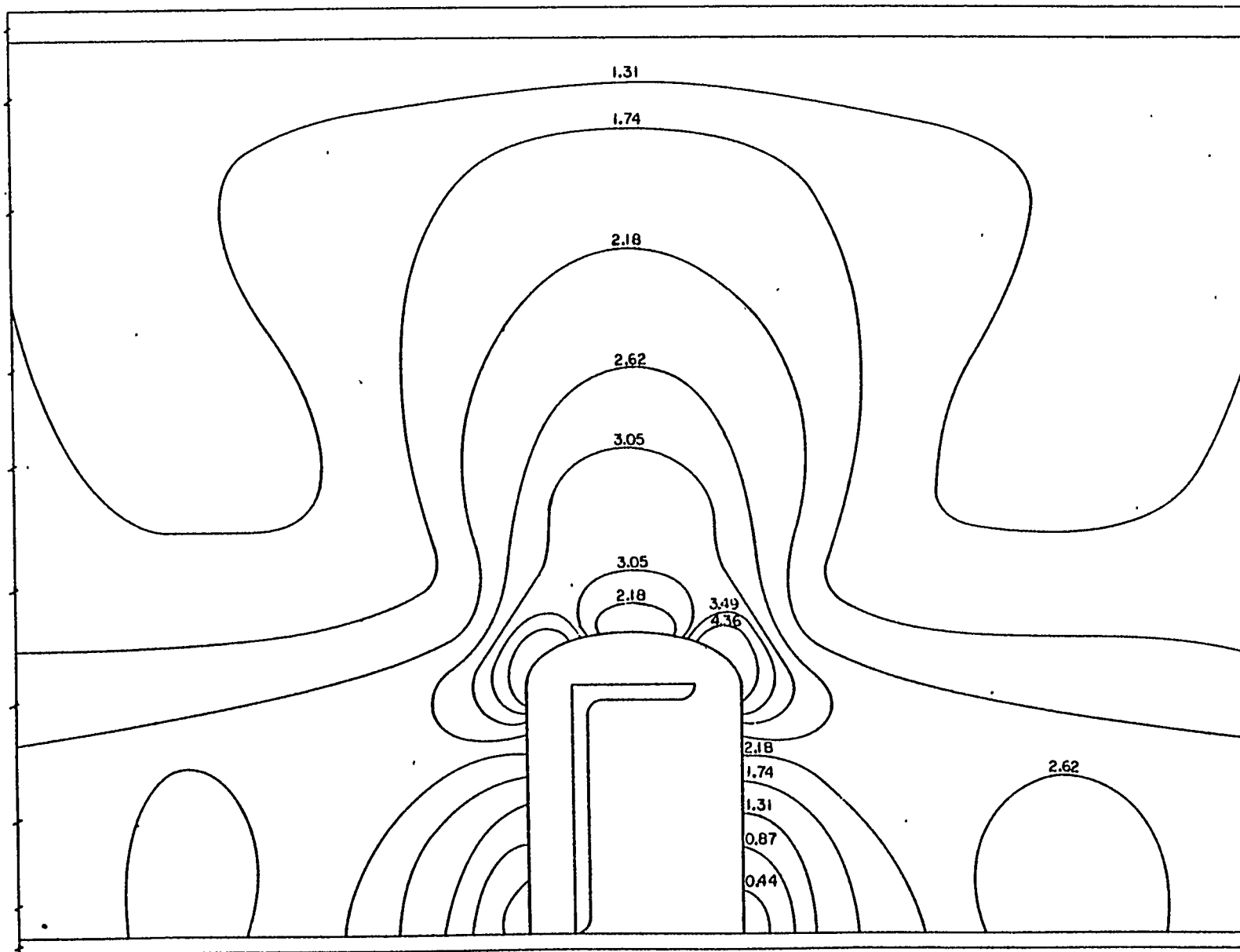
|LOAD CASE NO. 3: SHEAR |STRESS MAGNIFICATION FACTOR

Figure 3-12

LOAD CASE NO. 3: SHEAR STRESS MAGNIFICATION FACTOR
DETAIL 9 CUTOUT

Figure 3-13

SCALE

NOTE: NO CUT OUT
= 1.0

4.4

4.4
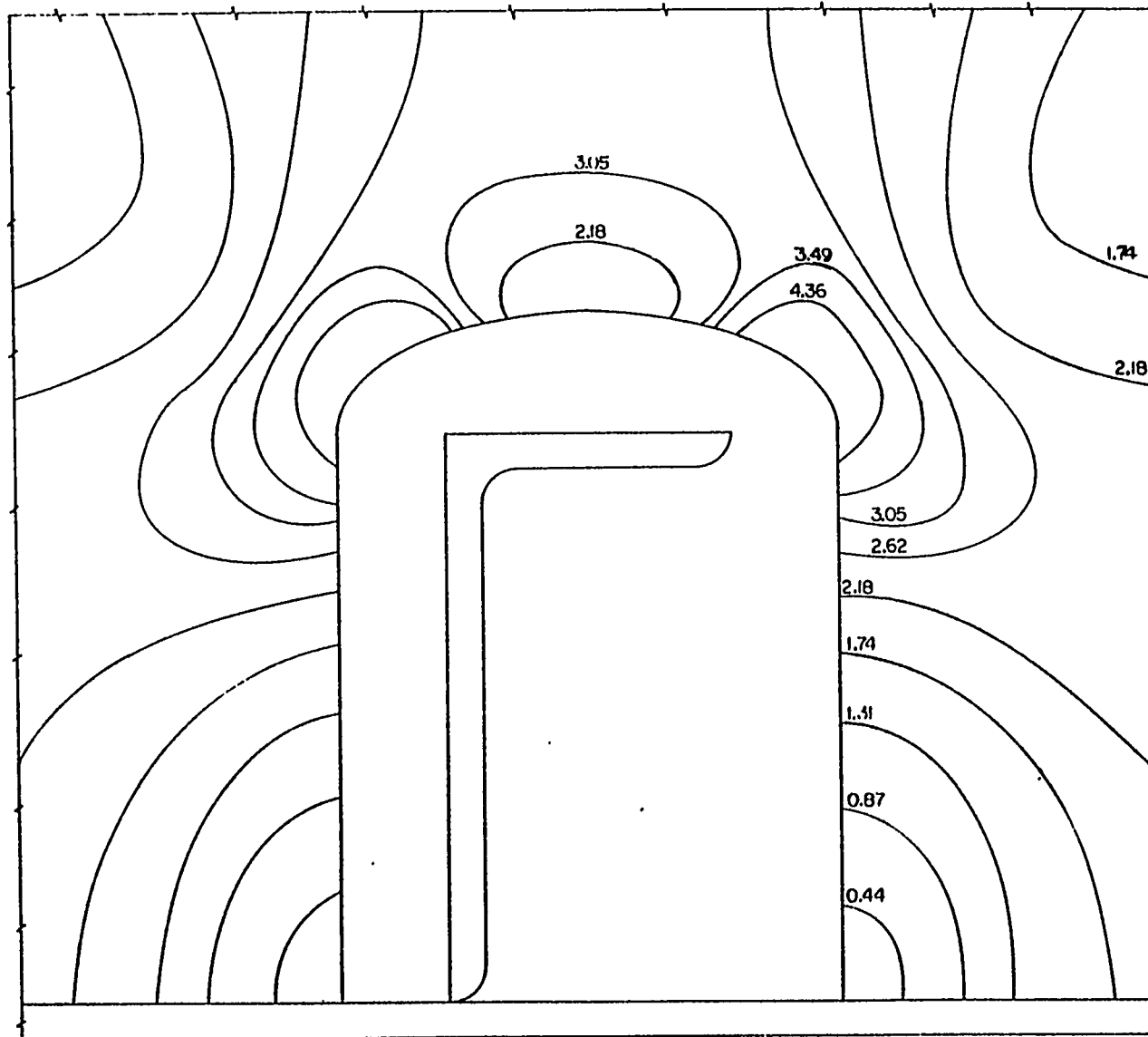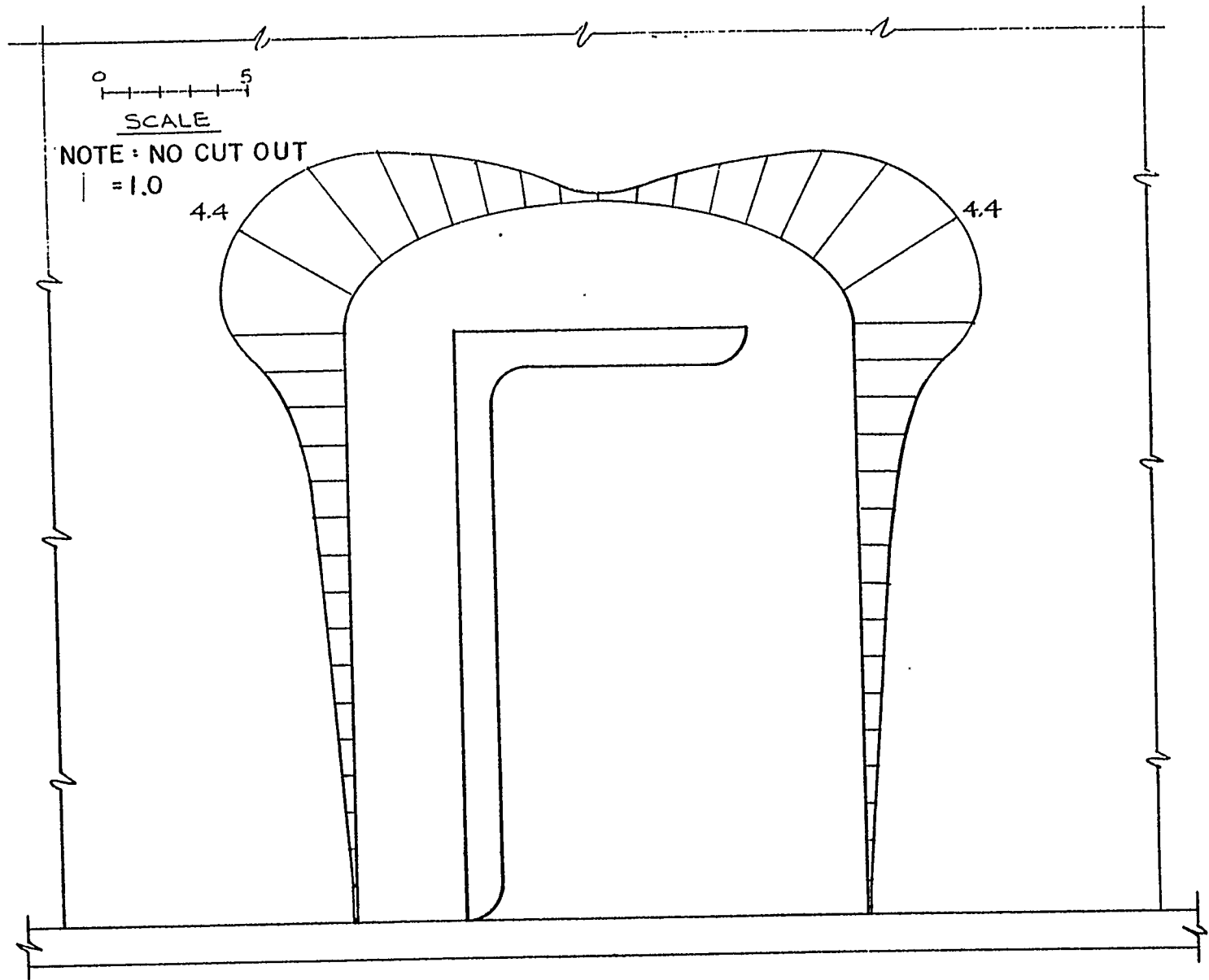
SHEAR STRESS CONCENTRATION FACTOR
ELLIPTICAL CUTOUT
Figure 3-14

3.2.3   Clearance Cuts - Straight

The analytical model configuration is described in Figures
3-15 to 3-18. Load cases considered were identical to
those discussed in Section 3.2.

3.2.4   Straight - Results

The stress magnification factor due to axial load (Figure
3-19) is less than for the elliptic cutout at the center-
line, but results in a slightly larger maximum factor
occurring at an upper corner.

A plot of magnification factors based on von Mises stresses
is presented in Figure 3-20, pointing to similar magnitudes
but steeper stress gradients than were calculated for the
elliptic cut. The bending case is shown in Figure 3-21 and
3-22, leading to the same conclusion stated in Section 3.3:
that bending has negligible effect on cutout stresses.

Stress magnification factors for shear, Figures 3-23, 3-24
and 3-25, are the same as for the elliptical cutout, with
slightly smaller gradients.

The choice of the elliptic cutout as a tentative standard
detail in Section 4 is admittedly somewhat arbitrary, since
no measurable difference is suggested by the analysis. As
stated in Section 2, it is expected that manual cutting and
trimming (and the workmanship inherent thereto) will be
avoided by specifying a cutout shape that is preferably
produced by automated processes.

FIXED END

FINITE ELEMENT ANALYSIS MODEL
STRAIGHT CUTOUT

Figure 3-15
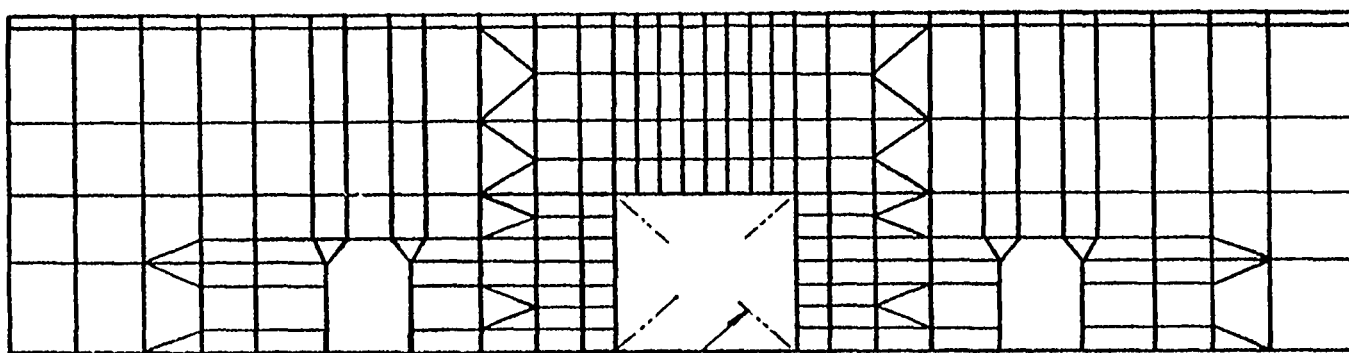
FOR MODEL
OF THIS AREA
SEE FIG. 3-18

FINITE ELEMENT ANALYSIS MODEL
STRAIGHT CUTOUT

Figure 3-16

3-19

$1\frac{1}{2}"$ R.
(TYP)

$1\frac{1}{2}"$

$1\frac{1}{2}"$
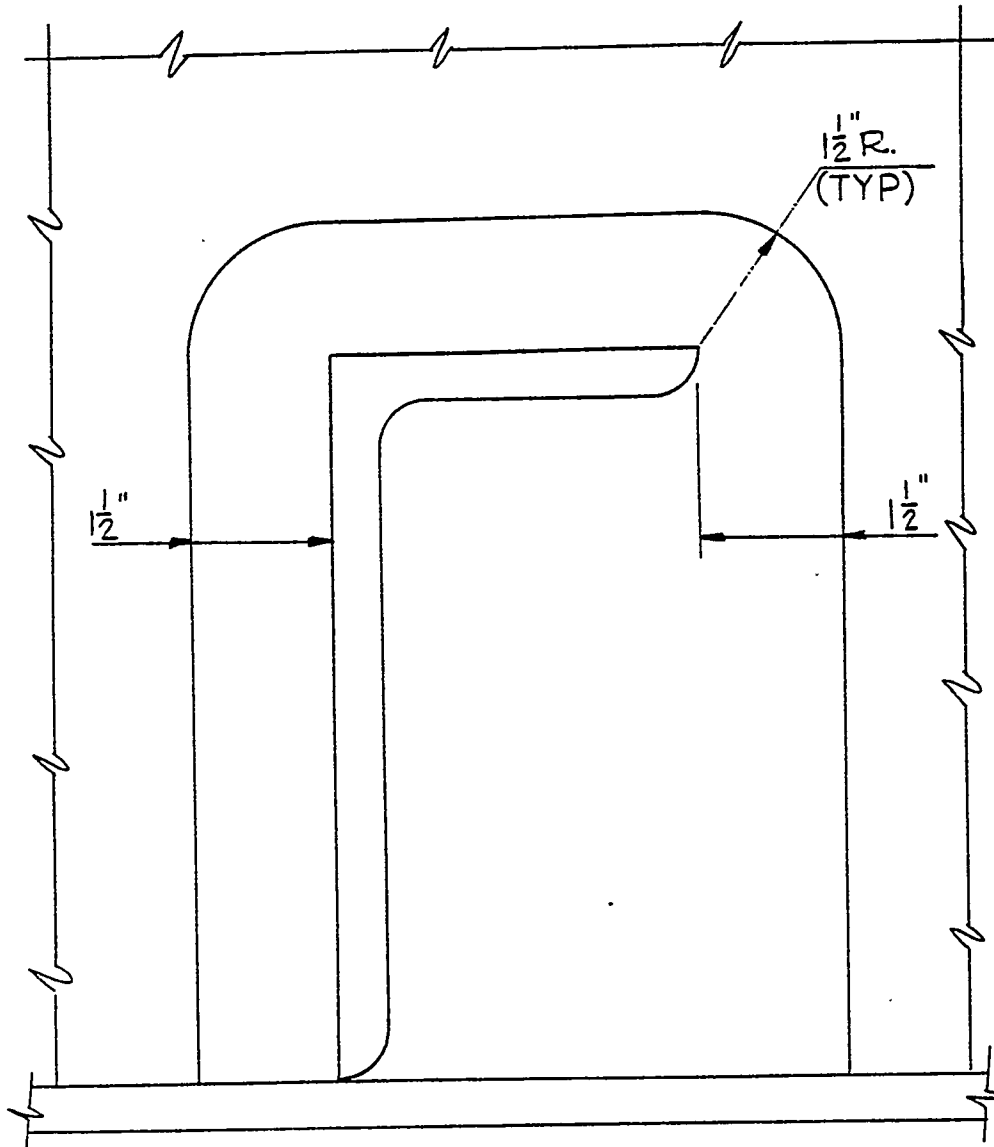
STRAIGHT CUTOUT

Figure 3-17
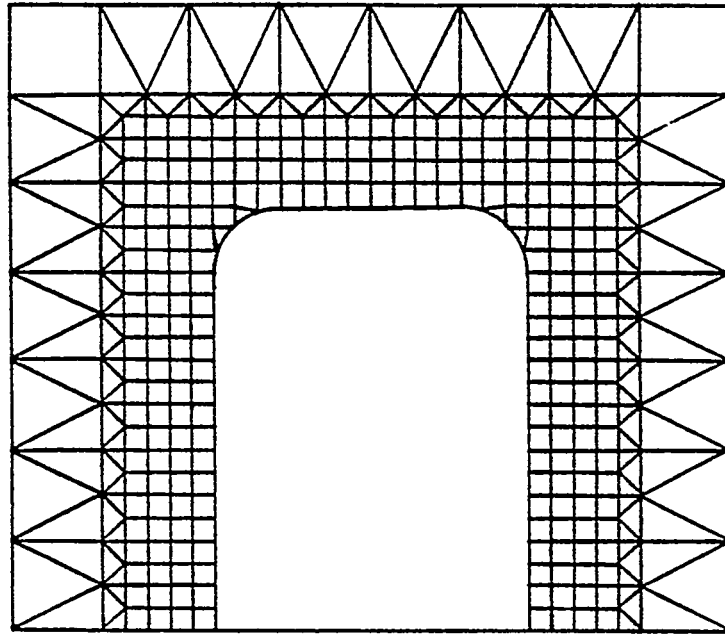
DETAILED MODEL OF CUTOUT AREA
STRAIGHT CUTOUT

Figure 3-18
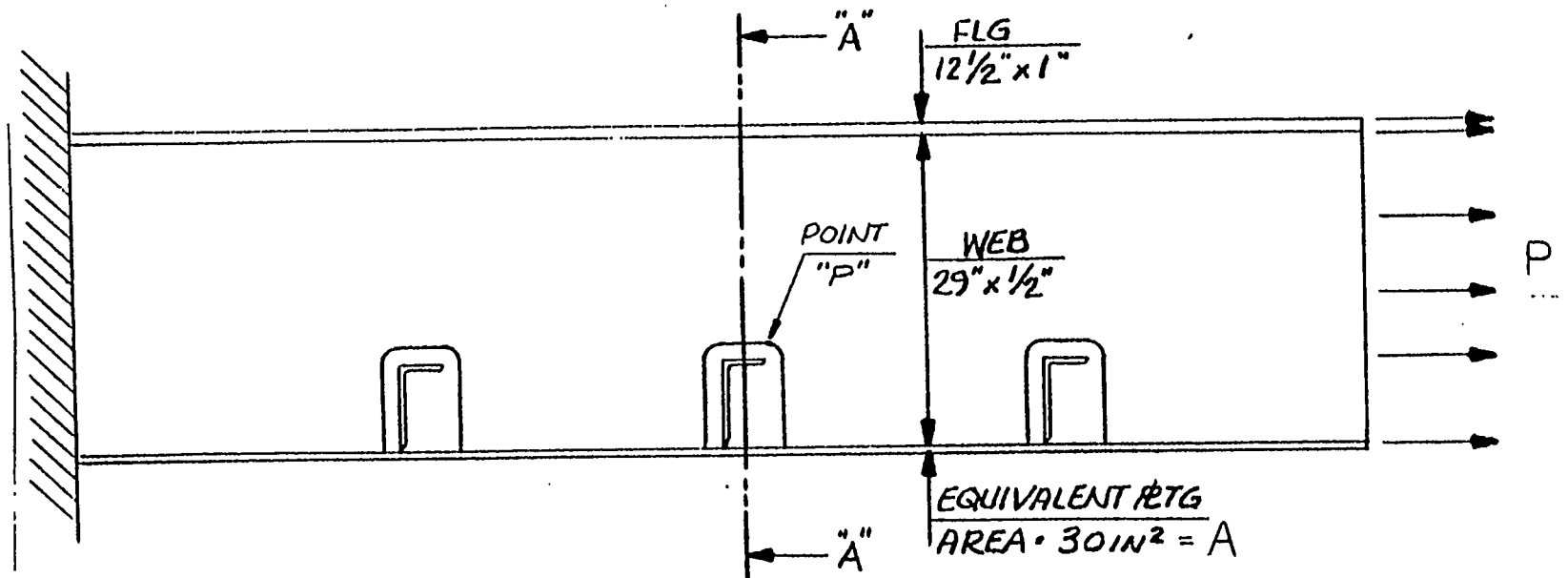
"A"

FLG
12½" x 1"

POINT
"P"

WEB
29" x ½"

EQUIVALENT RTG
AREA · 30 IN² = A

"A"

P

LOAD CASE NO.1: AXIAL LOAD

0.97

VON MISES STRESS
DISTRIBUTION
AT ℄ OF CUT OUT
AT WORST SECTION

1.87

2.62 @
POINT "P"

1.12

1.00

$\sigma = \dfrac{P}{A}$

STRESS @ "A-A"
(WITH CUT-OUT)

STRESS @ "A-A"
(WITH NO CUT-OUT)

Figure 3-19

LOAD CASE NO.I: AXIAL LOAD STRESS MAGNIFICATION FACTOR

DETAIL @ CUTOUT

Figure 3-20

"A" ← | FLG
12½"×1"

WEB
29"×½"

NEUTRAL AXIS

10.89"

EQUIVALENT RTG
AREA = 30 IN²

"A" ←

LOAD CASE NO. 2 : BENDING
(SHEAR = O)

1.02

VON MISES STRESS
DISTRIBUTION @
₵ CUT-OUT

-0.15

-0.54

STRESS @ "A-A"
(WITH CUT-OUT)

1.00

$\sigma_T = \dfrac{M}{S_T}$

$\sigma_B = \dfrac{M}{S_B}$

-0.55
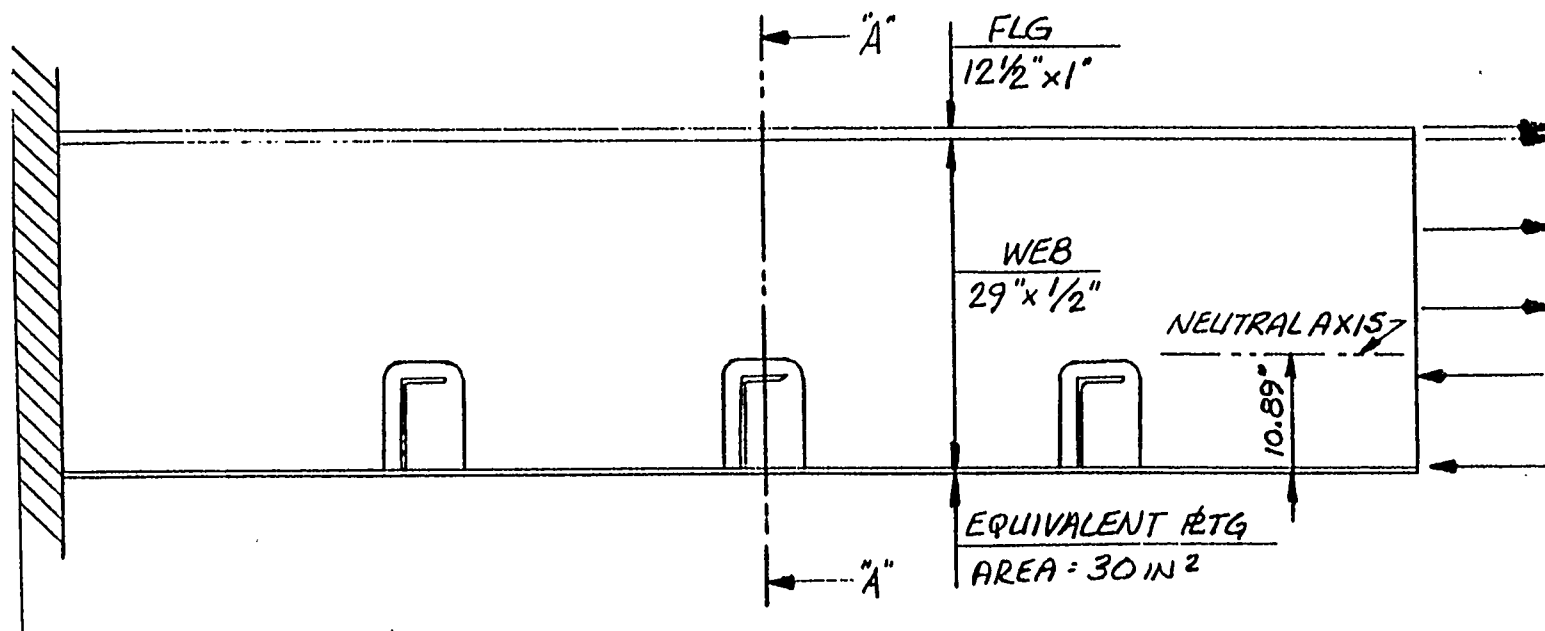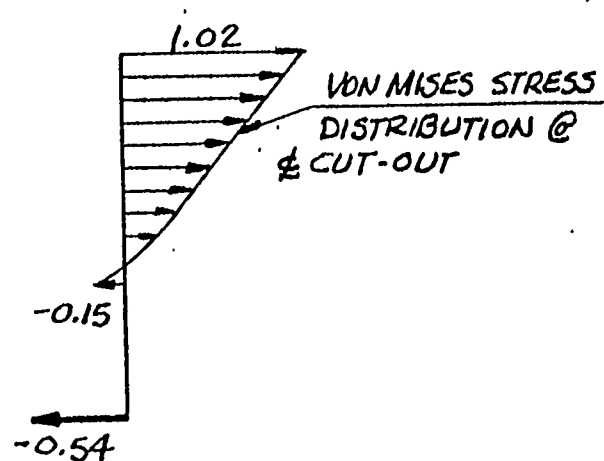
CALCULATED STRESS DISTRIBUTION

Figure 3-21

LOAD CASE NO. 2 : BENDING STRESS MAGNIFICATION FACTOR
DETAIL 9 CUTOUT

Figure 3-22

FLG
12½"×1"

WEB
29"×½"

"A"

"A"

EQUIVALENT RTG
AREA = 30 IN²

V

M

LOAD CASE NO. 3: SHEAR
(MOMENT = 0 @ CUT-OUT)

SHEAR STRESS
DISTRIBUTION

VON MISES STRESS
DISTRIBUTION @
CUT-OUT

0.90

3.38

0.39

1.95

0.03

NOTE: VON MISES STRESS =
1.73× SHEAR STRESS

STRESS @ "A-A"
(WITH CUT-OUT)

0.73

$\sigma_{xy} = \dfrac{VQ}{Ib}$

$\sigma_{VON\ MISES}$

$\sigma_{xy} = 1.00$
MAX @ N.A.

0.93
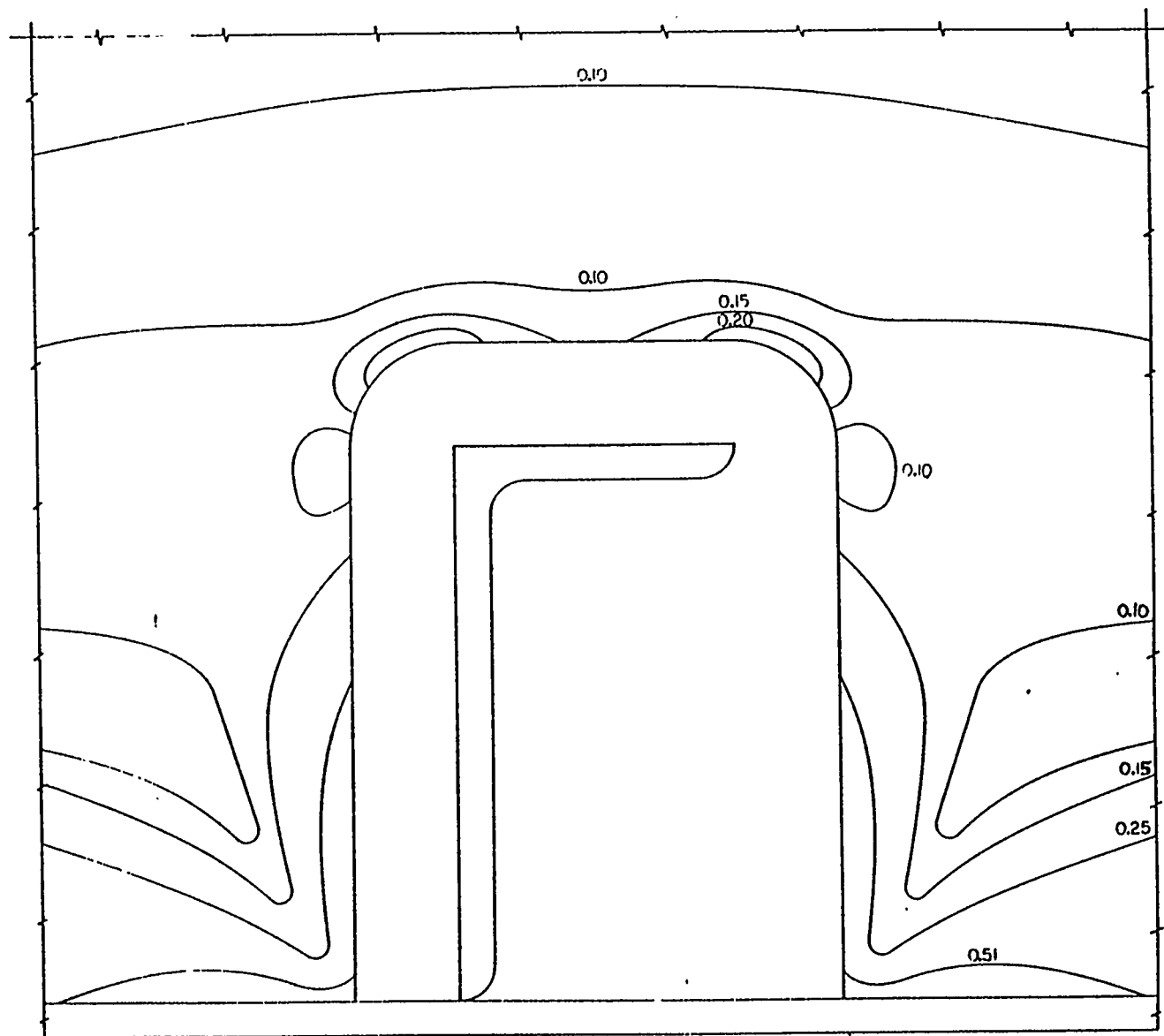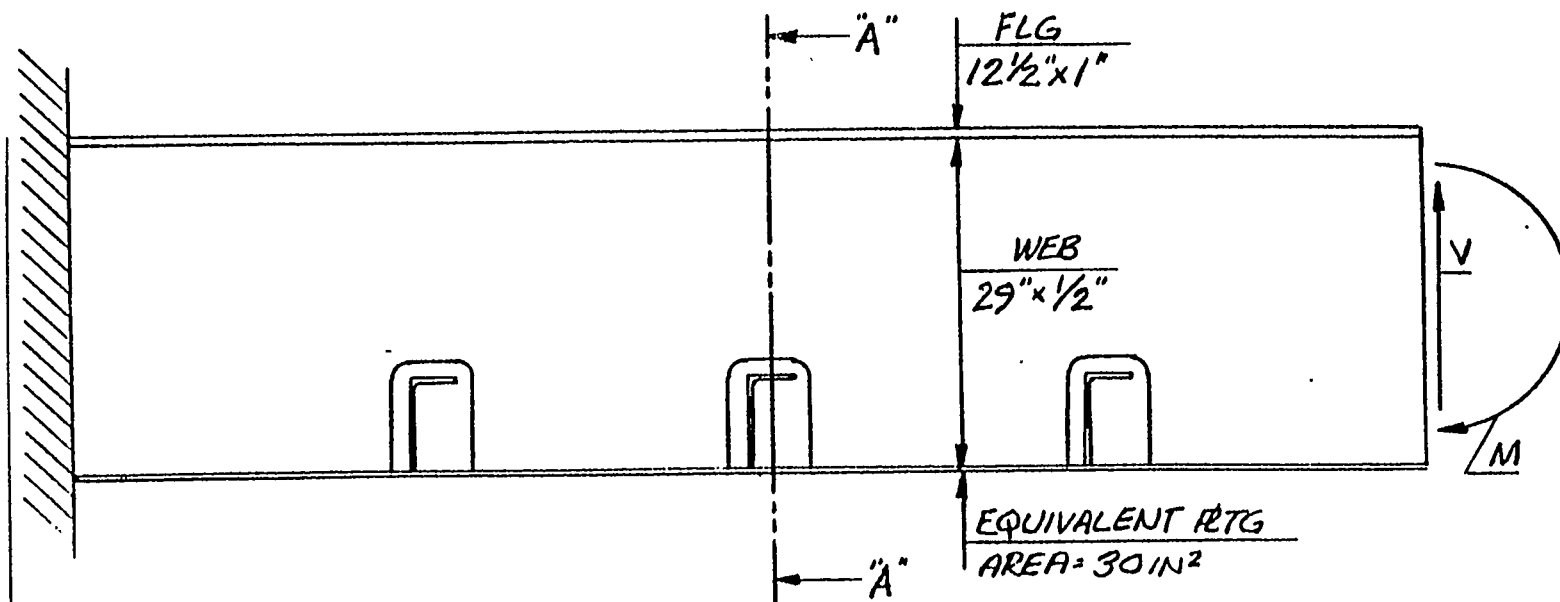
CALCULATED STRESS DISTRIBUTION
@ A-A (WITH NO CUT-OUT)
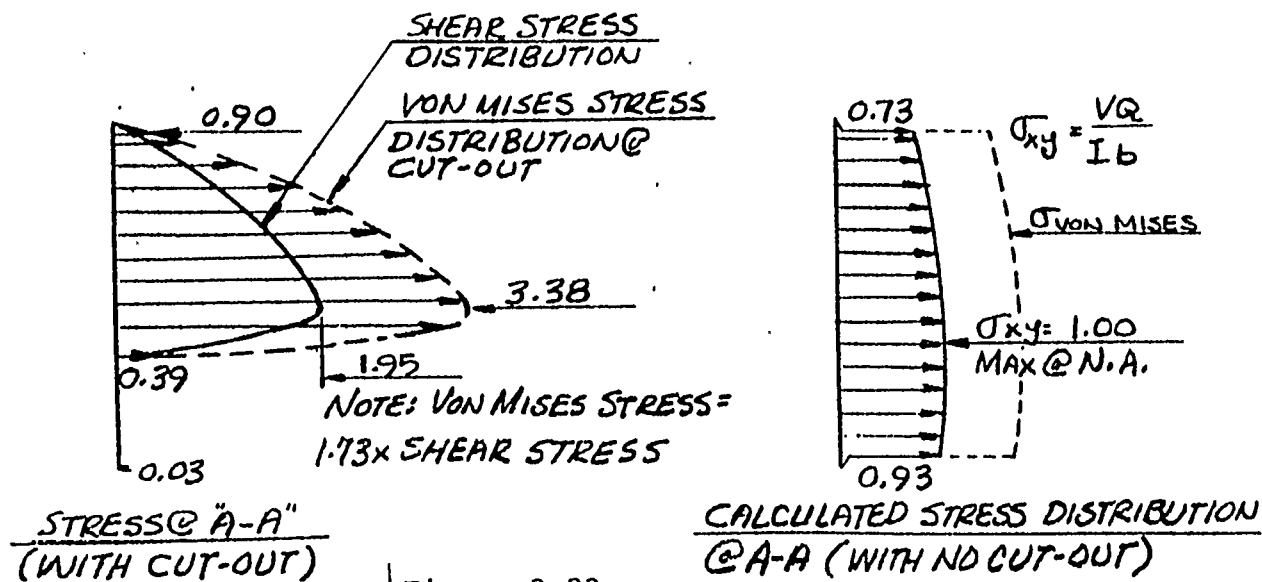
Figure 3-23

LOAD CASE NO.3: SHEAR STRESS MAGNIFICATION FACTOR
DETAIL @ CUTOUT

Figure 3-24

SCALE

NOTE : NO
CUT OUT, =1.0

4.5

4.5
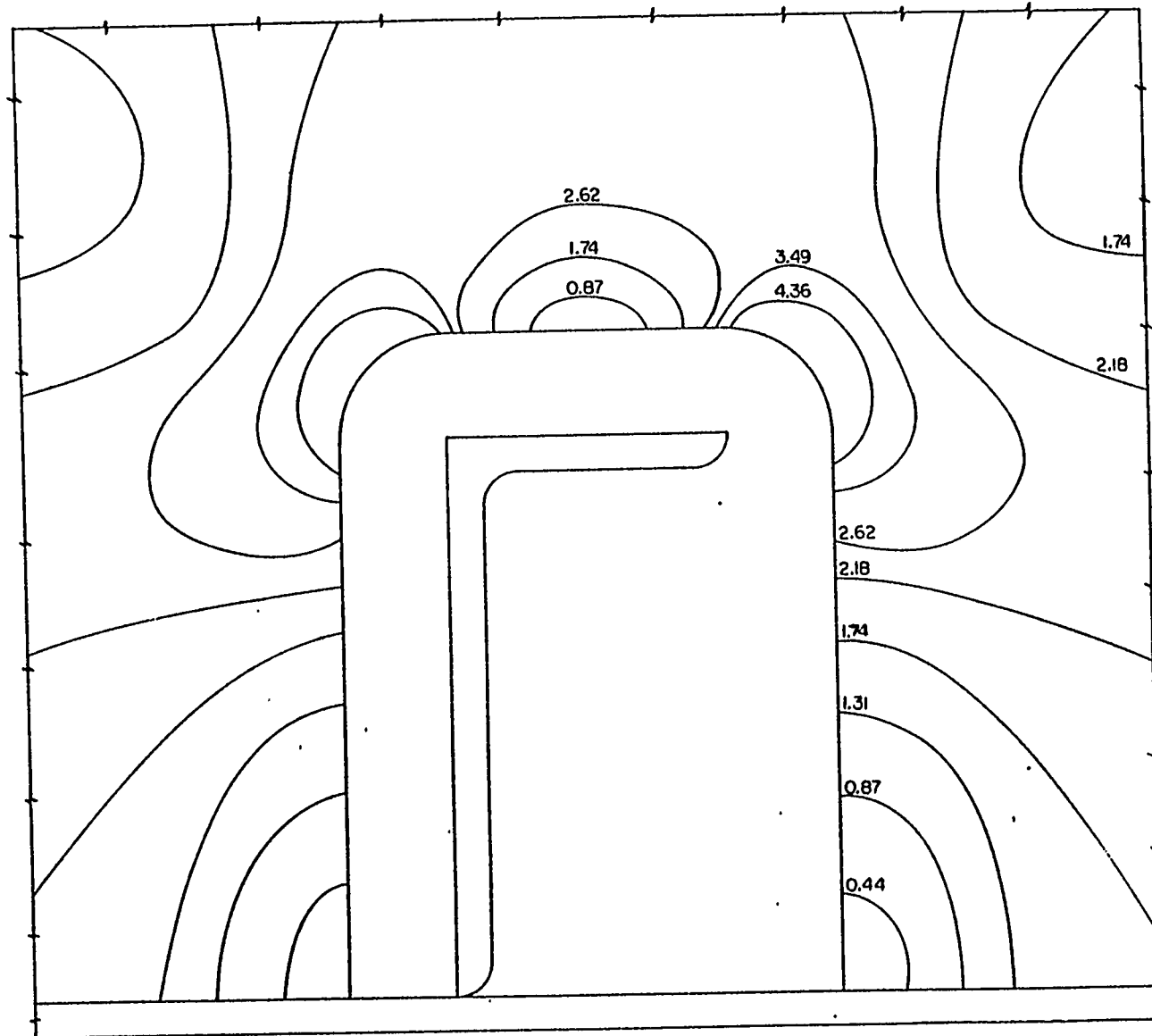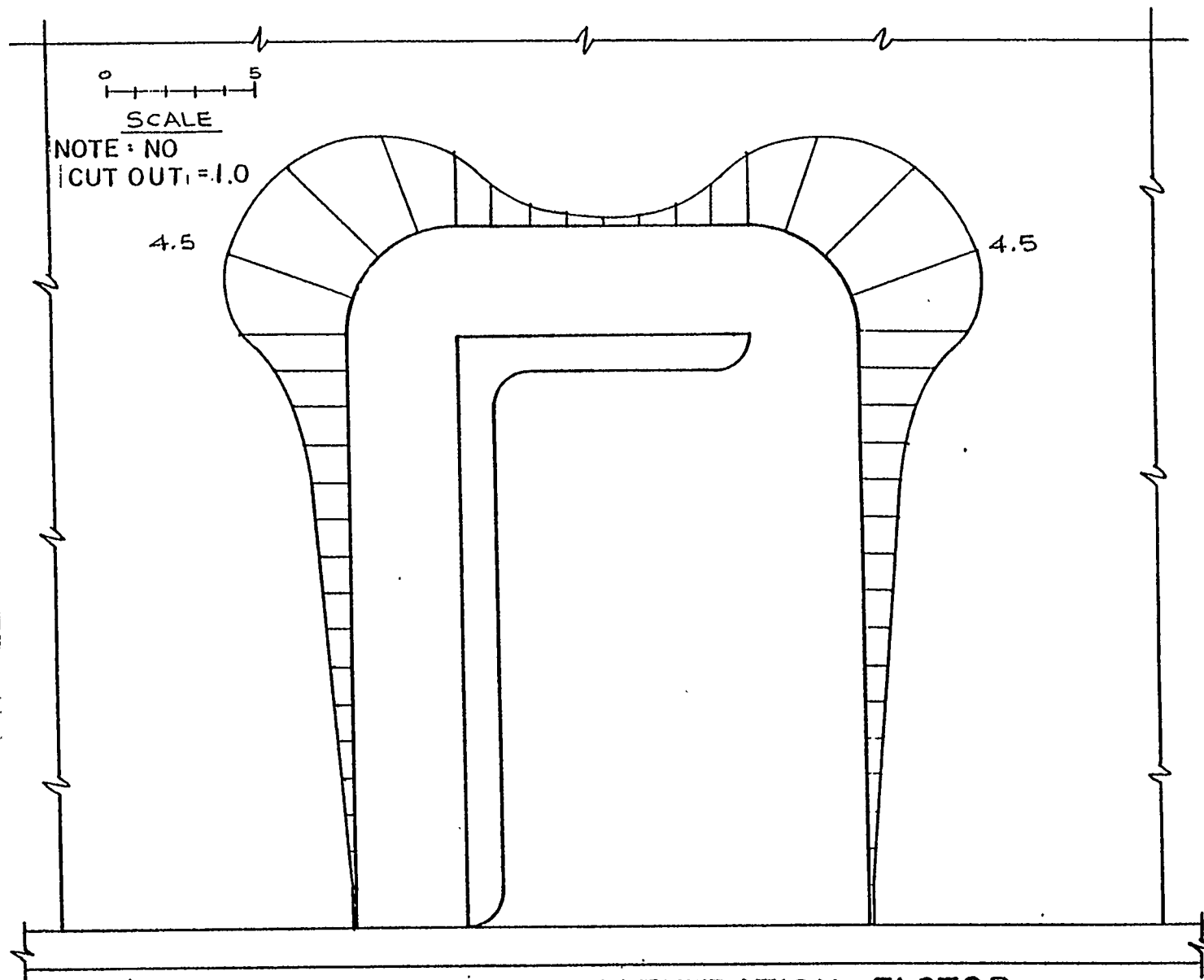
SHEAR STRESS CONCENTRATION FACTOR
STRAIGHT CUTOUT
Figure 3-25

3.3   COLLARED INTERSECTIONS

The model employed for finite element analysis consists of
a beam-plate combination as described in Section 3.2.   The
beam is 90 inches long to its center of symmetry, and fixed
at the end.   The load on intersecting longitudinals was
applied at either end of the longitudinals.   *Four* conditions
of support are considered for the stiffeners: a tab to the
heel with and without panel stiffener support, and tabs to
heel and bosom with and without panel stiffener support.

3.3.1   Single Tab

The analytical model is shown in Figures 3-26 and 3-27.   Only
the left cutout and the intersecting stiffener are modeled
in detail (Figures 3-28 and 3-29).

For this support case only, analysis was performed for a load
at one stiffener (Figure 3-30).   The equivalent von Mises
stresses were ratioed to similar stresses calculated for a
model of an intact (i.e. reeved) member, and the resulting
amplification factors are plotted in Figure 3-31 along the
cutout boundary.   Note stress amplification factors in the
range of 7-8 versus the ideal or reeved case.

The more general and realistic case of all (five) stiffeners
equally loaded is shown in Figure 3-32, and resulting stress
amplification factors are plotted in Figure 3-33.

As an interesting aside, an error Was made in establishing
the coordinates of two adjacent elements along the periphery
of the radius-sniped corner at the web of the longitudinal.
That error is shown in Figure 3-34.   The resultant amplifi-
cation of stress at those elements was 1.8 times higher than
for the smooth contour, which was established when this
error was later corrected.   The sensitivity to small changes
in cut outline can be considered a strong indication of the
need for clean automatic burning, though it is possible that
the effect was exaggerated by the inherently peculiar behaviour
of triangular elements.   Further investigation of this sensi-
tivity to cut outline would seem to be called for.

FIXED END

CENTER OF SYMMETRY
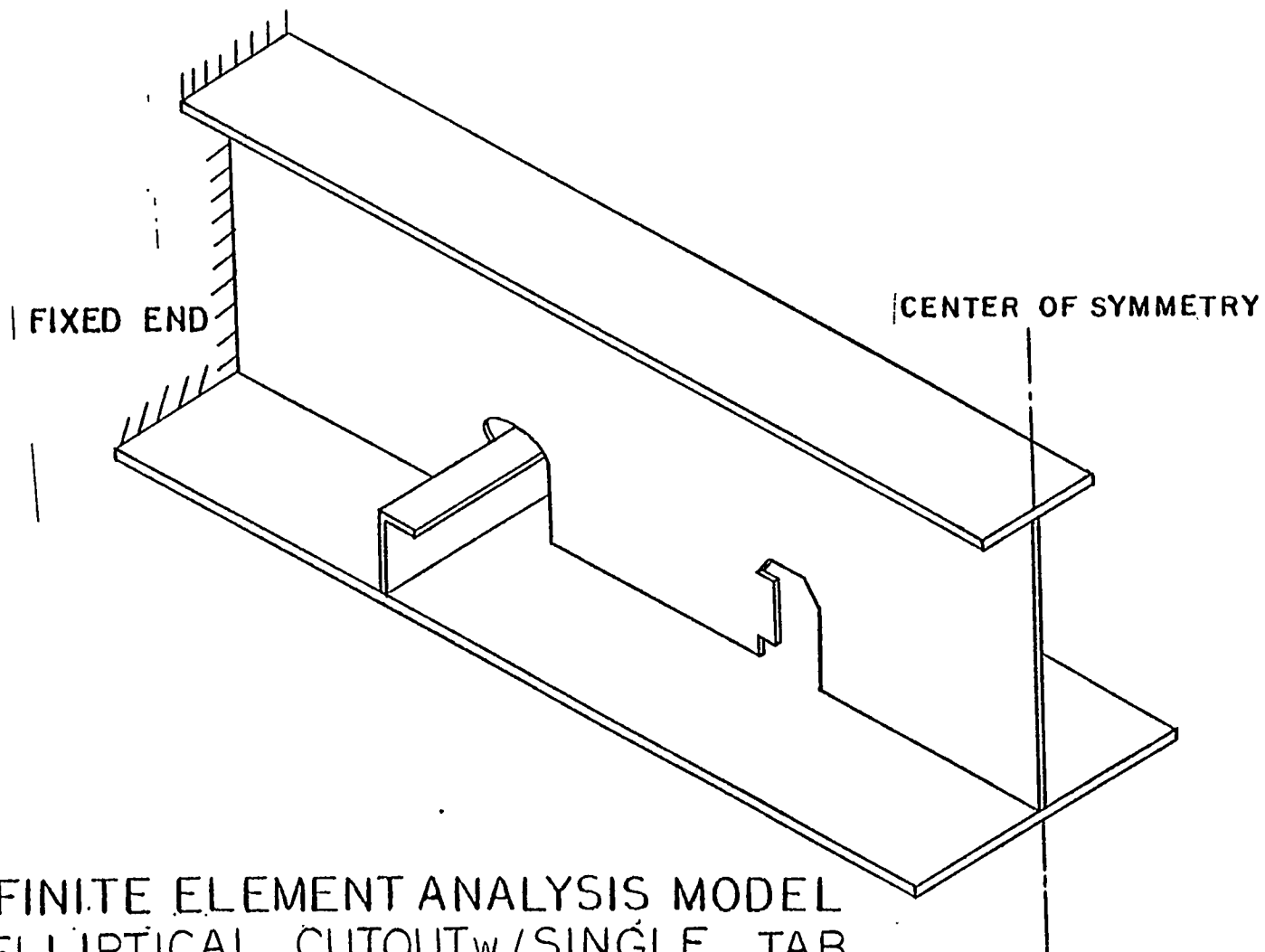
FINITE ELEMENT ANALYSIS MODEL
ELLIPTICAL CUTOUTw/SINGLE TAB
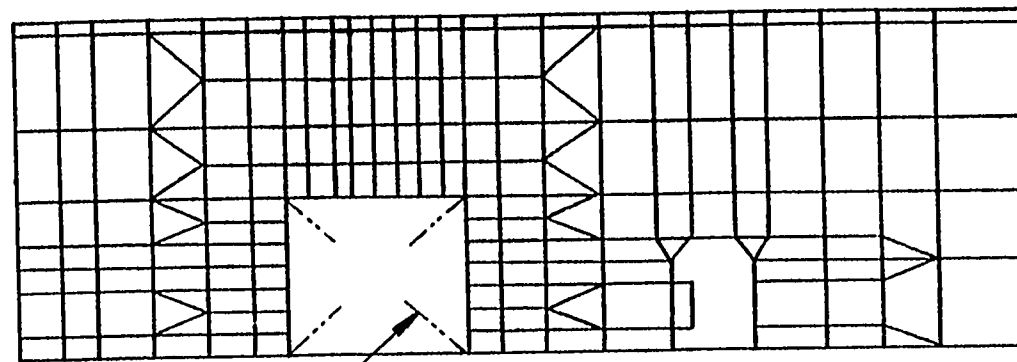
Figure 3-26
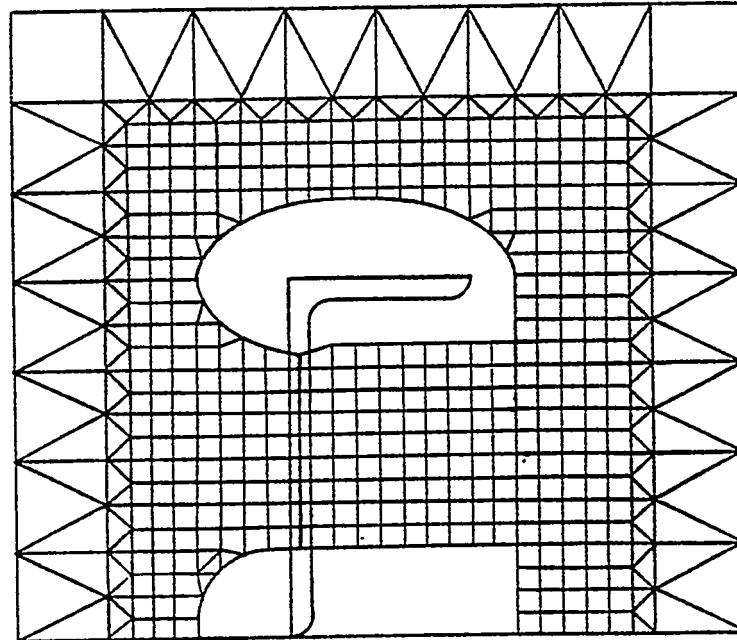
FOR MODEL OF THIS
AREA SEE FIG. 3-29

FINITE ELEMENT ANALYSIS MODEL
ELLIPTICAL CUTOUT w/ SINGLE TAB
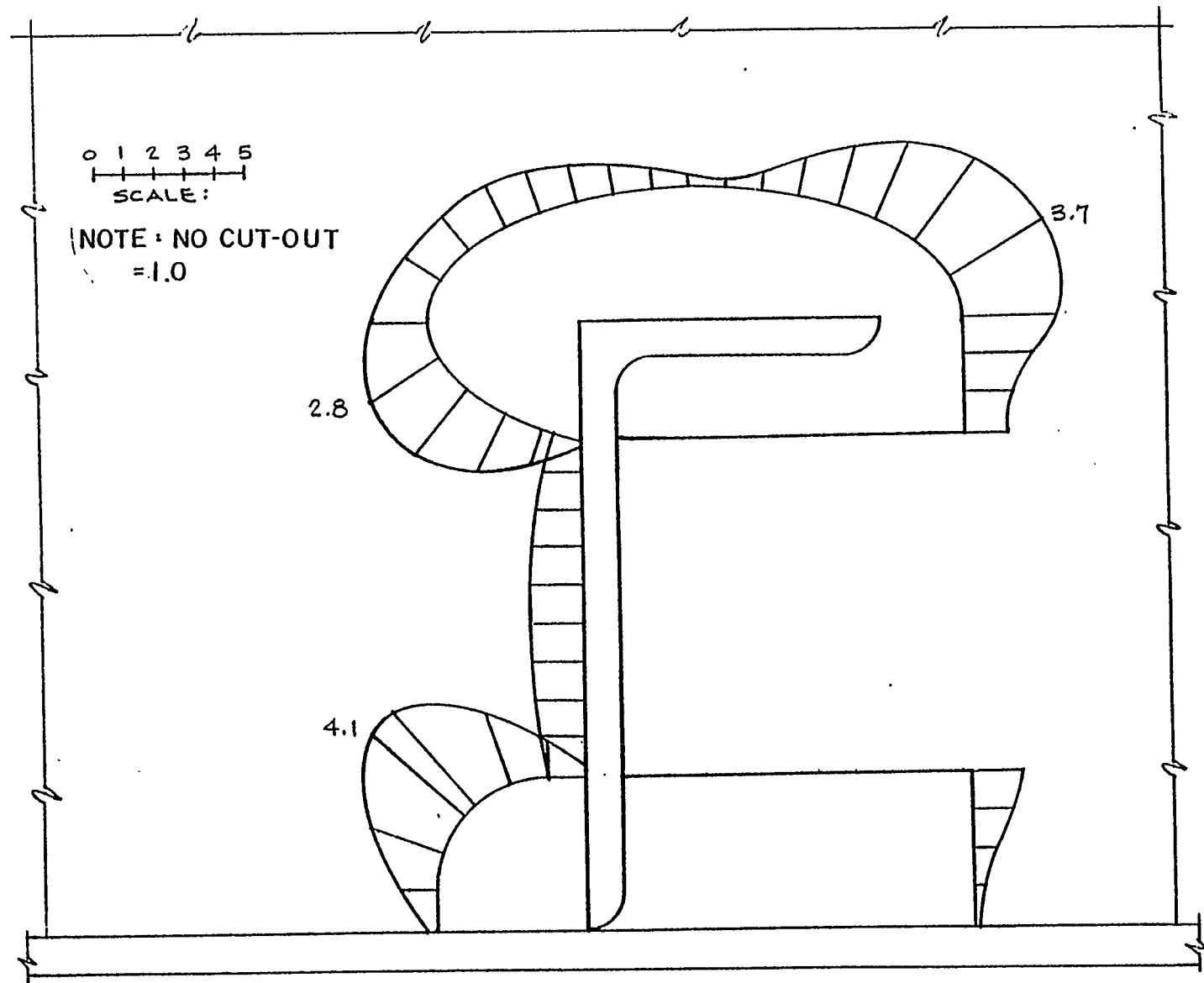
Figure 3-27
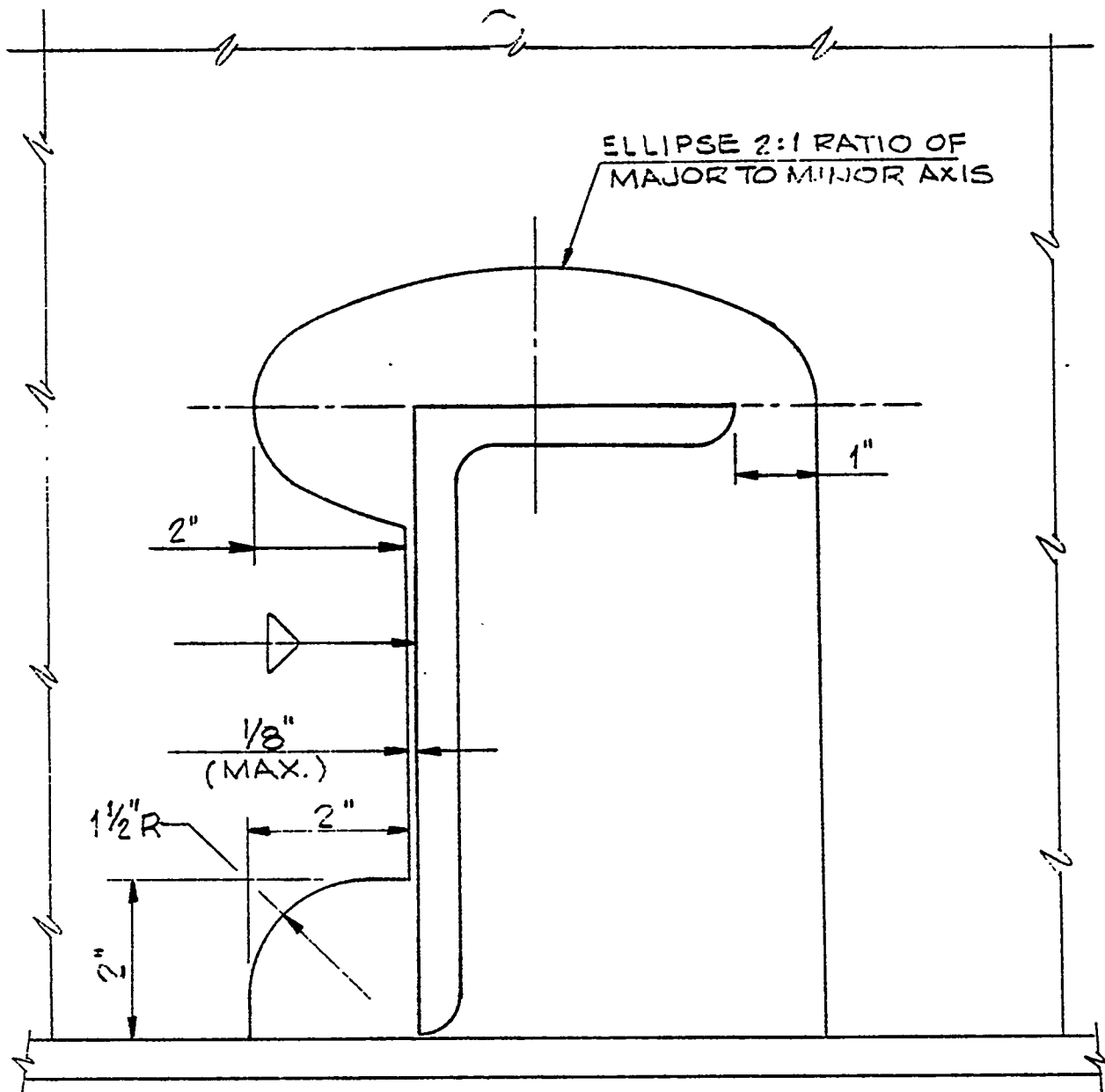
ELLIPTICAL CUTOUT w/ SINGLE TAB

Figure 3-28
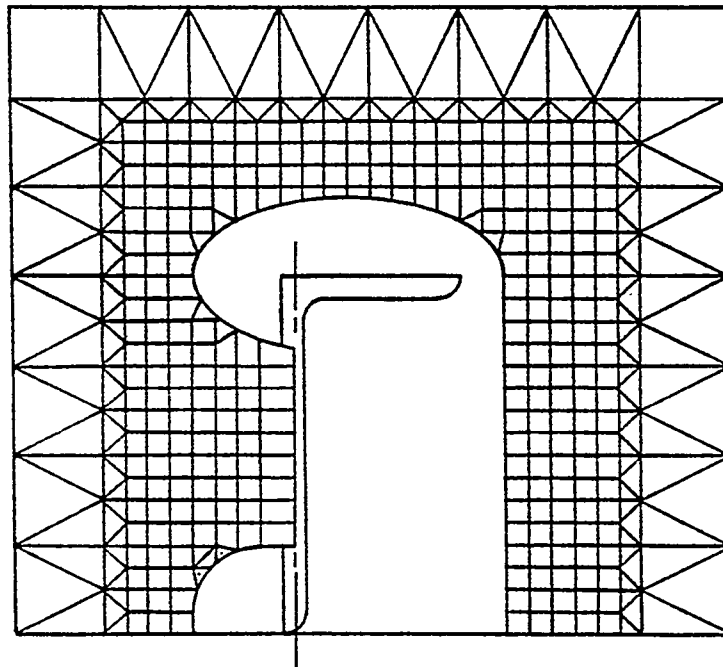
€ ANGLE

DETAILED MODEL OF CUTOUT AREA

ELLIPTICAL CUTOUT w/ SINGLE TAB

Figure 3-29

FLG
12 1/2"x 1"

WEB
29"x 1/2"

FIXED END

P
LOAD APPLIED
TO LONGITUDINAL

EQUIVALENT PLTG.
AREA = 30 in²   CENTER OF SYMMETRY
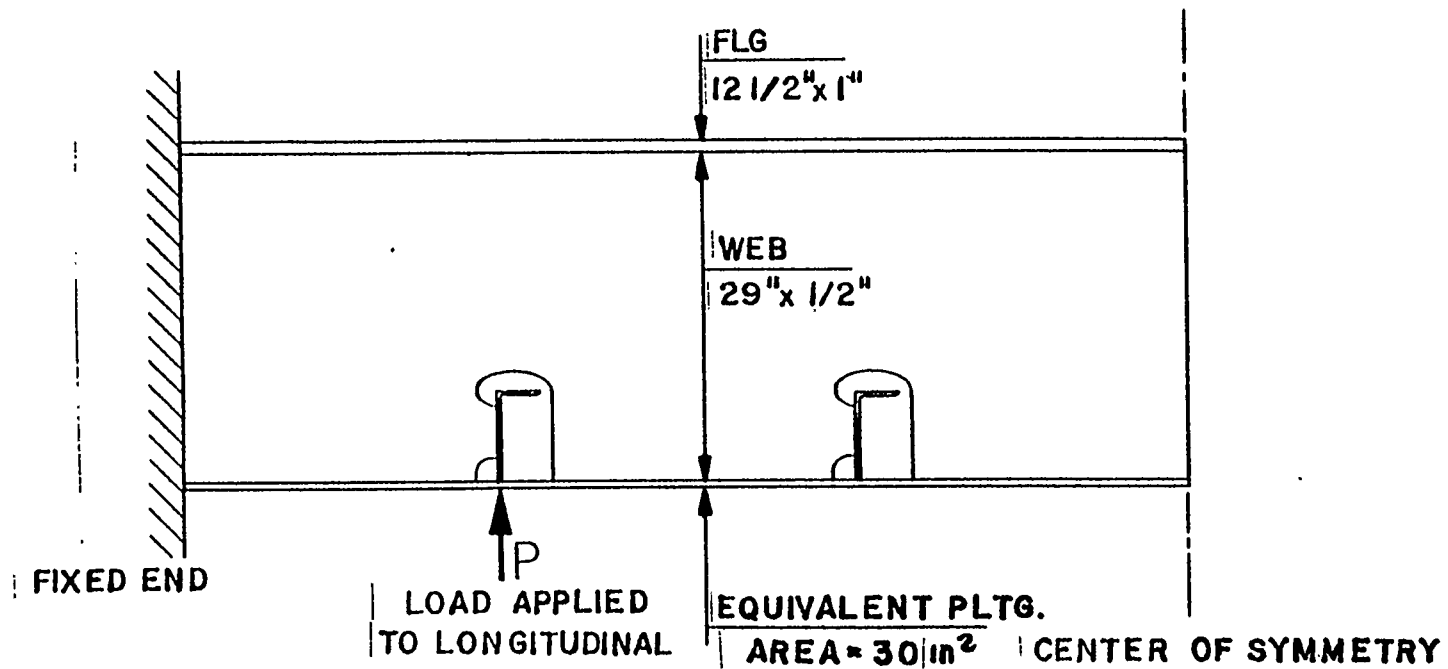
· LOAD CASE I: LOAD ON OUTSIDE LONGITUDINALS

Figure 3-30
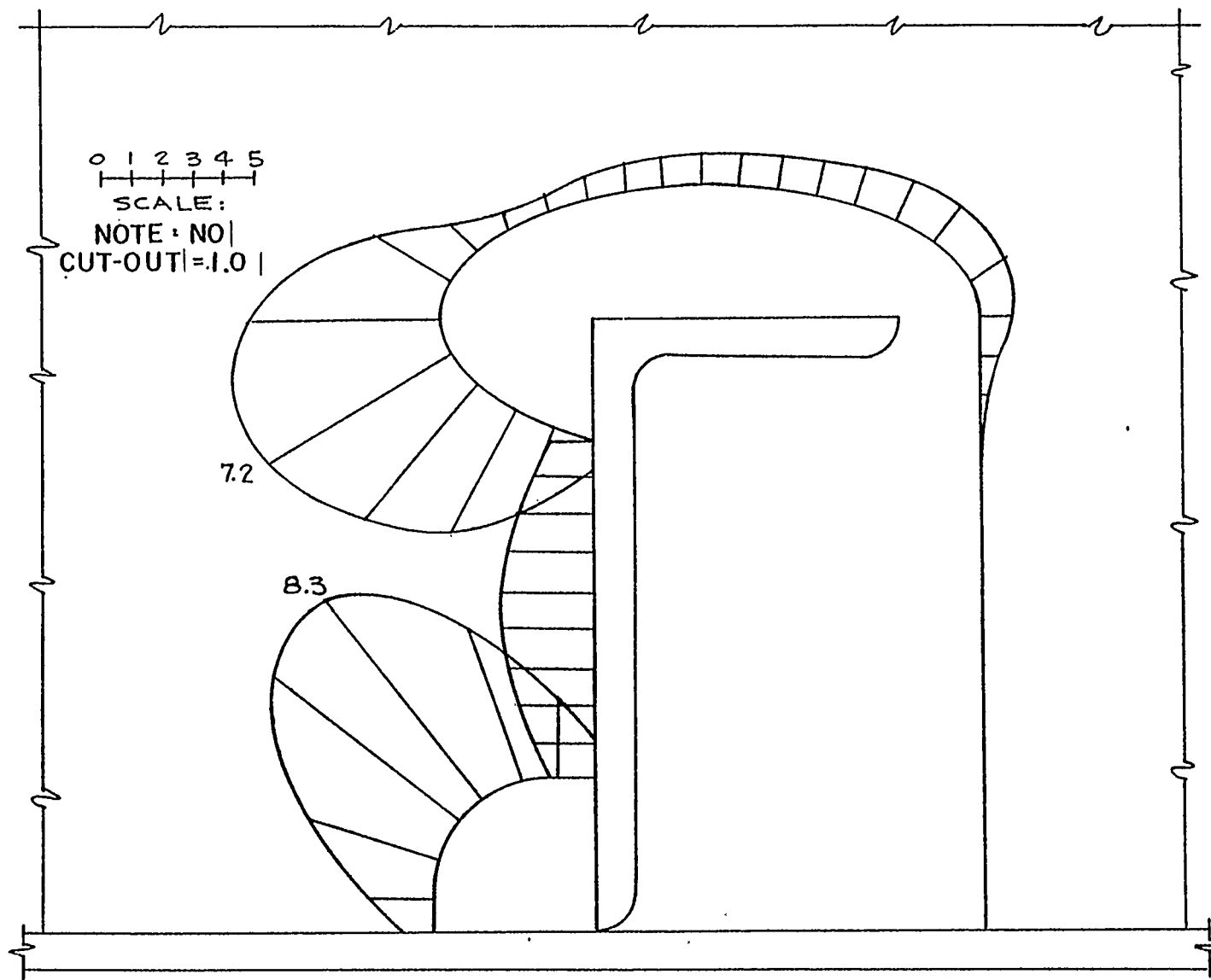
STRESS CONCENTRATION FACTOR
FOR LOAD CASE I

Figure 3-31

FLG
12 1/2"x 1"

WEB
29"x 1/2"

FIXED END

P
LOAD APPLIED
TO LONGITUDINAL

P
EQUIVALENT PLTG.
AREA = 30 in²

P/2

CENTER OF SYMMETRY
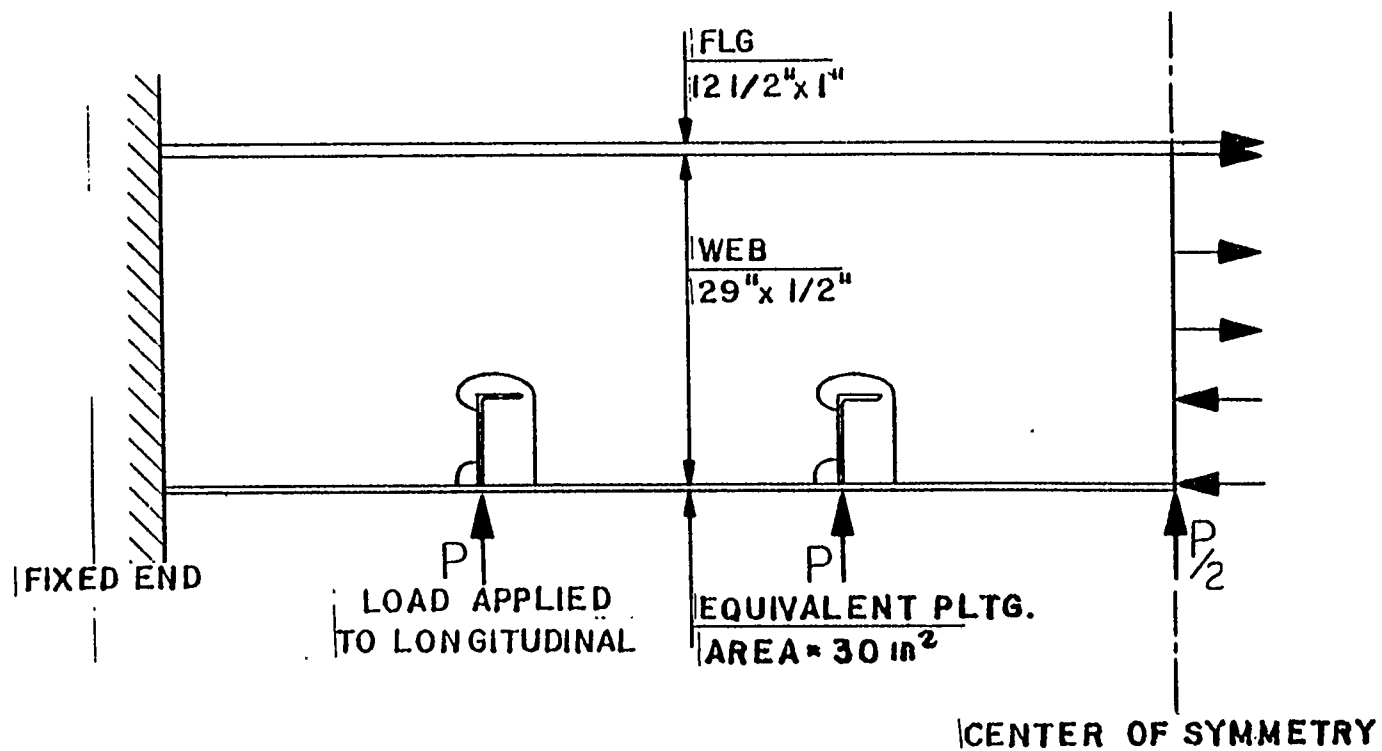
LOAD CASE 2 : ALL LONGITUDINALS LOADED

Figure 3-32

O I 2 3 4 5
SCALE:

NOTE: NO
CUT-OUT=.1.0

3.5

3.3

4.9

STRESS CONCENTRATION FACTOR
FOR LOAD CASE 2
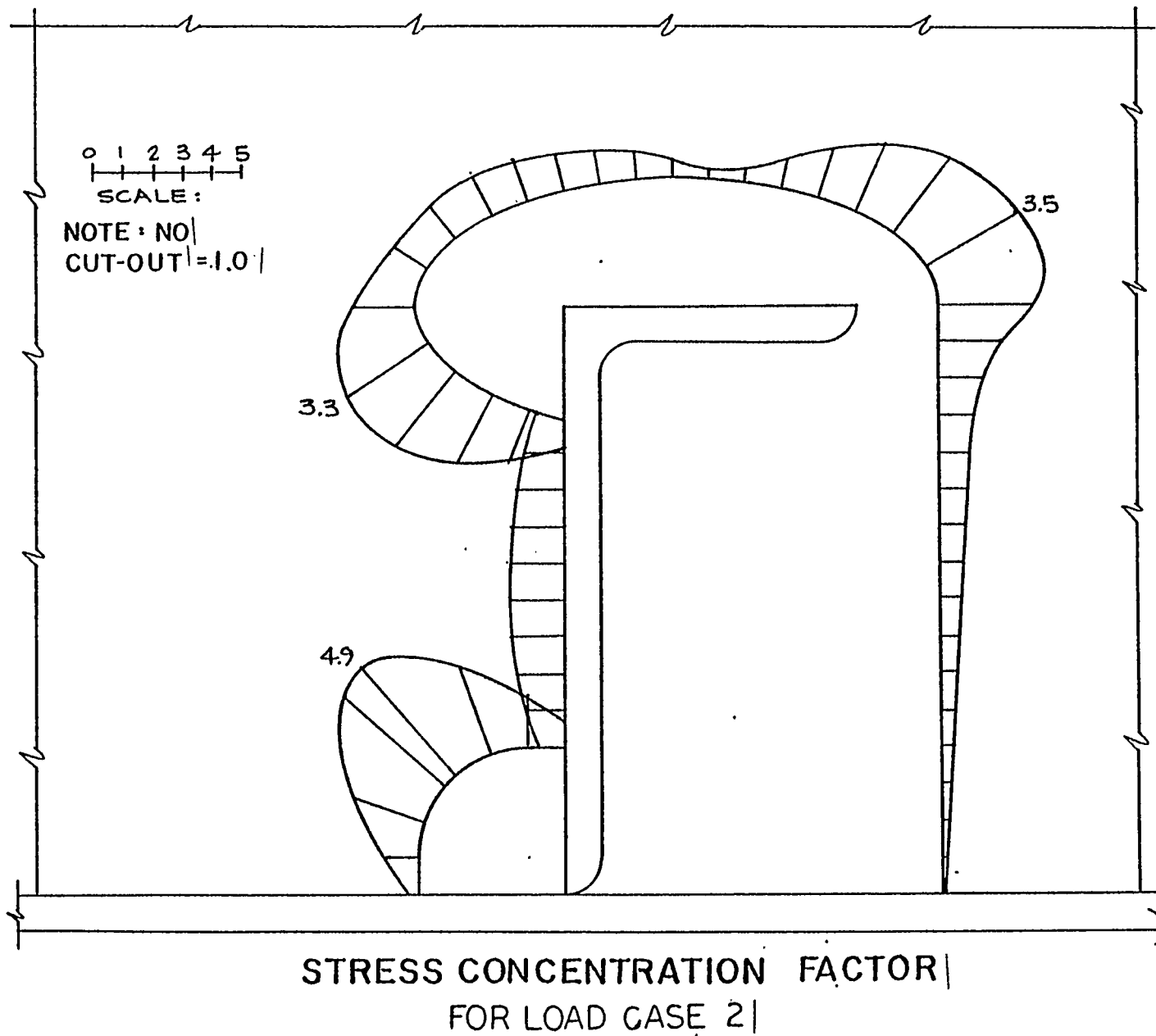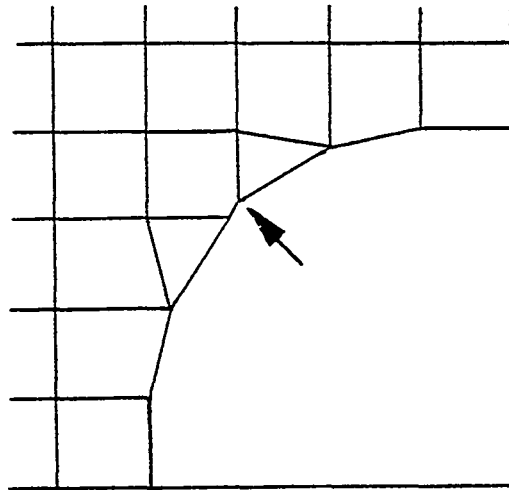
Figure 3-33

Figure 3-34

3.3.2 Double Tab

Figures 3-35 to 3-39 describe the model used to analyze the
effect of adding a tab to the bosom of the stiffener. The
stress amplification plot in Figure 3-40 indicates that the
bosom collar reduces stress amplification at base snipe and
clearance cut by only about 16 percent. This can be explained
in terms of the much greater flexibility of the longer tab.
For symmetrical stiffeners such as tees or flat bars the
effect of double tabs should be significantly greater.

3.3.3 Single Tab With Panel Stiffener

Figures 3-41 to 3-45 describe the analytical model used to
define the load carrying contribution of a panel stiffener
attached to the heel of the penetrating member. The plot of
stress magnification ratios along the cutout shown in
Figure 3-46 suggests only a slightly greater stress reduction
 (to 18 percent) due to connection to the panel stiffener
than was obtained by addition of the bosom tab.

3-38

FIXED END

CENTER OF SYMMETRY

FINITE ELEMENT ANALYSIS MODEL
ELLIPTICAL CUTOUT w/ DOUBLE TABS
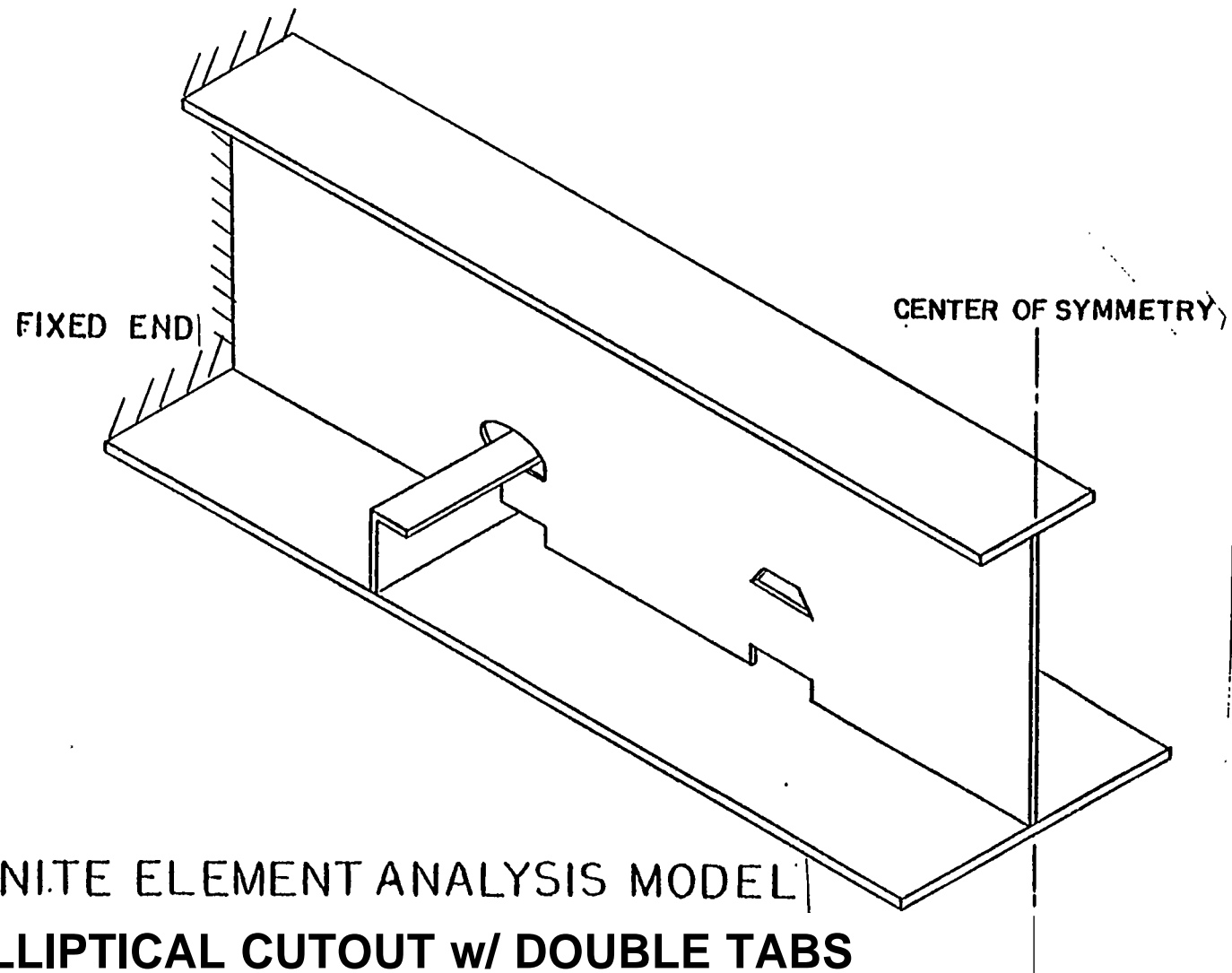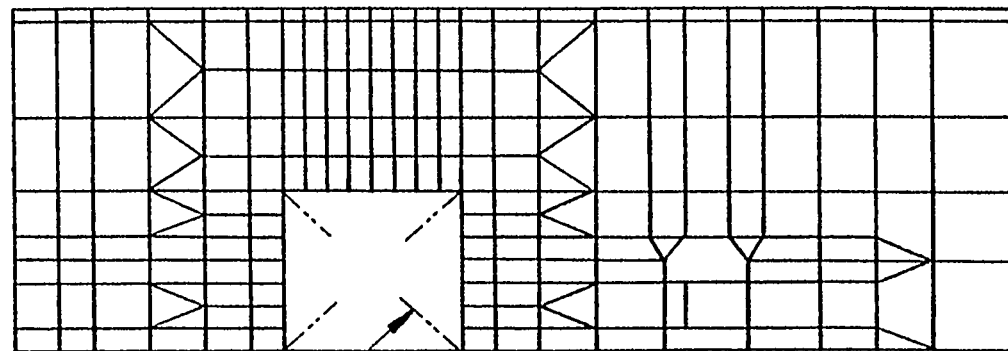
Figure 3-35

FOR MODEL OF THIS
AREA SEE FIG.3-38

FINITE ELEMENT ANALYSIS MODEL
ELLIPTICAL CUTOUT w/DOUBLE TABS

Figure 3-36

ELLIPSE 2:1 RATIO OF
MAJOR TO MINOR AXIS

1"

1½"R.

2"

2" LAP
(MIN.)

⅛"
(MAX.)

1½"R

2"

1½"R

2"

2"
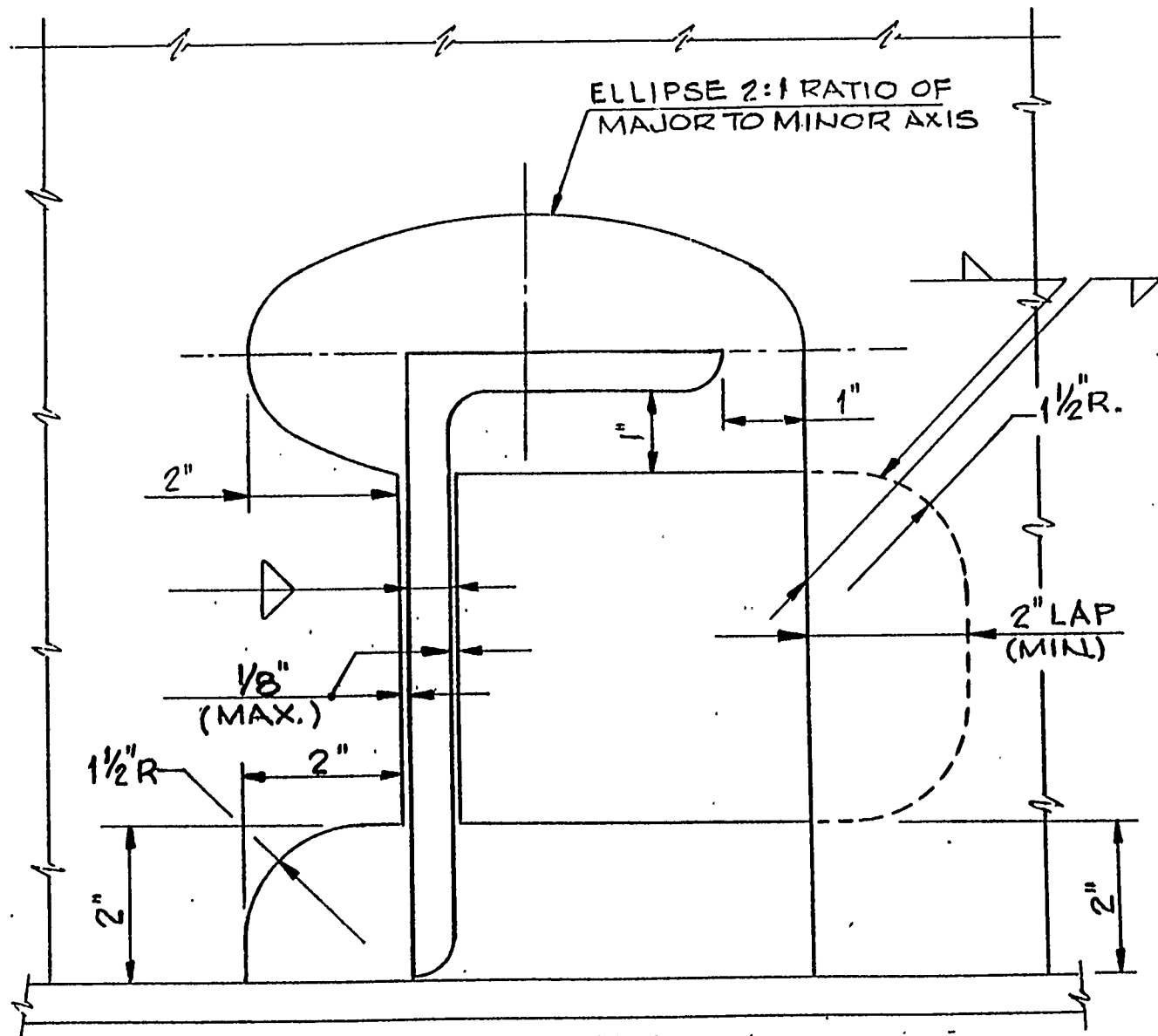
ELLIPTICAL CUTOUT w/ DOUBLE TABS

Figure 3-37

DETAILED MODEL OF CUTOUT AREA
ELLIPTICAL CUTOUT w/DOUBLEc- TABS

Figure 3-38
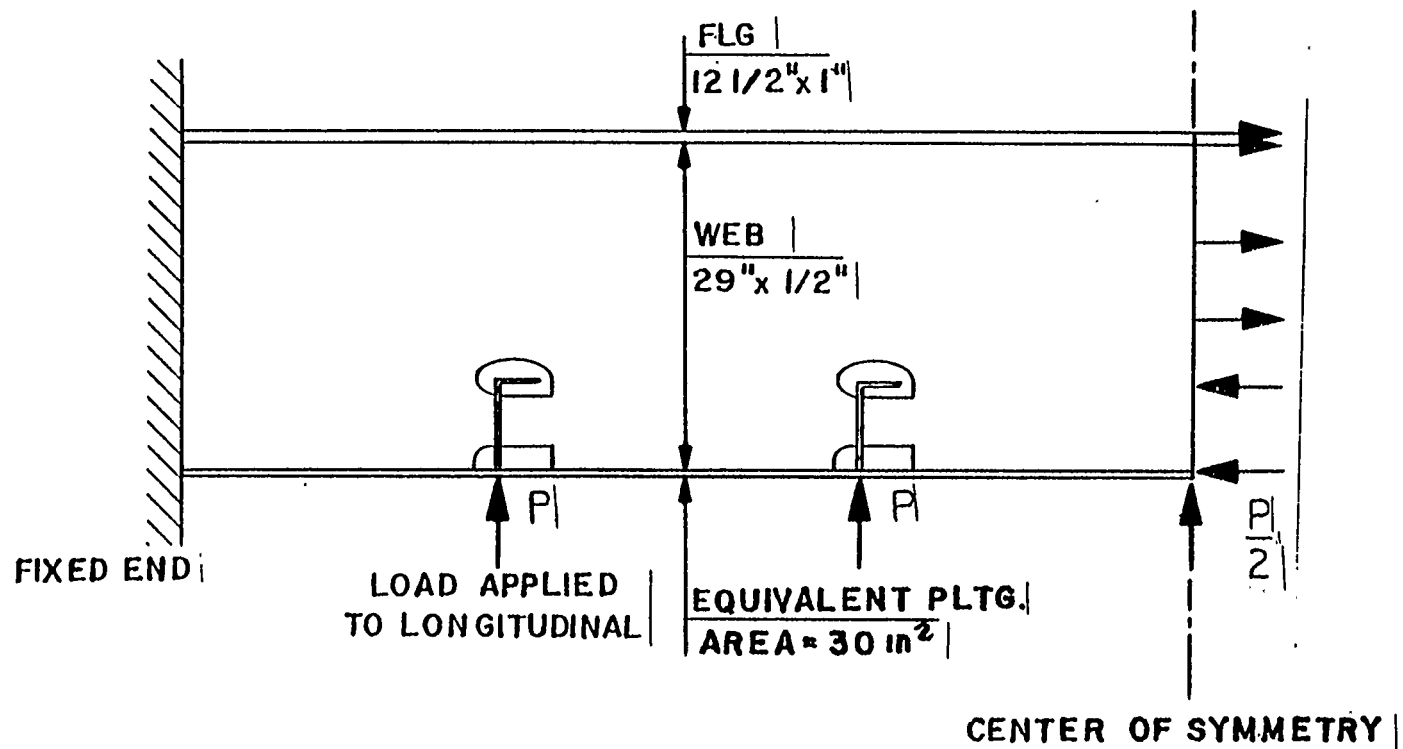
FLG
12 1/2" x 1"

WEB
29" x 1/2"

FIXED END

LOAD APPLIED
TO LONGITUDINAL

EQUIVALENT PLTG.
AREA = 30 in²

P

P

$\frac{P}{2}$

CENTER OF SYMMETRY

LOAD FOR ELLIPTICAL CUTOUT w/DOUBLE TABS

Figure 3-39

o 1 2 3 4 5
SCALE:

NOTE: NO CUT-OUT
=1.0

2.8

3.7

4.1

STRESS CONCENTRATION FACTOR
ELLIPTICAL CUTOUT w/DOUBLE TABS
Figure 3-40

FIXED END

CENTER OF SYMMETRY

FINITE ELEMENT ANALYSIS MODEL
ELLIPTICAL CUTOUT w/ SINGLE TAB AND PANEL STIFFENER

Figure 3-41

FOR MODEL OF THIS
AREA SEE FIG. 3-44
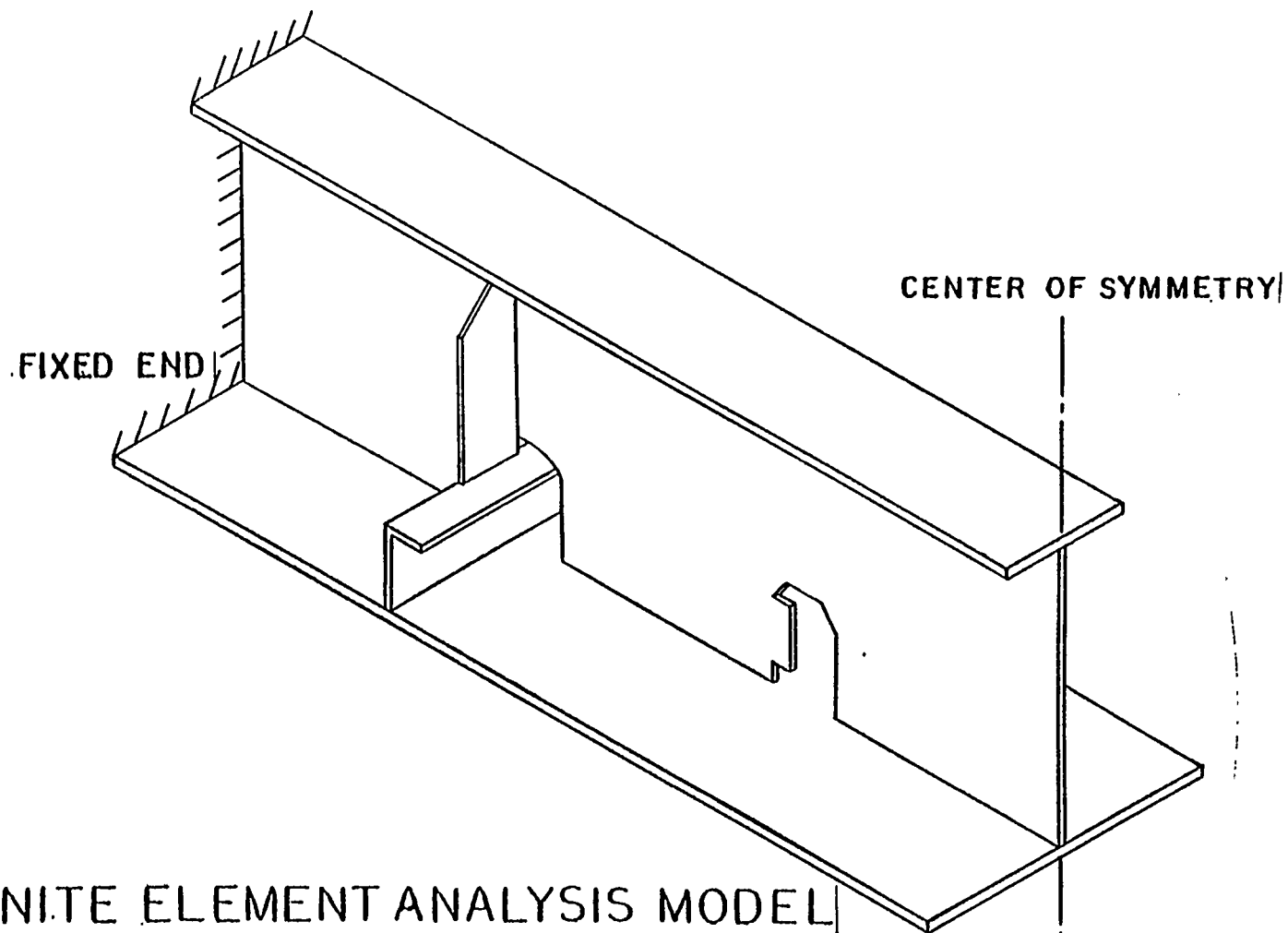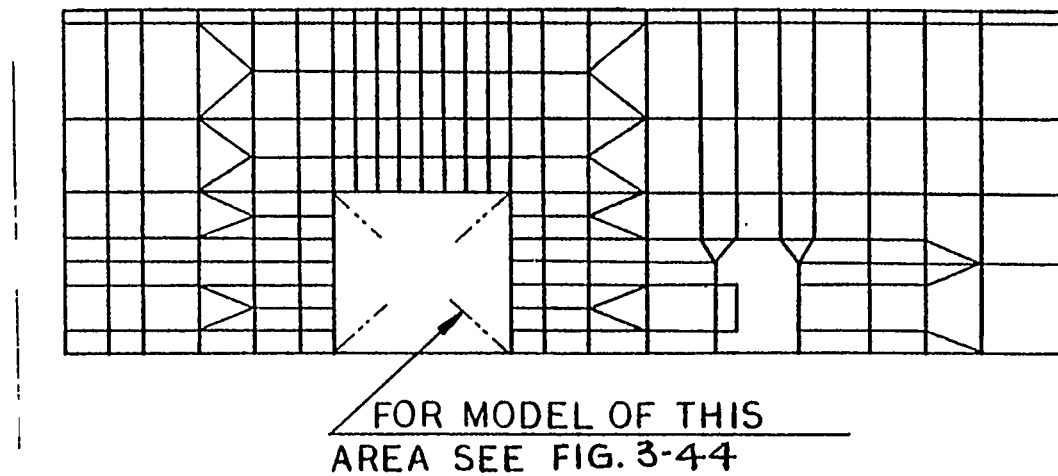
FINITE ELEMENT ANALYSIS MODEL
ELLIPTICAL CUTOUT w/SINGLE TAB AND PANEL STIFFENER

Figure 3-42

ELLIPSE 2:1 RATIO OF
MAJOR TO MINOR AXIS

1"

2"

1/8"
(MAX.)

1½"R

2"

2"
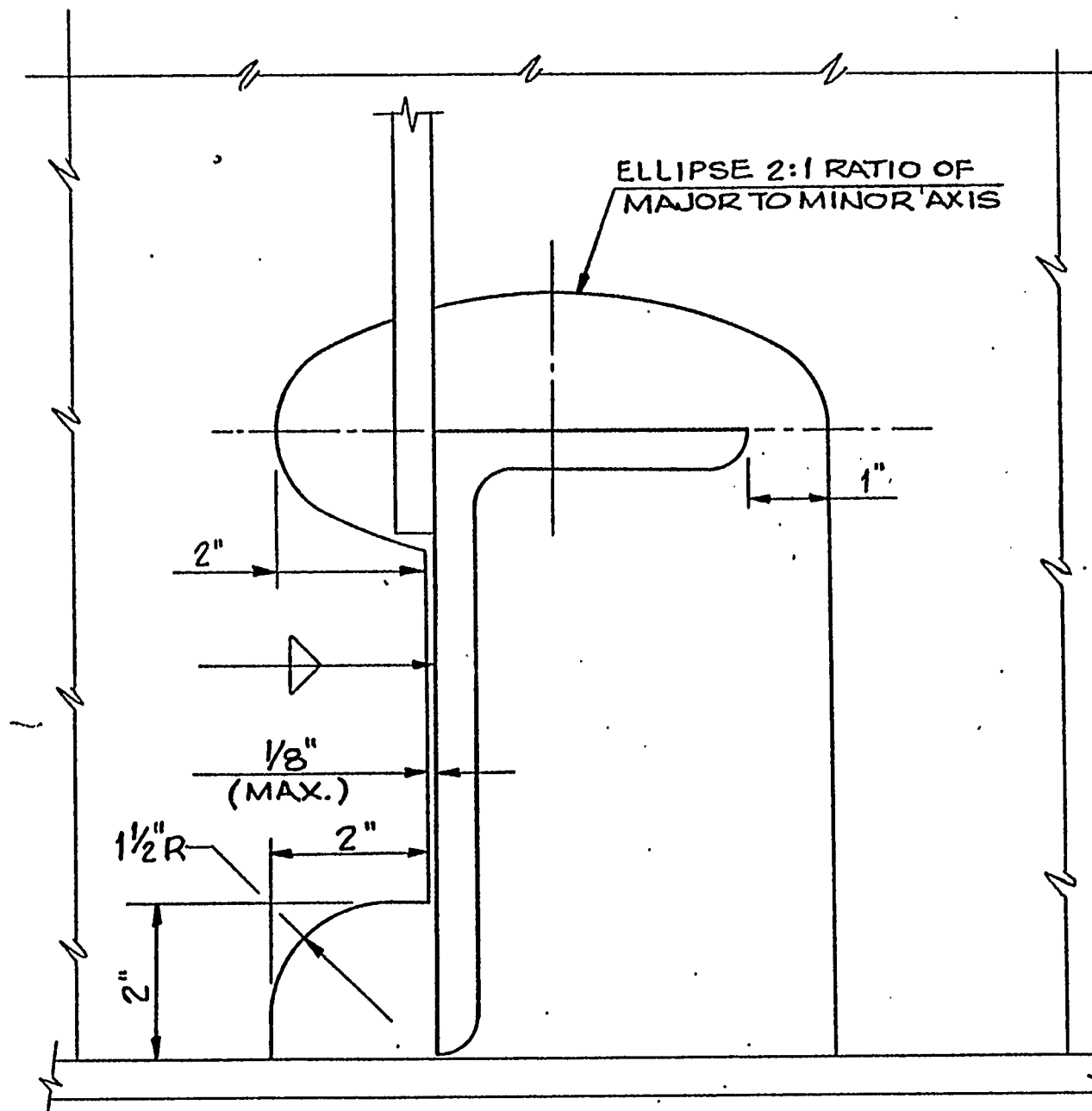
ELLIPTICAL CUTOUT w/ SINGLE TAB AND PANEL STIFFENER
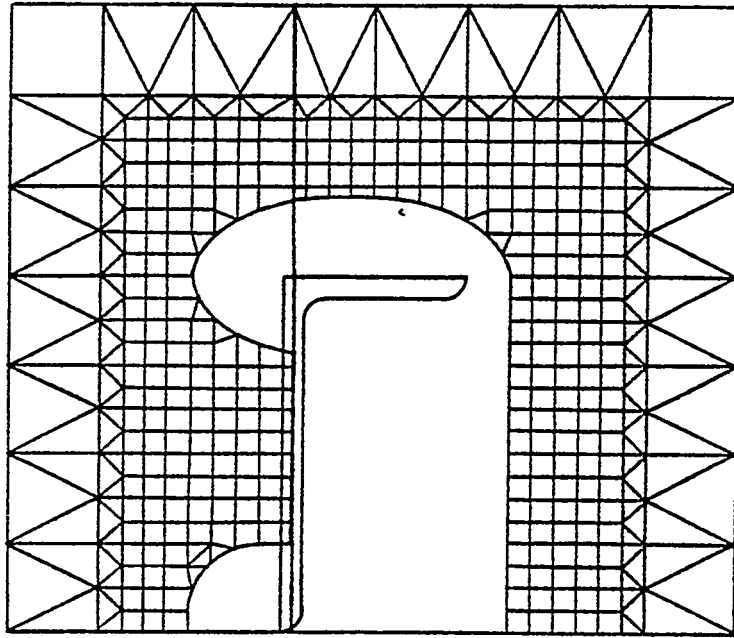
Figure 3-43

DETAILED MODEL OF CUTOUT AREA
ELLEPTICAL CUTOUT w/ SINGLE TAB AND PANEL STIFFENER

Figure 3-44
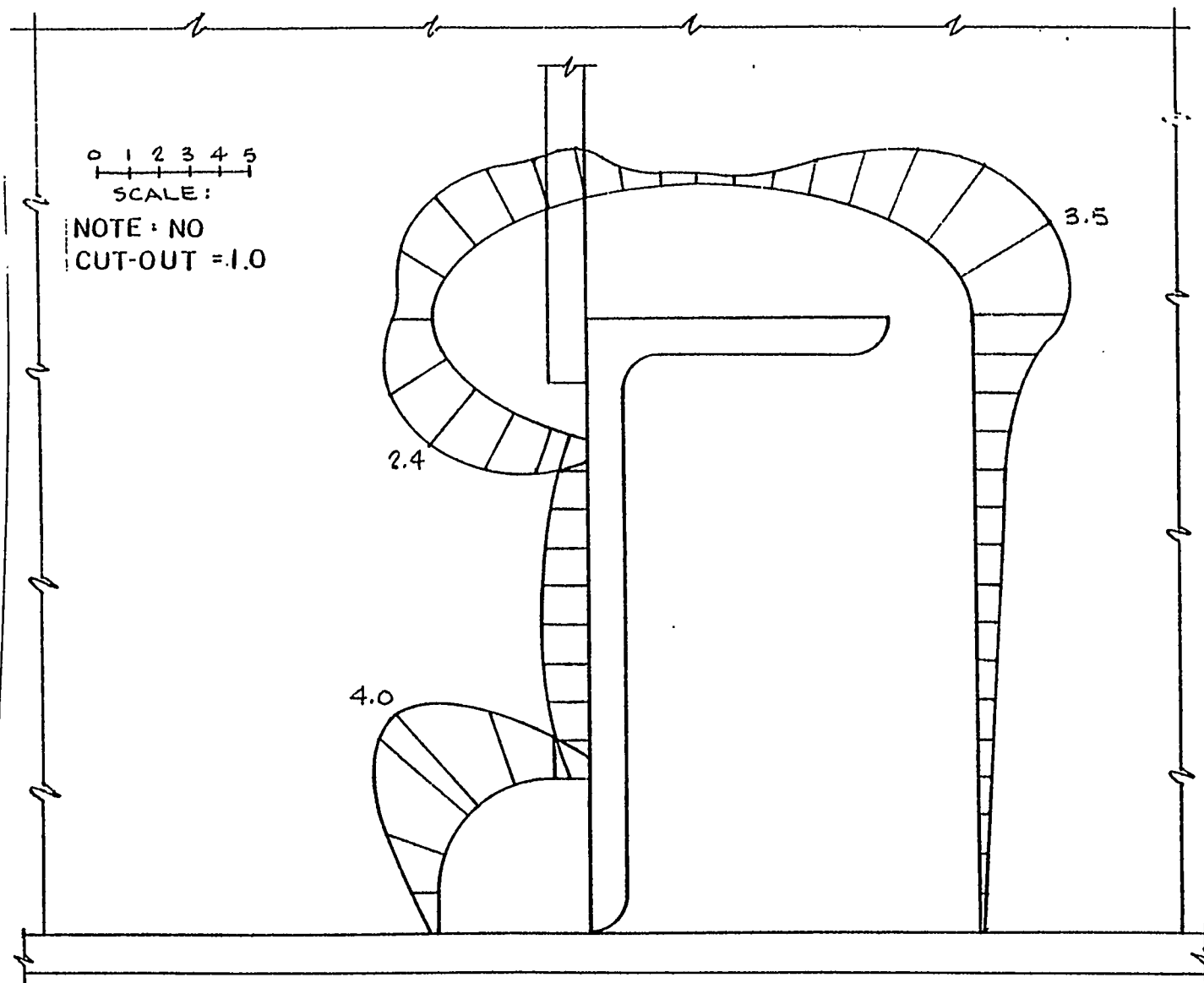
FLG
12 1/2"x 1"

WEB
29"x 1/2"

FIXED END

LOAD APPLIED
TO LONGITUDINAL

P

P

EQUIVALENT PLTG.
AREA = 30 in²

$\frac{P}{2}$

CENTER OF SYMMETRY

LOAD FOR ELLIPTICAL CUTOUT w/ SINGLE TAB
AND PANEL STIFFENER

Figure 3-45

STRESS CONCENTRATION FACTOR
ELLIPTICAL CUTOUT w/ SINGLE TAB and PANEL STIFFENER
Figure 3-46

3.3.4   Double Tab With Panel Stiffener

The model for this extreme support case is described in Figures 3-47 to 3-51, and stress magnification factors are plotted in Figure 3-52. The conclusion is that the addition of the bosom tab has no measurable benefit over and above attachment of the panel stiffener.

3.3.5   Analysis Summary

The analysis in this section provided the somewhat surprising results that addition of a second tab and/or panel stiffener has little effect on the stresses of an angle stiffener supported by a tab to the heel. Equally surprising is that the additional support provided by a panel stiffener is not measurably greater than that provided by a tab to the angle bosom.
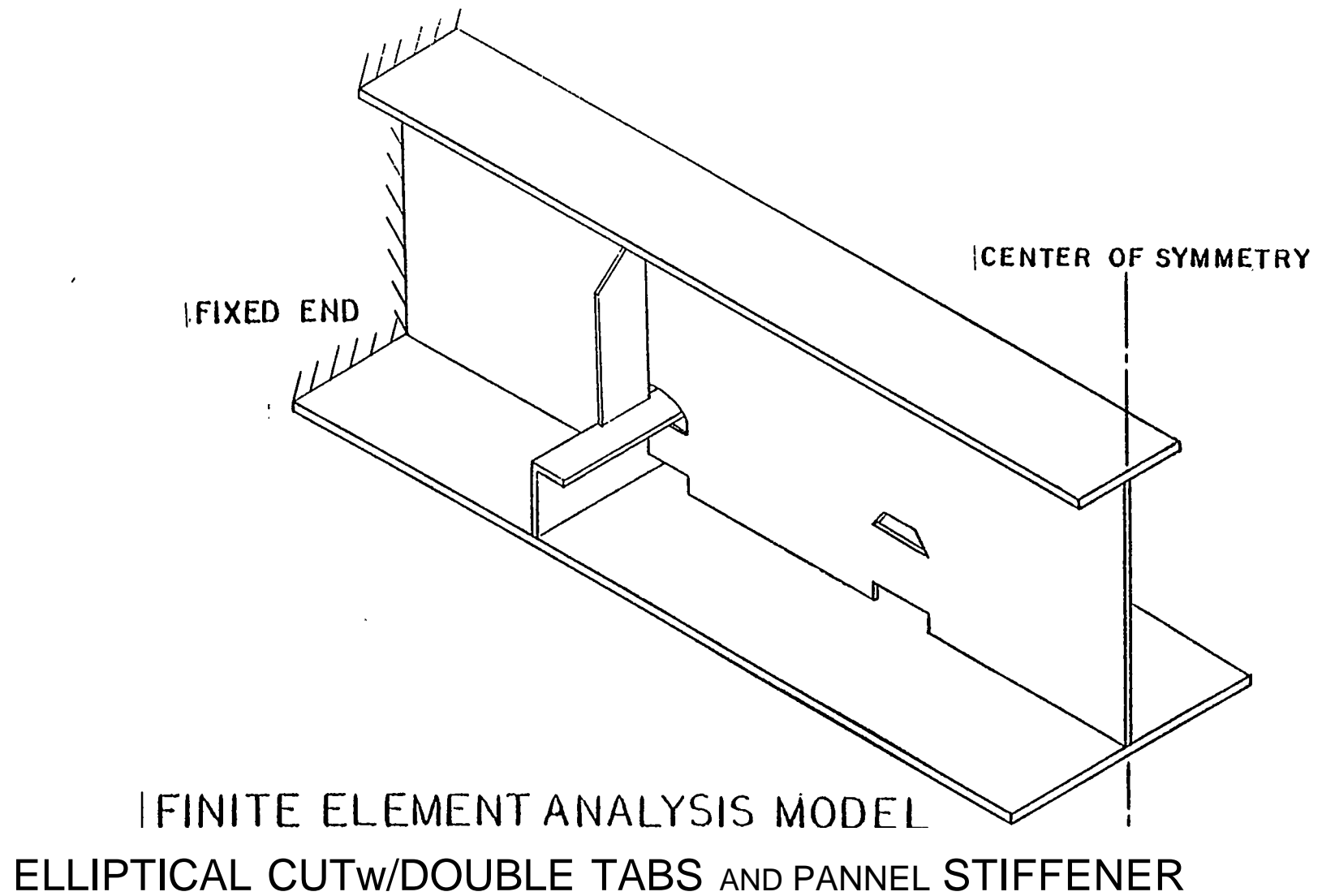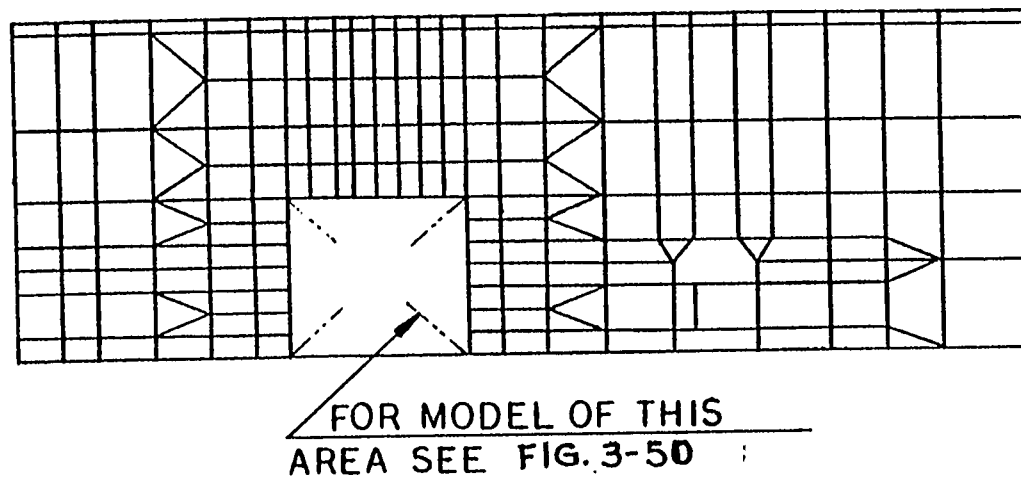
CENTER OF SYMMETRY

FIXED END

FINITE ELEMENT ANALYSIS MODEL
ELLIPTICAL CUTw/DOUBLE TABS AND PANNEL STIFFENER

Figure 3-47

FOR MODEL OF THIS
AREA SEE FIG. 3-50

FINITE ELEMENT ANALYSIS MODEL
ELLIPTICAL CUTOUT w/ DOUBLE TABS AND PANEL STIFFENER

Figure 3-48

ELLIPTICAL CUTOUT w/DOUBLE TABS AND PANEL STIFFENER
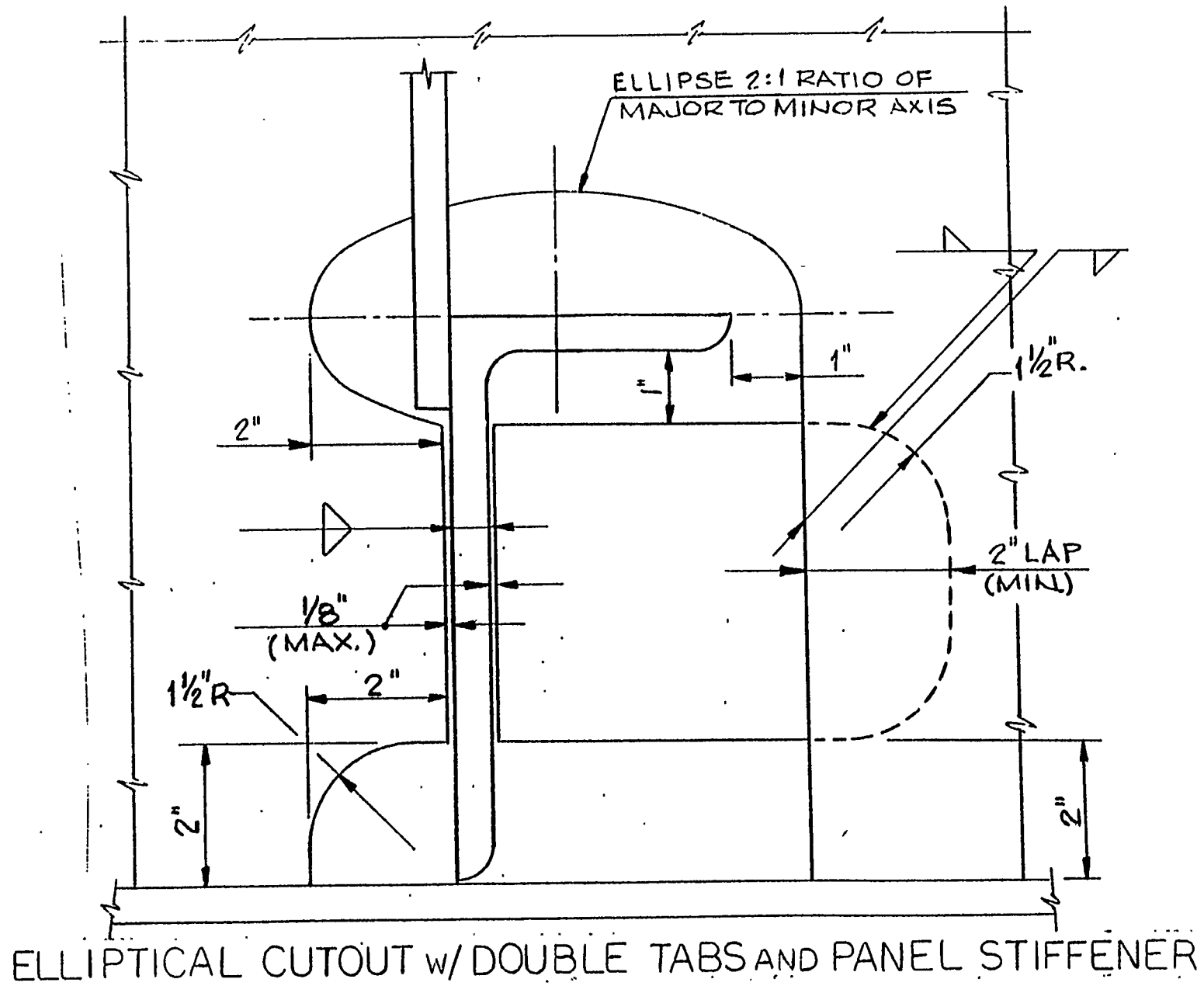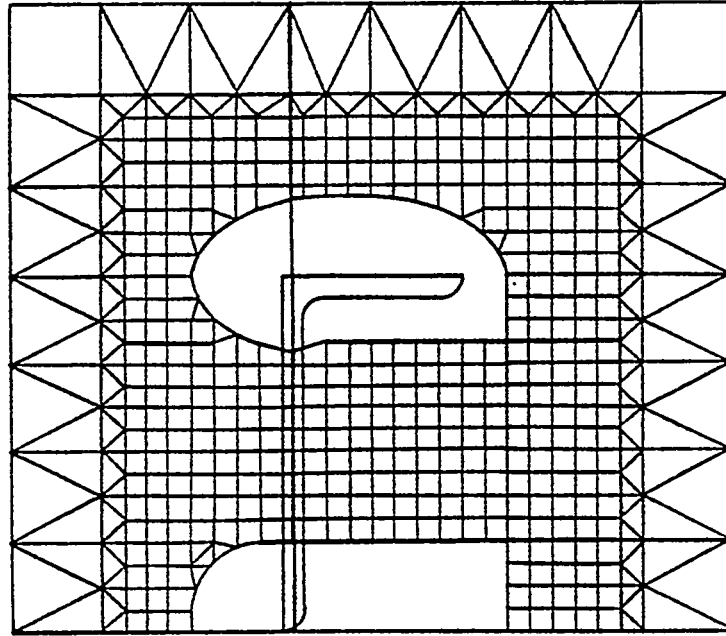
Figure 3-49

**DETAILED MODEL OF CUTOUT AREA
ELLIPTICAL CUTOUT WITH DOUBLE
TABS AND PANEL STIFFENER**

Figure 3-50
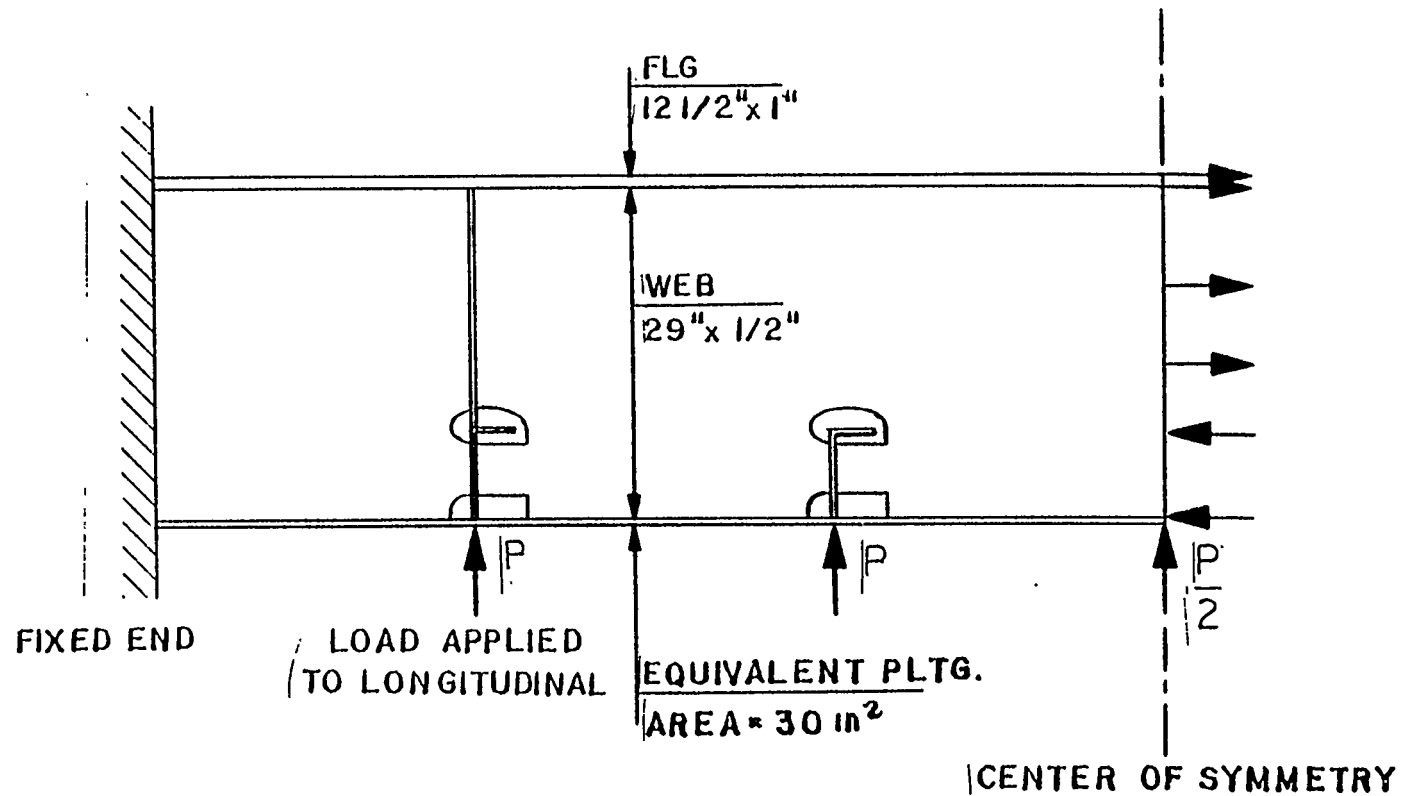
FLG
12 1/2"x 1"

WEB
29"x 1/2"

FIXED END

LOAD APPLIED
TO LONGITUDINAL

P

P

EQUIVALENT PLTG.
AREA = 30 in^2

$\dfrac{P}{2}$

CENTER OF SYMMETRY

LOAD FOR ELLIPTICAL CUTOUT w/ DOUBLE TABS
AND PANEL STIFFENER

Figure 3-51

0 — 5
SCALE

NOTE : NO
CUT-OUT = 1.0

3.2

2.3

4.0
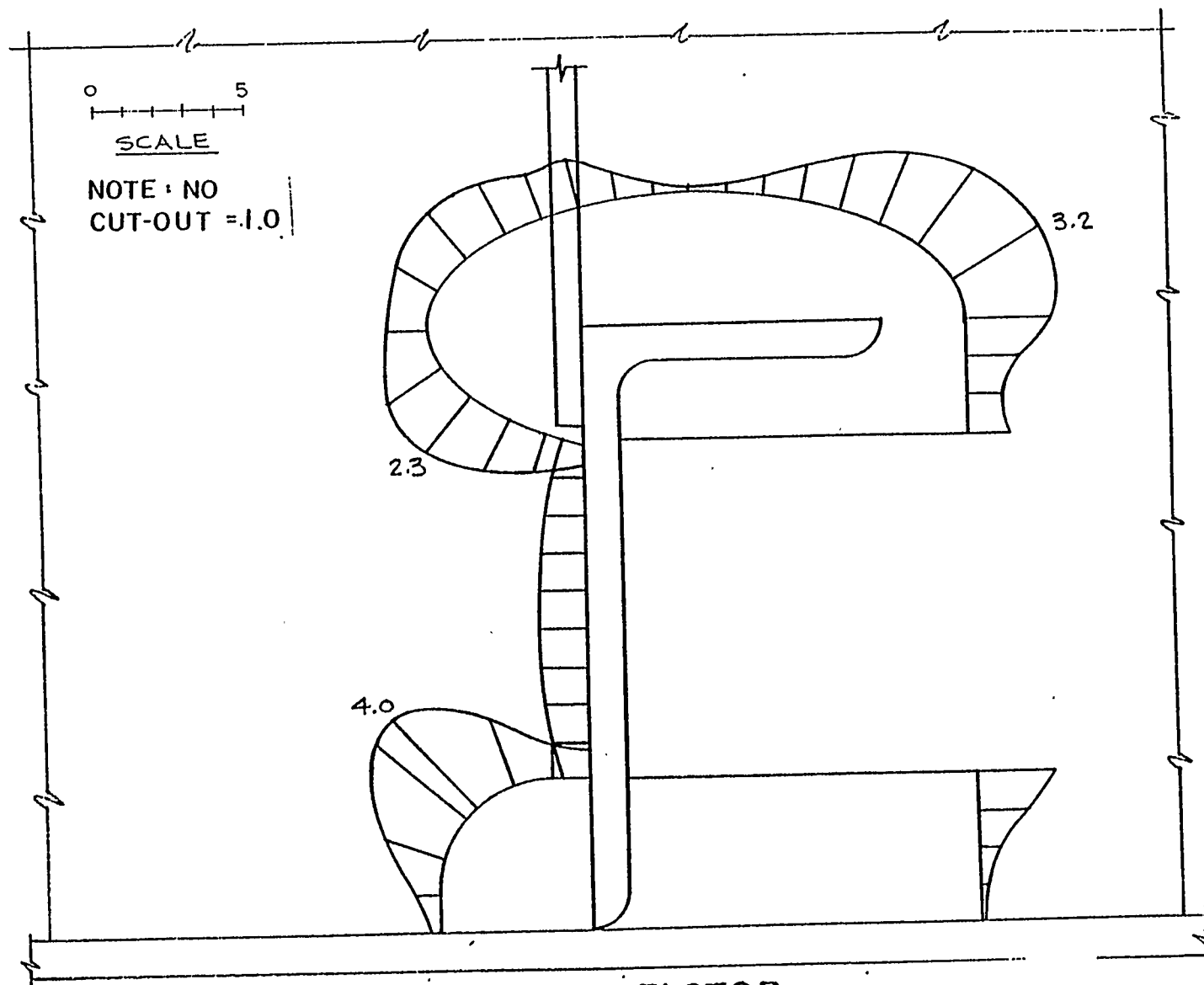
STRESS CONCENTRATION FACTOR
ELLIPTICAL CUTOUT w/DOUBLE TABS AND PANEL STIFFENERS

Figure 3-52

Section 4
TENTATIVE COLLECTION OF STANDARD SHIP
STRUCTURAL DETAILS

To assist in the future development of standards, this section presents a collection of ship structural details that represent either a direct adoption of what seems the best now in use in the U. S. shipbuilding industry, or the development of slightly modified configurations based on comments in Section 2.

Details are presented in the following categories:

	DETAIL TYPE	FIGURE NO.	PAGE NO.
1.	Clearance Cutouts	4-1 to 4-4	4-3 & 4-4
2.	Clearance Cutouts With Nontight Lapped Collars	4-5 to 4-11	4-5 to 4-8
3.	Clearance Cutouts With Web Attachments	4-12 to 4-14	4-9 & 4-10
4.	Clearance Cutouts With Flange Attachments	4-15	4-11
5.	Clearance Cutouts With Web & Flange Attachments	4-16 & 4-17	4-12
6.	Clearance Cutouts With Web Attachments & Nontight Lapped Collars	4-18 to 4-20	4-13 & 4-14
7.	Clearance Cutouts with Flange Attachments & Nontight Lapped Collars	4-21	4-15
8.	Clearance Cutouts With Web & Flange Attachments & Nontight Lapped Collars	4-22 to 4-23	4-16
9.	Clearance Cutouts With Tight Lapped Collars	4-24 to 4-27	4-17 & 4-18
10.	Clearance Cutouts With Tight Flush Collars	4-28 to 4-31	4-19 & 4-20
11.	Miscellaneous Cutouts	4-32 to 4-36	4-21 to 4-23
12.	Nontight Penetrations	4-37	4-24
13.	Chocks and Brackets	4-38 to 4-45	4-25 to 4-28
14.	Stiffener Endings	4-46 to 4-52	4-29 to 4-31
15.	Panel Stiffeners	4-53 to 4-58	4-32 to 4-35
16.	Stanchion Endings	4-59 & 4-60	4-36

The key to selection is adequate strength and good producibility and maintainability. As an example, the rounded corners of the collars in Figures 4-5 and 4-6 permit continuous welding with adequate all around access. Similarly the tight lapped collars in Figures 4-24 and 4-25 are intended for easy welding access to the base of the collar. This philosophy has been carried throughout the remainder of the applicable details in this section and is most apparent in the details presenting stiffener endings and panel stiffeners.

The miscellaneous cutouts in Figures 4-34 and 4-35 have found application in Europe. They are only suggested to U.S. shipbuilders as an excellent method of reducing the stress at the base of any cutout terminating normal to ship plating. These details have the obvious drawback of being susceptible to damage prior to installation.

Only two beam brackets have been illustrated, Figures 4-44 and 4-45, but they demonstrate the essential characteristics that the many possible variations should possess.

Similarly the great variety of possible stanchion end connections causes the listing here to include only two that are generally illustrative of good practice, see Figures 4-59 and 4-60.

It is the intent of this section to serve as a basis of individual or committee discussion and review, thereby possibly leading to consensus standards. Reference 2 and Section 2 of this report will be of assistance in that review.

MAJOR AXIS

FABRICATED ANGLE

ELLIPSE 2:1 RATIO OF
MAJOR TO MINOR AXIS

1½"   1½"

ROLLED ANGLE

Figure 4-1

ELLIPSE 2:1 RATIO OF
MAJOR TO MINOR AXIS

1½"   1½"
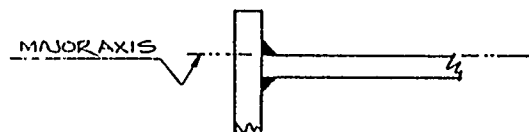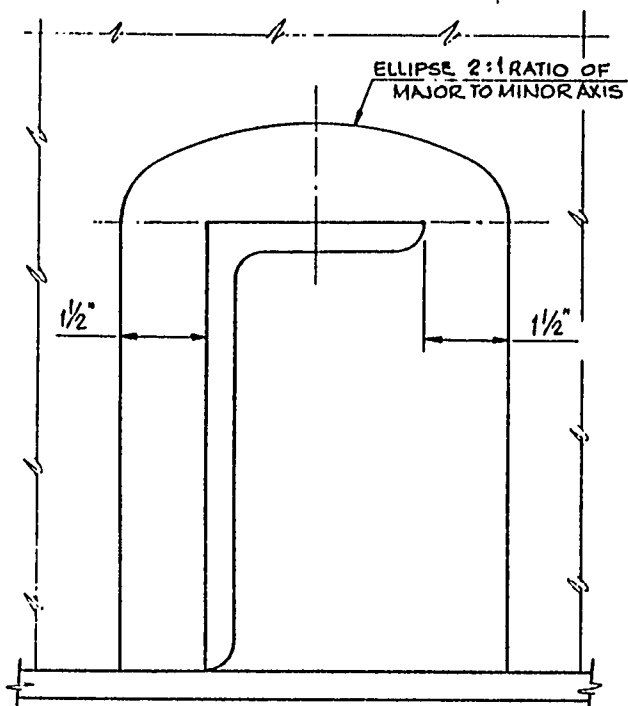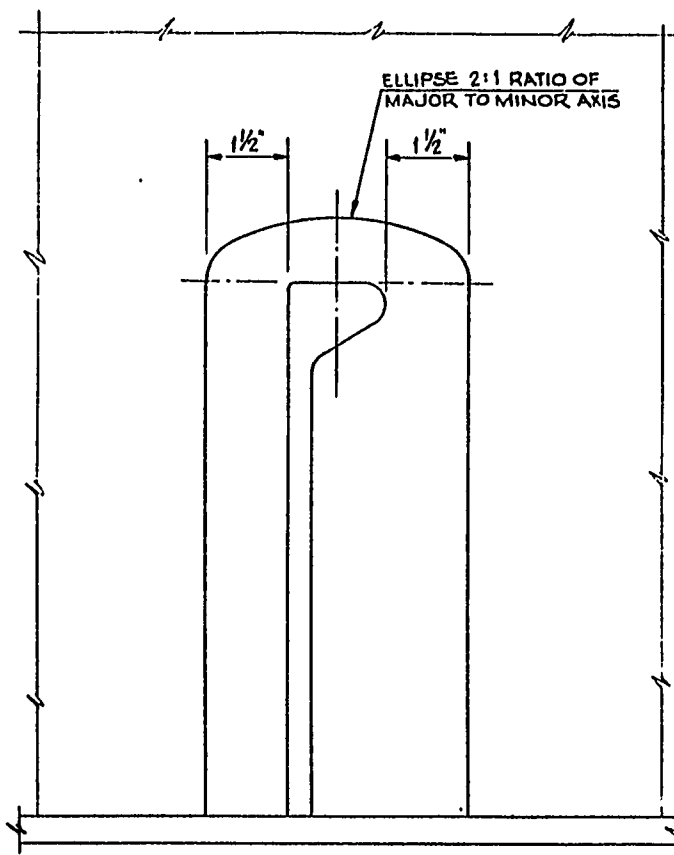
BULB FLAT

Figure 4-2

CLEARANCE CUTOUTS

ELLIPSE 4:1 RATIO OF
MAJOR TO MINOR AXIS

$1\frac{1}{2}"$ $1\frac{1}{2}"$

TEE

Figure 4-3

2"

2"R.
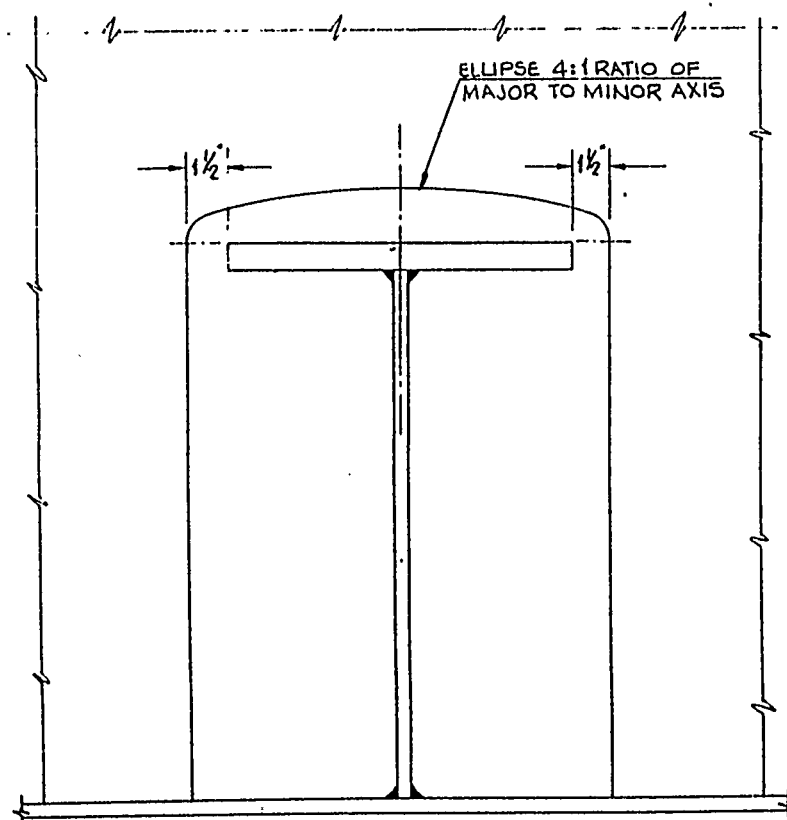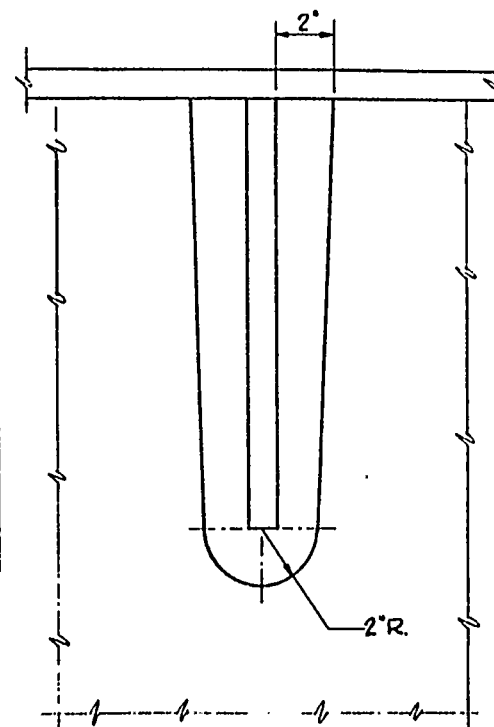
SLAB/FLAT BAR

Figure 4-4

CLEARANCE CUTOUTS

Use where web must be dropped
over stiffener with adequate clearance.

MAJOR AXIS

FABRICATED ANGLE

ELLIPSE 2:1 RATIO OF
MAJOR TO MINOR AXIS

1½"

½"

1½"R.

2"LAP
(MIN.)

⅛"
(MAX.)

1½"

2"

ROLLED ANGLE
COLLAR AT HEEL OF ANGLE
Figure 4-5

Use tab to bosom only if tab
to heel is very difficult.

MAJOR AXIS

FABRICATED ANGLE

ELLIPSE 2:1 RATIO OF
MAJOR TO MINOR AXIS

1½"

1½"

1"

1½"R

1½"

2"LAP
(MIN.)

⅛"
(MAX.)

2"

ROLLED ANGLE
COLLAR AT BOSOM OF ANGLE
Figure 4-6

CLEARANCE CUTOUTS WITH
NONTIGHT LAPPED COLLARS

4-5

ELLIPSE 2:1 RATIO OF
MAJOR TO MINOR AXIS

1½"   1½"

1½"

1/2"

1/8"
(MAX)

2" LAP
(MIN.)

"L"
SEE CHART
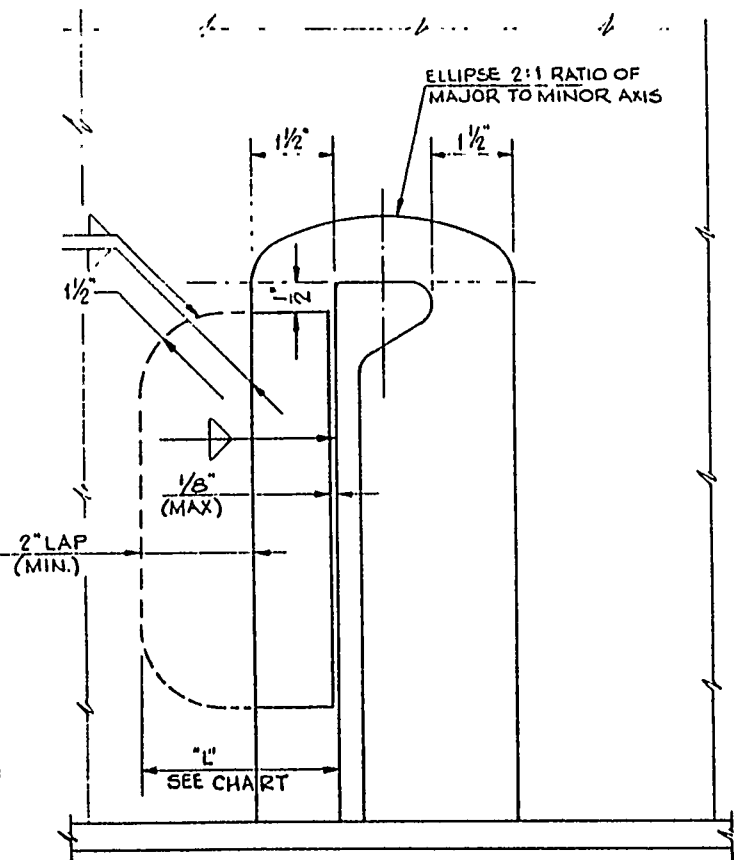
BULB FLAT
COLLAR AT HEEL

Figure 4-7

ELLIPSE 2:1 RATIO OF
MAJOR TO MINOR AXIS

1½"   1½"

1½"R.

1/8"
(MAX.)

2"LAP
(MIN.)

2"
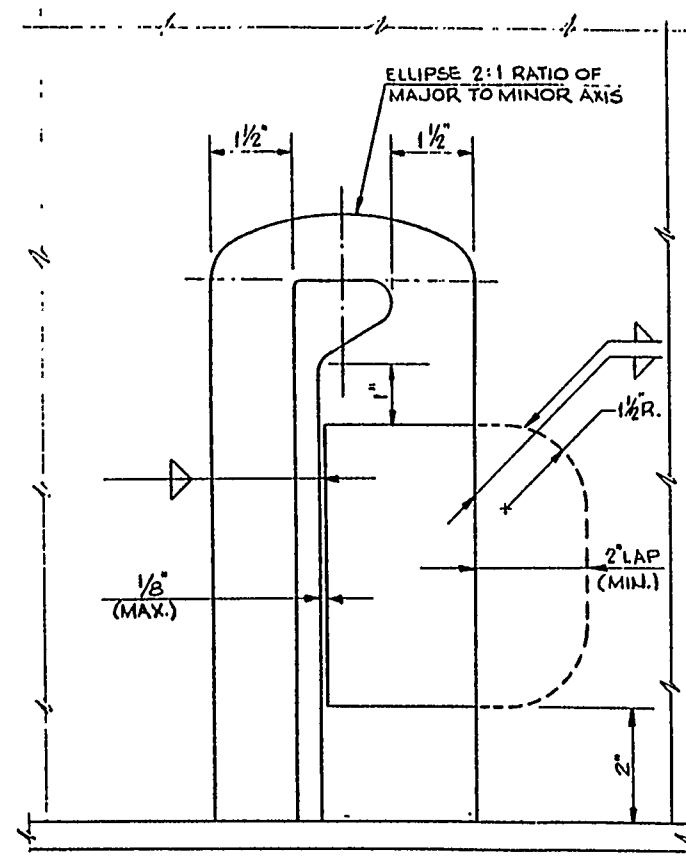
BULB FLAT
COLLAR AT BOSOM

Figure 4-8

CLEARANCE CUTOUTS WITH
NONTIGHT LAPPED COLLARS

ELLIPSE 4:1 RATIO OF
MAJOR TO MINOR AXIS

$1\frac{1}{2}$" $1\frac{1}{2}$"

2"

$1\frac{1}{2}$R

$\frac{1}{8}$"
(MAX.)

2"LAP
(MIN.)

2"
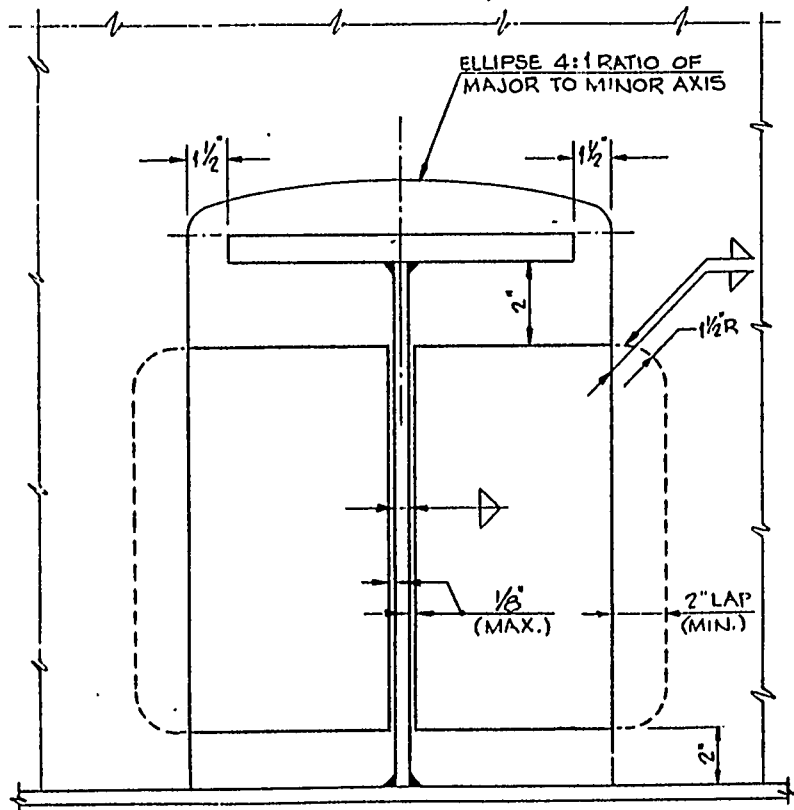
TEE
WEB ATTACHMENT ONLY

Figure 4-9

ELLIPSE 4:1 RATIO OF
MAJOR TO MINOR AXIS

$1\frac{1}{2}$" $1\frac{1}{2}$"

$1\frac{1}{2}$"R

$\frac{1}{8}$"
(MAX)

$\frac{1}{8}$"
(MAX.)

2"LAP
(MIN.)

2"
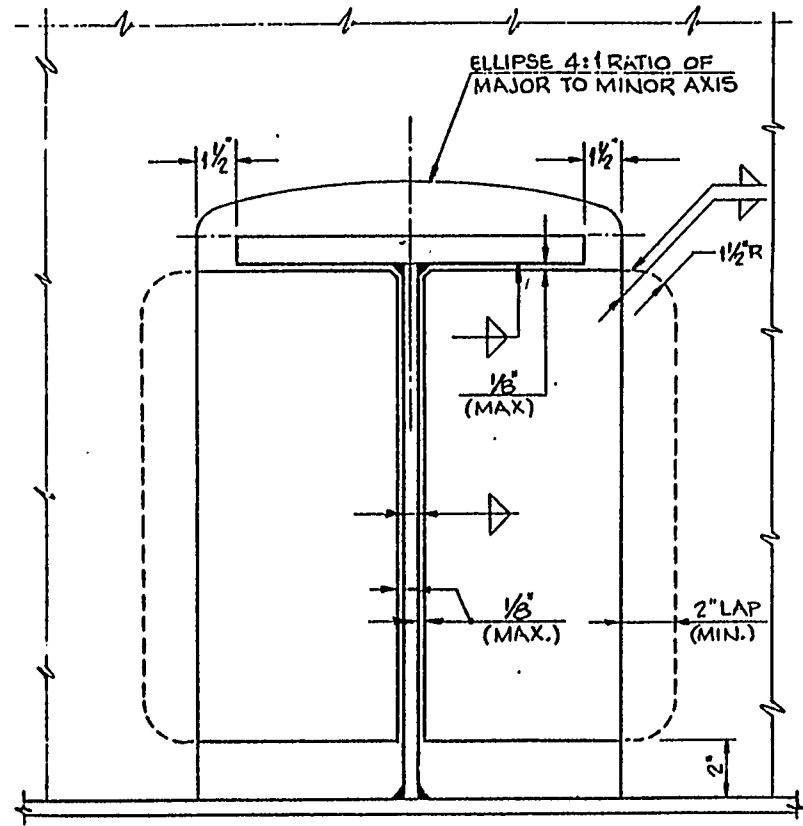
TEE
WEB AND FLANGE ATTACHMENT

Figure 4-10

CLEARANCE CUTOUTS WITH
NONTIGHT LAPPED COLLARS
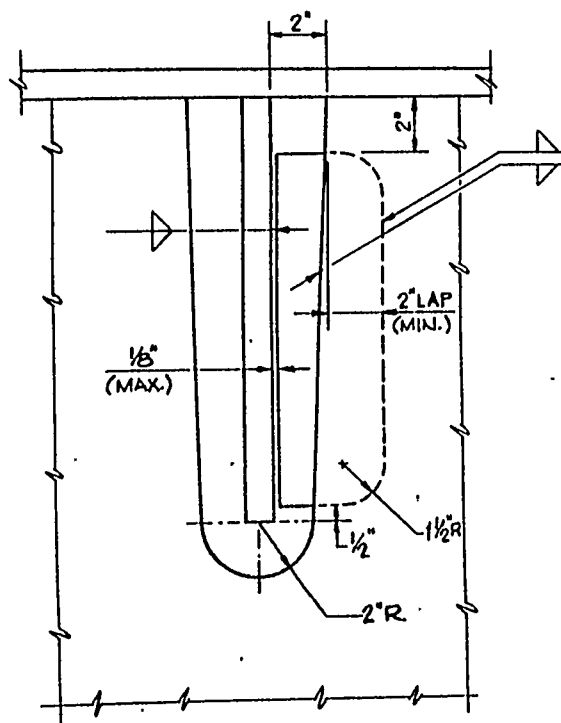
SLAB/FLAT BAR

Figure 4-11

CLEARANCE CUTOUTS WITH
NONTIGHT LAPPED COLLARS

ELLIPSE 2:1 RATIO OF
MAJOR TO MINOR AXIS

2"

1"

⅛"
(MAX.)

1½"R

2"

2"

ROLLED ANGLE

Figure 4-12

ELLIPSE 2:1 RATIO OF
MAJOR TO MINOR AXIS

2"

1"

⅛"
(MAX.)

2"

1½"R.
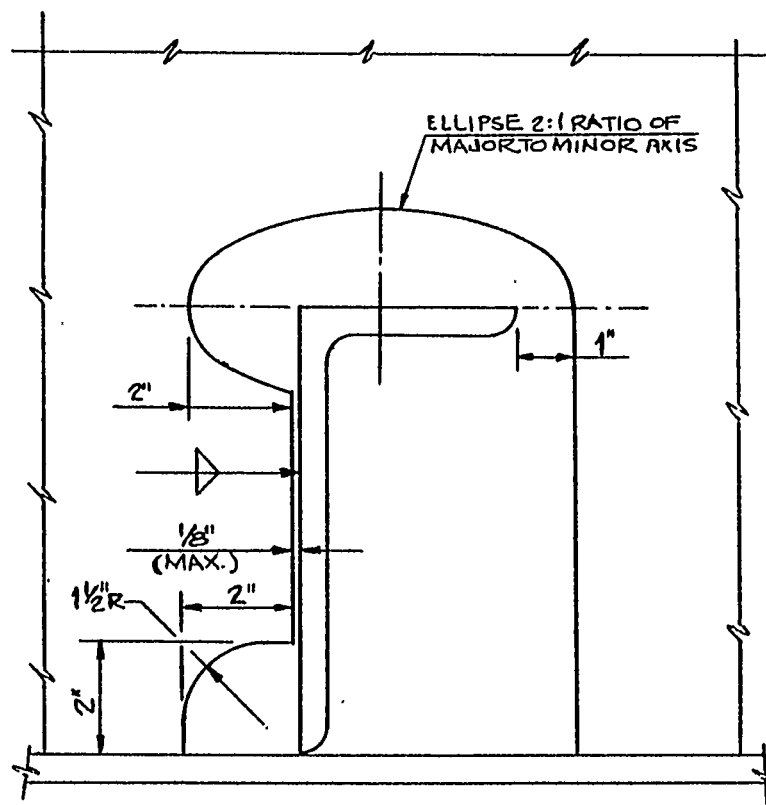
2"
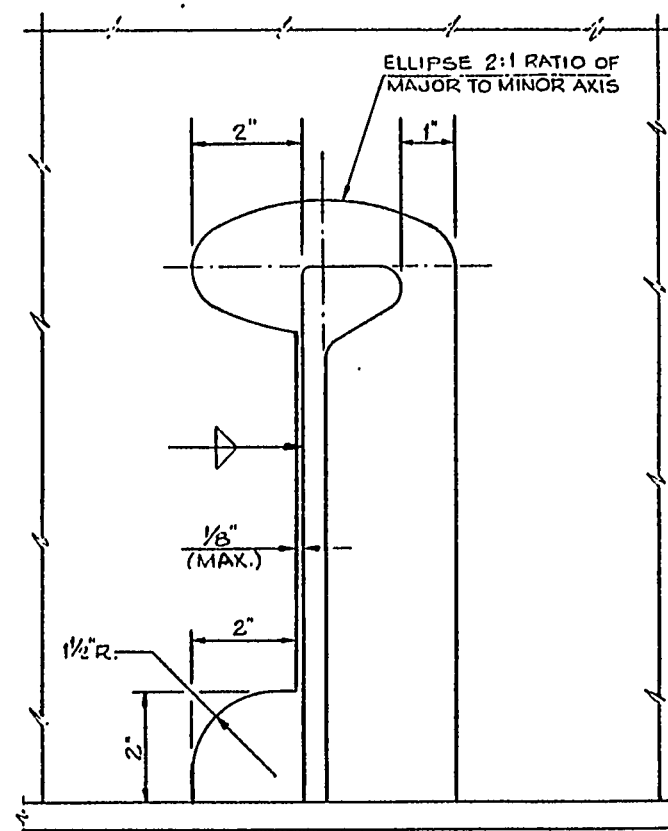
BULB FLAT

Figure 4-13

CLEARANCE CUTOUTS WITH
WEB ATTACHMENT
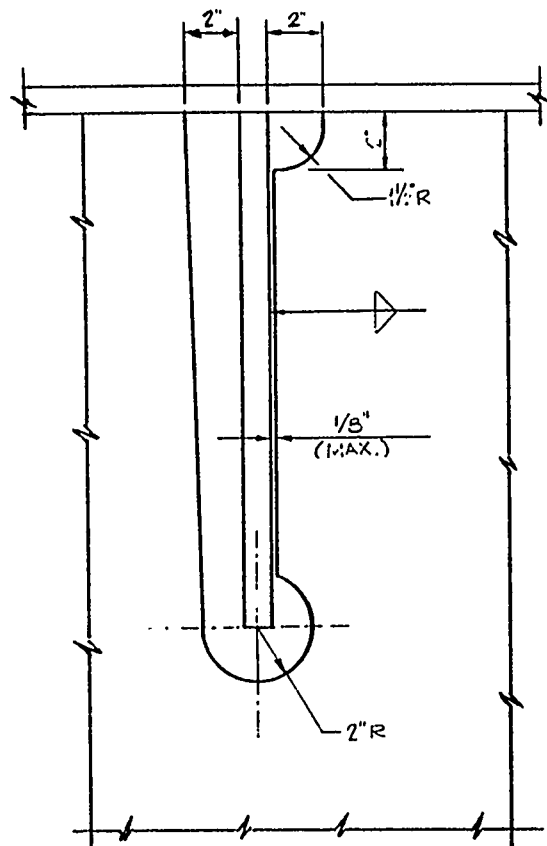
SLAB

Figure 4-14

CLEARANCE CUTOUTS WITH
WEB ATTACHMENT

TEE

Figure 4-15

2"R.

⅛" (MAX.)

1"R.

⅛" (MAX.)

3"
2" FOR 10" L

1½"R.

3"
2" FOR 10" L
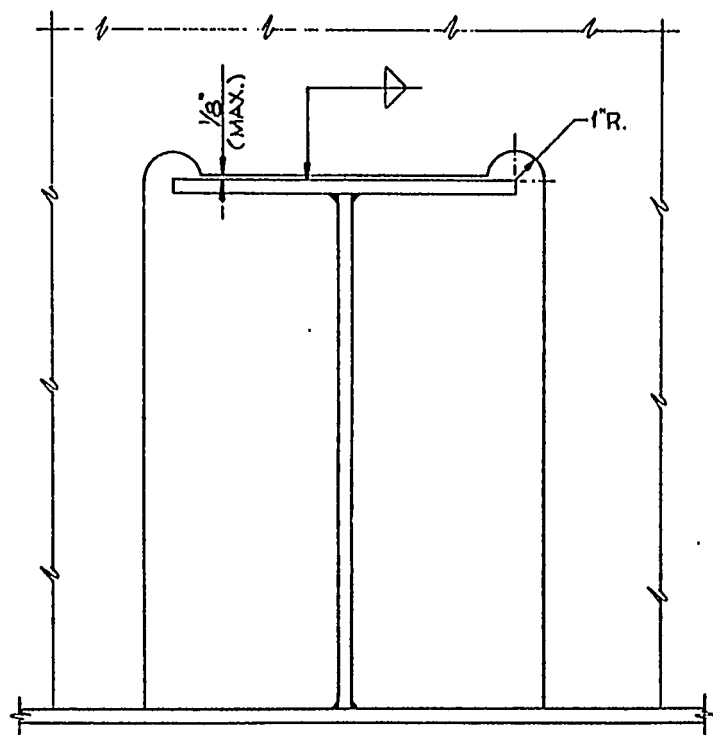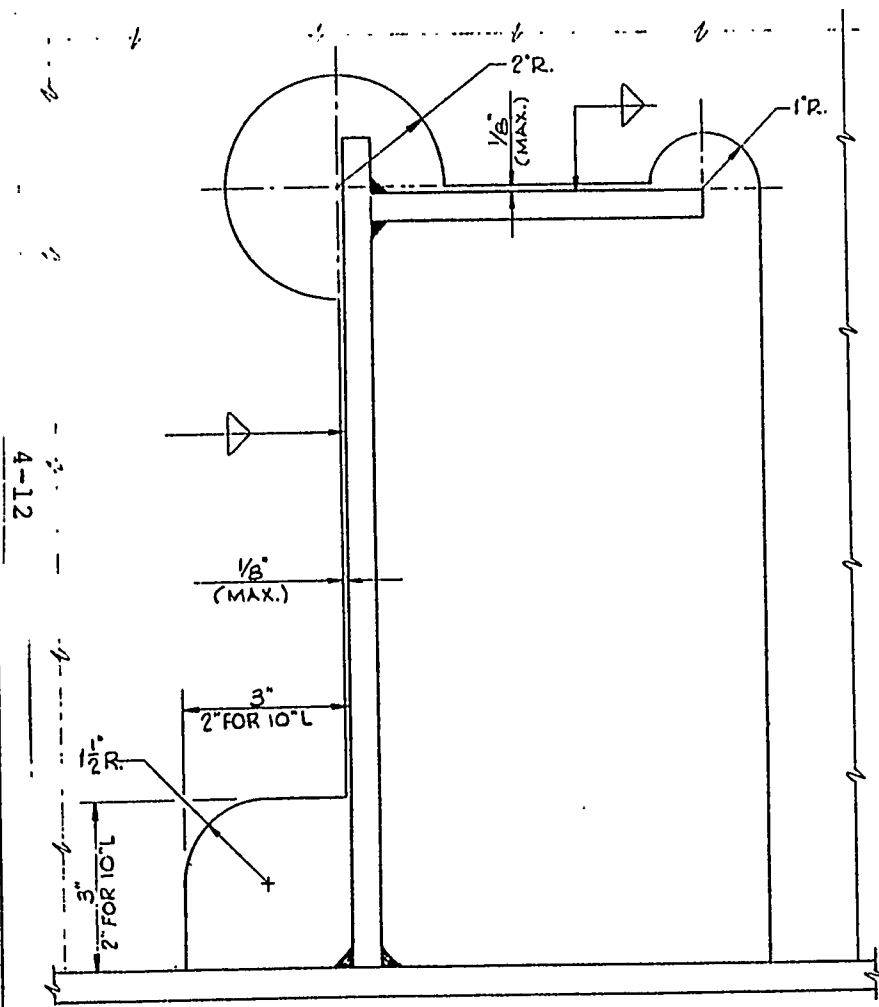
FABRICATED ANGLE

Figure 4-16

1"R.

⅛" (MAX)

1"R.

⅛" (MAX)

2"

1½"R.

2"
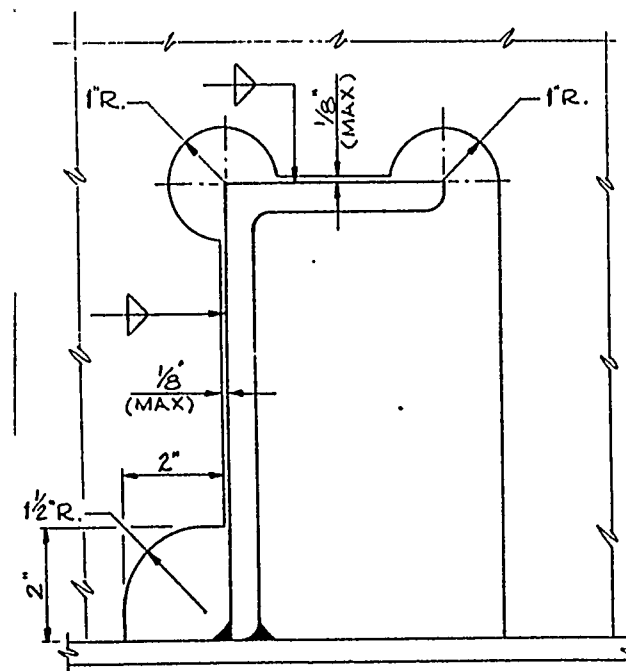
ROLLED ANGLE

Figure 4-17

CLEARANCE CUTOUTS WITH
WEB & FLANGE ATTACHMENT

ELLIPSE 2:1 RATIO OF
MAJOR TO MINOR AXIS

ELLIPSE 2:1 RATIO OF
MAJOR TO MINOR AXIS

2"

1"

1½"R.

2"

1"

1½"R.

2"LAP
(MIN)

2"LAP
(MIN)

⅛"
(MAX.)

⅛"
(MAX.)

1½"R

2"

2"

2"

1½"R.

2"

2"

2"
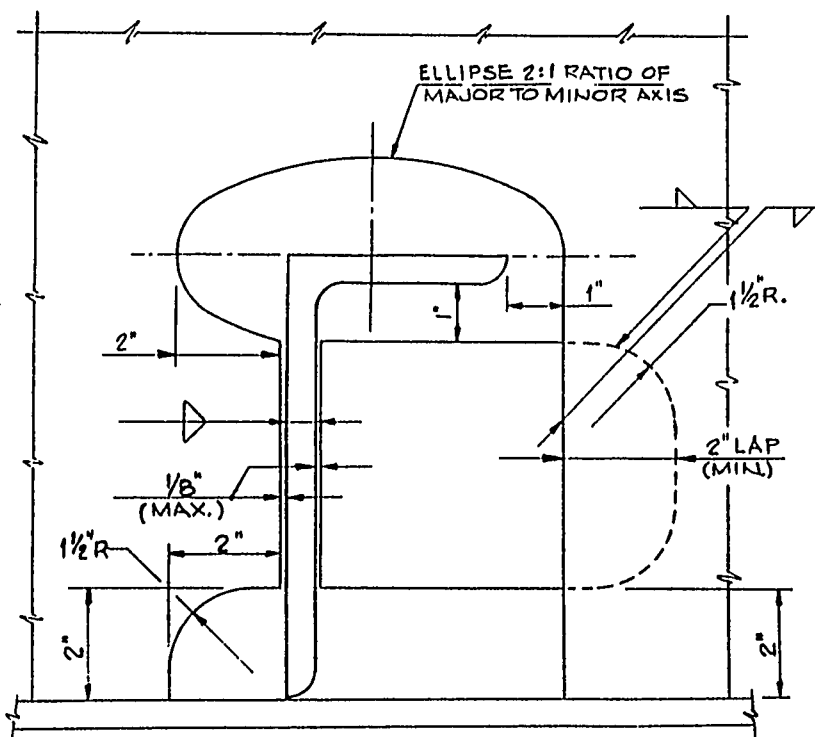
ANGLE
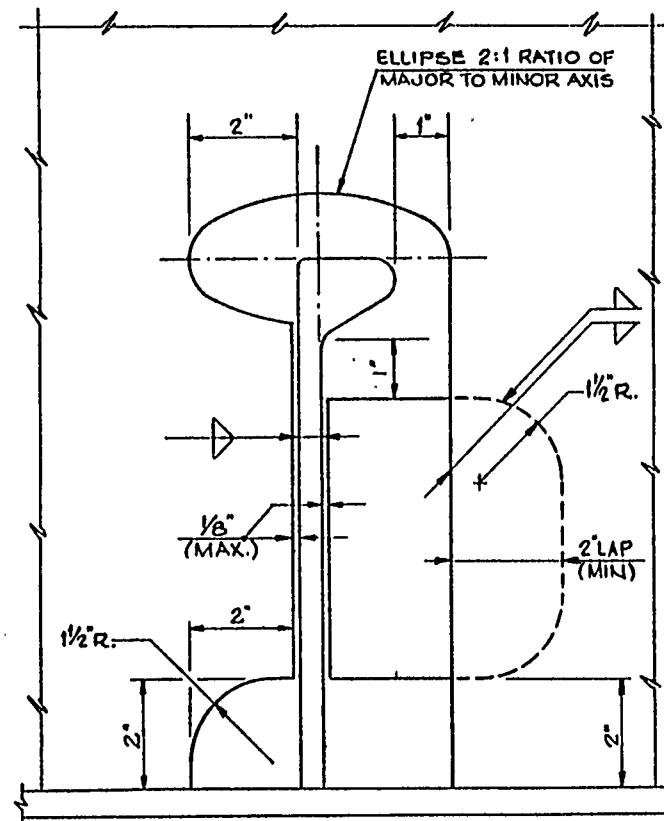
BULB FLAT

Figure 4-18

Figure 4-19

CLEARANCE CUTOUTS
WITH WEB ATTACHMENT &
NONTIGHT LAPPED COLLARS
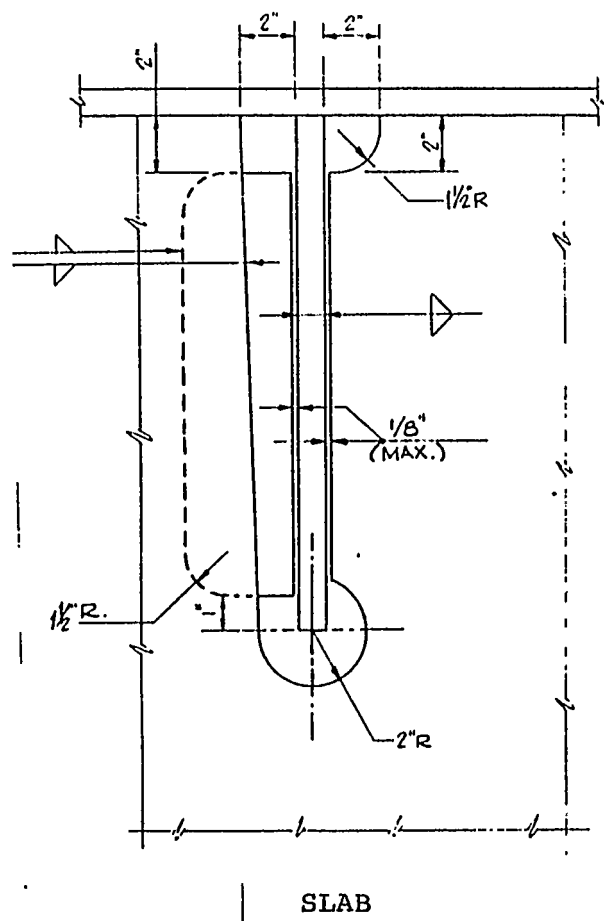
2" 2"

2"

1½R

1½" R.

⅛" (MAX.)

2"R

SLAB

Figure 4-20

TEE

Figure 4-21

CLEARANCE CUTOUTS
WITH WEB & FLANGE ATTACHMENT
& NONTIGHT LAPPED COLLARS

FABRICATED ANGLE

Figure 4-22

ROLLED ANGLE

Figure 4-23

CLEARANCE CUTOUTS WITH
WEB & FLANGE ATTACHMENT
AND NONTIGHT LAPPED COLLARS
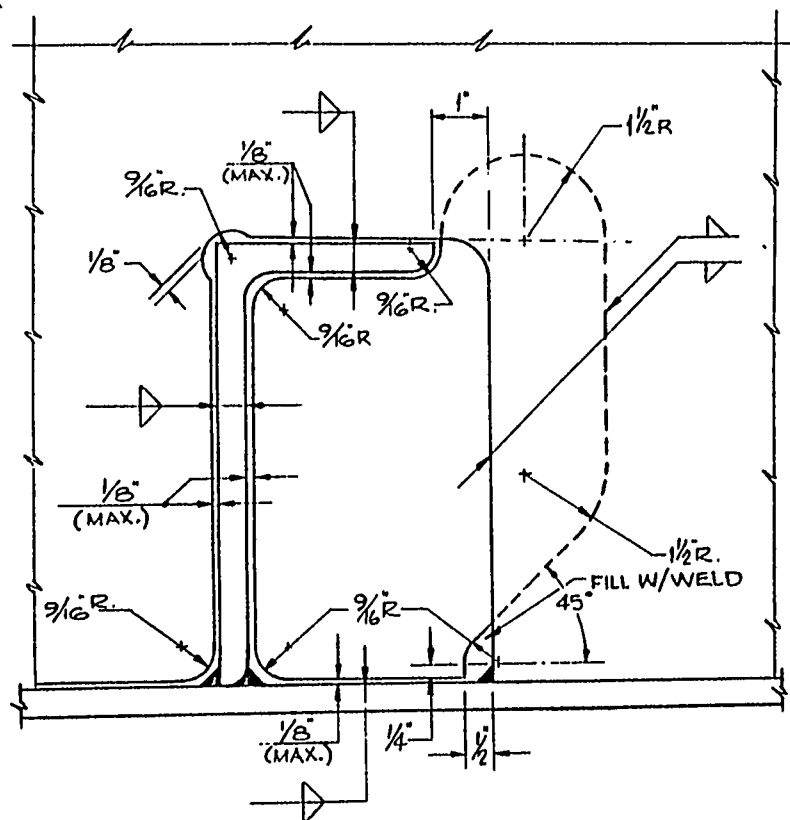
ROLLED ANGLE
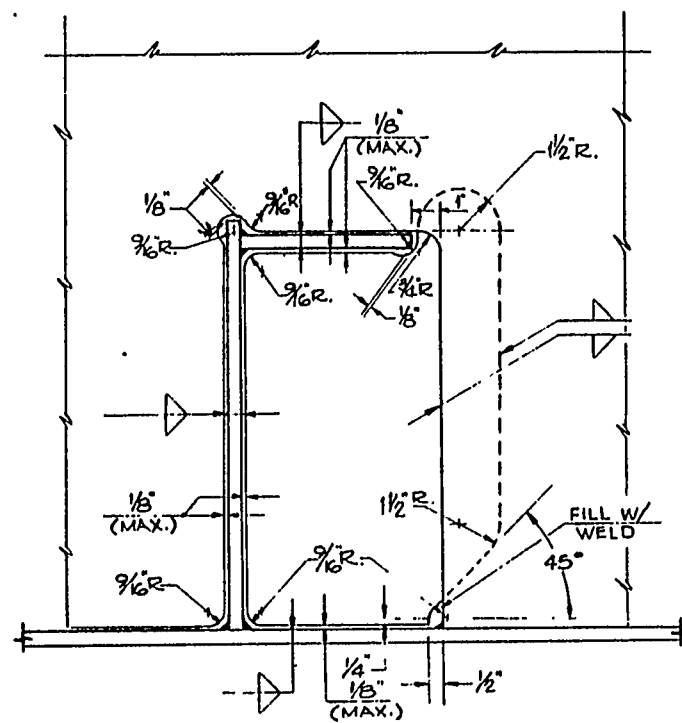
Figure 4-24

FABRICATED ANGLE

Figure 4-25
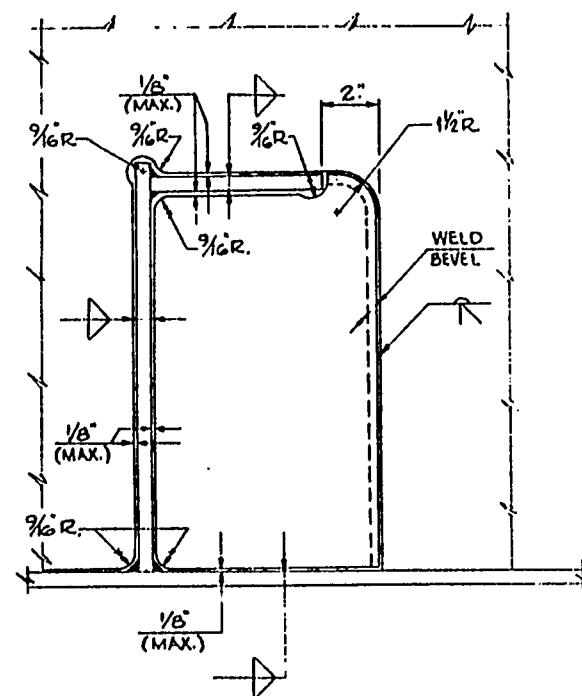
CLEARANCE CUTOUTS
WITH TIGHT LAPPED COLLARS

BULB FLAT

Figure 4-26

TEE

Figure 4-27

CLEARANCE CUTOUTS
WITH TIGHT LAPPED COLLARS

ROLLED ANGLE

Figure 4-28

FABRICATED ANGLE

Figure 4-29

CLEARANCE CUTOUTS
WITH TIGHT FLUSH COLLARS

1/8"
(MAX.)

9/16R.

1/8°

9/16"R.

2"

1 1/2"R.

WELD
BEVEL

1/8°
(MAX.)

9/16"R.

1/8°
(MAX.)

| BULB FLAT

Figure 4-30

1/8"
(MAX.)

2"

1 1/2"R.

9/16"R.

WELD
BEVEL

1/8"
(MAX.)

9/16"R.

1/8"
(MAX.)
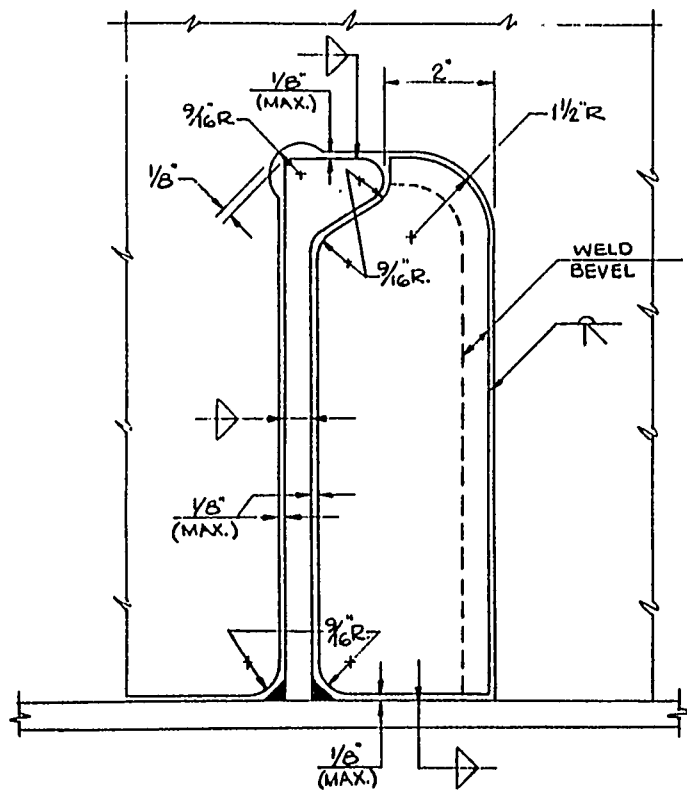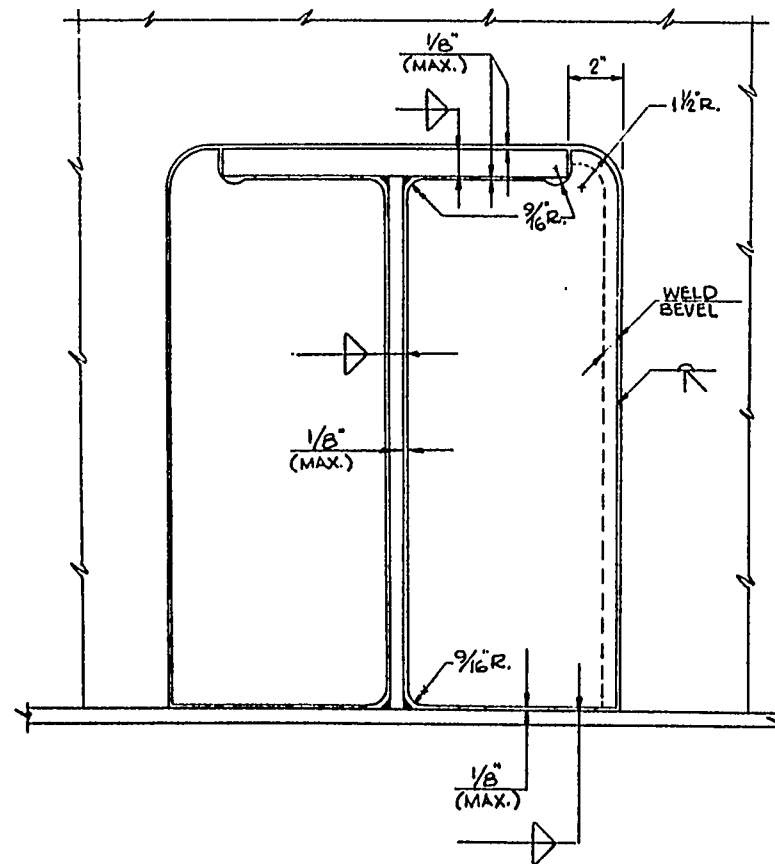
| TEE

| Figure 4-31

CLEARANCE CUTOUTS
WITH TIGHT FLUSH COLLARS
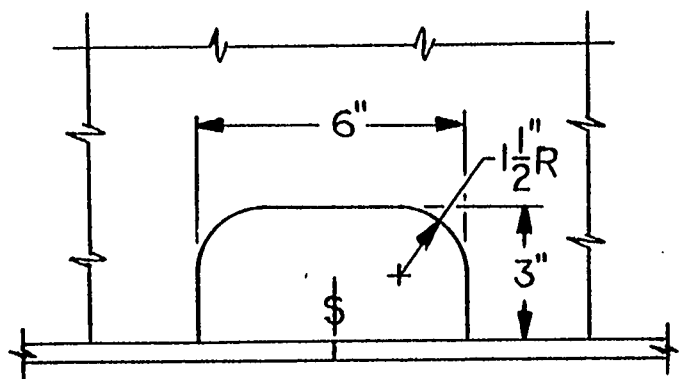
Figure 4-32
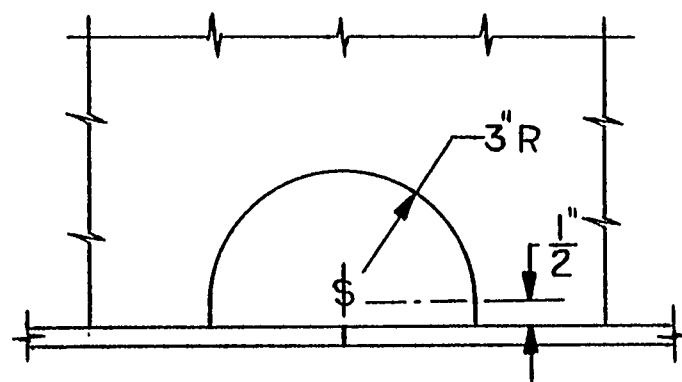
Figure 4-33

MISCELLANEOUS CUTOUTS
CLEARANCE CUTS AT PLATE BUTT

6"

3"

$

3"

Figure 4-34

$1\frac{1}{2}$"R

2"

2"
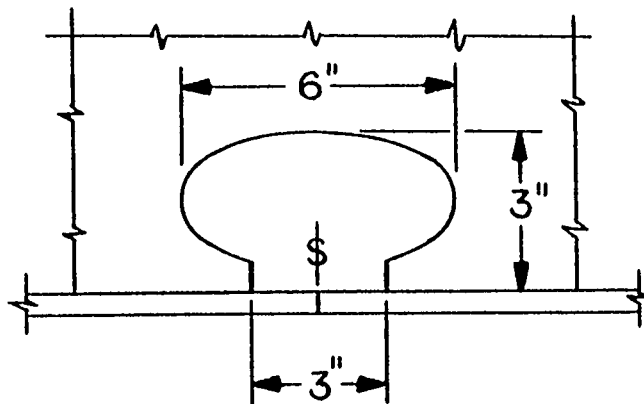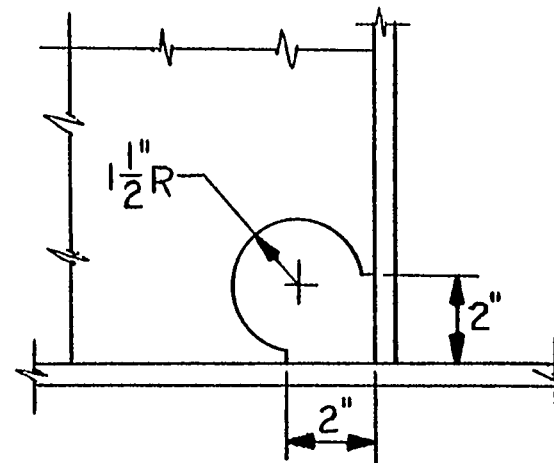
Figure 4-35

MISCELLANEOUS CUTOUTS
ALTERNATE DETAILS

3"

$1\frac{1}{2}$"R

3"
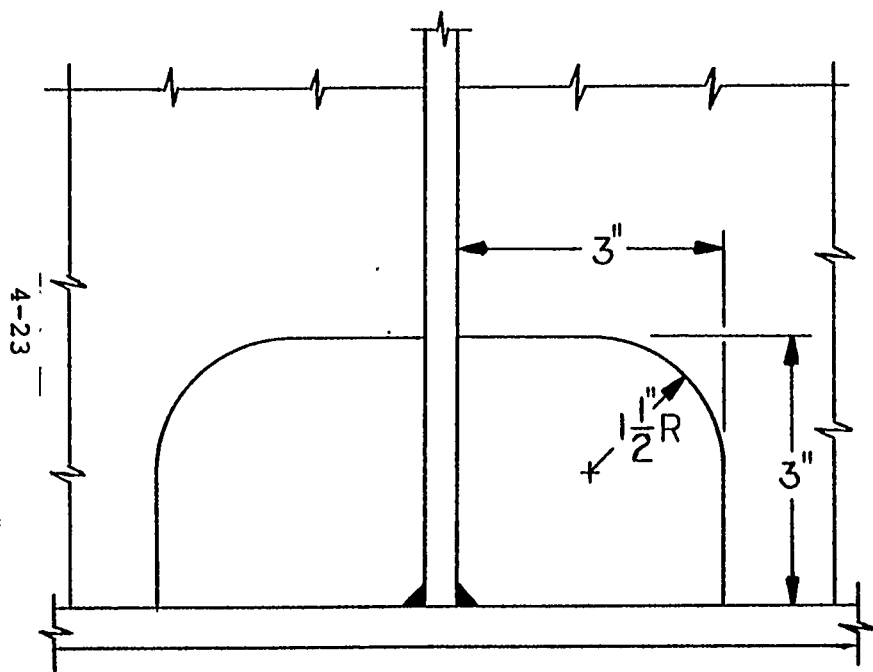
TYPICAL DRAIN AND LIMBER HOLE
IN DEEP STRUCTURE

Figure 4-36

MISCELLANEOUS CUTOUTS

$$\frac{10.2^{\#} \text{P.} \text{ OR EQUIV}}{\text{STD PIPE}}$$

$$\frac{\text{ABT}}{1/2''}$$

ABT 3''

$\frac{1''}{2}$

$\frac{\text{N T}}{\text{DECK}}$
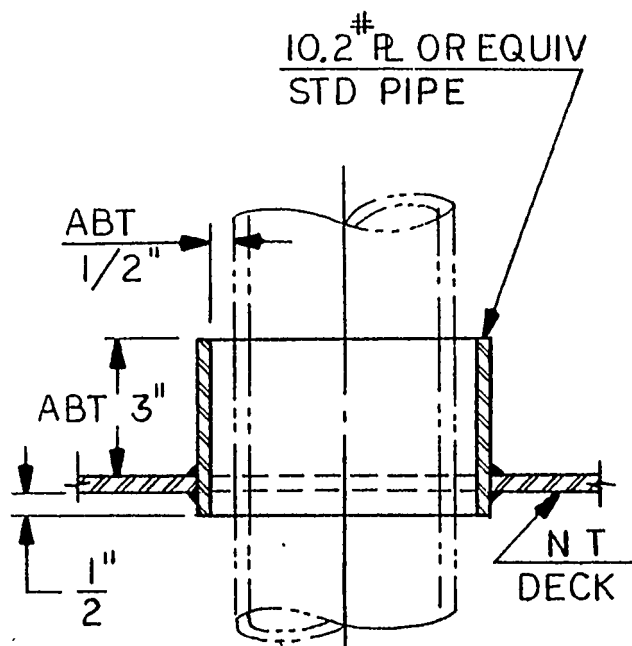
Figure 4-37

MISCELLANEOUS CUTOUTS
NONTIGHT PENETRATIONS

$2W$

W

$\dfrac{1}{2}"$ (TYP)

Figure 4-38

$2W$

W

$\dfrac{1}{2}"$ (TYP)

Figure 4-39

CHOCKS & BRACKETS

USE WHEN $D \leq 2W$
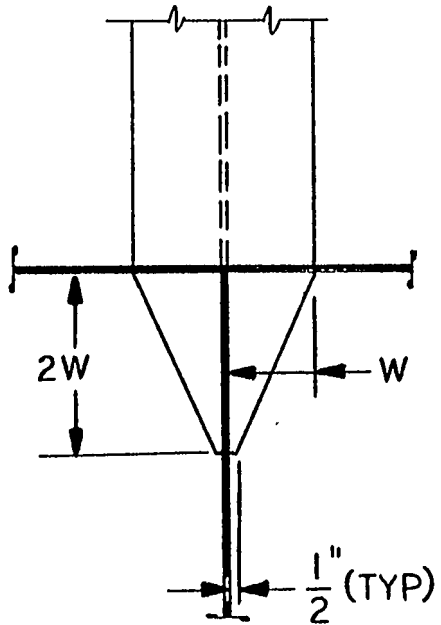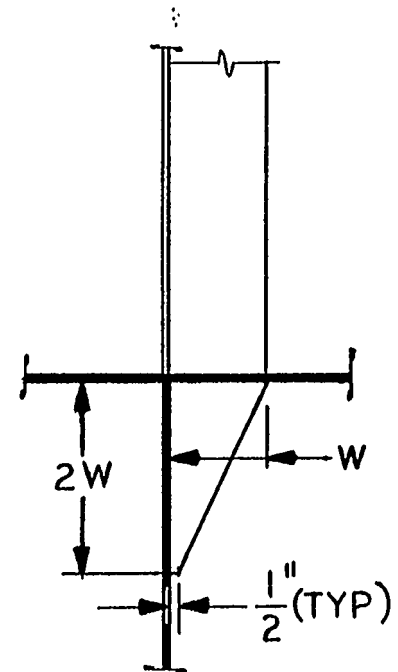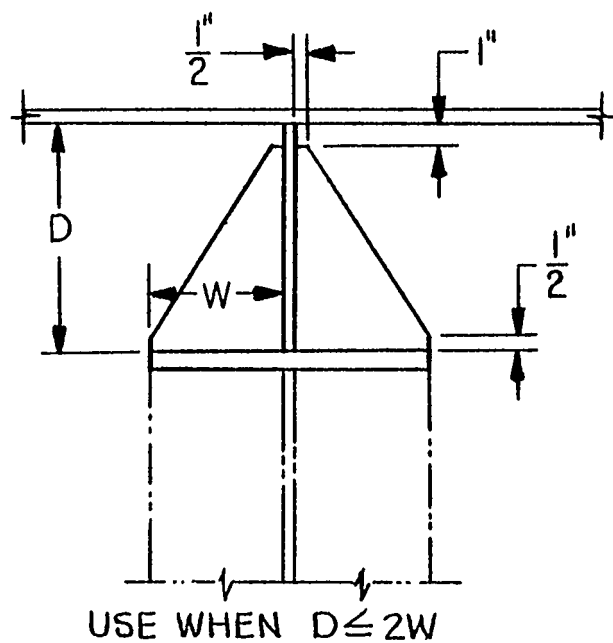
Figure 4-40
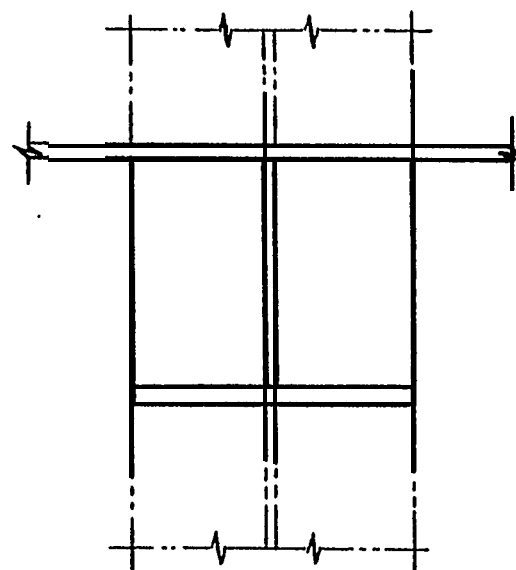
Figure 4-41

CHOCKS & BRACKETS

Use primarily to avoid knife
edge crossings at foundations
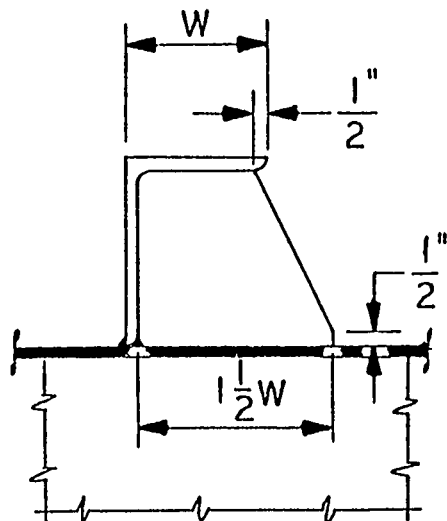
Figure 4-42

Bolting chock adjacent to
bolt hole and not in line
with backup structure

Figure 4-43

CHOCKS & BRACKETS

2" LAP

I"R (TYP)

FLANGE
(IF REQ.D)

ABT 2"
(TYP)

Figure 4-44

SEE FIG. 4-38
OR 4-40

SEE FIG. 4-41
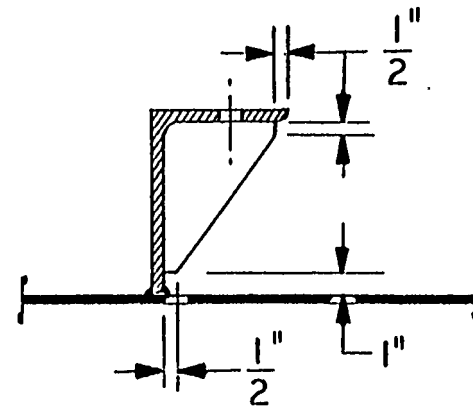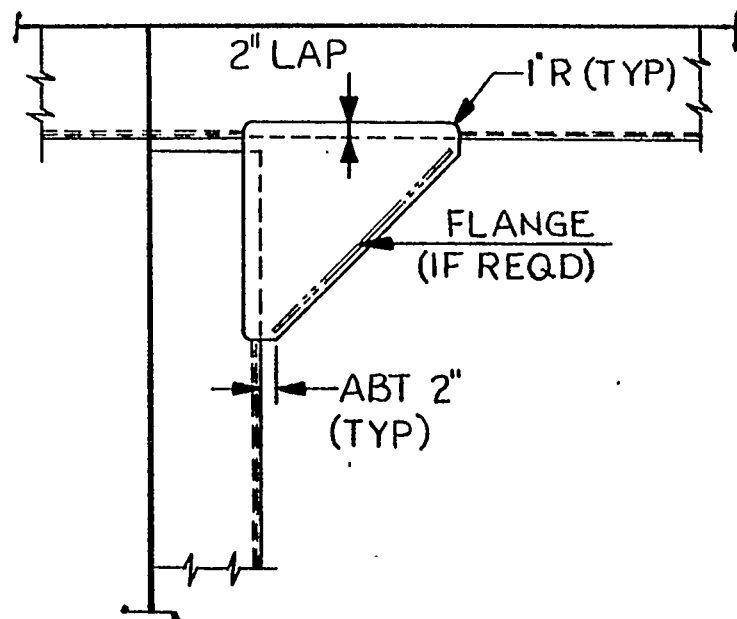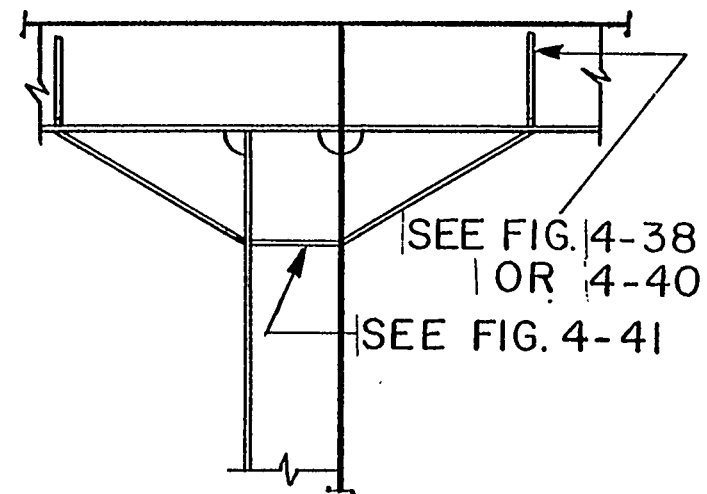
Figure 4-45

CHOCKS & BRACKETS

Stiffener endings for non-
tight opening which permits
access from both sides
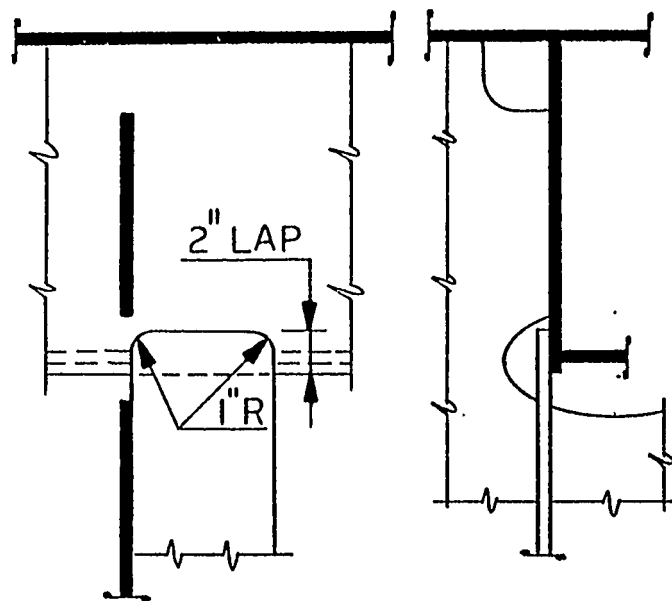
Stiffener endings for tight
intersection which permits
welding from one side only

2" LAP

1"R

Figure 4-46

1"R

2"
LAP

30°

Figure 4-47

STIFFENER ENDINGS

ABT I"   30°

2" R   I" R

ABT
2" LAP

I"
2
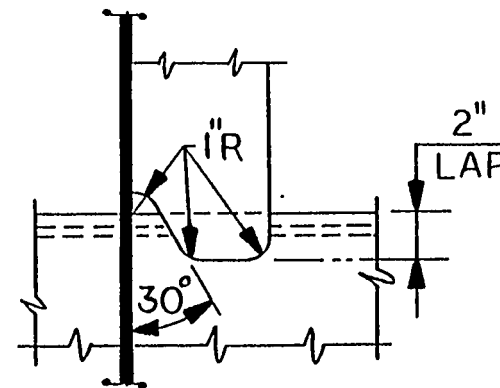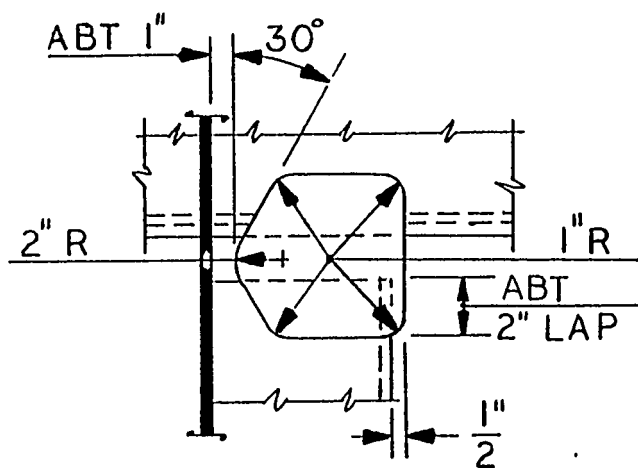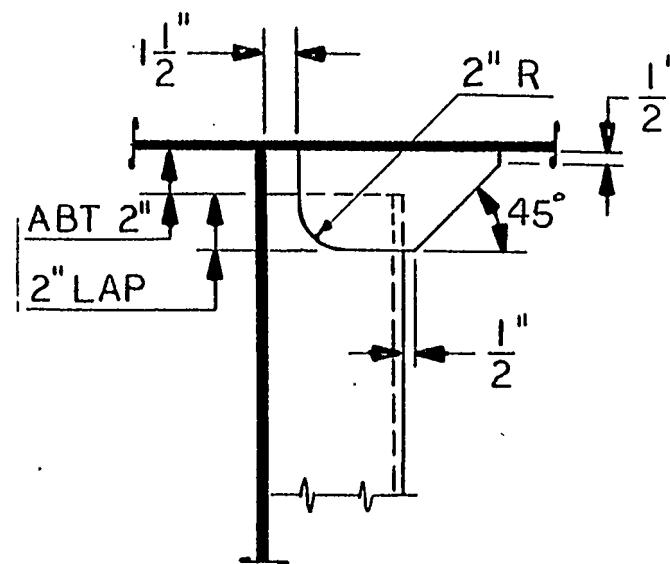
Figure 4-48

Longer tab improves end
restraint and can be used
with minimal backup

I I"
2

2" R   I"
2

ABT 2"   45°

2" LAP

I"
2

Figure 4-49

STIFFENER ENDINGS

ABT 2"
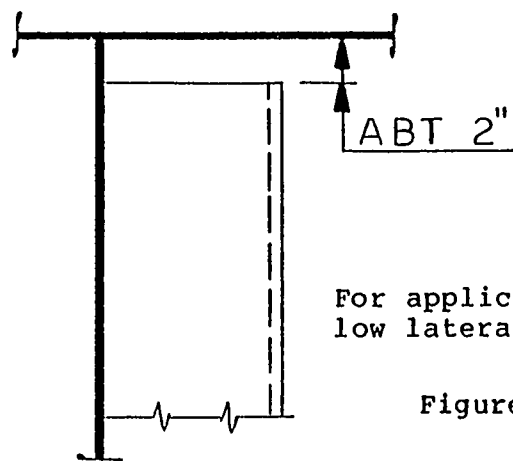
For applications with low lateral load

Figure 4-50

2"R

Figure 4-51

2"R

30"

1"

2"R
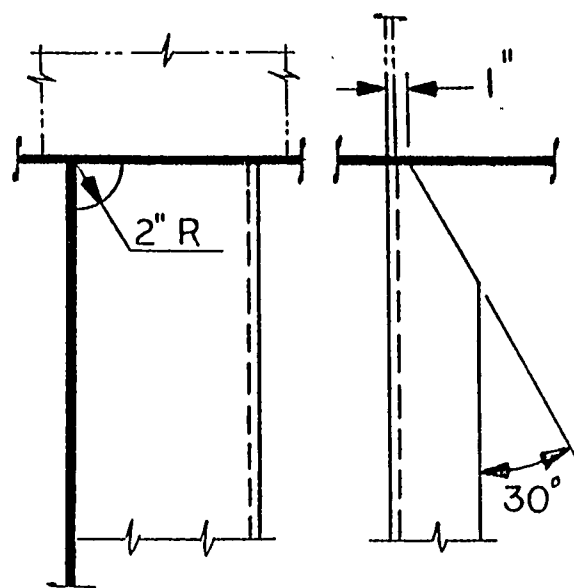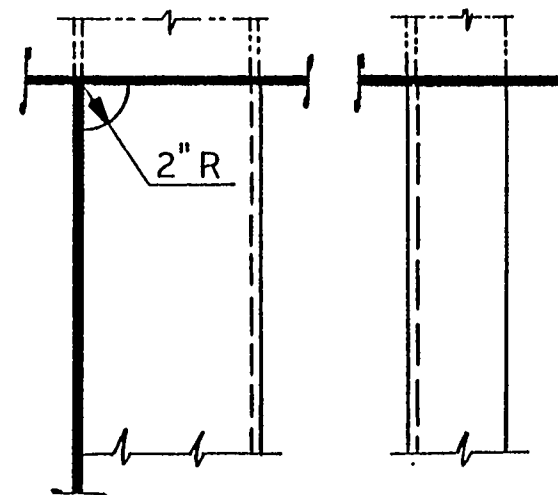
Figure 4-52

STIFFENER ENDINGS

$\frac{1"}{2}$

ABT 2"

45°

FLAT BAR
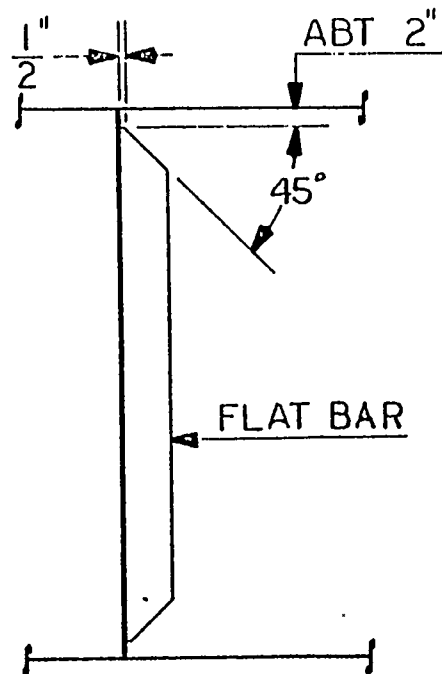
Figure 4-53

Arrangement for L or Tee
panel stiffenear in presence
of large lateral load

—2" R

ANGLE
OR TEE

SNIPE FLG
30° TO 1" SEE FIG.
4-51
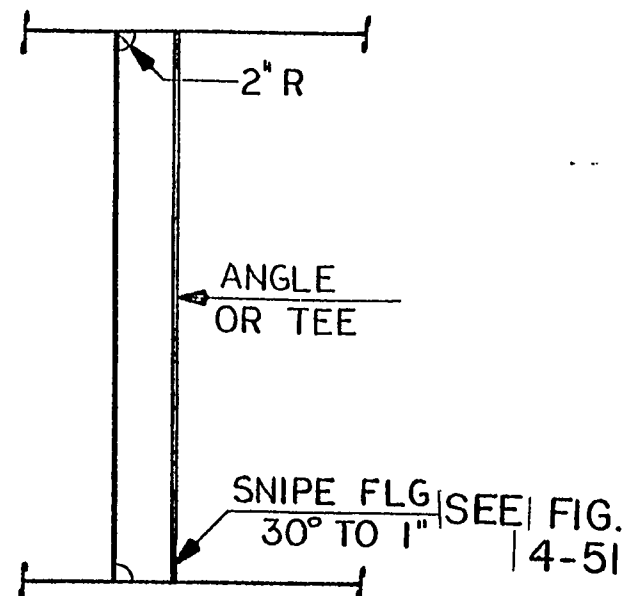
Figure 4-54

PANEL STIFFENERS

Limit application to panels
with low lateral load

ABT 2"

ANGLE
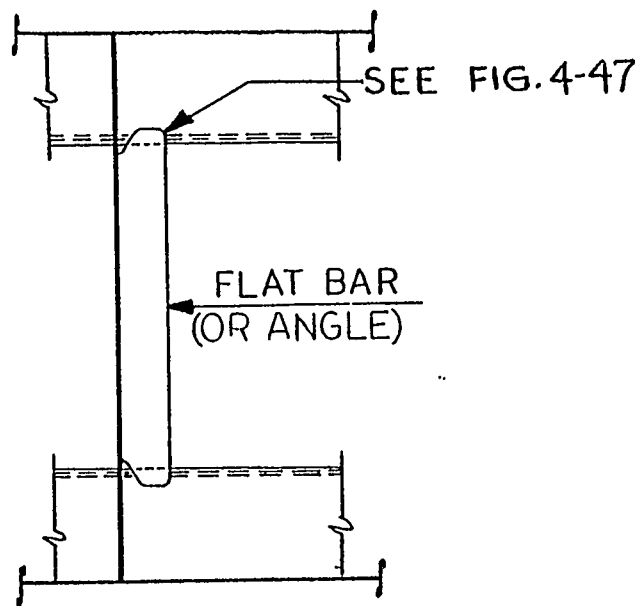
Figure 4-55

PANEL STIFFENERS

SEE FIG. 4-47

FLAT BAR
(OR ANGLE)
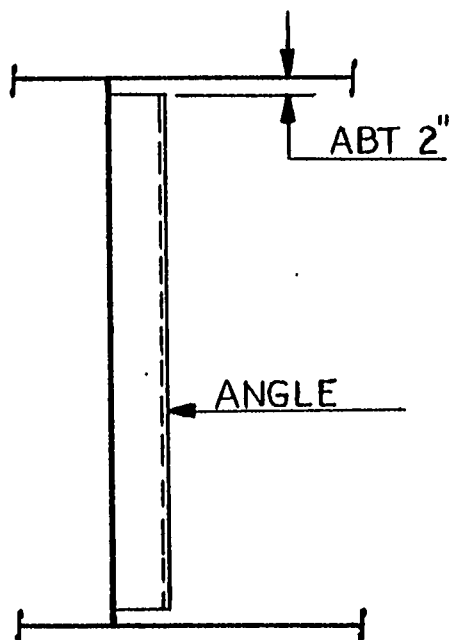
Figure 4-56

Good arrangement for L stif-
fener with lateral load.
Common plane for stiffeners,
reduces error. In horizontal.
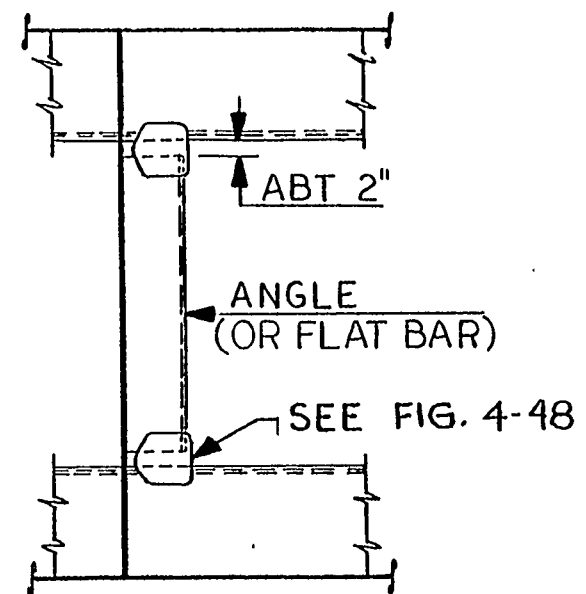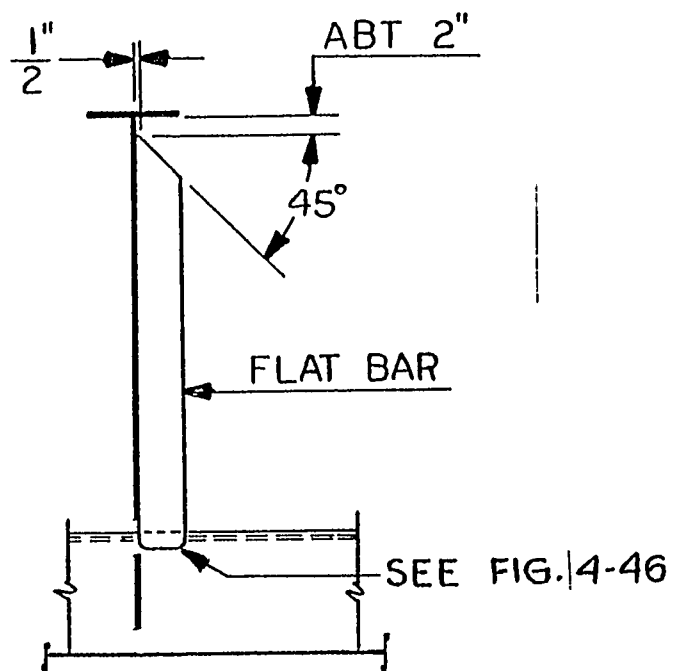application avoids turning
stiffener leg up.

ABT 2"

ANGLE
(OR FLAT BAR)

SEE FIG. 4-48

Figure 4-57

PANEL STIFFENERS

$\dfrac{1"}{2}$

ABT 2"

45°

FLAT BAR
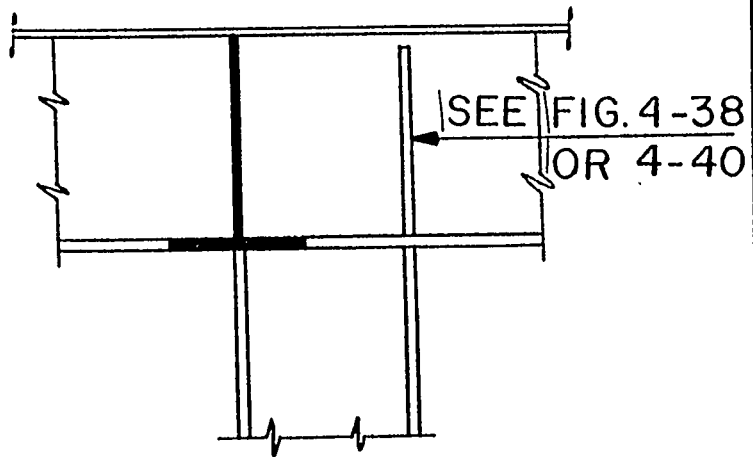
SEE FIG. 4-46

Figure 4-58

PANEL STIFFENERS

SEE FIG. 4-38
OR 4-40

Figure 4-59
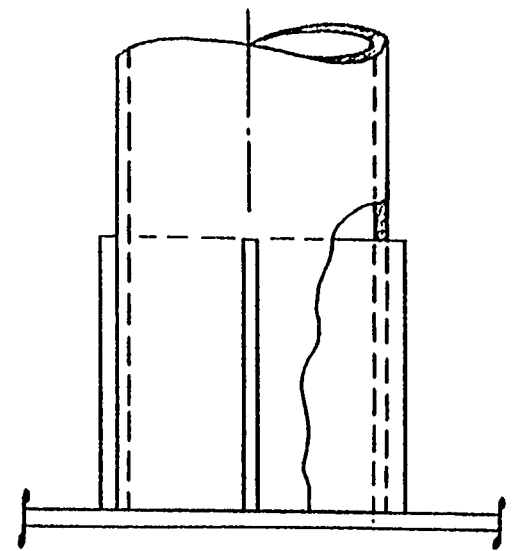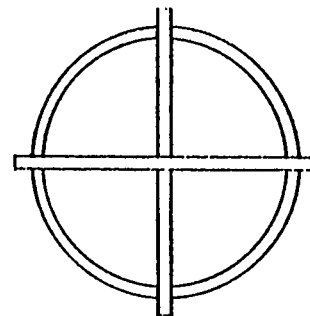
Figure 4-60

Section 5

REFERENCES

1. Glasfeld, et al, "Review of Ship Structural Details", Ship Structure Committee Report SSC-266, 1977.

2. "In-Service Performance of Structural Details", Ship Structure Committee Report SSC-272, 1978.

3. Higuchi, M., et al, "Study on Hull Structure Analysis", Nippon Kokan Technical Report Overseas, June 1973.

4. Broelman, J., et al, "Investigation of Details of Longitudinal Intersections on Tanker Frames" (In German), Schiffahrt-Schiffbau Hafen, 1975.

5. "Progress Summary - Standard Structural Arrangements", General Dynamics, Quincy Shipbuilding Division Report of July 1976.